Politecnico di Milano

Department of Electronics, Information, and Bioengineering

The emergence of diversity in the Adaptive Dynamics framework: Theory and applications

Pietro Landi
PhD Dissertation

Advisor
Prof. Fabio DERCOLE

Co-Advisor
Prof. Sergio RINALDI

Tutor
Prof. Carlo PICCARDI

Coordibator
Prof. Carlo FIORINI

PhD Program in Information Technology
Systems and Control
Cycle XXVII October

Abstract

Innovation and competition processes are often identifiable in science. They are responsible for evolutionary dynamics driven by innovative changes in the characteristics of individual agents and by competitive interactions that promote better performing ones. Genetic mutations and natural selection play this role in biology, but the potential applicability of the evolution paradigm can be extended to social, economic, information sciences and engineering. Quantitative approaches to evolutionary dynamics were born from genetics and economic game theory. While biologists traditionally consider evolutionary change separated from the demography of the interacting populations, game theorists study the relative diffusion of a given set of alternative strategies and the robustness of the corresponding equilibria with respect to invasion from potential dissident. By contrast, the more recent approach of Adaptive Dynamics (AD) takes explicitly into account both the evolutionary and the demographic change and characterizes both the evolutionary equilibria and transients and non-stationary regimes. AD represents a flexible framework, based on the hypothesis of rare and small mutations, for the formal description of evolution of the characteristics of the system in terms of ordinary differential equations. Diversity increases in the system each time competition between innovative and resident strategies gives rise to their coexistence (evolutionary branching), and reduces when evolution brings groups of agents to extinction. Evolutionary branching is particularly interesting: in appropriate conditions, innovative agents can coexist with resident ones and their strategies, initially very similar, can then diverge generating two resident forms with different characteristics. The evolution of this enlarged system can still bring to the situation in which evolutionary branching is possible for one or both forms of agents present in the system. Thus, this succession of evolutionary branchings brings simple systems (with few resident forms) toward more complex and diversified configurations.

The study of the possible branching scenarios is then very interesting in biology (where it gives an interpretation of the diversification of species from a common ancestor), but also in social sciences, economics, technology, engineering, etcetera. Moreover, some theoretical aspects of branching are still unstudied. For example, mathematical conditions under which branching occurs are expressed as sign conditions on appropriate second derivatives of the competition model, but theoretical results in critical cases in which such derivatives annihilate are not yet available. Although mathematically non generic, these situations are quite common in applications, in which particular symmetries of the model bring some derivatives to annihilate systematically. In conclusion, the main goal of the thesis is to focus both on the analysis of theoretical aspects of evolutionary branching in the framework of AD and on the development of models to interpret diversification phenomena in the above mentioned fields of science.

The thesis is organized as follows. The first three chapters are just an introduction to evolution and to the existing theory of Adaptive Dynamics, with particular focus on evolutionary branching. Chapter 4 extends the theory of evolutionary branching in critical cases, expanding our knowledge on the phenomenon and providing more general conditions under which it occurs. The next three chapter are more applicative: the first concerns the evolution of biodiversity in ecological coevolving communities and develops a general methodology to study diversification scenarios in evolutionary systems; the second focuses on fisheries-induced diversification of fish stocks; while the third is about the emergence of fashion diversity in social groups.

In particular, chapter 1 is an introduction on the theory of evolution, starting from its history, passing through its basic elements (mutation and selection), and closing with the mathematical approaches to the study of the evolutionary dynamics. The concept of evolutionary diversification and evolutionary extinction are also intuitively introduced. Chapter 2 is dedicated to the Adaptive Dynamics approach, the resident-mutant competition model, the computation of the invasion fitness, and the AD canonical equation, that models the expected long-term evolution of the phenotypic traits of the coevolving community. In chapter 3 we focus on the emergence of diversity in the AD framework, that is, evolutionary branching. We classify the evolutionary equilibria with respect to their convergence and evolutionary stability, recovering the classical branching conditions, i.e., the two mathematical conditions in terms of second derivatives of the invasion fitness under which the system becomes dimorphic and ex-

perience disruptive selection, thus increasing its diversity. Chapter 4 is devoted to the study of the branching bifurcation, namely, the transition from evolutionary stability to evolutionary instability along with the change in a model parameter. This bifurcation occurs when the branching condition ruling evolutionary stability changes sign. To study such critical case, a particular third order approximation of the invasion fitness must be computed, and a novel property of the resident-mutant competition model must be exploited in order to obtain simple and general results. The case in which the other branching condition is critical is more complicated and is left for future research, but our theoretical approach is general and remains valid, also for further degenerate cases (e.g., when both the branching conditions are critical). In chapter 5 we develop a general methodology to study the evolution of biodiversity in eco-evolutionary two-species communities, with an application to prey-predator interactions. We then use such methodology in two fields of science different from biology. In chapter 6 we analyze the possibility that the interplay of natural and artificial selection due to fishing could lead to disruptive selection on exploited fish stocks. Finally, in chapter 7 we study the evolution of fashion purely driven by social interactions, with particular focus on the emergence of style diversity, and find out that different styles can successively emerge starting from a single style society. Chapter 8 discusses and summarizes the achievements of the work and close up the thesis with suggestions on extensions and future research.

Contents

Chapter 1

Introduction

In this chapter we introduce the history of evolutionary theory and the two fundamental processes driving evolutionary dynamics: mutation (innovation), that introduces new variants in the system, and selection (competition), that promotes the better performing ones. Afterwards, we intuitively discuss the possibility that evolution can both increase and decrease biodiversity through evolutionary branching and evolutionary extinction. Finally, we report a short review of the possible modelling approaches to evolution. More details can be found in Dercole and Rinaldi [2008], on which this introduction is based.

1.1 History of evolution theory

The idea that living organisms on Earth have diversified in time starting from a common ancestor goes back to the Greek naturalistic philosophy (VII-V century BC). However, no further contributions of the evolutionary theory aroused until the XVIII century, because the most diffused idea among European intellectuals was that of a universe which was created in its actual and final state. During the XVIII century, the work of enlightened intellectuals known as "Encyclopedist" showed, through a systematic classification of living organisms into groups, the presence of structural common features among all life forms. This led to a better understanding of the concept of species and revealed fundamental similarities among widely disparate organisms. These observations were in contrast with the idea of Creation and set the ground for evolution theory. Considerable contributions came from George-Louis Leclerc Buffon (1707-1788) and Erasmus Darwin (1731-1802), Charles' grandfather, who first introduced the hypoth-

esis that life could have evolved from a common ancestor and posed the question of how a species could evolve into another. The first explicit evolutionary theory was formulated by Jean Baptiste Lamarck (1744-1829), disciple of Buffon, who first introduced the concept of inheritance. The "Lamarckian" hypothesis has been widely criticized by naturalists of the time. At this point Charles Darwin (1809-1882) and Alfred Russel Wallace (1823-1913) formulated the evolution theory that is still accepted today. In 1858 they separately presented the theory of evolution through *natural selection* [Darwin and Wallace, 1858], arguing that

- there exist individual variations in a great number of features in a population, some of which may affect the individual probability of survival and reproductive success;
- there probably exist an inheritable component at the basis of these variations, but the evolutionary process mainly relies on the birth of new forms of organisms, called *mutants*;
- from generation to generation there exist a natural selection of the features associated with a higher probability of survival or a better reproductive success, whose frequencies in the population thus increase over time;
- cumulative effects of mutations and natural selection change the features of the species from those of their ancestors in the long term;
- all living organisms descend through successive modifications from a common ancestor, thus presenting hierarchical and recurrent similarities.

Darwin and Wallace combined empirical observations with the theory derived from the work of Thomas Robert Malthus (1766-1834) on competition and population growth [Malthus, 1798]. They had a precise idea of natural selection and of the possibility of mutations, but they were not aware of the laws of genetics, discovered seven years later by Gregor Mendel (1822-1884), who discovered the discrete nature of inheritance through what we now call genes [Mendel, 1865].

More than a century after the publication of the theory of evolution, it can be said that its impact on human thinking has widely spread beyond the field of biology. Essentially, the evolutionary dynamics can be described by a two-step process:

- *innovation*, that is, the birth of variations;
- *competition*, that selects for the better performing variants.

This abstract paradigm can be applied to many processes and thus explain the evolution of complex systems, both natural and artificial, in which a great number of agents, each characterized by its individual traits which are transmitted, with possible variations, to the next generation, are selected naturally or artificially through their performance with respect to some optimality criteria. After the "Darwinian" revolution, very different phenomena (such as socio-cultural networks, global and market economy, industrial processes, technological systems) can be interpreted and studied as evolutionary processes (see, e.g., Dawkins [1976], Dawkins [1982], and Dercole and Rinaldi [2008]).

1.2 Basic elements of evolution theory

1.2.1 Mutation

As Darwin and Wallace first realized, evolutionary changes are based on the birth of new forms of organisms, called mutants, characterized by variations in their *phenotypes*[1] with respect to their conspecific individuals. These phenotypic changes reflect inheritable changes in the genetic material, which are called *mutations*. Inheritable phenotypic changes have been documented in many organisms and for many types of features, including intelligence and behavioral strategies. Variations in these features, or *traits*, can give advantages or disadvantages in the competition for common resources or in terms of survival and reproductive ability. Mutations are the first fundamental step for the evolutionary dynamics and they are the basis on which natural selection acts. Notice, however, that this is not the only way to introduce a variant in a system, since different traits can come from outside the system through a process of immigration. However this occurs, new traits are always present in a single individual or in very low fraction of the population. Thus, this variations can have a long-term impact only if other processes (e.g., selection) lead to the increase of the frequency of the new trait in the population.

[1] The *genotype* of an individual consist in a particular realization of the *genome* of its species, and it's composed of the chromosomes effectively possessed by the individual. Otherwise, any individual feature determined by the genotype is called *phenotype*, that is, an inheritable feature from generation to generation [Li, 1955].

1.2.2 Selection

From the evolutionary point of view, what matters is the effect of the mutation on the phenotype of the mutant individual. Indeed, the success of an individual in the struggle for survival depends on its phenotypic features and on the environmental conditions it is facing. Such environmental conditions consist in both physical factors (e.g., clime, height, sea level, air or water pollution, etc.) that define the *abiotic environment*, and in all individuals of its same or different species interacting with the considered individual, that define the *biotic environment* (see, e.g., Lewontin [1983]). The result of the struggle for life of an individual facing intra- and interspecific competition and certain environmental conditions thus depend on its phenotype, on the abundances and phenotypes of the interacting individuals, and on the abiotic components of the environment, which typically fluctuate in time.

Individuals with different phenotypes with respect to the rest of the population can thus have a different probability of survival during the reproductive period (*viability*), a different reproductive success or a different abundance of their offspring (*fertility*). As a result, if we imagine a constant abiotic environment, with no mutations or immigration phenomena, then the demographic dynamics of the population will tend to promote the phenotype that is better adapting to all conditions, which in the long term will dominate the whole population. Therefore, under these assumptions, selection is an autonomous dynamical process and will bring the system toward a regime, which can be stationary as non-stationary (cyclic or even *chaotic*, see, e.g., Turchin [2003]). These regimes correspond to the *attractors* of the dynamical process, since they attract nearby states.

Approaching an attractor, some phenotypes could disappear from the community, since the individuals characterized by such features are eliminated by better performing and competitive individuals. When an attractor is reached, the phenotypes coexisting in the population are called *residents*, as the group of individuals carrying such features. If a population is composed by individuals characterized by the same phenotype it is called *monomorphic*. In reality, selection could be interrupted by a mutation or by a perturbation of the abiotic environment, events that would prevent the system to converge to the attractor. However, in the great majority of cases, the time interval between two successive mutations or environmental perturbations are usually so long to allow selection to bring the system on the attractor

and thus to define the resident groups of the population.

The timescale on which selection acts is the *demographic timescale*. Analogously, the dynamics driven by selection and the attractors to which this dynamic tends are called *demographic*. In the literature, the term *ecological* is also often used, since ecology studies living organisms on a timescale for which mutations and external environmental perturbations can be neglected (see, e.g., Roughgarden [1983]).

For convenience, in the biological context the term *fitness* is used to indicate the probability to survive and reproduce. Quantitatively speaking, the fitness of an individual is defined as the abundance of its offspring in the next generation, or the per-capita growth rate of the group of individuals with the same phenotype (i.e., the variation of the abundance in the unit time with respect to the total abundance). These two definitions (the first for a discrete-time and the second for a continuous-time approach) say that the abundance of the individuals characterized by a particular phenotypic trait will grow, in a given instant, if the fitness associated to that phenotype is greater than one ore positive, respectively. This quantitative approach will be fundamental for the modeling of the evolutionary dynamics (see Chapter 2).

As discussed in Paragraph 1.2.1, a mutation generally occurs in a single individual or in a very small fraction of the resident group. Disadvantageous mutations reduce survival and the reproductive success of the mutant individuals, so that they will be eliminated by the competition with the resident individuals. This is another fundamental role of selection, namely, it keeps under control mutations that translates into undesirable and disadvantageous features for the individuals. By opposite, mutations that bring advantages to the mutant individuals will be selected, leading the the increase of the abundance of the mutant group. However, in the initial phase in which the mutant abundance is scarce, these innovative individuals face the risk of accidental extinction and could not spread in the population and invade the resident group even if the mutation brings some advantages to the mutant individuals. When the mutation has just born, the fitness of the mutants is called *invasion fitness* [Metz et al., 1992], and its value gives a quantitative information of the advantages or disadvantages for the mutant individuals. As will be discussed in Paragraph 1.2.3, the evolutionary process goes on until there exist some phenotypic traits that favorably influence the fitness of the mutants that escape accidental extinction and invade the resident population.

1.2.3 Evolution

Intuitively, the evolutionary dynamics could be defined as the long-term dynamics of the phenotypic distributions of interacting populations. If populations of different species are interacting (e.g., through predation, symbiosis, competition for common resources, etc.) the evolution of a population of a species will probably influence the evolution of all other populations, so their *coevolution* [Futuyma and Slatkin, 1983, Thompson, 1994] must be studied.

Natural evolution thus results from the combination of the process of mutation (whose probability typically is of the order of one over a million on the demographic timescale) and natural selection, that typically occurs through interactions of predation, symbiosis, competition for space or common resources, exploitation of ecological niches, thus being a smooth and gradual phenomenon.

The evolutionary dynamic concerns phenotypic traits that influence the demography of interacting populations through the invasion fitness of the mutant individuals, which can increase their abundance and spread in the population by means of natural selection if the mutation gives some advantages to the mutants with respect to some optimality criteria. Phenotypic traits that influence the fitness are capable to adapt to the environmental conditions and are therefore called *adaptive*. In principle, there can exist phenotypes that do not have any influence on fitness, or mutations that have no effect on phenotypes. These traits do not experiment any selective pressure and their evolution follows the rules of *genetic drift*. Therefore, two different types of evolution can be distinguished:

- mutation and selection processes, that involve phenotypes that have some effect on the fitness of the individuals;
- genetic drift of the phenotypes that do not influence the fitness of the individuals.

Notice that mutant individuals are initially present in very low densities, therefore with no selective pressure the probability of facing accidental extinction is very high. Thus, genetic drift is a very slow phenomenon and it is typically dominated by the mutation-selection evolution.

It is now convenient to introduce the different timescales involved in the evolutionary dynamics:

- demographic (or ecological) timescale, on which selection acts;

- *evolutionary* timescale, on which the effects of successive mutations and selection of the best variant are appreciable.

Indeed, as introduced in Paragraph 1.2.2, the time interval between two successive mutations is generally sufficiently long to allow selection to act and bring the system to an attractor and thus define the resident group. More precisely, if a mutation brings some advantages to the mutants and if these individuals escape the mechanisms of accidental extinction, then selection brings the system on a new attractor, where typically the mutants have replaced the former residents, becoming the new resident group. Otherwise, the system goes back to the former attractor.

In this way, in the case of rare mutations, it is possible to define as *evolutionary dynamics* the sequence of attractors visited by the demographic dynamics. Under this assumption the two timescales are completely separated. In addition of being rare on the demographic timescale, mutations also often have small phenotypic effects, so that the evolutionary dynamics results to be slow and smooth. If we imagine a sequence of mutations with small effect on the phenotypes and assume that each time the mutant group is favored with respect to the resident, thus completely substituting them in the population, it is possible to draw an evolutionary trajectory. At a certain time instant on the evolutionary timescale, it is possible to define a phenotypic trait space, with an axis for each trait of the resident group, so that the current state corresponds to a point in this trait space. Such a point slowly moves along the evolutionary process, that is, each time a mutant group substitutes the resident group. Notice that the dimension of the trait space changes each time a new resident group appear in the community or each time a resident group disappears in favor of a mutant group.

As we will see in Chapter 2, these two simplifying assumptions are the basis of many modeling approaches of the evolutionary dynamics, and even though they may seem extreme simplifications of reality, they allow a description of the demographic and evolutionary dynamics that, at least qualitatively, can give very useful insights on the real dynamics of the system.

As for the demographic dynamics (see Paragraph 1.2.2), it is possible to study the attractors of the evolutionary dynamics. However, the evolutionary process is not autonomous, since it depends by particular sequences of mutations and on the abiotic environment fluctuations. Nonetheless, in this thesis the abiotic environment will be assumed as constant, not only to simplify the analytical study of the

models, but also to focus on the evolutionary effects that derive from endogenous dynamics of the system and from the mutation-selection process, neglecting exogenous factors. In this way, evolution can be studied as an autonomous dynamical process and the obtained results remain also valid if the exogenous variations of the abiotic environment have frequencies that are not comparable with the ones typical for the ecological and evolutionary processes and if the results are interpreted as the average of all possible realizations of the mutation process. For this, the evolutionary dynamics will tend to stationary as well as non-stationary (periodic or chaotic) attractors. Moreover, the nonlinearities of the system makes the presence of multiple attractors possible, making the outcome of the evolutionary dynamics dependent on the ancestral condition of the system [Dercole and Rinaldi, 2008].

1.2.4 Emergence of diversity (evolutionary branching)

One of the assumptions on which the evolutionary theory is based is that all living organisms are the descendants of self-replying organic molecules originated by inorganic substances more than 3 billion years ago. All forms of life that have developed have been produced by the natural selection of the mutations that were better fitted to the environment. So far, the concept of *species* has been used without giving a formal definition. However, in the great majority of cases, a species can be defined as a group of morphologically, structurally, and genetically similar living organisms that are isolated from other groups and that (when reproduction is sexual) are capable of interbreeding to generate fertile offspring [Mayr, 1942]. For sexual species the distinction is then quite simple, that is not the case for asexual organisms, for which it is necessary to rely on similarity measures.

The birth of new species, called *speciation*, is certainly one of the central problems in the theory of evolution, and also one of the most debated (see, e.g., Hutchinson [1959], Maynard Smith [1966], Felsenstein [1981], Kawecki [1996], and Dieckmann et al. [2004]). Speciation occurs with the genetic and phenotypic divergence of conspecific populations that adapt to different environmental niches in the same or different habitat. In the case of sexual species, divergence has to be enough to produce some obstacles to interbreeding (morphological or structural incompatibility, sterility of the offspring, different habitat preferences or different mating periods, sites, and rituals.)

The mechanism which is traditionally accepted by the scientific

community (proposed by Darwin) is that two populations of the same species are geographically isolated and then will follow two different evolutionary paths. Since different selective pressures and different genetic drifts may occur in different environments, the two isolated populations can become two different species. This form of speciation is called *allopatric* when the two populations are geographically isolated by natural or artificial barriers, or *parapatric* when they evolve toward geographic isolation expoiting different niches of nearby habitats. Although these mechanisms are supported by many observations for which variants of the same species (candidate to be different species) often occupy different regions, the main ingredient, i.e., the geographic isolation, results to be somehow an exogenous factor more than an effect of the evolutionary process itself.

A different mechanism of speciation, called *sympatric* [Maynard Smith, 1966], considers populations in the same geographic region. In this case the most important ingredient is a selective pressure that favors extreme phenotypes in a range of polymorphism. This so-called *disruptive* selection can result, for example, from the competition for alternative environmental niches, where the specialization for a specific niche can be advantageous respect of being generalists. Under the pressure of disruptive selection a monomorphic species can become dimorphic with respect to a certain phenotype: this phenomenon is called *evolutionary branching*. The monomorphic population is divided into two resident groups, initially very similar, that successively diversify following two separate and opposite evolutionary *branches*, each one characterized by its own mutations. In the trait space, an evolutionary trajectory approaches an equilibrium, called *branching point*; at this point the trait space gains a new dimension, that is, the trait that characterize the new resident group [Dercole and Rinaldi, 2008].

What makes evolutionary branching very interesting is that this phenomenon gives an autonomous and evolutionary explanation for a possible process of speciation, without referring to exogenous factors such as the geographic isolation. It has however to be noticed that evolutionary branching does not imply an immediate speciation phenomenon, but favors a higher polymorphism in the phenotypes of a certain population that can thus be at the basis of a possible speciation process.

1.2.5 Evolutionary extinction

So far, we have seen how the mechanism of speciation could give an evolutionary explanation to diversity of life on Earth. Nonetheless estimations of the number of species in the history of life [Wilson, 1988] show that the actual biodiversity is the result of a small surplus of the birth of new species respect to the loss of species. This makes the drivers of these extinctions as important as those of speciation.

In the history of life, indeed, periods of decrease of biodiversity have existed, during which extinctions were greater than speciations. Among these periods, the 5 mass extinctions [Raup and Sepkoski, 1982] are the most important. Other than these mass extinctions, almost surely caused by natural catastrophes on global scales, there also exist many more evidences of minor extinction phenomena. However, even if caused by catastrophic events, these extinctions are not random processes. Indeed they are the consequence of a rapid change of the abiotic environmental conditions on the evolutionary timescale, that creates an evolutionary transient along which species try to adapt at the new conditions. Some may have succeeded, other may have failed, so it is correct to talk about *evolutionary extinctions*.

As already observed (see Paragraph 1.2.3), the coevolution of coexisting populations changes the biotic environment in which they live, which in turn influences their evolution. For this, as a change in the abiotic environment may lead to the extinction of some species, the same may occur also for a change in the biotic conditions. In other words, the coevolution of different populations in the same constant abiotic environment may lead the phenotypic traits of some of these populations to values for which such populations cannot survive. The idea that evolution can autonomously lead to extinction was already perceived by Darwin, who observed that the process of mutation-selection favors phenotypes that give advantages to the single individual, but that could, in the long term, reveal to be inconvenient for the population.

Recently, the possibility of the evolution toward extinction in a constant abiotic environment has been studied theoretically [Matsuda and Abrams, 1994, Gyllenberg and Parvinen, 2001, Dieckmann and Ferriére, 2004, Parvinen, 2005] and three basic mechanisms have been identified:

- the first, called *evolutionary runaway*, occurs when selection leads the phenotypes toward values at which the population has low density, thus increasing the risk of accidental extinction.

The other two mechanism are based on the fact that the region of the trait space that allows the coexistence of all the coevolving populations is typically closed by an extinction boundary, since extreme values of the phenotypes are usually morphologically or physiologically not compatible with the (abiotic and biotic) environmental conditions. In the course of evolution the abundance of the population can gradually vanish approaching the extinction boundary or can persist at high values also in the vicinity of such boundary, as often occurs in many systems for which a certain threshold is needed for survival. Therefore,

- in the first case the phenomenon is called *evolutionary murder*, since the rate of phenotypic variation of the population (being proportional to the number of mutants generated per unit time) gradually vanishes together with the population abundance. For this, the extinction boundary is reached because of the evolution of the other coevolving populations, that act as murders;

- by contrast, in the second case, called *evolutionary suicide*, the population actively evolve toward self-destruction, that is, mutations closer to the extinction boundary give advantages to the individuals with respect to the residents, even if the trait is closer and closer to the boundary. What is good for the single individual turns out to be catastrophic for the whole population.

The subtle difference between these three mechanisms is difficult to be observed empirically, but this approach remain the same valid and very important since it conceptually shows that evolution is also capable of autonomously destroying some species.

1.3 Modeling approaches

Evolutionary process reveals to be so complex that a detailed description remains practically impossible. Each mathematical modeling approach considers some relevant mechanisms and neglects the others. The tradeoff between the description of reality and the possibility of a mathematical analysis has produced a great variety of approaches, each one focusing on different aspects of the evolutionary process. Also a neat distinction between the different approaches is difficult, since often assumptions overlap. Following Dercole and Rinaldi [2008], seven different modeling approaches are cited:

- *population genetics* [Fisher, 1930, Wright, 1931, Haldane, 1932];

approach	geno-type	pheno-type	short term	long term	evol. tree	deter. mod.	stoch. mod.
population genetics*	✓		✓			✓	✓
individual-based models	✓	✓	✓	✓	✓		✓
quantitative genetics		✓	✓			✓	
evolutionary game theory		✓				✓	
replicator dynamics		✓	✓			✓	
fitness landscapes		✓		✓		✓	
Adaptive Dynamics		✓		✓	✓	✓	✓

*classic formulation: short-term genotypic distribution.

Table 1.1: Comparative analysis of the different modeling approaches.

- *individual-based evolutionary models* [Bolker and Pacala, 1997, Dieckmann and Law, 2000, Grimm and Railsback, 2005];
- *quantitative genetics* [Bulmer, 1980, Falconer, 1989];
- *evolutionary game theory* [Nash, 1950, von Neumann and Morgenstern, 1953, Maynard Smith and Price, 1973];
- *replicator dynamics* [Taylor and Jonker, 1978, Schuster and Sigmund, 1983];
- *fitness landscapes* [Levins, 1968, Leon, 1974, Metz et al., 1992];
- *Adaptive Dynamics* [Metz et al., 1996, Dieckmann and Law, 1996, Geritz et al., 1998].

The choice of one of the above approaches depends on the level of description one wants to obtain, on the particular question one wants to address, and on the technological tools of analysis available to reach one's goals. From a biological point of view, the main distinctions regard the genotype or phenotype base, the timescale, and the ability to produce the evolutionary tree of the studied community. By contrast, from a technical point of view, the main discriminant is between deterministic and stochastic models. See Table 1.1 for a comparative analysis of the cited modeling approaches, both respect the biological and the technical considerations.

Chapter 2

Adaptive Dynamics

In this chapter we present the *Adaptive Dynamics* approach. It is the modelling framework in which the whole thesis is cast. We first describe the main assumptions on which AD is based, to continue with a more specific and technical part in which we show how to compute from the resident-mutant competition model the invasion fitness, to be used in the derivation of the AD *canonical equation*, that models the expected evolutionary dynamics of the adaptive traits in the community. We close showing how the canonical equation can be used to produce evolutionary state portraits, describing evolutionary trajectories in the space of the adaptive traits. More details can be found in Dercole and Rinaldi [2008], on which this introduction to AD is based.

2.1 Description and assumptions

The most innovative among the dynamical approaches based on phenotypes is indeed Adaptive Dynamics (AD) [Metz et al., 1996, Dieckmann and Law, 1996, Geritz et al., 1998, Dercole and Rinaldi, 2008], that formulates the fitness functions explicitly considering the demographic interactions between residents and mutants. This allows to identify the conditions under which a resident trait is replaced by a mutant trait (*invasion implies substitution theorem* [Geritz, 2005, Meszéna et al., 2005, Dercole and Rinaldi, 2008]). Moreover, the phenomena of evolutionary branching (see Paragraph 1.2.4) and evolutionary extinctions (see Paragraph 1.2.5) are formally explained. This is very important for the aim of this thesis, especially for what concerns the evolutionary branching conditions.

With the AD approach, genetic details are neglected by means of the timescales separation (see Paragraph 1.2.3). This allows for the use of asexual population models [Dercole and Rinaldi, 2008]. In this way, when a mutation occurs, the demographic system can be considered at its regime. Moreover, the competition between the resident and the mutant populations is explicitly described by the *resident-mutant model*, an Ordinary Differential Equation (ODE) model that describes the dynamics of the resident and mutant populations for each values of the considered traits. When no mutants are present, the resident-mutant model degenerates into the *resident model*, that defines the region of the trait space in which all the resident populations coexist on the demographic timescale, called the *evolution set* of the community. When the evolutionary dynamics pushes the traits toward the boundary of such region, at least one of the resident populations go extinct (see Paragraph 1.2.5).

The use of deterministic population models is justified whenever populations are present in high abundances, i.e., in the absence of risk of accidental extinction (for example, through the mechanism of *demographic stochasticity*). However, this is not the case of a mutant population, which is initially very scarce (see Paragraph 1.2.1), so that the resident-mutant model can only be used to study the dynamics of populations that escaped the risk of accidental extinction. Mutations are described as a stochastic process and each time a mutation occurs, the probability of escaping accidental extinction is computed as the probability that the mutant population reaches a certain threshold of abundance that guarantees its survival. In this way, the evolutionary dynamics is the result of a sequence of mutations that substitute the resident group and can be described in the trait space by a *random-walk*-type model. The birth of a new resident trait occurs when a mutant population escapes the mechanisms of accidental extinction and coexists with the resident group, becoming a resident population itself (evolutionary branching, see Paragraph 1.2.4). By contrast, an evolutionary extinction occurs whenever the evolution of the traits leads to the extinction of one or more resident populations, thus reducing the trait space dimension. Very important, Champagnat et al. [2006] showed that such a model (individual and stochastic description of the mutation process plus the resident-mutant model) converges for very low values of the mutation probability. For this, the *canonical equation* of AD [Dieckmann and Law, 1996] describes the long term evolution of the phenotypic trait values characterizing a certain community in the limit of rare and infinitesimal mutations.

The AD canonical equation is an ODE system (one equation for each adaptive trait) that smoothly approximates the expected evolutionary dynamics of the phenotypes with respect to all possible realizations of the stochastic mutation process.

To derive the canonical equation is necessary to rely on the *invasion implies substitution theorem*, that has been proved [Geritz, 2005, Meszéna et al., 2005, Dercole and Rinaldi, 2008] in the following technical setting:

1. the spatial and physiological heterogeneity of the populations is not described, so that the resident-mutant model is composed by one equation for each population;

2. stationary coexistence of the resident populations;

3. the community is composed of

   (a) a single resident population characterized by independent mutations on different traits, or

   (b) different resident populations characterized by independent mutations in a single trait each.

However, the conditions under which the theorem holds are not met close to the equilibria of the canonical equation. For this, when such an evolutionary equilibrium is approached, a further analysis of the resident-mutant model is necessary. Specific analytic conditions exist to assess if the resident-mutant coexistence is possible and, if so, when the initially similar traits experience disruptive selection and, thus, tend to diversify. In this case, the evolutionary equilibrium is a *branching point*: the mutant population coexists with the resident on the demographic timescale and their similar traits diverge on the evolutionary timescale following a higher-dimensional canonical equation (see Paragraph 1.2.4 and Geritz et al. [1997, 1998]). In such a way, an initially monomorphic population turns into a dimorphic one, thus increasing the biodiversity of the community.

In summary, evolutionary trajectories produced by the canonical equation of AD can lead to stationary evolutionary regimes (that can be either terminal or branching points), non-stationary evolutionary regimes (cyclic or chaotic) or to evolutionary extinctions.

2.2 Evolving community

To introduce the AD approach, reference is made to a community composed of different resident populations, whose individuals are characterized by a single adaptive continuous phenotypic trait. This trait can be described by a real variable mapped to the actual phenotypic values through a suitable transformation (eventually nonlinear). In this way it is possible to consider the traits as adimensional variables.

Each population is a homogeneous group of individuals of the same species and with the same trait value. Some of the resident populations can be conspecific, but characterized by different forms or *morphs*, i.e., different trait values. Species with a single morph are called *monomorphic*, while species with different morphs are called *polymorphic* (*dimorphic* in the case of two forms). For this reason, monomorphic species are represented by a single population, while polymorphic species are composed of different populations, one for each morph.

The evolutionary dynamics is the result of a process of innovations (i.e., the mutations), that introduces new populations in the community, and by a process of competition (i.e., selection), that rules the dynamics of the community on the demographic timescale. Darwin first argued that the better adapted populations to survive and reproduce would have dominated the community, and called *natural selection* the demographic process that lead to the dominance of the better fitted population (see Chapter 1).

Natural selection is described by deterministic population models, with no spatial or physiological details. In this way all the individuals of a population are identical and uniformly distributed in a homogeneous habitat, so that each population is completely described by its abundance and by the value of the phenotypic trait of its individuals.

Mutations are assumed to affect the value of a single trait. The mutant population is then characterized by the same trait of the resident population, but with a slightly different value. After each mutation, the mutant population has a very low density, but has the potential to invade and replace the resident group. Since mutations are very rare on the demographic timescale, selection takes its time to act on the community and lead it to its regime, thus defining the new resident group. It is thus possible to focus on the effects of a single mutation at a time (even if this assumption can be relaxed [Meszéna et al., 2005]).

The notation that is used in the present chapter to describe the

AD approach is now introduced. The focus is on the trait affected by the mutation, which is indicated with x for the residents and with x' for the mutants. Residents and mutants abundance is indicated with n and n', respectively, while all other resident traits and abundances are packed in vectors X and N, respectively.

2.3 Resident-mutant model

The demography of the coevolving populations is ruled by the interactions of the single individuals with the surrounding environment, both the abiotic and the abiotic component. The biotic component is the community of interacting populations, represented by the resident and mutant abundances n, N, and n', and by a set of demographic parameters that can in turn depend on the phenotypic traits of the individuals.

The growth rates $\dot{n}$, $\dot{n}'$, and $\dot{N}$ are thus a function of all abundances n, n', and N, and all traits x, x', and X, as well as of all other constant demographic and environmental parameters that will not be explicitly indicated for brevity. Since populations are composed of identical individuals, the common practice is to define the growth rate of the population when its abundance is the unit, i.e., the per-capita growth rate.

Let's indicate the per-capita growth rate $\dot{n}/n$ of the focus resident population with $f(n, n', N, x, x', X)$. This per-capita growth rate is the difference between the per-capita birth rate and the per-capita death rate, that is,

$$f(n, n', N, x, x', X) = b(n, n', N, x, x', X) - d(n, n', N, x, x', X),$$

where $b(n, n', N, x, x', X)$ and $d(n, n', N, x, x', X)$ are the per-capita birth and death rates, respectively.

From functions b, d and f for the resident population, we can easily obtain the same functions for the mutant population. Residents and mutants are indeed conspecific individuals that differ only in the value of a single trait, so they are involved in the same intra- and inter-specific demographic and environmental interactions of the residents. In other words, each of the two populations can be considered as the mutant if the other is the resident and viceversa. It is thus sufficient to exchange the arguments of the functions, obtaining $b(n', n, N, x', x, X)$, $d(n', n, N, x', x, X)$, and $f(n', n, N, x', x, X)$.

As for the other resident populations, we can indicate their growth rates with vector $F(n, n', N, x, x', X)$. In this way, the demographic

dynamics of the community are described by the following equations:

$$\begin{aligned} \dot{n} &= nf(n, n', N, x, x', X) \\ \dot{n}' &= n'f(n', n, N, x', x, X) \\ \dot{N} &= F(n, n', N, x, x', X), \end{aligned} \tag{2.1}$$

in which the abundances n, n', and N are the state variables while the traits x, x', and X are constant parameters. Model (2.1) is the *resident-mutant model*.

At this point it is important to highlight some properties of functions f and F which are important for the study of the resident-mutant model (2.1). Recall that functions f and F give, by definition, the per-capita growth rate of population n and the growth rates of populations N, respectively.

P1 If the second argument vanishes, f and F cannot depend on the fifth argument, since the growth rate of a population cannot be influenced by the trait of an absent population, so that

$$\begin{aligned} f(n, 0, N, x, x', X) &= f(n, 0, N, x, \cdot, X) = f^{\mathrm{R}}(n, N, x, X) \\ F(n, 0, N, x, x', X) &= F(n, 0, N, x, \cdot, X), \end{aligned} \tag{2.2}$$

where the $(\cdot)$ notation stands for any trait value and the R-superscript stands for resident. By contrast, if n vanishes in f, the growth rate is still influenced by x, since the potential growth of a new population depends on its trait (analogously for F).

P2 A second property of f and F refers to the case of two identical resident and mutant populations, i.e., characterized by the same trait value $x = x'$. Actually, only one population exists, characterized by trait x and abundance $n + n'$, so that its per-capita growth rate and the growth rates of the other populations in N are

$$\begin{aligned} &f(n + n', 0, N, x, \cdot, X) \\ &F(n + n', 0, N, x, \cdot, X). \end{aligned}$$

Indeed, if one would divide the population into two subpopulations with abundances n and n' would obtain

$$\begin{aligned} (\dot{n} + \dot{n}')\Big|_{x'=x} &= nf(n, n', N, x, x, X) + n'f(n', n, N, x, x, X) \\ &= (n + n')f(n + n', 0, N, x, \cdot, X), \end{aligned}$$

that implies that the two subpopulations have the same per-capita growth rate, in particular

$$f(n, n', N, x, x, X) = f(n', n, N, x, x, X)$$

for each value of n and n', or, equivalently,

$$f(n, n', N, x, x, X) = f((1-\alpha)(n+n'), \alpha(n+n'), N, x, x, X) \tag{2.3}$$

for $0 \leq \alpha \leq 1$. And analogous results hold for function F.

P3 Moreover, for function F we have

$$F(n, n', N, x, x', X) = F(n', n, N, x', x, X), \tag{2.4}$$

since the growth rate of a resident population interacting with two other conspecific populations cannot depend on their order.

When no mutants are present, the resident-mutant model (2.1) becomes the *resident model*

$$\begin{aligned} \dot{n} &= nf(n, 0, N, x, \cdot, X) = nf^{\mathrm{R}}(n, N, x, X) \\ \dot{N} &= F(n, 0, N, x, \cdot, X), \end{aligned} \tag{2.5}$$

that identifies the demographic attractor of the resident populations dynamics before the appearance of the mutant population. Assuming that for suitable values of the traits x and X model (2.5) has a stable positive equilibrium, the abundances of the resident populations are constant and indicated with

$$n = \bar{n}(x, X) \quad \text{and} \quad N = \bar{N}(x, X), \tag{2.6}$$

defined by

$$\begin{aligned} f(\bar{n}(x, X), 0, \bar{N}(x, X), x, \cdot, X) &= 0 \\ F(\bar{n}(x, X), 0, \bar{N}(x, X), x, \cdot, X) &= 0. \end{aligned} \tag{2.7}$$

This is sometimes referred to as *the principle of selective neutrality of the residents*. It is also assumed that equilibrium (2.6) is the only positive attractor of the resident model (2.5) on which the resident populations can coexist. This assumption, that is not necessary but greatly simplifies the explanation, can be relaxed [Dieckmann and Law, 1996]. In this way, the evolutionary dynamics of the community can be defined only in the open set χ of the trait space (x, X) in

which equilibrium (2.6) exists. The set χ is called *evolution set* of the community (see Paragraph 2.1).

Equilibrium (2.6) is a fixed point in the demographic space (n, N) that is stable and positive for each $(x, y) \in \chi$, while crossing the boundary of χ it loses at least one of its properties (existence, stability, and/or positivity). More precisely, equilibrium (2.6) can disappear colliding with a positive *saddle*, lose stability giving rise to a small limit cycle, or lose positivity (and stability) crossing one of the faces of the demographic state space (n, N). Since such faces are *invariants* of the resident model (2.5), the only way for equilibrium (2.6) to cross one of them is through the collision with a saddle lying on the face. Technically, all the above mentioned cases are *bifurcations*, and can thus be revealed from the study of the eigenvalues of the *Jacobian matrix* of model (2.5), evaluated at equilibrium (2.6), i.e.,

$$J^{\mathrm{R}}(x, X) = \left[\begin{matrix} n\frac{\partial}{\partial n} f & n\frac{\partial}{\partial N} f \\ \frac{\partial}{\partial n} F & \frac{\partial}{\partial N} F \end{matrix} \right] \Bigg|_{\substack{n=\bar{n}(x,X), n'=0 \\ N=\bar{N}(x,X)}} \tag{2.8}$$

Since equilibrium (2.6) is stable, the real part of the eigenvalues of matrix (2.8) is negative for $(x, y) \in \chi$. When a bifurcation occurs, the real part of at least one of such eigenvalues vanish.

2.4 Invasion (generically) implies substitution

In the present paragraph competition between resident and mutant populations is studied. In particular, we look for the conditions under which the mutant population spreads in the community (*invasion*) and substitutes the resident population (*substitution*), thus entailing a small step (from x to x') in the evolution of the trait affected by the mutation. The obtained conditions (for a deterministic demographic model such as the resident-mutant model (2.1)) are valid only if the mutant population, initially with a very low abundance, escapes the mechanisms of accidental extinction. If otherwise, even when the conditions are met, the mutant population would disappear leaving the trait unchanged. However, the effects of accidental extinction will be discussed in Paragraph 2.5.

Just before a mutation, the resident populations are, by assumption, at equilibrium (2.6) of the resident model (2.5). Just after the mutation, the resident and the mutant populations are, thus, close to the equilibrium

$$(n, n', N) = (\bar{n}(x, X), 0, \bar{N}(x, X)) \tag{2.9}$$

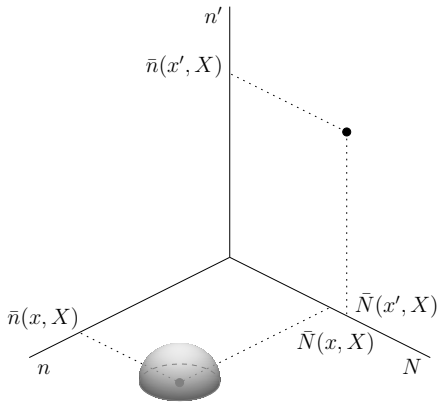

Figure 2.1: The demographic resident-mutant state space (n, n', N) in three dimensions. Just after the mutation, the state of the resident-mutant model (2.1) is close to equilibrium (2.9) (shaded region). Equilibrium (2.11) is also shown (reproduced from Dercole and Rinaldi [2008]).

of the resident-mutant model (2.1) (shaded region in Figure 2.1).

The faces $n = 0$ and $n' = 0$ of the demographic state space (n, n', N) are invariants of the resident-mutant model (2.1). In particular, on the face $n' = 0$ model (2.1) degenerates into the resident model (2.5), while on the face $n = 0$ it reduces to

$$\begin{aligned} \dot{n}' &= n' f(n', 0, N, x', \cdot, X) = n' f^{\mathrm{R}}(n', N, x', X) \\ \dot{N} &= F(n', 0, N, x', \cdot, X), \end{aligned} \tag{2.10}$$

that, using property P3 (equation (2.4)), is simply model (2.5) with n and x replaced by n' and x'. In this way, if $(x', y) \in \chi$, the equilibrium

$$(n', N) = (\bar{n}(x', X), \bar{N}(x', X))$$

is the only stable and positive equilibrium of model (2.10) and its eigenvalues are those of the Jacobian matrix $J^{\mathrm{R}}(x', X)$ obtained from (2.8) substituting x with x'. Moreover, point

$$(n, n', N) = (0, \bar{n}(x', X), \bar{N}(x', X)) \tag{2.11}$$

shown in Figure 2.1, is another equilibrium of the resident-mutant model (2.1).

Stability of equilibrium (2.9) can be studied through linearization. It is easy to show [Dercole and Rinaldi, 2008] that the Jacobian matrix

of the resident-mutant model (2.1) evaluated at equilibrium (2.9) is given by

$$J(x,x',X) = \begin{bmatrix} J^{\mathrm{R}}(x,X) & \cdots \\ 0 & f(0,\bar{n}(x,X),\bar{N}(x,X),x',x,X) \end{bmatrix}. \quad (2.12)$$

Due to the triangular structure of matrix (2.12), the eigenvalues of equilibrium (2.9) are those of the matrix $J^{\mathrm{R}}(x,X)$ (which has negative real part by assumption) and the eigenvalue

$$\lambda(x,x',X) = f(0,\bar{n}(x,X),\bar{N}(x,X),x',x,X), \quad (2.13)$$

that is, the per-capita growth rate of a mutant population with very low abundance. If this eigenvalue is positive, the abundance of this mutant population will increase, so that the mutants will invade the community. For this reason, $\lambda(x,x',X)$ is called *invasion eigenvalue*.

The invasion eigenvalue gives the initial per-capita growth rate of the scarce mutant population appearing in the community. This quantity has been traditionally called *invasion fitness* (or, simply, *fitness*, see Paragraph 1.2.3) of the mutant population and function (2.13) will often be called *fitness function*. A positive fitness characterize mutations that brings some advantages to the mutants, in terms of survival, reproductive success, or in the competition with the resident individuals, while negative values of the fitness are associated to disadvantageous mutations. In the same way, the eigenvalues of equilibrium (2.11) are those of the matrix $J^{\mathrm{R}}(x',X)$ and the invasion eigenvalue is $\lambda(x',x,X)$. To conclude, since matrices $J^{\mathrm{R}}(x,X)$ and $J^{\mathrm{R}}(x',X)$ has negative real-part eigenvalues (see Paragraph 2.3), the stability of equilibria (2.9) and (2.11) is only related to the sign of the invasion eigenvalues.

It is important to notice that $\lambda(x,x,X) = 0$. In fact, if the resident and the mutant populations are identical ($x = x'$), we can use properties P2 (equation (2.3) with $\alpha = 0$), P1 (equation (2.2)), and the resident equilibrium condition (2.7) to obtain

$$\begin{aligned} \lambda(x,x,X) &= f(0,\bar{n}(x,X),\bar{N}(x,X),x,x,X) \\ &= f(\bar{n}(x,X),0,\bar{N}(x,X),x,\cdot,X) = 0. \end{aligned} \quad (2.14)$$

Moreover, using properties P2 and P3, we obtain that

$$\begin{aligned} f((1-\alpha)\bar{n}(x,X),\alpha\bar{n}(x,X),\bar{N}(x,X),x,x,X) = 0 \\ F((1-\alpha)\bar{n}(x,X),\alpha\bar{n}(x,X),\bar{N}(x,X),x,x,X) = 0 \end{aligned}$$

for all $0 \leq \alpha \leq 1$, i.e., all points

$$(n, n', N) = ((1-\alpha)\bar{n}(x, X), \alpha\bar{n}(x', X), (1-\alpha)\bar{N}(x, X) + \alpha\bar{N}(x', X)) \tag{2.15}$$

of the segment connecting the two equilibria (2.9) and (2.11) are equilibria of the resident-mutant model (2.1) when $x' = x$. All these equilibria are neutrally stable because they have a zero eigenvalue ($\lambda(x, x, X)$) while all the other eigenvalues are those of the Jacobin matrix $J^{\mathrm{R}}(x, X)$.

Moreover, the invasion eigenvalues $\lambda(x, x', X)$ and $\lambda(x', x, X)$ usually have opposite sign, so that, if equilibrium (2.9) is stable, equilibrium (2.11) will be unstable, and viceversa. In fact, for each value of X, function $\lambda(x, x', X)$ vanishes for $x' = x$. This implies that, excluding non-generic cases,

$$\frac{\partial}{\partial x'}\lambda(x, x', X)\bigg|_{x'=x} \neq 0,$$

so that function $\lambda(x, x', X)$ has opposite sign for $x' > x$ and $x' < x$ (with x' close to x).

Looking at the eigenvectors of the Jacobian matrix $J(x, x', X)$ it is possible to exploit again its triangular structure (see (2.12)) and conclude that all eigenvectors of $J^{\mathrm{R}}(x, X)$, that lie in the space (n, N), become eigenvectors of $J(x, x', X)$ simply adding the component $n' = 0$. By contrast, the eigenvector associated to the invasion eigenvalue $\lambda(x, x', X)$ (called invasion eigenvector) is almost aligned with the segment (2.15) and tends to it for x' tending to x (as in Figure 2.2).

Expanding $\lambda(x, x', X)$ in Taylor series around $x' = x$ up to first order we obtain

$$\lambda(x, x', X) \approx \frac{\partial}{\partial x'}\lambda(x, x', X)\bigg|_{x'=x}(x' - x), \tag{2.16}$$

that is positive if

$$\frac{\partial}{\partial x'}\lambda(x, x', X)\bigg|_{x'=x} > 0 \qquad \text{and} \qquad x' > x$$

or if

$$\frac{\partial}{\partial x'}\lambda(x, x', X)\bigg|_{x'=x} < 0 \qquad \text{and} \qquad x' < x.$$

In this case equilibrium (2.9) is unstable while equilibrium (2.11) is stable. Conversely, if $\lambda(x, x', X)$ is negative equilibrium (2.9) is stable while equilibrium (2.11) is unstable (see Figure 2.2). Moreover,

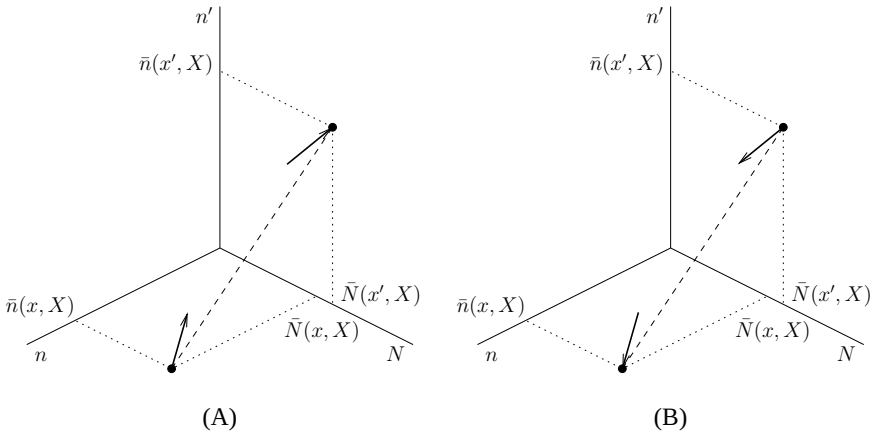

Figure 2.2: Stability of equilibria (2.9) and (2.11) of the resident-mutant model (2.1). (A) Positive (2.16): equilibrium (2.9) is unstable while equilibrium (2.11) is stable. (B) Negative (2.16): equilibrium (2.9) is stable while equilibrium (2.11) is unstable. Arrows point in the direction of the resident-mutant dynamics along the invasion eigenvector (dashed segment (2.15)) (reproduced from Dercole and Rinaldi [2008]).

trajectories quickly approaches the invasion eigenvector and follow it approaching or leaving the equilibrium depending on its stability.

Up to now we showed, through linearization, that, if the first order term (2.16) in the fitness Taylor expansion is positive, the mutant population invades, while if (2.16) is negative the mutants go extinct. But proving that invasion implies substitution is not possible through a local analysis of the resident-mutant model (2.1), but, in principle, a global study is necessary. The fact that invasion implies substitution has been assumed as true since the first formulation of the canonical equation of AD [Dieckmann and Law, 1996] and even before (in the fitness landscape approaches, see Paragraph 1.3). Such assumption, called *invasion implies substitution principle*, has been proved and became a theorem [Geritz, 2005, Meszéna et al., 2005, Dercole and Rinaldi, 2008, Dercole and Geritz, 2014]. The proof is given under the same assumptions made so far, namely:

1. $(x, X) \in \chi$;

2. x' close to x;

3. equation (2.16) positive;

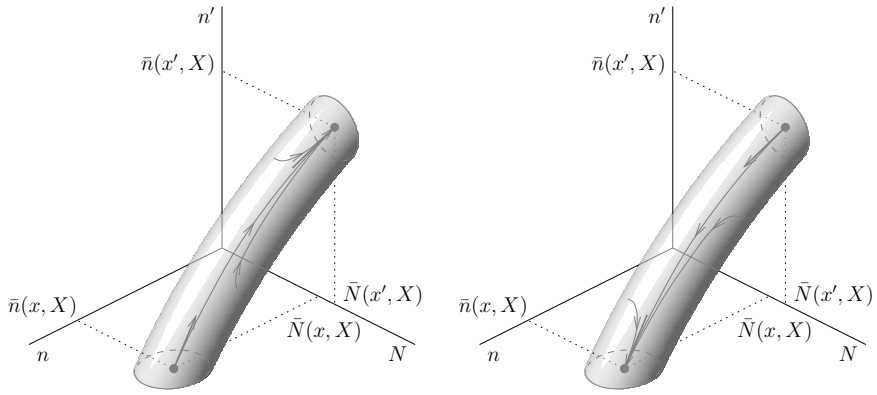

Figure 2.3: Invasion implies substitution (reproduced from Dercole and Rinaldi [2008]).

4. initial condition of the invasion transient close to equilibrium (2.9) (see Figure 2.1).

The first two conditions guarantee that there exist an invariant tube [Geritz et al., 2002] connecting equilibrium (2.9) and (2.11) (see Figure 2.3). If the third condition is true, all trajectories starting from the inside of the tube converge to equilibrium (2.11), implying the substitution. If, otherwise, the third condition is not met (equation (2.16) is negative), trajectories converge to equilibrium (2.9), implying the extinction of the mutant population.

2.5 The canonical equation of AD

In this paragraph we discuss the derivation of the AD canonical equation, that describes the evolution of each trait x characterizing the community with the Ordinary Differential Equation

$$\dot{x} = \frac{1}{2}\mu(x)\sigma^2(x)\bar{n}(x, X)\frac{\partial}{\partial x'}\lambda(x, x', X)\Big|_{x'=x}, \tag{2.17}$$

where the time refers to the evolutionary timescale and $\mu(x)$ and $\sigma(x)$ are the probability that a newborn individual is a mutant and the standard deviation of the mutational step $x' - x$, respectively. Moreover,

$$k(x) = \frac{1}{2}\mu(x)\sigma^2(x)$$

is often called *mutation rate* and describe the statistics of the mutational process.

The evolution of each trait is the result of a sequence of advantageous mutations after which the mutant population substitutes the resident one, thus becoming itself the new resident population. The Adaptive Dynamics transforms this step-by-step process into a continuous process described by the canonical equation under the assumption of rare and small mutations.

In this way, x' can be considered close to x and the resident populations are at their demographic equilibrium (2.6) when the mutation occurs. The initial state of the resident-mutant model (2.1) just after the mutation is, thus, inside the tube in Figure 2.3. From Paragraph 2.4 follows that if

$$\frac{\partial}{\partial x'}\lambda(x, x', X)\Big|_{x'=x} \tag{2.18}$$

is positive (resp., negative) the mutant population characterized by trait $x' > x$ (resp., $x' < x$) will replace the resident population, while mutations characterized by $x' < x$ (resp., $x' > x$) will go extinct on the demographic timescale, leaving the community unchanged.

Equation (2.18) measures the selective pressure acting on trait x, selecting greater (resp., smaller) values if positive (resp., negative) and, for this reason, it is called *selection derivative* or *selection gradient*. In other words, $\dot{x}$ has the same sign of equation (2.18), so that the dynamics of the traits are ruled by the sign of (2.18).

As already mentioned in Paragraph 2.1, evolution is a stochastic process mainly based on two forms of stochasticity: the mutation process and the demographic stochasticity, i.e., the fact that even advantageous mutations (with the same sign of (2.18)) might not be able to invade, since the mutant individuals are initially very scarce and, thus, face the risk of accidental extinction. In this way, a deterministic description of the evolution rate $\dot{x}$ can be interpreted as the average of all the possible realizations of the mutation and of the demographic stochasticity processes, that is,

$$\dot{x} = \lim_{dt\to 0} \frac{E[x(t+dt) - x(t)]}{dt}, \tag{2.19}$$

where $E[\cdot]$ is the standard expected value operator and t refers to the evolutionary timescale.

Denoting with

$$P(x, x', X, dt)dx' \tag{2.20}$$

the probability that a community characterized by traits (x, X) at time t will be characterized by traits in (x', X) and $(x' + dx', X)$ at time $t + dt$, we can writhe equation (2.19) as

$$\dot{x} = \lim_{dt \to 0} \frac{1}{dt} \int_{-\infty}^{+\infty} (x' - x) P(x, x', X, dt) dx'. \tag{2.21}$$

To explicitly compute the integral in (2.21), it is necessary to assess the probability (2.20), that is the product of three probabilities, namely:

- the probability that a mutation occurs in the infinitesimal time step $[t, t + dt]$;
- the probability that the mutant trait is between x' and $x' + dx'$;
- the probability that mutant individuals escape the risk of accidental extinction and substitute the resident population.

It is possible to show [Dercole and Rinaldi, 2008] that computing all these probabilities and substituting them into equation (2.21) leads to equation (2.17).

2.6 A schematic summary

Figure 2.4 schematically summarizes the Adaptive Dynamics approach and emphasizes the relationships between the three introduced models: the resident-mutant model (2.1), the resident model (2.5), and the canonical equation (2.17). Notice that the resident-mutant model and the mutation statistics are the main source of information for the canonical equation.

Given an ancestral condition $(x(0), X(0)) \in \chi$, the canonical equation (2.17) describes the evolutionary trajectory $(x(t), X(t))$, with $t > 0$, followed by the traits characterizing the community. Along this evolution, the demographic equilibrium (2.6) of the resident model (2.5) is entrained on the evolutionary timescale by the variation of the traits.

2.7 Evolutionary state portraits

The canonical equation (2.17) is a time-continuous dynamical system whose trajectories are defined in the evolution set χ and in which the state variables are the phenotypic traits characterizing the evolving

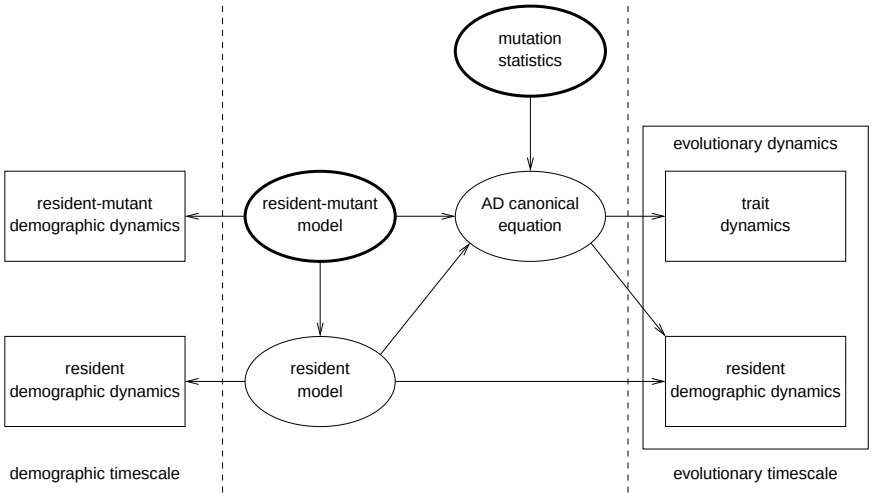

Figure 2.4: Schematic summary of the relationships between the resident-mutant model (2.1), the resident model (2.5), the mutation statistics, the canonical equation (2.17) of Adaptive Dynamics, and the respective demographic and evolutionary dynamics (reproduced from Dercole and Rinaldi [2008]).

community. Moreover, the canonical equation is typically nonlinear, so the evolutionary dynamics will be as complex as the nonlinear dynamics typically are. The attractors of the canonical equation, called *evolutionary attractors*, can thus be evolutionary equilibria, as well as evolutionary cycles, tori, and strange attractors, provided the number of adaptive traits are in sufficient number (in particular, at least two for cycles and at least three for tori and strange attractors). Evolutionary equilibria, cycles, tori, and strange invariants can also be unstable (saddles or repellers) and the evolutionary dynamics can be characterized by multiple invariants, e.g., multiple attractors, whose basins of attraction are separated by stable manifolds of evolutionary saddles, in which case the regime evolutionary dynamics is dependent from the ancestral conditions. The set of all trajectories of the canonical equation (2.17), one for each ancestral condition in the evolution set χ, gives the so-called *evolutionary state portrait*. Obviously, they are very useful graphical representations of the dynamics when the trait space is at most three-dimensional, and the maximum of their efficacy is in the two-dimensional case, when are typically shown the boundary of the evolution set χ, the invariants and some significant trajectory from which all others can be deducted.

Figure 2.5 shows an example of a two-dimensional evolutionary

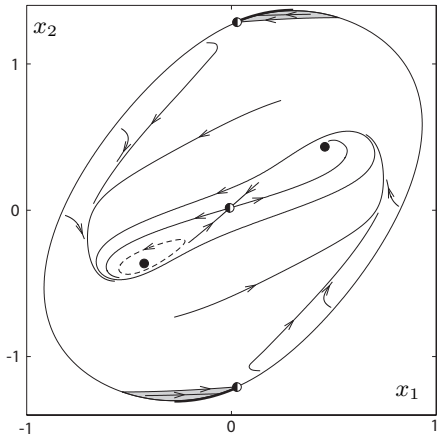

Figure 2.5: Example of evolutionary state portrait. Filled points: stable evolutionary equilibria. Half-filled points: evolutionary saddles. Closed trajectories: stable evolutionary cycles. Closed dotted trajectories: unstable evolutionary cycles. White regions: viable set, i.e., long term persistence set. Grey regions: unviable set, i.e., long term extinction set. Thick segments: extinction segments (reproduced from Dercole and Rinaldi [2008]).

state portrait, relative to a prey-predator community [Dercole et al., 2003]. Notice that the evolution set χ is bounded, since extreme values of the traits typically are unfeasible with the coexistence of the interacting resident populations.

Evolutionary equilibria are points in the trait space where all the selection derivatives (2.18) (one for each trait) vanish for all resident traits x and X characterizing the community. When such points are approached, the canonical equation is no more justified, since the invasion implies substitution theorem does not guarantee anymore that the mutant population that invades escaping accidental extinction will actually replace the resident population. For this reason, in the neighborhood of an evolutionary equilibrium, a deeper analysis of the resident-mutant model (2.1) is necessary (see Chapter 3).

From Figure 2.5 it is also possible to notice that evolutionary trajectories can tend toward the boundary of the evolution set χ. On such boundary the (demographic) equilibrium abundance of at least one population vanish (in this case the predator abundance), so the evolutionary trajectories approach the boundary horizontally, since $\dot{x}_2$ is zero ($\bar{n}_2(x_1, x_2) = 0$, see equation (2.17)). In this way the equilibrium abundance of the resident predator gradually vanish

while the evolutionary trajectory is approaching such boundary. In other words, the evolution of the predator population slows down and the boundary of the evolution set is reached (in finite time) due to the evolution of the other resident population (the prey population). When the boundary is reached the predator goes extinct, so that the the prey acts as murder (see Paragraph 1.2.5, evolutionary murder). By contrast, without murders, evolutionary extinction would have occurred asymptotically (see Paragraph 1.2.5, evolutionary runaway).

In any case, reaching the boundary of the evolution set χ leads to the evolutionary extinction of one or more resident populations. After an evolutionary extinction, if the remaining resident populations coexist at a demographic equilibrium, the evolutionary dynamics of the community follows a canonical equation with a reduced dimension, since the traits of the extinct populations have been lost.

To conclude, it is possible to partition the evolution set χ in a subset of ancestral conditions that gives rise to a trajectory that will always remain in χ, called *viable set*, and in another subset of ancestral conditions that lead to an evolutionary extinction, called *unviable set* (see Figure 2.5). The segments of the boundary in the unviable set on which extinction occurs are called *extinction segments*. In each point of an extinction segment the vector $(\dot{x}_1, \dot{x}_2)$ tangent to the evolutionary trajectory points outside the boundary of χ, so that the extremes of the extinction segments are points in which the tangent vector $(\dot{x}_1, \dot{x}_2)$ is either tangent to the boundary of χ (for this reason called *tangent points*) or vanish on an evolutionary equilibrium on the boundary of χ (see Figure 2.5). Another interesting geometric property is that the boundaries separating the viable from the unviable set are either evolutionary trajectories passing through a tangent point or stable manifolds of saddles on the boundary or inside χ (see Figure 2.5).

Chapter 3

Evolutionary branching

In this chapter we focus on the phenomenon of evolutionary branching, that is, the phenomenon through which diversity emerge in the AD framework. We first introduce a new more compact notation for the residents and mutants per-capita growth rate and then we focus on the branching conditions. In particular, we present the catalog of all possible dynamics around evolutionary equilibria, with particular emphasis on the possibility of dimorphic coexistence and subsequent evolutionary divergence. We then classify evolutionary equilibria with respect to their convergence and evolutionary stability and, finally, divide them into two classes, namely branching and terminal points. More details can be found in Dercole and Rinaldi [2008], on which this introduction to evolutionary branching is based.

3.1 The g-function

We start introducing a new and more compact notation for the description of the resident-mutant interactions. We initially consider two similar competing populations, with densities n and n' and characterized by one-dimensional traits (or strategies) x and x' very close to each other, coexisting with other resident populations, whose densities and traits are packed in vectors N and X, respectively. We consider x and x' as the resident and mutant traits, respectively. Their competition dynamics is described by the resident mutant model (see also equation (2.1))

$$\begin{aligned} \dot{n} &= ng(n, n', N, x, x', X, x) \\ \dot{n}' &= n'g(n, n', N, x, x', X, x') \\ \dot{N} &= F(n, n', N, x, x', X), \end{aligned} \tag{3.1}$$

where $g(n, n', N, x, x', X, y)$ is the so-called *generating fitness function* [Vincent and Brown, 2005], that gives the per-capita growth rate of a vanishing population with a "virtual" strategy y in an environment where strategies x and x' are present with densities n and n', respectively. Therefore, suitably evaluating g at densities (n, n') and traits (x, x') we obtain the per-capita growth rate of the two similar competing populations. E.g., we have that $g(n, n', N, x, x', X, x) = f(n, n', N, x, x', X)$ and $g(n, n', N, x, x', X, x') = f(n', n, N, x', x, X)$ (see Paragraph 2.3). From now on, we make arguments N and X implicit for notation convenience (see Dercole and Rinaldi [2008], Dercole [2014], Dercole and Geritz [2014], Dercole et al. [2014] and Paragraph 4.2.3.5 for analyses in the most general case). Here and in the rest of the thesis, we assume smoothness of the g-function and use lists of integer superscripts to indicate the order of differentiation and the position of the arguments w.r.t. which we take derivatives, e.g.,

$$\begin{aligned} g^{(1,0,0,0,0)}(n, n', x, x', y) &:= \tfrac{\partial}{\partial n} g(n, n', x, x', y), \\ g^{(1,1,0,0,0)}(n, n', x, x', y) &:= \tfrac{\partial^2}{\partial n n'} g(n, n', x, x', y), \\ g^{(2,0,0,0,0)}(n, n', x, x', y) &:= \tfrac{\partial^2}{\partial n^2} g(n, n', x, x', y). \end{aligned}$$

In the next chapter, consistency properties of the g-function, similar to those introduced in Paragraph 2.3 for functions f and F, plus a new property recently introduced by Dercole [2014], will be widely exploited for the study of the branching bifurcation.

If we now assume rare mutations, we can evaluate the (monomorphic) invasion fitness of the mutation as

$$\lambda_1(x, x') = g(\bar{n}(x), 0, x, \cdot, x'),$$

which is the per-capita growth rate of a very scarce mutant population characterized by trait x' competing with the resident population characterized by trait x and attained at its demographic equilibrium $\bar{n}(x)$ (see also equation (2.13)). Away from evolutionary singularities, the outcome of the competition is always the dominance of one of the two populations (the better fitted) and the extinction of the other. In this way, the trait follows a slow evolution led by a series of subsequent mutations and possible substitutions between residents and mutants, in the direction of a better performing (or fitted) trait. This evolutionary dynamics can be approximated in the limit of infinitesimal mutational steps by the one-dimensional AD canonical equation

$$\dot{x} = k(x)\bar{n}(x)\lambda_1^{(0,1)}(x, x),$$

where $k(x) = \frac{1}{2}\mu(x)\sigma^2(x)$ is the mutation rate scaling the speed of evolution and $\lambda_1^{(0,1)}(x,x) = g^{(0,0,0,0,1)}(\bar{n}(x), 0, x, \cdot, x)$ is the selection gradient (see also equations (2.17) and (2.18)).

3.2 The branching conditions

As already mentioned in Paragraphs 2.1 and 2.7, when the trait dynamics approaches an evolutionary equilibrium point $\bar{x}$, that is, a point in the evolution set χ at which all selection derivatives vanish, condition 3 of Paragraph 2.4 is no more valid, so that the invasion of a mutant population does not imply the substitution of the resident population. It is therefore necessary a deeper study of the resident-mutant model 3.1 and of the fitness function $\lambda_1(x, x')$ up to second order (see equation (2.16)). Under a certain condition, in the vicinity of evolutionary equilibria, a mutant population can invade and coexist with the resident populations, becoming a new resident population itself with a trait value initially very similar to that of the population in which the mutation occurred. At this point, the evolutionary dynamics of the community will be described by a new canonical equation, with an extra ODE for the new resident trait. Under a second condition, the traits of the two similar populations will experience disruptive selection and, thus, diverge on the evolutionary timescale, giving rise to the phenomenon of evolutionary branching (see Paragraph 1.2.4). It is now possible that the new enlarged system (with an extra trait) will again approach a stationary regime and that a new evolutionary branching will be possible. This possible branching cascade can lead to the increase of the diversity of the community, starting from a minimal diversity community (a single trait for each population, see Chapters 5 and 7). This is in line with the evolutionary idea that life developed from a common ancestor to the impressive biodiversity we observe today.

Technically speaking (see Geritz et al. [1998] and Dercole and Rinaldi [2008]), resident and mutant coexistence is possible for x and x' close to $\bar{x}$ if

$$\bar{\lambda}_1^{(1,1)} < 0, \tag{3.2}$$

where

$$\bar{\lambda}_1^{(i,j)} = \lambda_1^{(i,j)}(\bar{x}, \bar{x}) = \left.\frac{\partial^{(i+j)}}{\partial x^i x'^j}\lambda_1(x, x')\right|_{x=x'=\bar{x}}.$$

Condition (3.2) implies the existence of a region of coexistence in the strategy space (x, x') locally to $(\bar{x}, \bar{x})$, that is, a cone with ver-

tex centered in $\bar{x}$, in which the two strategies are mutually invadable ($\lambda_1(x, x') > 0$ and $\lambda_1(x', x) > 0$) and coexist at a positive demographic equilibrium. The boundaries of such region are the curves in the strategies space (x, x') where this dimorphic demographic equilibrium collides with one of the two boundary monomorphic equilibria, $(\bar{n}(x), 0)$ or $(0, \bar{n}(x'))$ (see also (2.9) and (2.11)). This is a transcritical bifurcation [Kuznetsov, 2004, Meijer et al., 2009] described by

$$\lambda_1(x, x') = 0 \tag{3.3}$$

when the dimorphic equilibrium collides with the boundary monomorphic equilibrium $(\bar{n}(x), 0)$, and by the same expression with x and x' reversed when the dimorphic equilibrium collides with the monomorphic equilibrium $(0, \bar{n}(x'))$. Geritz et al. [1997, 1998] showed that mutual invasibility occurs in the cone, whereas the existence of a unique stable equilibrium of coexistence has been only recently shown [Geritz, 2005, Meszéna et al., 2005, Dercole and Rinaldi, 2008, Dercole and Geritz, 2014].

Resident densities after coexistence are indicated with n_1 and n_2, while resident traits are denoted with x_1 and x_2, initially close to $\bar{x}$. Selection can be disruptive (favoring outer rather than intermediate phenotypes) thus leading to trait divergence in the new enlarged system if

$$\bar{\lambda}_1^{(0,2)} > 0. \tag{3.4}$$

This leads the two traits to diverge following two different series of mutant-resident substitutions in the two different branches. This diverging dynamics is ruled by a two-dimensional canonical equation. If we evaluate $g(n_1, n_2, x_1, x_2, x')$ at the demographic coexistence equilibrium $(\bar{n}_1(x_1, x_2), \bar{n}_2(x_1, x_2))$, with traits (x_1, x_2) initially close to the evolutionary equilibrium $\bar{x}$, we obtain the dimorphic fitness function

$$\lambda_2(x_1, x_2, x') = g(\bar{n}_1(x_1, x_2), \bar{n}_2(x_1, x_2), x_1, x_2, x'),$$

that is, the per-capita growth rate of a rare mutant population with trait x' appearing in an environment set by the two resident populations at their demographic equilibrium $(\bar{n}_1(x_1, x_2), \bar{n}_2(x_1, x_2))$. The dimorphic trait dynamics is ruled by the two-dimensional canonical equation

$$\dot{x}_i = k_i(x_i)\bar{n}_i(x_1, x_2)\lambda_2^{(0,0,1)}(x_1, x_2, x_i),$$

with $i = 1, 2$. Conditions (3.2) and (3.4) are called *branching conditions*.

3.2.1 The coexistence condition (3.2)

In this paragraph we consider the resident-mutant model (3.1) for trait values x and x' close to $\bar{x}$. As already done in Paragraph 2.4, we now study the sign of the fitness function.

Recalling the principle of selective neutrality of the residents (that is, the demographic equilibrium condition $g(\bar{n}(x), 0, x, \cdot, x) = 0$), we can write

$$\begin{aligned} &\lambda_1(x,x) = 0 \\ &\lambda_1^{(1,0)}(x,x) + \lambda_1^{(0,1)}(x,x) = 0 \\ &\lambda_1^{(2,0)}(x,x) + 2\lambda_1^{(1,1)}(x,x) + \lambda_1^{(0,2)}(x,x) = 0 \end{aligned} \tag{3.5}$$

(see also equation (2.14)), so that $\bar{\lambda}_1^{(1,0)}$ is null since the selection gradient $\bar{\lambda}_1^{(0,1)}$ vanishes at evolutionary equilibrium.

Thus, the sign of $\lambda_1(x,x')$ in a small neighborhood of $(\bar{x},\bar{x})$ is determined by second-order terms of the Taylor expansion

$$\begin{aligned} &\lambda_1(x,x') = \\ &\frac{1}{2}\bar{\lambda}_1^{(2,0)}(x-\bar{x})^2 + \bar{\lambda}_1^{(1,1)}(x-\bar{x})(x'-\bar{x}) + \frac{1}{2}\bar{\lambda}_1^{(0,2)}(x'-\bar{x})^2 + O(\|(x-\bar{x}, x'-\bar{x})\|^3). \end{aligned} \tag{3.6}$$

Recalling (3.5), we can substitute $\bar{\lambda}_1^{(2,0)} = -2\bar{\lambda}_1^{(1,1)} - \bar{\lambda}_1^{(0,2)}$ into (3.6) to obtain

$$\begin{aligned} &\lambda_1(x,x') = \\ &\quad \frac{1}{2}\Big(\big(-2\bar{\lambda}_1^{(1,1)} - \bar{\lambda}_1^{(0,2)} \big)(x-\bar{x}) - \bar{\lambda}_1^{(0,2)}(x'-\bar{x}) \Big)(x-x') \\ &\qquad\qquad + O(\|(x-\bar{x}, x'-\bar{x})\|^3). \end{aligned} \tag{3.7}$$

Thus, $\lambda_1(x,x')$ changes sign when $x' = x$ and when $x' - \bar{x} = \tan\theta_{\mathrm{T}2}(x - \bar{x})$, with

$$\theta_{\mathrm{T}2} = \arctan\left(-2\frac{\bar{\lambda}_1^{(1,1)}}{\bar{\lambda}_1^{(0,2)}} - 1 \right),$$

where the subscript T stands for "Transcritical" and the 2 tells that population 2, i.e., the mutant, goes extinct at the bifurcation. The reason for this choice will be clear reading Chapter 4.

There are therefore two curves in the (x,x') plane passing through the equilibrium point $(\bar{x},\bar{x})$, with slope $\pi/4$ and $\theta_{\mathrm{T}2}$, along which $\lambda_1(x,x') = 0$. These two curves are obviously the diagonal $x' =$

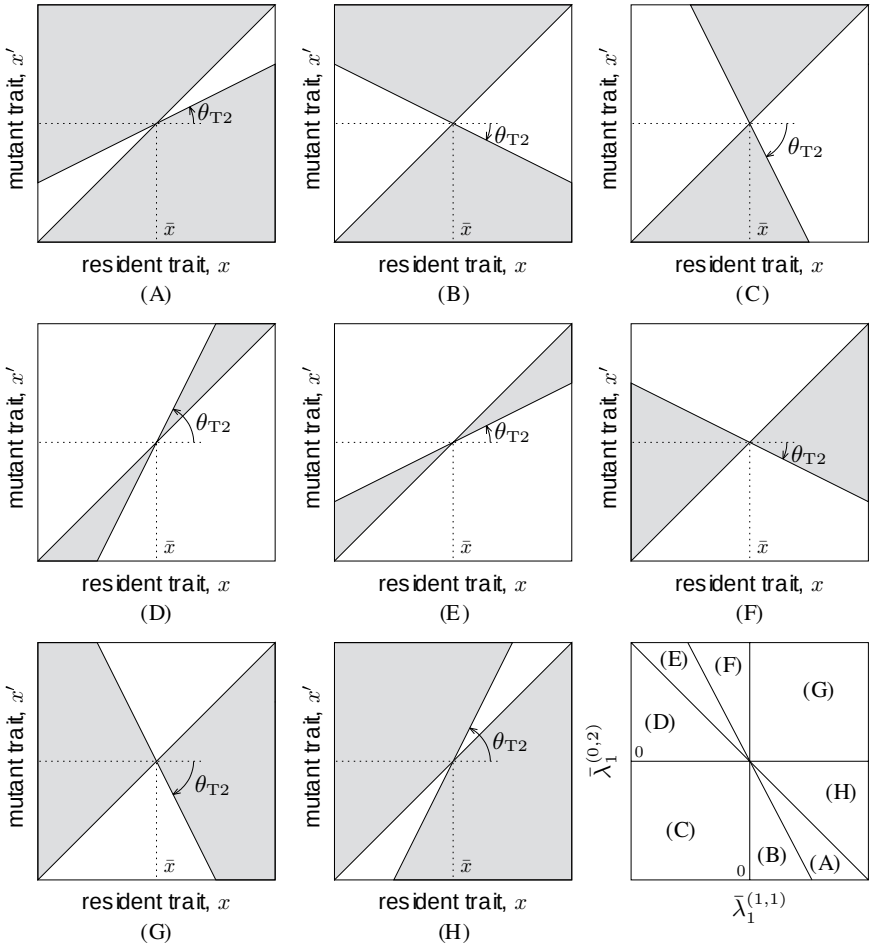

Figure 3.1: Classification of evolutionary equilibria $\bar{x} \in \chi$. Panels A-H show the sign of the fitness $\lambda_1(x, x')$ (white: positive; gray: negative) in a small neighborhood of $(\bar{x}, \bar{x})$ in the (x, x') plane and corresponds to cases A-H in the last panel (reproduced from Dercole and Rinaldi [2008]).

x and the transcritical bifurcation curve (described in the previous paragraph and defined by (3.3)) approximated with a straight line, and they partition the neighborhood of $(\bar{x}, \bar{x})$ into four regions: in two of them $\lambda_1(x, x')$ is positive, while in the other two it is negative.

As shown in Figure 3.1 (see also Geritz et al. [1998]), it is possible to distinguish eight qualitatively different cases, identified by different inequalities among the second derivatives of the fitness shown in the last panel. For example, the anti-diagonal $\bar{\lambda}_1^{(0,2)} = -\bar{\lambda}_1^{(1,1)}$ in the

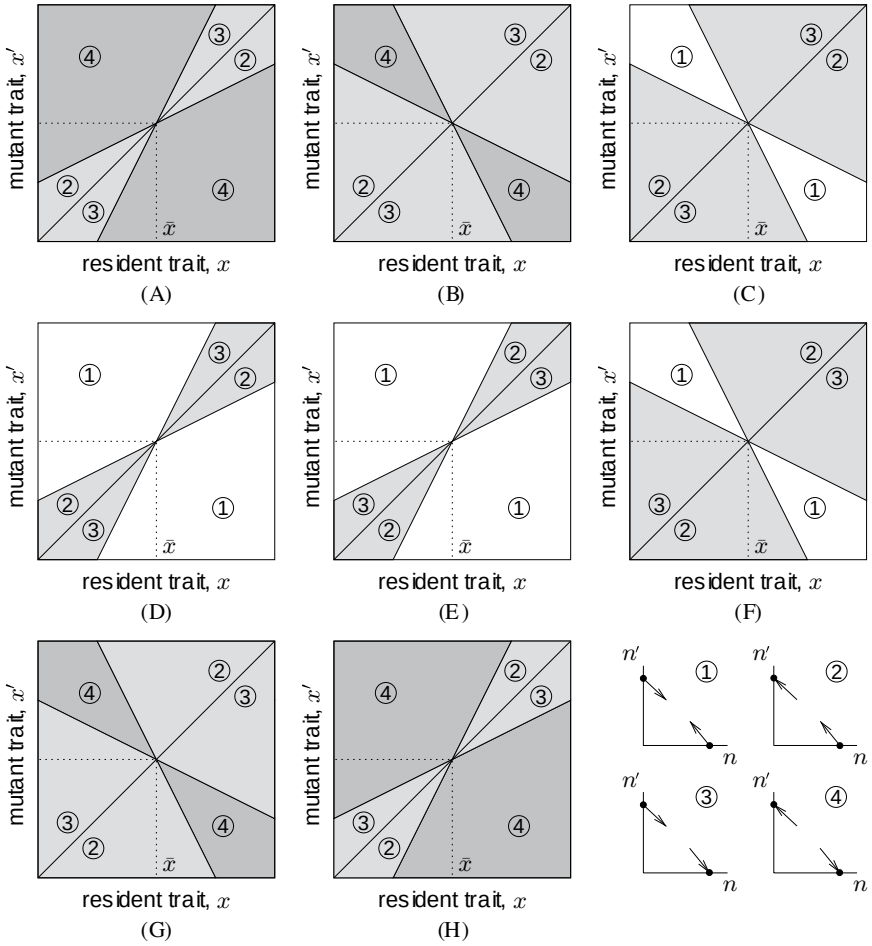

Figure 3.2: Classification of evolutionary equilibria $\bar{x} \in \chi$. Panels A-H show the sign of the invasion eigenvalues $\lambda_1(x, x')$ (positive in regions ① and ②; negative in regions ③ and ④) and $\lambda_1(x', x)$ (positive in regions ① and ③; negative in regions ② and ④) in a small neighborhood of $(\bar{x}, \bar{x})$ in the (x, x') plane and corresponds to cases A-H in the last panel of Figure 3.1. As shown in the last panel, equilibria $(\bar{n}(x), 0)$ and $(0, \bar{n}(x'))$ of the resident-mutant model 3.1 are both unstable (resp., stable) in region ① (resp., ④), while $(\bar{n}(x), 0)$ is unstable (resp., stable) and $(0, \bar{n}(x'))$ stable (resp., unstable) in region ② (resp., ③) (reproduced from Dercole and Rinaldi [2008]).

last panel corresponds to $\theta_{\mathrm{T2}} = \pi/4$, the line $\bar{\lambda}_1^{(0,2)} = -2\bar{\lambda}_1^{(1,1)}$ corresponds to $\theta_{\mathrm{T2}} = 0$, while the vertical axis $\bar{\lambda}_1^{(1,1)} = 0$ corresponds to $\theta_{\mathrm{T2}} = -\pi/4$. Panels A-H show the sign of the fitness $\lambda_1(x, x')$ in a

small neighborhood of $(\bar{x}, \bar{x})$ in the (x, x') plane. White (resp., gray) regions indicate positive (resp., negative) values of $\lambda_1(x, x')$. On the boundaries of such regions $\lambda_1(x, x') = 0$.

In the AD jargon, diagrams A-H are called *pairwise invasibility plots* (PIPs) [Metz et al., 1996]. A PIP gives information on the invasion of the mutant population: if the point (x, x') falls in a white (resp., gray) region, then the invasion eigenvalue $\lambda_1(x, x')$ is positive (resp., negative) and the mutant population invades (resp., goes extinct), so that equilibrium $(\bar{n}(x), 0)$ of the resident-mutant model (3.1) is unstable (resp., stable). PIPs are called "pairwise" since the symmetric point (x', x) w.r.t. the diagonal gives the same information about equilibrium $(0, \bar{n}(x'))$.

The superposition of the PIP with its mirror image w.r.t. the diagonal $x' = x$ is called *mutual invasibility plot* (MIP). It contains three types of regions, as shown in Figure 3.2: white-white regions (white regions ① in panels C-F), in which both equilibria $(\bar{n}(x), 0)$ and $(0, \bar{n}(x'))$ are unstable; white-gray regions (light gray regions ② and ③ in all panels), in which one of the two equilibria is stable and the other unstable; and gray-gray regions (dark grey regions ④ in panels A, B, G, and H), in which both equilibria are stable. Moreover, in regions ② and ③ the invasion implies substitution theorem implies that one population replaces the other (see the corresponding demographic state portraits in the last panel), while in regions ① and ④ a coexistence equilibrium is present, stable in region ① and unstable (a saddle) in region ④ (see the corresponding demographic state portraits in the last panel). These four are all the possible resident-mutant dynamics in the neighborhood of an evolutionary equilibrium.

To conclude, it has been shown that in the neighborhood of an evolutionary equilibrium resident and mutant types can coexist. This happens in cases C-F, where region ① is present (see Figure 3.2). Looking at the last panel of Figure 3.1, such cases corresponds to condition (3.2).

3.2.2 The divergence condition (3.4)

Once residents and mutants coexist at a strictly positive equilibrium in the demographic state space (n, n'), the mutant population becomes by definition a new resident population. For this reason abundances n, n' and traits x, x' are now indicated with n_1, n_2 and x_1, x_2, respectively. We can denote with $(\bar{n}_1(x_1, x_2), \bar{n}_2(x_1, x_2))$ this dimorphic coexistence equilibrium and derive the two-dimensional canonical

equation

$$\dot{x}_i = k_i \bar{n}_i(x_1, x_2) \lambda_2^{(0,0,1)}(x_1, x_2, x_i), \tag{3.8}$$

with $i = 1, 2$, where $\lambda_2(x_1, x_2, x') = g(\bar{n}_1(x_1, x_2), \bar{n}_2(x_1, x_2), x_1, x_2, x')$ is the dimorphic fitness function. In the next chapter we will show that, with a proper Taylor expansion, the second-order approximation of the dimorphic fitness $\lambda_2(x_1, x_2, x')$ in the neighborhood of the singular strategy $(\bar{x}, \bar{x}, \bar{x})$ is

$$\lambda_2(x_1, x_2, x') = \frac{1}{2} \bar{\lambda}_1^{(0,2)} (x' - x_1)(x' - x_2) + O(\|(\ldots)\|^3), \tag{3.9}$$

where the term $O(\|(\ldots)\|^3)$ will be carefully discussed. The two-dimensional canonical equation (3.8) thus becomes

$$\dot{x}_i = k_i \bar{n}_i(x_1, x_2) \frac{1}{2} \bar{\lambda}_1^{(0,2)} (2x_i - x_1 - x_2) + O(\|(\ldots)\|^2), \tag{3.10}$$

with $i = 1, 2$. This means that $\dot{x}_1$ and $\dot{x}_2$ has opposite sign and trait x_1 and x_2 diverge (resp., converge) when $\bar{\lambda}_1^{(0,2)}$ is positive (resp., negative), so the divergence condition is nothing but (3.4) (see also Geritz et al. [1998]). The evolutionary trajectories described by the canonical equation (3.10) in cases C-F where coexistence is possible are reported in Figure 3.3. In particular, if (3.4) is satisfied (cases D-F), traits x_1 and x_2 initially diverge, and a nonlocal analysis of the canonical equation (3.8) is required to determine the fate of the community. Notice, however, that in case F the boundaries of the coexistence region are attractive, meaning that the evolutionary trajectory of the two diverging traits likely tends toward such boundaries, where one of the two populations is driven to extinction by the evolution of the other (evolutionary murder, see Paragraphs 1.2.5 and 2.7). By contrast, if (3.4) is not satisfied (case C), traits x_1 and x_2 converge and also in this case the evolutionary trajectory likely tends to the boundary of the coexistence region, driving one of the two populations to evolutionary extinction. Notice that there is a particular evolutionary trajectory reaching the evolutionary monomorphic equilibrium, along which the two similar coexisting populations do not vanish and merge in trait value (the opposite phenomenon of evolutionary branching that has been called *evolutionary merging* [Dercole and Rinaldi, 2008]).

Geometrically, positive (resp., negative) values of $\bar{\lambda}_1^{(0,2)}$ mean that the evolutionary equilibrium $\bar{x}$ is a local minimum (resp., maximum) of the fitness landscape $\lambda_1(\bar{x}, x')$ experienced by the mutant with trait x' at the evolutionary equilibrium $\bar{x}$. At fitness minima (resp., maxima), points (x_1, x_2) just above or below point $(\bar{x}, \bar{x})$ in Figure 3.1 lie

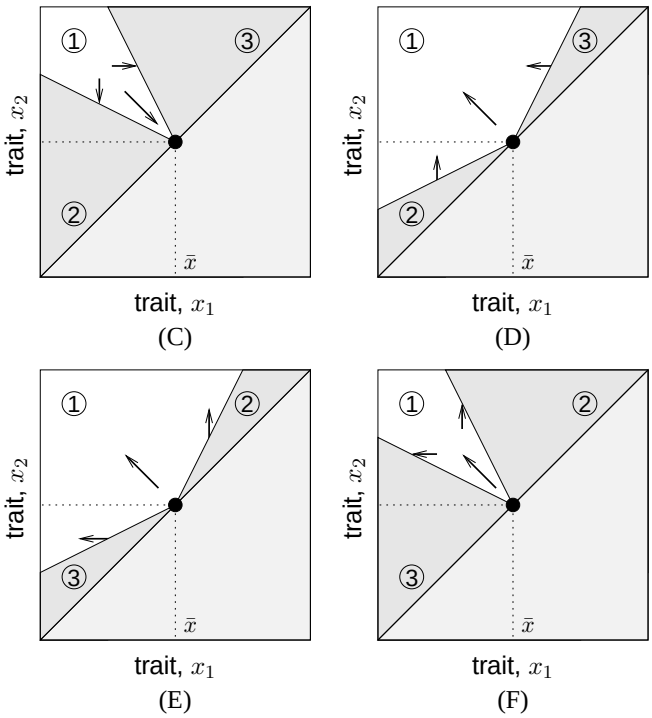

Figure 3.3: Evolutionary branching (cases D-F) and evolutionary merging (case C) (reproduced from Dercole and Rinaldi [2008]).

in white (resp., gray) regions of the PIP, i.e., cases D-G (resp., A-C, H). Thus, small mutations x' either larger or smaller than $\bar{x}$ invade at fitness maxima, while fitness minima are uninvadable. Since stability of evolutionary equilibrium $\bar{x}$ is not related only with $\bar{\lambda}_1^{(0,2)}$, evolution on an adaptive landscape may drive communities toward fitness maxima (as traditionally expected) as well as toward fitness minima [Abrams et al., 1993].

3.3 Classification of evolutionary equilibria

It is then possible to classify evolutionary equilibria w.r.t. their *convergence* stability [Christiansen, 1991] and *evolutionary* stability [Maynard Smith and Price, 1973]. An evolutionary equilibrium $\bar{x}$ is convergence stable if a population of a nearby phenotype can be invaded by mutants that are even closer to $\bar{x}$, i.e., if $\lambda_1(x, x') > 0$ for $x < x' < \bar{x}$ and $\bar{x} < x' < x$. It is the classical notion of asymptotic stability of dynamical systems, for which any perturbation from the

singular state tends to zero. The concept of evolutionary stability is related to the concept of ESS (Evolutionarily Stable Strategy) of evolutionary game theory (see Paragraph 1.3). An evolutionary equilibrium is ESS-stable if cannot be invaded by nearby mutants, i.e., if $\lambda_1(\bar{x}, x') < 0$ for both $x' < \bar{x}$ and $x' > \bar{x}$ close to $\bar{x}$.

Technically, convergence stability can be assessed looking at the eigenvalue of the linearized canonical equation at $\bar{x}$, that, in the case of a single trait population, is

$$\frac{d}{dx}\left(\frac{1}{2}\mu(x)\sigma^2(x)\bar{n}(x)\lambda_1^{(0,1)}(x,x)\right)\Big|_{x=\bar{x}} = \frac{1}{2}\mu(\bar{x})\sigma^2(\bar{x})\bar{n}(\bar{x})\left(\bar{\lambda}_1^{(1,1)}+\bar{\lambda}_1^{(0,2)}\right), \tag{3.11}$$

so that $\bar{x}$ is convergence stable (resp., unstable) if $\bar{\lambda}_1^{(1,1)} + \bar{\lambda}_1^{(0,2)}$ is negative (resp., positive). Therefore, the evolutionary equilibrium (in a single trait population) is convergence stable in cases A-D of Figure 3.1 (see last panel), while it is convergence unstable (or an evolutionary repellor) in cases E-H of Figure 3.1. However, in multiple trait communities, such analysis is not so simple [Matessi and Di Pasquale, 1996, Cohen et al., 1999].

An evolutionary equilibrium $\bar{x}$ is evolutionarily stable if $\lambda_1(\bar{x}, x') < 0$ for all $x' \neq \bar{x}$ in a small neighborhood of $\bar{x}$. This is verified when $\bar{\lambda}_1^{(0,2)} < 0$, i.e., $\bar{x}$ is a fitness maximum. Therefore, $\bar{x}$ is ESS-stable in cases A-C and H of Figure 3.1 (see last panel). This condition can be easily generalized in the case of multiple trait communities [Brown and Vincent, 1987, 1992].

Recalling (3.11), it is possible to notice that in a single trait population convergence stability ($\bar{\lambda}_1^{(1,1)} + \bar{\lambda}_1^{(0,2)} < 0$) and evolutionary instability ($\bar{\lambda}_1^{(0,2)} > 0$) imply resident-mutant coexistence ($\bar{\lambda}_1^{(1,1)} < 0$). Thus, the branching conditions are both satisfied. By contrast, in multiple trait communities, convergence stability and evolutionary instability do not imply evolutionary branching. For this to occur, $\bar{\lambda}_1^{(1,1)}$ must be negative, that is, in cases C-F of Figure 3.1.

We are now ready to classify all cases A-H w.r.t. convergence and evolutionary stability (in the case of multiple trait communities we always assume converge stability of the evolutionary equilibrium, since convergence unstable points are not reached by the evolutionary dynamics).

- Single trait population
  - A-B: Continuously Stable Strategies (CSS) [Eshel and Motro, 1981, Eshel, 1983];

  - C: ESSs at which resident-mutant coexistence is allowed (but the dimorphic dynamics lead one of the two populations to extinction or the two traits to merge into one). Therefore this ESSs can be characterized by temporary invasion (a new concept w.r.t. the traditional ESS formulation of Game Theory [Dercole and Rinaldi, 2008]);
  - D: Convergence stable equilibria at which resident mutant coexistence is allowed and the dimorphic dynamics is unstable, leading away from such points;
  - E-F: Resident-mutant coexistence is allowed, but the monomorphic dynamics go away from these points;
  - G: The monomorphic dynamics go away from these points;
  - H: Unstable ESSs or Gardens of Eden [Eshel and Motro, 1981, Eshel, 1983, Nowak, 1990].

- Multiple traits communities (with M resident traits)
  - A-B and H: Evolutionary Stable Coalitions (co-ESS);
  - C: co-ESS with temporary invasion;
  - D-F: Convergence stable equilibria at which resident mutant coexistence is allowed and the $(M+1)$-morphic dynamics is unstable, leading away from such points;
  - G: Evolutionary unstable equilibria at which resident-mutant coexistence is not possible. For this reason, each mutation leads to the substitution of the resident group, but the convergence stability guarantees that the traits will tend again toward the equilibrium.

Transitions between these cases happen when the second derivatives $\bar{\lambda}_1^{(1,1)}$ and $\bar{\lambda}_1^{(0,2)}$ assume critical values (see Figure 3.1, last panel). Therefore, they can be seen as particular *bifurcations*. In the next chapter we will study the *branching bifurcation*, that is, the change of evolutionary stability ($\bar{\lambda}_1^{(0,2)} = 0$) of the singular strategy, under the genericity condition of resident-mutant coexistence ($\bar{\lambda}_1^{(1,1)} < 0$), i.e., the transition between cases C and D.

3.4 Branching and terminal points

To conclude, we can summarize by considering only two classes:

- *branching points* (BP), i.e., convergence stable equilibria at which resident mutant coexistence is allowed and the dimorphic dynamics is unstable, leading away from $\bar{x}$ (both branching conditions are satisfied for at least one population). They corresponds to case D for single trait populations and to cases D-F for multiple traits communities;

- *terminal points* (TP), i.e., convergence stable equilibria at which the dimorphic dynamics is not possible or it is stable (no branching can occur for any trait, with the consequent halt of the evolutionary dynamics). They correspond to cases A-C for single trait populations and to cases A-C and G-H for multiple traits communities (assuming convergence stability of the evolutionary equilibrium).

Notice that branching points, although technically equilibria of the canonical equation, are not equilibria of the evolutionary process. Indeed, the evolution of the community continues with an enlarged system (with an extra trait) following a higher-dimensional canonical equation. Moreover, notice that there exists terminal points which are however not ESSs (case G in multiple traits communities).

If, in the vicinity of an equilibrium, the branching conditions are satisfied for more than one population, it means that all of them will (initially) gain a new resident form. But (generically), as long as diverge takes place following the higher-dimensional canonical equation (with an extra ODE for each of the populations satisfying the branching conditions), only one of the nascent branching events will survive (this is the phenomenon of *missed branching*, see Kisdi [1999] and Paragraph 5.2.3.2).

At each branching, one of the resident populations gains one form, increasing its polymorphism. Branching points are, thus, a source of diversity for the evolving community and can be considered at the base of a possible mechanism of sympatric speciation (see Paragraph 1.2.4).

Chapter 4

The branching bifurcation

In this chapter we unfold the bifurcation involving the loss of evolutionary stability of an equilibrium of the canonical equation of Adaptive Dynamics. The equation deterministically describes the expected long-term evolution of the inheritable traits—phenotypes or strategies—of coevolving populations, in the limit of rare and small mutations. In the vicinity of a stable equilibrium of the AD canonical equation, a mutant type can invade and coexist with the present—resident—types, whereas the fittest always win far from equilibrium. After coexistence, residents and mutants effectively diversify, according to the enlarged canonical equation, only if natural selection favors outer rather than intermediate traits—the equilibrium being evolutionarily unstable, rather than stable. Though the conditions for evolutionary branching—the joint effect of resident-mutant coexistence and evolutionary instability—have been known for long, the unfolding of the bifurcation remained a missing tile of AD, the reason being related to the nonsmoothness of the mutant invasion fitness at the branching point. In this chapter, we develop a methodology that allows the approximation of the invasion fitness after branching in terms of the expansion of the (smooth) fitness before branching. We then derive a canonical model for the branching bifurcation and perform its unfolding around the loss of evolutionary stability. We cast our analysis in the simplest (but classical) setting of asexual, unstructured populations living in an isolated, homogeneous, and constant abiotic environment; individual traits are one-dimensional; intra- as well as inter-specific ecological interactions are described in the vicinity of a stationary regime. More details can be found in Dercole et al. [2014].

4.1 Introduction

Since its funding publications [Metz et al., 1996, Geritz et al., 1997, 1998], Adaptive Dynamics has been widely used for modeling the long-term evolutionary dynamics of genetically transmitted phenotypic traits (see Dercole and Rinaldi [2008] and the references therein), with special emphasis on the emergence of diversity through evolutionary branching. Evolutionary branching takes place when a resident and a similar mutant type coexist in the same environment and natural selection is disruptive, i.e., it favors outer rather than intermediate phenotypes. Series of subsequent mutations hence lead to the diversification of the two traits. Analogous phenomena can be observed in socio-economic contexts (see Chapter 7 and Dercole et al. [2008], Landi and Dercole [2014b]), where behavioral strategies, innovations, and competition play the role of phenotypic traits, mutations, and natural selection [Ziman, 2000].

In the limit of extremely rare mutations of infinitesimal effect, evolution can be approximated by a continuous dynamics in terms of an ODE model, called the canonical equation of AD [Dieckmann and Law, 1996, Champagnat et al., 2006]. The AD canonical equation describes the expected long-term evolution as an ascent of the traits on an adaptive fitness landscape [Levins, 1968, Gavrilets, 2004]. All kind of evolutionary attractors can be displayed, from stationary—called singular strategies in the AD jargon—to periodic [Dieckmann et al., 1995] and chaotic [Dercole et al., 2010a, Dercole and Rinaldi, 2010], and attractor multiplicity questions the replicability of evolutionary history [Dercole et al., 2006]. When mutational steps are finite and stochastically drawn, evolution proceeds as a random walk in the trait space of coevolving populations, again showing the full plethora of nonlinear behaviors [Doebeli and Ruxton, 1997].

Evolutionary branching can be formally described in terms of the stability properties of the singular strategies, seen as the evolutionary equilibria of the AD canonical equation. Specifically, resident-mutant coexistence can only occur in the vicinity of an evolutionary equilibrium, so the equilibrium must be stable (convergence stability) to be reached by the evolutionary dynamics, and unstable (evolutionary instability [Maynard Smith and Price, 1973]) for the higher-dimensional canonical equation to be used after resident-mutant coexistence to produce phenotypic divergence. Whereas branching cannot occur if coexistence is not possible close to the evolutionary equilibrium or if the equilibrium is evolutionarily stable—the equilibrium then repre-

sents a terminal point of the evolutionary dynamics.

The transition from terminal to branching point (or vice-versa) along with changes in the relevant demographic, environmental, or control parameters, can therefore be interpreted as a *bifurcation* of the AD canonical equation. The unfolding of the bifurcation is however a missing tile of AD theory. The reason why it has been left behind is related to difficulties in developing a suitable normal form for the bifurcation. In fact, the fitness landscape after branching is nonsmooth at the branching point and this prevents the Taylor expansion approach typical of normal form analysis.

In this chapter we develop a methodology that allows the approximation of the dimorphic fitness landscape—the invasion fitness of a mutant in the presence of the two resident types at the incipient branching—in terms of the expansion of the monomorphic fitness—the invasion fitness before the branching—up to any order locally to the branching point. We cast our analysis in the simplest (but classical) setting of unstructured populations (no distinction in age, state, location, etc., of individuals) varying in continuous time in an isolated, homogeneous, and constant abiotic environment; individual traits are quantified by one-dimensional strategies; intra- as well as inter-specific ecological interactions are described in the vicinity of a stationary regime. We exploit an expansion in the radial direction in the plane of the two diverging strategies and show that the fitness landscape is smooth on each given ray, thus obtaining an approximation that is parametric in the ray angle.

By means of a third-order approximation, we unfold the *branching bifurcation* involving the change in evolutionary stability of the evolutionary equilibrium. In particular, it is the third derivative of the monomorphic fitness with respect to the mutant strategy the main parameter ruling branching in the degenerate case we analyze. The transition involving the possibility of resident-mutant coexistence near the evolutionary equilibrium is more involved and is left for future research. This, as well as bifurcations of higher codimension (more degeneracies occurring together), can be however dealt with the same methodology.

Interestingly, our approximation coincides up to second-order to the one obtained by Geritz et al. [1997, 1998] by erroneously assuming a smooth dimorphic fitness. Thus, the branching conditions derived by Geritz et al. [1997, 1998] in terms of the second derivatives of the monomorphic fitness at the singular strategy are confirmed. The third-order terms in the approximation however differ from those one

would obtain under the smoothness assumption. Worth to remark is that they are given in terms of the monomorphic fitness derivatives (in contrast to what preliminarily found in Durinx [2008], in the special case of Lotka-Volterra models), so the evolutionary dynamics locally to a branching point are determined by quantities that can be evaluated without waiting for the mutation that triggers the branching. This is possible thanks to the new property (P4) of the ecological model that we will introduce in the next paragraph. This property derives from a generalized law of *mass action*, i.e., the fact that ecological models describe pairwise interactions between individuals that are, in turn, involved in pairwise interactions.

The chapter is organized as follows. In the next Paragraph we introduce the basic notation and the methodology used for approximating the dimorphic invasion fitness. For simplicity of notation, we consider a single species generic model (as done in Geritz et al. [1997, 1998]) and we focus on the transition from the monomorphic to the dimorphic situation. Only later, in Paragraph 4.2.3.5, we will consider higher polymorphisms and/or other inter-specific interactions. The results are fully analogous, but more involved to be derived. In Paragraphs 4.3 and 4.4 we present the normal form and the unfolding of the branching bifurcation. Paragraph 4.5 is dedicated to an example, where the developed theory is applied to an AD eco-evolutionary model taken from the literature. Finally, in Paragraph 4.6, we discuss possible extensions for future work. In particular, similar results are expected to hold for the case of structured populations characterized by multi-dimensional strategies. All analytical computations have been handled symbolically and a detailed commented *Mathematica* script can be found in Dercole et al. [2014].

4.2 Methods

4.2.1 Notation, assumptions, and preliminaries

We consider two similar competing populations, with abundances measured by densities $n_1(t)$ and $n_2(t)$ at time t and characterized by a one-dimensional strategy (or trait) x taking values x_1 and $x_2 \simeq x_1$ in populations 1 and 2 (the case in which other conspecific populations and/or other species are present is treated in Paragraph 4.2.3.5). In the monomorphic situation, we refer to populations 1 and 2 as resident and mutant, respectively, whereas they are both residents after branching.

Populations 1 and 2 being conspecific, their per-capita growth rates $\dot{n}_1/n_1$ and $\dot{n}_2/n_2$ can be expressed through the same g-function (see also Paragraph 3.1) $g(n_1, n_2, x_1, x_2, x')$—the per-capita growth rates of a population with strategy x' and infinitesimally small density in the environment where strategies x_1 and x_2 are present with densities n_1 and n_2. Then, $\dot{n}_1/n_1$ and $\dot{n}_2/n_2$ are given by the g-function evaluated for $x' = x_1$ and $x' = x_2$, respectively:

$$\dot{n}_1 = n_1\, g(n_1, n_2, x_1, x_2, x_1) \tag{4.1a}$$
$$\dot{n}_2 = n_2\, g(n_1, n_2, x_1, x_2, x_2). \tag{4.1b}$$

To define reasonable population dynamics, function g enjoys the four basic properties summarized below. The first three are rather obvious and has already been introduced in Paragraph 2.3in terms of f and F, but are here recalled in terms of g-function; whereas the last is more involved and has been recently introduced in [Dercole, 2014]. We recall that we assume g to be smooth and we use lists of integer superscripts to indicate the arguments w.r.t. which we take derivatives and the order of differentiation, e.g.

$$\begin{aligned} g^{(1,0,0,0,0)}(n_1, n_2, x_1, x_2, x') &:= \tfrac{\partial}{\partial n_1} g(n_1, n_2, x_1, x_2, x'), \\ g^{(1,1,0,0,0)}(n_1, n_2, x_1, x_2, x') &:= \tfrac{\partial^2}{\partial n_1 n_2} g(n_1, n_2, x_1, x_2, x'), \\ g^{(2,0,0,0,0)}(n_1, n_2, x_1, x_2, x') &:= \tfrac{\partial^2}{\partial n_1^2} g(n_1, n_2, x_1, x_2, x'). \end{aligned}$$

P1 $g(n_1, 0, x_1, x_2, x') = g(n_1, 0, x_1, \cdot, x') = g_1(n_1, x_1, x')$,
for a suitable function g_1, i.e., the per-capita growth rate of a strategy x' is not affected by the strategy x_2 of an absent population.

P2 $g(n_1, n_2, x, x, x') = g(\alpha(n_1+n_2), (1-\alpha)(n_1+n_2), x, x, x')$,
for any $0 \leq \alpha \leq 1$, i.e., any partitioning of the total density (n_1+n_2) into two populations with same strategy x must result in the same per-capita growth rate for strategy x'.

P3 $g(n_1, n_2, x_1, x_2, x') = g(n_2, n_1, x_2, x_1, x')$,
i.e., the order in which populations 1 and 2 are considered does not matter.

P4

$$g^{(0,0,p,0,0)}(n_1,n_2,x,x,x') = \sum_{i=1}^{p} \phi_{p,i}(n_1+n_2,x,x')\, n_1^i$$

$$g^{(0,0,p_1,p_2,0)}(n_1,n_2,x,x,x') = \sum_{i_1=1}^{p_1}\sum_{i_2=1}^{p_2} \phi_{p_1,p_2,i_1,i_2}(n_1+n_2,x,x')\, n_1^{i_1} n_2^{i_2},$$

for suitable functions $\phi_{p,i}$ and ϕ_{p_1,p_2,i_1,i_2} and $p, p_1, p_2 \geq 1$. This property follows from a generalized principle of *mass-action*, i.e., the assumption that g describes pairwise interactions between a target individual with strategy x' and other individuals which are, in turn, involved in pairwise interactions (see Dercole [2014]). Thus, when considering identical resident and invader strategies, $x' = x$, the sensitivity (i.e., the derivative) of the growth rate g w.r.t. the x at fourth or fifth argument is proportional to the density of the corresponding individuals, n_1 or n_2, whose strategy is being perturbed by the derivative, with a proportionality coefficient that can be density-dependent only as a function of the total density n_1+n_2. Moreover, due to nonlinear density dependencies in g, higher powers of n_1 and n_2 may appear in further derivatives (up to the order of differentiation p, p_1, or p_2), with coefficients $\phi_{p,i}$ or ϕ_{p_1,p_2,i_1,i_2}.

Examples of property P4 are

$$\begin{aligned} g^{(0,0,1,0,0)} &= \phi_{1,1}\, n_1 \\ g^{(0,0,1,1,0)} &= \phi_{1,1,1,1}\, n_1 n_2 \\ g^{(0,0,2,0,0)} &= \phi_{2,1}\, n_1 + \phi_{2,2}\, n_1^2, \end{aligned}$$

(where arguments have been omitted for notation simplicity) from which we write equations like

$$\begin{aligned} g^{(1,0,1,0,0)} &= \phi_{1,1}^{(1,0,0)} n_1 + \phi_{1,1}, \\ g^{(0,1,1,0,0)} &= \phi_{1,1}^{(1,0,0)} n_1, \\ g^{(1,0,1,1,0)} &= \phi_{1,1,1,1}\, n_2 + \phi_{1,1,1,1}^{(1,0,0)} n_1 n_2, \\ g^{(1,0,2,0,0)} &= \phi_{2,1} + (\phi_{2,1}^{(1,0,0)} + 2\phi_{2,2}) n_1 + \phi_{2,2}^{(1,0,0)} n_1^2. \end{aligned}$$

Properties P1–4 can be combined to produce further relations among g-derivatives that will be taken into account in our expansions in Paragraph 4.2.3. For example:

P1-2a $g^{(l_1,l_2,0,0,0)}(n_1,n_2,x,x,x') = g_1^{(l_1+l_2,0,0)}(n_1+n_2,x,x')$,
i.e., n_1- and n_2-perturbations simply perturb the total density (n_1+n_2) if the two populations have the same strategy x;

P1-2b $\sum_{i=0}^{p}\binom{p}{i} g^{(l_1,l_2,i,p-i,0)}(n_1,n_2,x,x,x') = g_1^{(l_1+l_2,p,0)}(n_1+n_2,x,x')$,
$p \geq 1$, obtained by x-differentiating P1-2a;

P1-3 $g(0,n_2,x_1,x_2,x') = g_1(n_2,x_2,x')$;

P1-4 $g_1^{(0,p,0)}(n,x,x') = \sum_{i=1}^{p} \phi_{p,i}(n,x,x')\, n^i$;

P1-2-4 $\sum_{i=i_1}^{p-i_2}\binom{p}{i}\phi_{i,p-i,i_1,i_2}(n,x,x') = \binom{i_1+i_2}{i_1}\phi_{p,i_1+i_2}(n,x,x')$,
for each $i_1, i_2 \geq 1$ with $i_1+i_2 \leq p \geq 2$, obtained by substituting P4 and P1-4 into P1-2b with $l_1 = l_2 = 0$.

P3-4a $g^{(0,0,0,p,0)}(n_1,n_2,x,x,x') = \sum_{i=1}^{p} \phi_{p,i}(n_1+n_2,x,x')\, n_2^i$;

P3-4b $\phi_{p_1,p_2,i_1,i_2} = \phi_{p_2,p_1,i_2,i_1}$.

Moreover, further derivatives w.r.t. to the target strategy x' can be added to all properties.

As anticipated in Paragraph 4.1, we consider the (simplest, but most typical) case of stationary coexistence. In particular, we assume that for all values of the strategy x_1 that we consider, the resident population 1 can persist alone at a strictly positive and (hyperbolically) stable equilibrium of equation (4.1a) with $n_2 = 0$ (see also Paragraph 2.3). We denote the equilibrium density with function $\bar{n}(x_1)$, implicitly defined by

$$g(\bar{n}(x_1),0,x_1,\cdot,x_1) = g_1(\bar{n}(x_1),x_1,x_1) = 0 \tag{4.2}$$

(see property P1 above). Note that the hyperbolicity of the resident equilibrium (i.e., nonzero real part of all associated eigenvalue) and the similarity between the resident and mutant populations ($x_1 \simeq x_2$), guarantee that the population 2 is also able to persist alone at the strictly positive (and hyperbolically stable) equilibrium $\bar{n}(x_2)$ of

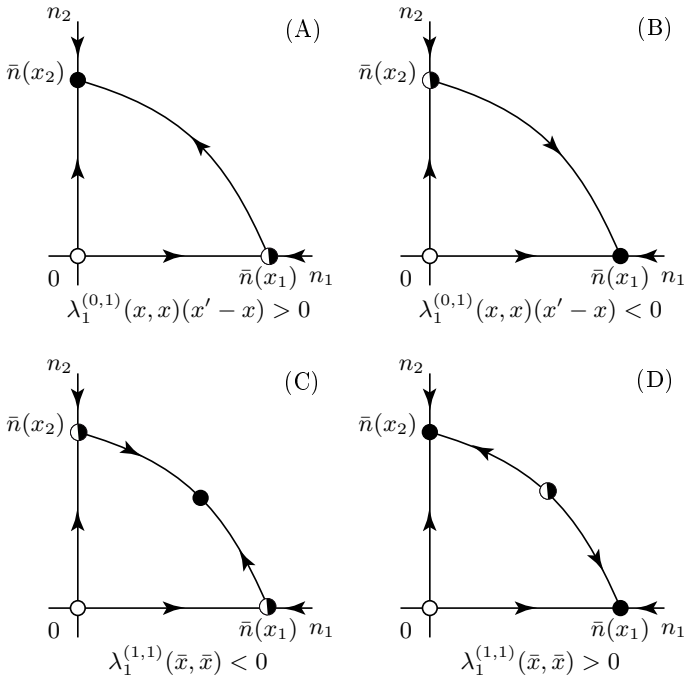

Figure 4.1: Resident-mutant competition scenarios. Top row, far from singular strategies: exclusion of population 1 (A) (resp., 2 (B)). Bottom row, close to a singular strategy $\bar{x}$: coexistence (C) or mutual exclusion (D). Full points: stable equilibria. Half-filled points: saddles. Empty points: unstable equilibria.

equation (4.1b) with $n_1 = 0$. In other words, the resident-mutant model (4.1) admits the two monomorphic equilibria $(\bar{n}(x_1), 0)$ and $(0, \bar{n}(x_2))$ for all the pairs (x_1, x_2) that we consider (see Figure 4.1, top panels).

The *monomorphic invasion fitness* is the initial (per-capita) growth rate of the mutant population, i.e.,

$$\lambda_1(x, x') := g(\bar{n}(x), 0, x, \cdot, x') = g_1(\bar{n}(x), x, x'), \tag{4.3}$$

the resident population settled at equilibrium mutations being rare. Generically (i.e., if $\lambda_1^{(0,1)}(x,x) \neq 0$ [Geritz, 2005, Meszéna et al., 2005, Dercole and Rinaldi, 2008]) the best performing population wins the competition, so x evolves by small steps in the direction of the *selection gradient* $\lambda_1^{(0,1)}(x,x)$. And in the limit of extremely rare and small mutations, the expected evolutionary dynamics is deterministi-

cally described by the AD canonical equation

$$\dot{x} = \tfrac{1}{2}\,\mu(x)\sigma(x)^2\bar{n}(x)\lambda_1^{(0,1)}(x,x), \tag{4.4}$$

where $\mu(x)$ and $\sigma(x)^2$ scale with the frequency and variance of mutations in strategy x (half of which are at disadvantage and go extinct). The strategies annihilating the selection gradient are called singular and correspond to the equilibria of the canonical equation.

In the vicinity of a singular strategy $\bar{x}$, i.e.,

$$\lambda_1^{(0,1)}(\bar{x},\bar{x}) = 0, \tag{4.5}$$

the ecological and evolutionary dynamics are dominated by the second derivatives of the monomorphic fitness. In particular, resident-mutant coexistence is possible if

$$\lambda_1^{(1,1)}(\bar{x},\bar{x}) < 0. \tag{G1}$$

Geritz et al. [1997, 1998] showed that under (G1) resident and mutant mutually invade each other (the instability of the two monomorphic equilibria, see Figure 4.1C); and they mutually exclude if the inequality sign in (G1) is reversed (the stability of the two monomorphic equilibria, see Figure 4.1D). More recently, Dercole and Geritz [2014] showed the uniqueness and stability of the internal equilibrium of the ecological model (4.1). When possible, coexistence occurs for (x_1, x_2) in a conical region locally to $(\bar{x},\bar{x})$ (see Figure 4.2). The boundaries of the region are transcritical bifurcation curves [Kuznetsov, 2004, Meijer et al., 2009] on which the internal equilibrium collides with one of the monomorphic equilibria (see Paragraph 4.2.2). For (x_1, x_2) in the coexistence region, we denote the densities of the internal equilibrium with functions $\bar{n}_1(x_1, x_2)$ and $\bar{n}_2(x_1, x_2)$, implicitly defined by

$$g(\bar{n}_1(x_1,x_2),\bar{n}_2(x_1,x_2),x_1,x_2,x_1) = 0 \tag{4.6a}$$
$$g(\bar{n}_1(x_1,x_2),\bar{n}_2(x_1,x_2),x_1,x_2,x_2) = 0 \tag{4.6b}$$

(the equilibrium condition for model (4.1)).

After coexistence evolution is driven by a two-dimensional canonical equation

$$\dot{x}_i = \tfrac{1}{2}\,\mu(x_i)\sigma(x_i)^2\bar{n}_i(x_1,x_2)\lambda_2^{(0,0,1)}(x_1,x_2,x_i), \quad i = 1,2, \tag{4.7}$$

where

$$\lambda_2(x_1,x_2,x') := g(\bar{n}_1(x_1,x_2),\bar{n}_2(x_1,x_2),x_1,x_2,x'), \tag{4.8}$$

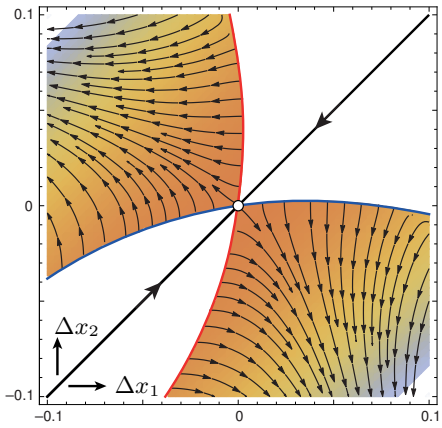

Figure 4.2: Coexistence region locally to $(\bar{x}, \bar{x})$. The colored shaded area represents trait pairs where coexistence is possible, and the color indicates the total abundance (blue: low, orange: high). In the white areas one of the two populations outcompetes the other. It is a higher-order approximation w.r.t. Figure 3.3D.

is the *dimorphic invasion fitness*—the initial (per-capita) growth rate of the mutant population of strategy x' appeared in an environment set by the two residents x_1 and x_2 at their equilibrium densities.

Note the symmetry of the resident-mutant coexistence region w.r.t. the diagonal $x_1 = x_2$ (Figure 4.2), that is due to the same symmetry in model (4.1). The dynamics of model (4.1) corresponding to point (x_1, x_2) below the diagonal are obtained by those corresponding to point (x_2, x_1) above the diagonal by exchanging n_1 and n_2—i.e., by exchanging the roles of resident and mutant (see property P3). Consequently, also model (4.7) has a diagonal symmetry—the vector field at (x_1, x_2) below the diagonal is obtained by that at (x_2, x_1) above the diagonal by exchanging the two components (see the blue arrows in Figure 4.2).

The singular strategy $\bar{x}$ is a *branching point* if the two similar strategies x_1 and x_2 tend to diversify according to the dimorphic evolutionary dynamics (4.7). Technically, this is so if $\dot{x}_1(0) < 0$ and $\dot{x}_2(0) > 0$ at a point $(x_1(0), x_2(0))$ of the coexistence region, with $x_2(0) > x_1(0)$, that is arbitrarily close to $(\bar{x}, \bar{x})$ (see the blue arrows above the diagonal in Figure 4.2). The singular strategy is a *terminal point* of the evolutionary dynamics, otherwise.

Geritz et al. [1997, 1998] concluded that the condition for evolutionary divergence is

$$\lambda_1^{(0,2)}(\bar{x}, \bar{x}) > 0, \tag{4.9}$$

i.e., the condition for evolutionary instability—mutant invasion at $x_1 = \bar{x}$. The conclusion is based on a second-order Taylor expansion of the dimorphic fitness at $(x_1, x_2, x') = (\bar{x}, \bar{x}, \bar{x})$, that is however nonsmooth there. In fact, by assuming smoothness and exploiting the following consistency relations:

C1 $\lambda_2(x, x, x') = \lambda_1(x, x')$,
the link between the dimorphic and monomorphic fitness functions (induced by properties P1 and P2),

C2 $\lambda_2(x_1, x_2, x') = \lambda_2(x_2, x_1, x')$,
the order irrelevance of the two residents (property P3)

C3 $\lambda_2(x_1, x_2, x_1) = \lambda_2(x_1, x_2, x_2) = 0$,
the resident equilibrium conditions (4.6),

one gets to nongeneric constraints on the monomorphic fitness, such as $\lambda_1^{(2,0)}(\bar{x}, \bar{x}) = \lambda_1^{(0,2)}(\bar{x}, \bar{x})$ at second order, and similar nonsenses at higher orders (see Paragraph 4.2.3.1). In Paragraph 4.2.3 we show that the divergence condition (4.9) is correct, as we rederive it through a proper (radial) expansion of the dimorphic fitness.

As in the previous chapter, we use overbars to denote evaluations at the singular strategy, e.g. $\bar{\lambda}_1^{(1,1)} = \lambda_1^{(1,1)}(\bar{x}, \bar{x})$ and $\bar{\lambda}_1^{(0,2)} = \lambda_1^{(0,2)}(\bar{x}, \bar{x})$. Moreover, taking into account that

$$\lambda_1(x, x) = 0 \tag{4.10}$$

for any x (this is nothing but the definition of $\bar{n}(x)$, see (4.2) and (4.3)), we can avoid the pure derivatives $\bar{\lambda}_1^{(k,0)}$, $k \geq 1$, since by the x-derivatives of (4.10) at $(\bar{x}, \bar{x})$ we have

$$\bar{\lambda}_1^{(1,0)} + \bar{\lambda}_1^{(0,1)} = 0, \tag{4.11a}$$

$$\bar{\lambda}_1^{(2,0)} + 2\bar{\lambda}_1^{(1,1)} + \bar{\lambda}_1^{(0,2)} = 0, \tag{4.11b}$$

$$\bar{\lambda}_1^{(3,0)} + 3\bar{\lambda}_1^{(2,1)} + 3\bar{\lambda}_1^{(1,2)} + \bar{\lambda}_1^{(0,3)} = 0, \tag{4.11c}$$

and so forth (see also (3.5)). We always try to express our results in terms of the monomorphic fitness derivatives, that are known prior to coexistence. For this, recalling its definition (4.3), we take into

account that

$$\begin{aligned}
\bar{\lambda}_1^{(1,0)} &= \bar{g}^{(1,0,0,0,0)}\bar{n}^{(1)} + \bar{g}^{(0,0,1,0,0)} \\
\bar{\lambda}_1^{(0,1)} &= \bar{g}^{(0,0,0,0,1)} \\
\bar{\lambda}_1^{(2,0)} &= \bar{g}^{(2,0,0,0,0)}\left(\bar{n}^{(1)}\right)^2 + 2\bar{g}^{(1,0,1,0,0)}\bar{n}^{(1)} + \bar{g}^{(1,0,0,0,0)}\bar{n}^{(2)} + \bar{g}^{(0,0,2,0,0)} \\
\bar{\lambda}_1^{(1,1)} &= \bar{g}^{(1,0,0,0,1)}\bar{n}^{(1)} + \bar{g}^{(0,0,1,0,1)} \\
\bar{\lambda}_1^{(0,2)} &= \bar{g}^{(0,0,0,0,2)},
\end{aligned} \tag{4.12}$$

and similar relations for higher-order derivatives.

4.2.2 Expansion of the resident-mutant coexistence region

The equilibrium $(\bar{n}_1(x_1,x_2),\bar{n}_2(x_1,x_2))$ of model (4.1), at which the two similar residents coexist along an incipient branching, is defined by equations (4.6). Under the genericity condition (G1), Dercole and Geritz [2014] showed that the coexistence equilibrium can only undergo transcritical bifurcations in the vicinity of point $(x_1,x_2) = (\bar{x},\bar{x})$ in the strategy plane, $\bar{x}$ being a singular strategy. Due to the symmetry of model (4.1) w.r.t. the diagonal $x_1 = x_2$, the diagonal itself is a (degenerate) transcritical bifurcation at which the segment $n_1+n_2 = \bar{n}(x_1)$ is composed of a continuum of (critically) stable equilibria. Moreover, two (standard) transcritical bifurcations are rooted at point $(\bar{x},\bar{x})$ and constitute the boundaries of the coexistence region (see Figures 1 and 2).

The transcritical bifurcation at which the coexistence equilibrium collides with the monomorphic one at $(\bar{n}(x_1),0)$ is defined by

$$\lambda_1(x_1,x_2) = 0,$$

i.e., the mutant "coexists at zero density" with the resident (see the definition (4.3)). To geometrically characterize the bifurcation curve, it is convenient to use the polar coordinates

$$x_1 := \bar{x} + \varepsilon\cos\theta, \quad x_2 := \bar{x} + \varepsilon\sin\theta, \tag{4.13}$$

and to ε-parameterize the curve as $\theta = \theta_{\mathrm{T2}}(\varepsilon)$ (as done in [Dercole and Geritz, 2014], with the notation introduced in the previous chapter). Then

$$\lambda_1(\bar{x} + \varepsilon\cos\theta_{\mathrm{T2}}(\varepsilon), \bar{x} + \varepsilon\sin\theta_{\mathrm{T2}}(\varepsilon)) = 0 \tag{4.14}$$

is an identity for any (sufficiently small) $\varepsilon \geq 0$, and by evaluating (4.14) and its ε-derivatives at $\varepsilon = 0$ we can solve the resulting expressions for $\theta_{\mathrm{T2}}(0)$ and the derivatives $\theta_{\mathrm{T2}}^{(k)}(0)$, $k \geq 1$. The angle $\theta_{\mathrm{T2}}(0)$

gives the tangent direction to the bifurcation curve at $\varepsilon = 0$, while the first nonvanishing derivative $\theta_{\mathrm{T2}}^{(k)}(0)$ determines the curvature of the curve (whether θ increases or decreases by moving away from $\varepsilon = 0$ in the $\theta_{\mathrm{T2}}(0)$-direction).

Specifically, taking into account the singularity condition (4.5) (and the properties in (4.11)), the first ε-derivative of (4.14) at $\varepsilon = 0$ is an identity, whereas the second and third derivatives give

$$\begin{aligned}&(\sin\theta_{\mathrm{T2}}(0) - \cos\theta_{\mathrm{T2}}(0))\\ &\quad\Big(2\bar{\lambda}^{(1,1)}\cos\theta_{\mathrm{T2}}(0) + \bar{\lambda}^{(0,2)}(\sin\theta_{\mathrm{T2}}(0) + \cos\theta_{\mathrm{T2}}(0))\Big) = 0 \qquad (4.15)\end{aligned}$$

and

$$\begin{aligned}&6\Big(\bar{\lambda}^{(1,1)}(\sin^2\theta_{\mathrm{T2}}(0) - 2\sin\theta_{\mathrm{T2}}(0)\cos\theta_{\mathrm{T2}}(0) +\\ &\qquad - \cos^2\theta_{\mathrm{T2}}(0)) - 2\bar{\lambda}^{(0,2)}\sin\theta_{\mathrm{T2}}(0)\cos\theta_{\mathrm{T2}}(0)\Big)\theta_{\mathrm{T2}}^{(1)}(0) =\\ &\qquad\qquad (\sin\theta_{\mathrm{T2}}(0) - \cos\theta_{\mathrm{T2}}(0))\\ &\Big(3\bar{\lambda}^{(2,1)}\cos^2\theta_{\mathrm{T2}}(0) + 3\bar{\lambda}^{(1,2)}\cos\theta_{\mathrm{T2}}(0)(\sin\theta_{\mathrm{T2}}(0) + \cos\theta_{\mathrm{T2}}(0)) +\\ &\quad \bar{\lambda}^{(0,3)}(\sin^2\theta_{\mathrm{T2}}(0) + \sin\theta_{\mathrm{T2}}(0)\cos\theta_{\mathrm{T2}}(0) + \cos^2\theta_{\mathrm{T2}}(0))\Big). \qquad (4.16)\end{aligned}$$

From the $(\sin\theta_{\mathrm{T2}}(0) - \cos\theta_{\mathrm{T2}}(0))$ factor in (4.15), we have the solutions $\theta_{\mathrm{T0}}(0) = \frac{1}{4}\pi$ and $\frac{5}{4}\pi$, which correspond to the diagonal $x_1 = x_2$, whereas solving the second factor we get

$$\tan\theta_{\mathrm{T2}}(0) = -\frac{2\bar{\lambda}^{(1,1)} + \bar{\lambda}^{(0,2)}}{\bar{\lambda}^{(0,2)}} \overset{(4.11\mathrm{b})}{=} \frac{\bar{\lambda}^{(2,0)}}{\bar{\lambda}^{(0,2)}} \qquad (4.17)$$

(see also Chapter 3). We only consider angles above the diagonal and we can assume $\tan\theta_{\mathrm{T2}}(0) \neq 1$. In fact, recalling our aim of studying the branching bifurcation at which $\bar{\lambda}^{(0,2)} = 0$ under (G1) (the transition from case C to D of the previous chapter, see in particular the lat panel of Figure 3.1), we see from (4.17) that close to the bifurcation (small $|\bar{\lambda}^{(0,2)}|$) we certainly have

$$\bar{\lambda}^{(1,1)} + \bar{\lambda}^{(0,2)} \overset{(4.11\mathrm{b})}{=} \tfrac{1}{2}\left(\bar{\lambda}^{(0,2)} - \bar{\lambda}^{(2,0)}\right) < 0 \qquad (4.18)$$

(preventing the singular strategy $\bar{x}$ to undergo a saddle-node bifurcation of the monomorphic AD canonical equation (4.4), see [Dercole and Geritz, 2014]). We therefore restrict our attention to

$$\tfrac{1}{4}\pi < \theta < \tfrac{5}{4}\pi \qquad (4.19\mathrm{a})$$

and

$$x_2 - x_1 = \varepsilon\,(\sin\theta - \cos\theta) > 0. \tag{4.19b}$$

Substituting (4.17) into (4.16) and solving for $\theta^{(1)}_{\mathrm{T}0}(0)$, we get

$$\theta^{(1)}_{\mathrm{T}2}(0)= - \frac{4\big(\bar\lambda^{(1,1)}\big)^2\bar\lambda^{(0,3)}-2\bar\lambda^{(1,1)}\bar\lambda^{(0,2)}\big(3\bar\lambda^{(1,2)}-\bar\lambda^{(0,3)}\big)+\big(\bar\lambda^{(0,2)}\big)^2\big(3\bar\lambda^{(2,1)}+\bar\lambda^{(0,3)}\big)}{6\sqrt{2}\Big(2\big(\bar\lambda^{(1,1)}\big)^2+2\bar\lambda^{(1,1)}\bar\lambda^{(0,2)}+\big(\bar\lambda^{(0,2)}\big)^2\Big)^{3/2}}. \tag{4.20}$$

Note that taking the solution for $\theta_{\mathrm{T}2}(0)$ below the diagonal, one gets same/opposite curvatures $\theta^{(k)}_{\mathrm{T}2}(0)$ for even/odd k, i.e., equivalently, one can keep the solution above the diagonal and use the expansion $\theta_{\mathrm{T}2}(\varepsilon) = \theta_{\mathrm{T}2}(0)+\theta^{(1)}_{\mathrm{T}2}(0)\varepsilon+\cdots+\theta^{(k)}_{\mathrm{T}2}(0)\varepsilon^k+O(\varepsilon^{k+1})$ also for negative ε to describe both branches (above and below the diagonal) of the bifurcation curve. Also note that substituting $\theta_{\mathrm{T}2}(0) = \frac{1}{4}\pi$ (or $\frac{5}{4}\pi$) into (4.16) we get $\theta^{(1)}_{\mathrm{T}2}(0) = 0$, which confirms the diagonal being a bifurcation (in this case $\theta^{(k)}_{\mathrm{T}2}(0) = 0$ for all $k \geq 1$).

The bifurcation curve $\theta = \theta_{\mathrm{T}1}(\varepsilon)$ corresponding to the standard transcritical at the monomorphic equilibrium $(0, \bar n(x_2))$ is symmetric w.r.t. the diagonal to the one occurring at $(\bar n(x_1), 0)$ (the index 1 tells that population 1 goes extinct at the bifurcation). It is indeed defined by $\lambda_1(x_2, x_1) = 0$, i.e., the resident "coexists at zero density" with the mutant. As a result, $\tan\theta_{\mathrm{T}1}(0)$ is the inverse of the expression in (4.17), i.e.,

$$\tan\theta_{\mathrm{T}1}(0) = \frac{\bar\lambda^{(0,2)}}{\bar\lambda^{(2,0)}}, \tag{4.21}$$

the derivatives $\theta^{(k)}_{\mathrm{T}1}(0)$ coincide with $\theta^{(k)}_{\mathrm{T}2}(0)$ for odd k, whereas $\theta^{(k)}_{\mathrm{T}1}(0) = -\theta^{(k)}_{\mathrm{T}2}(0)$ for even k.

The two (standard) transcritical bifurcation curves define the resident-mutant coexistence region. In Figure 4.2 the two curve are first-order approximated by $\theta_{\mathrm{T}i}(\varepsilon) = \theta_{\mathrm{T}i}(0) + \theta^{(1)}_{\mathrm{T}i}(0)\varepsilon$, $i = 1, 2$, for small (positive and negative) ε. Locally to $(\bar x, \bar x)$, the coexistence region is a cone spanned by the rays within the two angles $\theta_{\mathrm{T}2}(0)$ and $\theta_{\mathrm{T}1}(0)$. Close to the branching bifurcation we certainly have $\theta_{\mathrm{T}2}(0) < \theta_{\mathrm{T}1}(0)$ (see (4.17) and (4.18) with small $|\bar\lambda^{(0,2)}|$), so the cone of coexistence is defined by $\theta_{\mathrm{T}2}(0) < \theta < \theta_{\mathrm{T}1}(0)$. At the bifurcation ($\bar\lambda^{(0,2)} = 0$), the tangent directions to the cone boundaries are respectively vertical

and horizontal, and their curvature is dominated by $\bar{\lambda}^{(0,3)}$ (see (4.20) with $\bar{\lambda}^{(0,2)} = 0$ under (G1)). Generically, we assume

$$\bar{\lambda}^{(0,3)} \neq 0. \tag{G2}$$

4.2.3 Expansion of the dimorphic invasion fitness

As anticipated at the end of Paragraph 4.2.1, the dimorphic invasion fitness $\lambda_2(x_1, x_2, x')$ cannot be Taylor expanded at $(x_1, x_2, x') = (\bar{x}, \bar{x}, \bar{x})$. This is due to the nonsmoothness of the resident-mutant coexistence equilibrium $(\bar{n}_1(x_1, x_2), \bar{n}_2(x_1, x_2))$, e.g. $\bar{n}_1(x_1, x_2)$ approaches $\bar{n}(\bar{x})$ along one of the boundaries of the coexistence region, being zero on the other boundary. The key observation, made in [Durinx, 2008] and [Dercole and Geritz, 2014], is that the equilibrium densities $\bar{n}_1(x_1, x_2)$ and $\bar{n}_2(x_1, x_2)$ can be smoothly defined at $(\bar{x}, \bar{x})$ along each ray $(x_1, x_2) = (\bar{x} + \varepsilon\cos\theta, \bar{x} + \varepsilon\sin\theta)$ with θ in the cone of coexistence ($\theta \in [\theta_{\mathrm{T2}}(0), \theta_{\mathrm{T1}}(0)]$; actually any θ in the interval (4.19a) could be used, though either $\bar{n}_1(x_1, x_2)$ or $\bar{n}_2(x_1, x_2)$ is negative outside the cone).

Specifically, Dercole and Geritz [2014] made use of new variables (following Meszéna et al. [2005] and Dercole and Rinaldi [2008]), the sum of the resident densities $s = n_1 + n_2$ and the relative mutant density $r = n_2/(n_1 + n_2)$ (the inverse transformation giving $n_1 = (1-r)s$ and $n_2 = rs$), and exploited their fast-slow nature for small ε. At constant r, s quickly converges to the *fast-equilibrium manifold* $\{s_f(r, \varepsilon, \theta),\ r \in [0, 1]\}$ connecting the two monomorphic equilibria (see Figure 4.1), so the dynamics of r can be studied by restricting n_1 and n_2 to $(1-r)s_f(r, \varepsilon, \theta)$ and $r\,s_f(r, \varepsilon, \theta)$.

From the resident-mutant model (4.1), the fast-equilibrium manifold is defined by

$$\begin{aligned} 0 &= \dot{n}_1 + \dot{n}_2 \\ &= (1-r)\,g\big((1-r)s_f(r,\varepsilon,\theta), rs_f(r,\varepsilon,\theta), \bar{x}+\varepsilon\cos\theta, \bar{x}+\varepsilon\sin\theta, \bar{x}+\varepsilon\cos\theta\big) \\ &+ \ rg\big((1-r)s_f(r,\varepsilon,\theta), rs_f(r,\varepsilon,\theta), \bar{x}+\varepsilon\cos\theta, \bar{x}+\varepsilon\sin\theta, \bar{x}+\varepsilon\sin\theta\big) \end{aligned} \tag{4.22}$$

whereas the slow dynamics of r restricted to the fast-equilibrium manifold is ruled by

$$\begin{aligned} \dot{r} &= r(1-r)\,g\big((1-r)s_f(r,\varepsilon,\theta), rs_f(r,\varepsilon,\theta), \bar{x}+\varepsilon\cos\theta, \bar{x}+\varepsilon\sin\theta, \bar{x}+\varepsilon\sin\theta\big) \\ &- \ r(1-r)\,g\big((1-r)s_f(r,\varepsilon,\theta), rs_f(r,\varepsilon,\theta), \bar{x}+\varepsilon\cos\theta, \bar{x}+\varepsilon\sin\theta, \bar{x}+\varepsilon\cos\theta\big). \end{aligned}$$

The equilibrium solutions for r are $r = 0$ and $r = 1$, corresponding to the monomorphic equilibria of model (4.1), together with the solutions

$\bar{r}(\varepsilon,\theta) \in [0,1]$ of

$$g\big((1-\bar{r}(\varepsilon,\theta))s_f(\bar{r}(\varepsilon,\theta),\varepsilon,\theta), \bar{r}(\varepsilon,\theta)s_f(\bar{r}(\varepsilon,\theta),\varepsilon,\theta), \bar{x}+\varepsilon\cos\theta, \bar{x}+\varepsilon\sin\theta, \bar{x}+\varepsilon\sin\theta\big) -$$
$$g\big((1-\bar{r}(\varepsilon,\theta))s_f(\bar{r}(\varepsilon,\theta),\varepsilon,\theta), \bar{r}(\varepsilon,\theta)s_f(\bar{r}(\varepsilon,\theta),\varepsilon,\theta), \bar{x}+\varepsilon\cos\theta, \bar{x}+\varepsilon\sin\theta, \bar{x}+\varepsilon\cos\theta\big) = 0. \tag{4.23}$$

The equilibrium densities $\bar{n}_1(x_1,x_2)$ and $\bar{n}_2(x_1,x_2)$ can then be expressed in terms of (ε,θ) as

$$\bar{n}_1(\varepsilon,\theta) = (1-\bar{r}(\varepsilon,\theta))s_f(\bar{r}(\varepsilon,\theta),\varepsilon,\theta), \quad \bar{n}_2(\varepsilon,\theta) = \bar{r}(\varepsilon,\theta)s_f(\bar{r}(\varepsilon,\theta),\varepsilon,\theta), \tag{4.24}$$

and can be evaluated also at $\varepsilon = 0$ for any given θ in the cone of coexistence, the result being of course θ-dependent (see Tables 4.1 and 4.2, first row).

The dimorphic fitness can be rewritten in terms of ε, θ, and $\Delta x' := x' - \bar{x}$ as

$$\lambda_2(\varepsilon,\theta,\Delta x') :=$$
$$g\big((1-\bar{r}(\varepsilon,\theta))s_f(\bar{r}(\varepsilon,\theta),\varepsilon,\theta), \bar{r}(\varepsilon,\theta)s_f(\bar{r}(\varepsilon,\theta),\varepsilon,\theta), \bar{x}+\varepsilon\cos\theta, \bar{x}+\varepsilon\sin\theta, \bar{x}+\Delta x'\big), \tag{4.25}$$

and can be Taylor expanded around $(\varepsilon,\Delta x') = (0,0)$ at given θ. We proceed up to third order. This involves up to third ε-derivatives of the fast-equilibrium manifold, whereas only the first ε-derivative of the slow equilibrium $\bar{r}$ is involved.

The required zero- and higher-order terms of the fast-equilibrium manifold (w.r.t. ε and mixed (r,ε)) are reported in Table 4.1, whereas those of the slow equilibrium $\bar{r}$ are in Table 4.2. They are obtained by differentiating equations (4.22) and (4.23) at $\varepsilon = 0$ and solving for the unknown terms (see Paragraphs 4.2.3.3 and 4.2.3.4). E.g., equation (4.23) and its first derivative give trivial identities at $\varepsilon = 0$, while the second derivative can be solved for the zero-order term $\bar{r}(0,\theta)$. Note in particular the expression of $\bar{r}(0,\theta)$, which goes from zero to one when θ moves from $\theta_{\mathrm{T2}}(0)$ to $\theta_{\mathrm{T1}}(0)$, i.e., from one extreme to the other of the cone of coexistence, passing through $\frac{1}{2}$ when $\theta = \frac{3}{4}\pi$ (see Table 4.2, first row, and Figure 4.2).

The derivatives $s_f^{(0,k,0)}(r,0,\theta)$, $k \geq 1$, characterize the ε-perturbations of the fast-equilibrium manifold from the zero-order solution $s_f(r,0,\theta) = \bar{n}(\bar{x})$. Note that they are polynomial expressions in r with degree equal to the order of differentiation and coefficients that are ultimately functions of the singular strategy $\bar{x}$ and of the perturbation direction θ. This is due to property P4, where $n_1 + n_2$ becomes $\bar{n}(\bar{x})$ when

$\varepsilon \to 0$, while $n_1^{i_1} n_2^{i_2}$ becomes $(1-r)^{i_1} r^{i_2} \bar{n}(\bar{x})^{i_1+i_2}$. The mixed derivatives of s_f characterize joint (ε, r)-perturbations, i.e., involving both changes in the shape of the manifold and movements along it. Note that they can be simply obtained by r-differentiating $s_f^{(0,k,0)}(r, 0, \theta)$. The derivatives $\bar{r}^{(k,0)}(0, \theta)$, $k \geq 1$, describe how the coexistence equilibrium (4.24) moves from $((1 - \bar{r}(0, \theta))\bar{n}(\bar{x}), \bar{r}(0, \theta)\bar{n}(\bar{x}))$ along the fast-equilibrium manifold when ε is perturbed in the direction θ.

That the third derivative of the slow equilibrium is not needed in the cubic ε-expansion of the dimorphic fitness is easy to note. In fact, if the $\bar{r}$ in front of s_f is ε-differentiated three times, then no differentiation is taken w.r.t. the ε in x_1 and x_2 (the third and fourth arguments of the g-function), so at $x_1 = x_2 = \bar{x}$ the densities n_1 and n_2 (at first and second arguments) sum up due to property P2 and the $\bar{r}$ in front of s_f plays no role in (4.25). And also the third derivative of the $\bar{r}$ at first argument of s_f does not appear, since it is multiplied by the r-derivative of s_f that vanishes with ε, the fast-equilibrium manifold becoming the straight segment $n_1 + n_2 = \bar{n}(\bar{x})$ as $\varepsilon \to 0$ (see Table 4.1, first row). More involved to see is that also the second derivative of the slow equilibrium is not needed. The derivative $\bar{r}^{(2,0)}(0, \theta)$ is, e.g., multiplied by

$$
\begin{aligned}
&s_f^{(1,1,0)}(r, 0, \theta)\, \bar{g}^{(1,0,0,0,0)} + \\
&-\bar{n} \left(\cos\theta\, \bar{g}^{(1,0,1,0,0)} + \sin\theta\, \bar{g}^{(1,0,0,1,0)} - \cos\theta\, \bar{g}^{(0,1,1,0,0)} - \sin\theta\, \bar{g}^{(0,1,0,1,0)} \right)
\end{aligned}
$$

and all of the above terms are generically nonzero. However, their sum vanishes thanks again to property P4.

Taking the results in Tables 4.1 and 4.2 into account, exploiting the properties P1–4 of Paragraph 4.2.1, and assuming genericity (G1), the dimorphic fitness derivatives appearing in the third-order expansion

$$
\begin{aligned}
&\lambda_2(\varepsilon, \theta, \Delta x') = \\
&\bar{\lambda}_2 + \bar{\lambda}_2^{(1,0,0)} \varepsilon + \bar{\lambda}_2^{(0,0,1)} \Delta x' + \\
&\tfrac{1}{2}\, \bar{\lambda}_2^{(2,0,0)} \varepsilon^2 + \bar{\lambda}_2^{(1,0,1)} \varepsilon \Delta x' + \tfrac{1}{2}\, \bar{\lambda}_2^{(0,0,2)} (\Delta x')^2 + \\
&\tfrac{1}{6}\, \bar{\lambda}_2^{(3,0,0)} \varepsilon^3 + \tfrac{1}{2}\, \bar{\lambda}_2^{(2,0,1)} \varepsilon^2 \Delta x' + \tfrac{1}{2}\, \bar{\lambda}_2^{(1,0,2)} \varepsilon (\Delta x')^2 + \tfrac{1}{6}\, \bar{\lambda}_2^{(0,0,3)} (\Delta x')^3 + \\
&O(\|(\varepsilon, \Delta x')\|^4)
\end{aligned}
\tag{4.26}
$$

(overbars here denote evaluations at $(\varepsilon, \Delta x') = (0, 0)$) result as in Table 4.3. Rewriting the dimorphic fitness back in terms of the resident and mutant strategies $(\bar{x} + \Delta x_1, \bar{x} + \Delta x_2, \bar{x} + \Delta x')$, $\Delta x_i := x_i - \bar{x}$,

$s_f(r,0,\theta) = \bar{n}(\bar{x})$

$s_f^{(k,0,0)}(r,0,\theta) = 0$

$s_f^{(0,1,0)}(r,0,\theta) = \big((1-r)\cos\theta + r\sin\theta\big)\bar{n}^{(1)}(\bar{x})$

$s_f^{(0,2,0)}(r,0,\theta) = \big((1-r)\cos\theta + r\sin\theta\big)^2\bar{n}^{(2)}(\bar{x}) - \frac{r(1-r)(\cos\theta-\sin\theta)^2}{\bar{g}^{(1,0,0,0,0)}}(\bar{\lambda}_1^{(0,2)} + \bar{\phi}_{2,1}\bar{n}(\bar{x}))$

$s_f^{(1,1,0)}(r,0,\theta) = (\sin\theta - \cos\theta)\bar{n}^{(1)}(\bar{x})$

$s_f^{(0,3,0)}(r,0,\theta) = \big((1-r)\cos\theta + r\sin\theta\big)^3\bar{n}^{(3)}(\bar{x}) - \frac{r(1-r)(\cos\theta-\sin\theta)^2}{\bar{g}^{(1,0,0,0,0)}}\Big(\big(\cos\theta+\sin\theta\big)(\bar{\lambda}_1^{(0,3)} + \bar{\phi}_{3,1}\bar{n}(\bar{x}))+$
$\big((1-r)\cos\theta + r\sin\theta\big)\Big(\bar{\lambda}_1^{(0,3)} + 3\bar{\lambda}_1^{(1,2)} + \bar{\phi}_{3,2}\bar{n}(\bar{x})^2 + \bar{\phi}_{3,1}\bar{n}(\bar{x}) + 3\bar{\phi}_{2,1}^{(0,0,1)}\bar{n}(\bar{x}) + 3\bar{\phi}_{2,1}\bar{n}^{(1)}(\bar{x}) + 3\bar{\phi}_{2,1}^{(1,0,0)}\bar{n}(\bar{x})\bar{n}^{(1)}(\bar{x}) +$
$-\frac{3}{\bar{g}^{(1,0,0,0,0)}}\big((\bar{\lambda}_1^{(0,2)} + \bar{\phi}_{2,1}\bar{n}(\bar{x}))(\bar{g}^{(1,0,0,0,1)} + \bar{g}^{(2,0,0,0,0)}\bar{n}^{(1)}(\bar{x}) + \bar{\phi}_{1,1}^{(1,0,0)}\bar{n}(\bar{x}) + \bar{\phi}_{1,1})\big)\Big)\Big)$

$s_f^{(2,1,0)}(r,0,\theta) = 0$

$s_f^{(1,2,0)}(r,0,\theta) = 2\big((1-r)\cos\theta + r\sin\theta\big)(\sin\theta - \cos\theta)\bar{n}^{(2)}(\bar{x}) - \frac{(1-2r)(\cos\theta-\sin\theta)^2}{\bar{g}^{(1,0,0,0,0)}}(\bar{\lambda}_1^{(0,2)} + \bar{\phi}_{2,1}\bar{n}(\bar{x}))$

Table 4.1: ε-expansion of the fast-equilibrium manifold $\{s_f(r,\varepsilon,\theta),\, r\in[0,1]\}$ (see Paragraph 4.2.3.3 for computation details).

$$\bar{r}(0,\theta) = \frac{(\cos\theta+\sin\theta)\bar{\lambda}_1^{(0,2)}+2\cos\theta\bar{\lambda}_1^{(1,1)}}{2(\cos\theta-\sin\theta)\bar{\lambda}_1^{(1,1)}}$$

$$\bar{r}^{(1,0)}(0,\theta) = \frac{1}{6(\cos\theta-\sin\theta)\bar{\lambda}_1^{(1,1)}}$$

$$\Big(\bar{\lambda}_1^{(0,3)} + \cos\theta\sin\theta\bar{\lambda}_1^{(0,3)} + 3\cos\theta\big((\cos\theta+\sin\theta)\bar{\lambda}_1^{(1,2)} + \cos\theta\bar{\lambda}_1^{(2,1)}\big) + 3\bar{r}(0,\theta)^2(\cos\theta-\sin\theta)^2(\bar{\lambda}_1^{(2,1)} - \bar{\phi}_{2,1}^{(0,0,1)}\bar{n}(\bar{x}))+$$

$$-3\bar{r}(0,\theta)\Big((\cos\theta-\sin\theta)\big((\cos\theta+\sin\theta)\bar{\lambda}_1^{(1,2)} + 2\cos\theta\bar{\lambda}_1^{(2,1)}\big) - (\cos\theta-\sin\theta)^2\bar{\phi}_{2,1}^{(0,0,1)}\bar{n}(\bar{x})\Big)+$$

$$-3\bar{r}(0,\theta)\big(1-\bar{r}(0,\theta)\big)(\cos\theta-\sin\theta)^2\frac{\bar{g}^{(1,0,0,0,1)}}{\bar{g}^{(1,0,0,0,0)}}(\bar{\lambda}_1^{(0,2)} + \bar{\phi}_{2,1}\bar{n}(\bar{x}))\Big)$$

Table 4.2: ε-expansion of the slow equilibrium $\bar{r}(\varepsilon,\theta)$ (see Paragraph 4.2.3.4 for computation details).

$$\lambda_2(0,\theta,0) = 0$$
$$\lambda_2^{(0,0,q)}(0,\theta,0) = \bar{\lambda}_1^{(0,q)}$$
$$\lambda_2^{(1,0,q)}(0,\theta,0) = ((1-\bar{r}(0,\theta))\cos\theta + \bar{r}(0,\theta)\sin\theta)\bar{\lambda}_1^{(1,q)}$$
$$\lambda_2^{(1,0,0)}(0,\theta,0) = 0$$
$$\lambda_2^{(2,0,0)}(0,\theta,0) = \cos\theta\sin\theta\bar{\lambda}_1^{(0,2)}$$
$$\lambda_2^{(1,0,1)}(0,\theta,0) = -\tfrac{1}{2}(\cos\theta+\sin\theta)\bar{\lambda}_1^{(0,2)}$$
$$\lambda_2^{(3,0,0)}(0,\theta,0) = \cos\theta\sin\theta(\cos\theta+\sin\theta)\left(\bar{\lambda}_1^{(0,3)} - \tfrac{3}{2}\frac{\bar{\lambda}_1^{(0,2)}\bar{\lambda}_1^{(1,2)}}{\bar{\lambda}_1^{(1,1)}}\right)$$
$$\lambda_2^{(2,0,1)}(0,\theta,0) = \tfrac{1}{6}\left(3(\cos\theta+\sin\theta)^2\frac{\bar{\lambda}_1^{(0,2)}\bar{\lambda}_1^{(1,2)}}{\bar{\lambda}_1^{(1,1)}} - 2(\cos\theta\sin\theta+1)\bar{\lambda}_1^{(0,3)}\right)$$
$$\lambda_2^{(1,0,2)}(0,\theta,0) = -\tfrac{1}{2}(\cos\theta+\sin\theta)\frac{\bar{\lambda}_1^{(0,2)}\bar{\lambda}_1^{(1,2)}}{\bar{\lambda}_1^{(1,1)}}$$

Table 4.3: $(\varepsilon,\Delta x')$-expansion of the dimorphic fitness (see Paragraph 4.2.3.2 for computation details).

$i = 1,2$, i.e., recalling the definition (4.13) of the polar coordinates (ε,θ), we then come to following third-order approximation:

$$\tilde{\lambda}_2(\Delta x_1,\Delta x_2,\Delta x') :=$$
$$\left(\tfrac{1}{2}\bar{\lambda}_1^{(0,2)} + \tfrac{1}{6}\bar{\lambda}_1^{(0,3)}(\Delta x_1+\Delta x_2+\Delta x') - \tfrac{1}{4}\frac{\bar{\lambda}_1^{(0,2)}\bar{\lambda}_1^{(1,2)}}{\bar{\lambda}_1^{(1,1)}}(\Delta x_1+\Delta x_2)\right)$$
$$(\Delta x'-\Delta x_1)(\Delta x'-\Delta x_2). \quad (4.27)$$

Note that the right-hand side of equation (4.27) is an expansion taken at given $\theta \in [\theta_{\mathrm{T}2}(0),\theta_{\mathrm{T}1}(0)]$ around $(\varepsilon,\Delta x') = (0,0)$ (the higher-order terms are indeed $O(\|(\varepsilon,\Delta x')\|^4)$), and not an expansion w.r.t. (x_1,x_2,x') around $(\bar{x},\bar{x},\bar{x})$. It can be nevertheless used as an approximation of the dimorphic fitness (4.8) for (x_1,x_2) in the resident-mutant coexistence region locally to $(\bar{x},\bar{x})$ and x' close to $\bar{x}$.

Interestingly, the second-order terms in (4.27) coincide with those obtained by Geritz et al. [1997, 1998] assuming a smooth dimorphic fitness (see equation A10 in [Geritz et al., 1998] Appendix 1; the zero- and first-order terms vanish at the singular point $(\Delta x_1,\Delta x_2,\Delta x') = (0,0,0)$). Thus, the (second-order) branching condition (4.9) of Geritz et al. [1997, 1998] is correct, though we recall that assuming smoothness implies senseless constraints on the monomorphic fitness derivatives (starting with the second-order, see Paragraph 4.2.3.1).

To illustrate our approach at work, the reader can go to Paragraph 4.2.3.2, where we compute the terms involving up to second derivatives of $\lambda_2(\varepsilon, \theta, \Delta x')$ step by step, that allow to recover the classical results of Geritz et al. [1997, 1998]. All other computations can be checked in Dercole et al. [2014].

4.2.3.1 The nonsmoothness of the dimorphic invasion fitness $\lambda_2(\Delta x_1, \Delta x_2, \Delta x')$

In this paragraph we show that assuming the dimorphic fitness $\lambda_2(x_1, x_2, x')$ smooth at $(\bar{x}, \bar{x}, \bar{x})$ brings to the nongeneric constraint

$$\bar{\lambda}_1^{(2,0)} = \bar{\lambda}_1^{(0,2)} \tag{4.28}$$

between the second derivatives of the monomorphic fitness $\lambda_1(x, x')$ at $(\bar{x}, \bar{x})$. And analogous constraints of the form

$$\frac{\partial^k}{\partial x^k} \lambda_1^{(0,1)}(x, x) = 0, \quad k \geq 2, \tag{4.29}$$

are obtained at any order, e.g.

$$\bar{\lambda}_1^{(2,1)} + 2\,\bar{\lambda}_1^{(1,2)} + \bar{\lambda}_1^{(0,3)} = 0 \quad \text{for} \quad k = 2, \tag{4.30a}$$

$$\bar{\lambda}_1^{(3,1)} + 3\,\bar{\lambda}_1^{(2,2)} + 3\,\bar{\lambda}_1^{(1,3)} + \bar{\lambda}_1^{(0,4)} = 0 \quad \text{for} \quad k = 3 \tag{4.30b}$$

(see Dercole et al. [2014]; note that, taking equation (4.11b) into account, also (4.28) is of the form (4.29) for $k = 1$). The smoothness of the dimorphic fitness would therefore imply that the selection gradient $\lambda_1^{(0,1)}(x, x)$ vanishes at $x = \bar{x}$ together with all its derivatives, whereas all such derivatives are generically expected to be nonzero (though some of them might vanish in specific models due to symmetries in the trait dependencies).

To show equation (4.28) we exploit the consistency properties C1–3 of section 4.2.1 and, in particular, their derivatives w.r.t. (x, x') (C1) (x_1, x_2, x') (C2) (x_1, x_2) (C3) at $x = x_1 = x_2 = x' = \bar{x}$, that can be taken under smoothness. Specifically, C1 and its second x-derivative give

C1a: $\bar{\lambda}_2^{(0,0,2)} = \bar{\lambda}_1^{(0,2)}$,

C1b: $\bar{\lambda}_2^{(2,0,0)} + 2\,\bar{\lambda}_2^{(1,1,0)} + \bar{\lambda}_2^{(0,2,0)} = \bar{\lambda}_1^{(2,0)}$,

the second x_1-derivative of C2 gives

C2a: $\bar{\lambda}_2^{(2,0,0)} = \bar{\lambda}_2^{(0,2,0)}$,

and, in C3, the mixed (x_1, x_2)- and the second x_2-derivatives of $\lambda_2(x_1, x_2, x_1) = 0$ give

C3a: $\bar{\lambda}_2^{(1,1,0)} + \bar{\lambda}_2^{(0,1,1)} = 0$,

C3b: $\bar{\lambda}_2^{(0,2,0)} = 0$,

whereas the second x_2-derivative of $\lambda_2(x_1, x_2, x_2) = 0$ gives

C3c: $\bar{\lambda}_2^{(0,2,0)} + 2\,\bar{\lambda}_2^{(0,1,1)} + \bar{\lambda}_2^{(0,0,2)} = 0$.

From C1b-C2a-C3b, we therefore conclude

$$\bar{\lambda}_2^{(1,1,0)} = \tfrac{1}{2}\,\bar{\lambda}_1^{(2,0)}, \tag{4.31}$$

whereas substituting $\bar{\lambda}_2^{(0,1,1)}$ from C3c into C3a and then applying C1a-C3b, we conclude

$$\bar{\lambda}_2^{(1,1,0)} = \tfrac{1}{2}\,\bar{\lambda}_1^{(0,2)}. \tag{4.32}$$

Equation (4.28) evidently follows from (4.31) and (4.32).

4.2.3.2 Derivatives of the dimorphic invasion fitness $\lambda_2(\varepsilon, \theta, \Delta x')$

In this paragraph we make use of the consistency property C1, linking the dimorphic to the monomorphic fitness, and of properties P1–P4 of section 4.2.1 to compute step by step the expansion (4.26) up to second order.

We start by noting that the x'-derivatives of C1 imply

$$\bar{\lambda}_2^{(0,0,q)} = \bar{\lambda}_1^{(0,q)}, \quad q \geq 0, \tag{4.33}$$

and by recalling that over-bars evaluations are taken at $(\varepsilon, \Delta x') = (0,0)$ for $\lambda_2(\varepsilon, \theta, \Delta x')$ and at $(\bar{x}, \bar{x})$ for $\lambda_1(x, x')$. The zero-order term $\bar{\lambda}_2$ and the first-order term $\bar{\lambda}_2^{(0,0,1)}$ are therefore null by the neutrality and singularity conditions (4.10) and (4.5), respectively.

More involved is the computation of the other first-order term, i.e., showing $\bar{\lambda}_2^{(1,0,0)} = 0$ (see Table 4.3). Computing $\bar{\lambda}_2^{(1,0,q)}$, $q \geq 0$, from the λ_2 definition (4.25), we obtain

$$\begin{aligned}\bar{\lambda}_2^{(1,0,q)} = \Big[\; & g^{(1,0,0,0,q)}\big(-\bar{r}^{(1,0)} s_f + (1-\bar{r})\big(s_f^{(1,0,0)}\,\bar{r}^{(1,0)} + s_f^{(0,1,0)}\big)\big) + \\ & g^{(0,1,0,0,q)}\big(\bar{r}^{(1,0)} s_f + \bar{r}\big(s_f^{(1,0,0)}\,\bar{r}^{(1,0)} + s_f^{(0,1,0)}\big)\big) + \\ & g^{(0,0,1,0,q)}\cos\theta + g^{(0,0,0,1,q)}\sin\theta\;\Big]\Big|_{\varepsilon=0,\Delta x'=0},\end{aligned} \tag{4.34}$$

(where functions' arguments, here omitted, are as in (4.25)). The right-hand side of (4.34) simplifies by taking into account that

$$g^{(1,0,0,0,q)}\big|_{\varepsilon=0,\Delta x'=0} = g^{(0,1,0,0,q)}\big|_{\varepsilon=0,\Delta x'=0} = \bar{g}^{(1,0,0,0,q)} \tag{4.35}$$

by P2 and that

$$g^{(0,0,1,0,q)}\big|_{\varepsilon=0,\Delta x'=0} = \bar{\phi}_{1,1}^{(0,0,q)}(1-\bar{r}(0,\theta))\, s_f(\bar{r}(0,\theta),0,\theta), \tag{4.36a}$$

$$g^{(0,0,0,1,q)}\big|_{\varepsilon=0,\Delta x'=0} = \bar{\phi}_{1,1}^{(0,0,q)}\bar{r}(0,\theta)\, s_f(\bar{r}(0,\theta),0,\theta) \tag{4.36b}$$

by P4 and P3,4a, respectively. The result is

$$\bar{\lambda}_2^{(1,0,q)} = \bar{g}^{(1,0,0,0,q)}\big(s_f^{(1,0,0)}(\bar{r}(0,\theta),0,\theta)\,\bar{r}^{(1,0)}(0,\theta) + s_f^{(0,1,0)}(\bar{r}(0,\theta),0,\theta)\big) + \bar{\phi}_{1,1}^{(0,0,q)} s_f(\bar{r}(0,\theta),0,\theta)\big((1-\bar{r}(0,\theta))\cos\theta + \bar{r}(0,\theta)\sin\theta\big). \tag{4.37}$$

Substituting in (4.37) the expressions in Table 4.1 for the fast-equilibrium manifold $s_f(\bar{r}(0,\theta),0,\theta)$ and for the derivatives $s_f^{(1,0,0)}(\bar{r}(0,\theta),0,\theta)$ and $s_f^{(0,1,0)}(\bar{r}(0,\theta),0,\theta)$ (computed below in section 4.2.3.3), we obtain

$$\bar{\lambda}_2^{(1,0,q)} = \big(\bar{g}^{(1,0,0,0,q)}\bar{n}^{(1)} + \bar{\phi}_{1,1}^{(0,0,q)}\bar{n}\big)\big((1-\bar{r}(0,\theta))\cos\theta + \bar{r}(0,\theta)\sin\theta\big),$$

that further simplifies to

$$\bar{\lambda}_2^{(1,0,q)} = \big((1-\bar{r}(0,\theta))\cos\theta + \bar{r}(0,\theta)\sin\theta\big)\bar{\lambda}_1^{(1,q)} \tag{4.38}$$

by taking equation (4.12) into account. With $q=0$, neutrality (4.11a) and singularity (4.5) yield $\bar{\lambda}_2^{(1,0,0)} = 0$, whereas substituting the expression for $\bar{r}(0,\theta)$ from Table 4.2 (computed below in section 4.2.3.3) into (4.38) with $q=1$, we obtain

$$\bar{\lambda}_2^{(1,0,1)} = -\tfrac{1}{2}(\cos\theta + \sin\theta)\bar{\lambda}_1^{(0,2)},$$

as in Table 4.3.

We finally need to compute $\bar{\lambda}_2^{(2,0,0)}$. Again from the λ_2 definition

(4.25), we have

$$\begin{aligned}\bar{\lambda}_2^{(2,0,0)} = \Big[\Big(&g^{(2,0,0,0,0,0)}\left(-\bar{r}^{(1,0)}s_f+(1-\bar{r})\left(s_f^{(1,0,0)}\bar{r}^{(1,0)}+s_f^{(0,1,0)}\right)\right)+\\ &g^{(1,1,0,0,0,0)}\left(\bar{r}^{(1,0)}s_f+\bar{r}\left(s_f^{(1,0,0)}\bar{r}^{(1,0)}+s_f^{(0,1,0)}\right)\right)+g^{(1,0,1,0,0,0)}\cos\theta+g^{(1,0,0,1,0,0)}\sin\theta\Big)\times\\ &\left(-\bar{r}^{(1,0)}s_f+(1-\bar{r})\left(s_f^{(1,0,0)}\bar{r}^{(1,0)}+s_f^{(0,1,0)}\right)\right)+\\ &g^{(1,0,0,0,0,0)}\Big(-\bar{r}^{(2,0)}s_f-2\bar{r}^{(1,0)}\left(s_f^{(1,0,0)}\bar{r}^{(1,0)}+s_f^{(0,1,0)}\right)+\\ &(1-\bar{r})\left(\left(s_f^{(2,0,0)}\bar{r}^{(1,0)}+2s_f^{(1,1,0)}\right)\bar{r}^{(1,0)}+s_f^{(1,0,0)}\bar{r}^{(2,0)}+s_f^{(0,2,0)}\right)\Big)+\\ &\Big(g^{(1,1,0,0,0,0)}\left(-\bar{r}^{(1,0)}s_f+(1-\bar{r})\left(s_f^{(1,0,0)}\bar{r}^{(1,0)}+s_f^{(0,1,0)}\right)\right)+\\ &g^{(0,2,0,0,0,0)}\left(\bar{r}^{(1,0)}s_f+\bar{r}\left(s_f^{(1,0,0)}\bar{r}^{(1,0)}+s_f^{(0,1,0)}\right)\right)+g^{(0,1,1,0,0,0)}\cos\theta+g^{(0,1,0,1,0,0)}\sin\theta\Big)\times\\ &\left(\bar{r}^{(1,0)}s_f+\bar{r}\left(s_f^{(1,0,0)}\bar{r}^{(1,0)}+s_f^{(0,1,0)}\right)\right)+\\ &g^{(0,1,0,0,0,0)}\Big(\bar{r}^{(2,0)}s_f+2\bar{r}^{(1,0)}\left(s_f^{(1,0,0)}\bar{r}^{(1,0)}+s_f^{(0,1,0)}\right)+\\ &\bar{r}\left(\left(s_f^{(2,0,0)}\bar{r}^{(1,0)}+2s_f^{(1,1,0)}\right)\bar{r}^{(1,0)}+s_f^{(1,0,0)}\bar{r}^{(2,0)}+s_f^{(0,2,0)}\right)\Big)+\\ &\cos\theta\Big(g^{(1,0,1,0,0,0)}\left(-\bar{r}^{(1,0)}s_f+(1-\bar{r})\left(s_f^{(1,0,0)}\bar{r}^{(1,0)}+s_f^{(0,1,0)}\right)\right)+\\ &g^{(0,1,1,0,0,0)}\left(\bar{r}^{(1,0)}s_f+\bar{r}\left(s_f^{(1,0,0)}\bar{r}^{(1,0)}+s_f^{(0,1,0)}\right)\right)+g^{(0,0,2,0,0,0)}\cos\theta+g^{(0,0,1,1,0,0)}\sin\theta\Big)+\\ &\sin\theta\Big(g^{(1,0,0,1,0,0)}\left(-\bar{r}^{(1,0)}s_f+(1-\bar{r})\left(s_f^{(1,0,0)}\bar{r}^{(1,0)}+s_f^{(0,1,0)}\right)\right)+\\ &g^{(0,1,0,1,0,0)}\left(\bar{r}^{(1,0)}s_f+\bar{r}\left(s_f^{(1,0,0)}\bar{r}^{(1,0)}+s_f^{(0,1,0)}\right)\right)+\\ &g^{(0,0,1,1,0,0)}\cos\theta+g^{(0,0,0,2,0,0)}\sin\theta\Big)\Big]\Big|_{\varepsilon=0,\Delta x'=0}. \qquad (4.39)\end{aligned}$$

Applying P2, i.e., taking (4.35) and

$$g^{(2,0,0,0,0,0)}\Big|_{\varepsilon=0,\Delta x'=0}=g^{(1,1,0,0,0,0)}\Big|_{\varepsilon=0,\Delta x'=0}=g^{(0,2,0,0,0,0)}\Big|_{\varepsilon=0,\Delta x'=0}=\bar{g}^{(2,0,0,0,0,0)}$$

into account, the right-hand side of (4.39) simplifies to

$$\begin{aligned}\bar{\lambda}_2^{(2,0,0)} = \Big[&\bar{g}^{(2,0,0,0,0,0)}\left(s_f^{(1,0,0)}\,\bar{r}^{(1,0)}+s_f^{(0,1,0)}\right)^2+\\ &\bar{g}^{(1,0,0,0,0,0)}\left(\left(s_f^{(2,0,0)}\,\bar{r}^{(1,0)}+2s_f^{(1,1,0)}\right)\bar{r}^{(1,0)}+s_f^{(1,0,0)}\,\bar{r}^{(2,0)}+s_f^{(0,2,0)}\right)+\\ &\Big(g^{(1,0,1,0,0,0)}\left(-\bar{r}^{(1,0)}s_f+(1-\bar{r})\left(s_f^{(1,0,0)}\,\bar{r}^{(1,0)}+s_f^{(0,1,0)}\right)\right)+\\ &g^{(0,1,1,0,0,0)}\left(\bar{r}^{(1,0)}s_f+\bar{r}\left(s_f^{(1,0,0)}\,\bar{r}^{(1,0)}+s_f^{(0,1,0)}\right)\right)\Big)2\cos\theta+\\ &\Big(g^{(0,1,0,1,0,0)}\left(\bar{r}^{(1,0)}s_f+\bar{r}\left(s_f^{(1,0,0)}\,\bar{r}^{(1,0)}+s_f^{(0,1,0)}\right)\right)+\\ &g^{(1,0,0,1,0,0)}\left(-\bar{r}^{(1,0)}s_f+(1-\bar{r})\left(s_f^{(1,0,0)}\,\bar{r}^{(1,0)}+s_f^{(0,1,0)}\right)\right)\Big)2\sin\theta+\\ &g^{(0,0,2,0,0,0)}\cos^2\theta+2g^{(0,0,1,1,0,0)}\sin\theta\cos\theta+g^{(0,0,0,2,0,0)}\sin^2\theta\Big]\Big|_{\varepsilon=0,\Delta x'=0}. \qquad (4.40)\end{aligned}$$

Applying P4, P3,4a, and P1–4, i.e.,

$$
\begin{aligned}
g^{(1,0,1,0,0)}\big|_{\varepsilon=0,\Delta x'=0} &= \bar{\phi}_{1,1}+\bar{\phi}_{1,1}^{(1,0,0)}(1-\bar{r}(0,\theta))\,s_f(\bar{r}(0,\theta),0,\theta),\\
g^{(0,1,1,0,0)}\big|_{\varepsilon=0,\Delta x'=0} &= \bar{\phi}_{1,1}^{(1,0,0)}(1-\bar{r}(0,\theta))\,s_f(\bar{r}(0,\theta),0,\theta),\\
g^{(0,1,0,1,0)}\big|_{\varepsilon=0,\Delta x'=0} &= \bar{\phi}_{1,1}+\bar{\phi}_{1,1}^{(1,0,0)}\bar{r}(0,\theta)\,s_f(\bar{r}(0,\theta),0,\theta),\\
g^{(1,0,0,1,0)}\big|_{\varepsilon=0,\Delta x'=0} &= \bar{\phi}_{1,1}^{(1,0,0)}\bar{r}(0,\theta)\,s_f(\bar{r}(0,\theta),0,\theta),\\
g^{(0,0,2,0,0)}\big|_{\varepsilon=0,\Delta x'=0} &= \bar{\phi}_{2,1}(1-\bar{r}(0,\theta))\,s_f(\bar{r}(0,\theta),0,\theta)+\bar{\phi}_{2,2}(1-\bar{r}(0,\theta))^2 s_f(\bar{r}(0,\theta),0,\theta)^2,\\
g^{(0,0,1,1,0)}\big|_{\varepsilon=0,\Delta x'=0} &= \bar{\phi}_{2,2}(1-\bar{r}(0,\theta))\,\bar{r}(0,\theta)\,s_f(\bar{r}(0,\theta),0,\theta)^2,\\
g^{(0,0,0,2,0)}\big|_{\varepsilon=0,\Delta x'=0} &= \bar{\phi}_{2,1}\,\bar{r}(0,\theta)\,s_f(\bar{r}(0,\theta),0,\theta)+\bar{\phi}_{2,2}\,\bar{r}(0,\theta)^2 s_f(\bar{r}(0,\theta),0,\theta)^2,
\end{aligned}
$$

the right-hand side of (4.40) becomes

$$
\begin{aligned}
\bar{\lambda}_2^{(2,0,0)} = {} & \bar{g}^{(2,0,0,0,0)}\Big(s_f^{(1,0,0)}(\bar{r}(0,\theta),0,\theta)\,\bar{r}^{(1,0)}(0,\theta)+s_f^{(0,1,0)}(\bar{r}(0,\theta),0,\theta)\Big)^2+\bar{g}^{(1,0,0,0,0)}\times\\
& \Big(\Big(s_f^{(2,0,0)}(\bar{r}(0,\theta),0,\theta)\,\bar{r}^{(1,0)}(0,\theta)+2s_f^{(1,1,0)}(\bar{r}(0,\theta),0,\theta)\Big)\bar{r}^{(1,0)}(0,\theta)+\\
& s_f^{(1,0,0)}(\bar{r}(0,\theta),0,\theta)\,\bar{r}^{(2,0)}(0,\theta)+s_f^{(0,2,0)}(\bar{r}(0,\theta),0,\theta)\Big)+\\
& 2\Big(\bar{\phi}_{1,1}+\bar{\phi}_{1,1}^{(1,0,0)}s_f(\bar{r}(0,\theta),0,\theta)\Big)\Big((1-\bar{r}(0,\theta))\cos\theta+\bar{r}(0,\theta)\sin\theta\Big)\times\\
& \Big(s_f^{(1,0,0)}(\bar{r}(0,\theta),0,\theta)\,\bar{r}^{(1,0)}(0,\theta)+s_f^{(0,1,0)}(\bar{r}(0,\theta),0,\theta)\Big)+\\
& 2\bar{\phi}_{1,1}s_f(\bar{r}(0,\theta),0,\theta)\bar{r}^{(1,0)}(0,\theta)(\sin\theta-\cos\theta)+\\
& \bar{\phi}_{2,1}s_f(\bar{r}(0,\theta),0,\theta)\Big((1-\bar{r}(0,\theta))\cos^2\theta+\bar{r}(0,\theta)\sin^2\theta\Big)+\\
& \bar{\phi}_{2,2}s_f(\bar{r}(0,\theta),0,\theta)^2\Big((1-\bar{r}(0,\theta))\cos\theta+\bar{r}(0,\theta)\sin\theta\Big)^2. \qquad (4.41)
\end{aligned}
$$

Substituting in (4.41) the fast-equilibrium manifold $s_f(\bar{r}(0,\theta),0,\theta)$ and its derivatives from Table 4.1, we obtain

$$
\begin{aligned}
\bar{\lambda}_2^{(2,0,0)} = {} & \Big(\bar{g}^{(2,0,0,0,0)}(\bar{n}^{(1)})^2+2\Big(\bar{\phi}_{1,1}+\bar{\phi}_{1,1}^{(1,0,0)}\bar{n}\Big)\bar{n}^{(1)}+\bar{g}^{(1,0,0,0,0)}\bar{n}^{(2)}+\bar{\phi}_{2,1}\bar{n}+\bar{\phi}_{2,2}\bar{n}^2\Big)\times\\
& \Big((1-\bar{r}(0,\theta))\cos\theta+\bar{r}(0,\theta)\sin\theta\Big)^2\\
& +2\bar{r}^{(1,0)}(0,\theta)(\sin\theta-\cos\theta)\Big(\bar{g}^{(1,0,0,0,0)}\bar{n}^{(1)}+\bar{\phi}_{1,1}\bar{n}\Big)+\\
& -\bar{\lambda}_1^{(0,2)}\bar{r}(0,\theta)(1-\bar{r}(0,\theta))(\cos\theta-\sin\theta)^2, \qquad (4.42)
\end{aligned}
$$

that further simplifies taking (4.12) into account and noting that, from the definition (4.2) of the resident equilibrium and P1,4, it results

$$
\bar{n}^{(1)} = -\frac{\bar{\phi}_{1,1}\bar{n}+\bar{g}^{(0,0,0,0,1)}}{\bar{g}^{(1,0,0,0,0)}} \overset{(4.5,4.12)}{=} -\frac{\bar{\phi}_{1,1}\bar{n}}{\bar{g}^{(1,0,0,0,0)}}. \qquad (4.43)
$$

Thanks to (4.43) we lose the $\bar{r}^{(1,0)}(0,\theta)$-term in (4.42) and obtain

$$\bar{\lambda}_2^{(2,0,0)} = \Big(\bar{g}^{(2,0,0,0,0)}(\bar{n}^{(1)})^2 + 2\big(\bar{\phi}_{1,1} + \bar{\phi}_{1,1}^{(1,0,0)}\bar{n}\big)\bar{n}^{(1)} + \bar{g}^{(1,0,0,0,0)}\bar{n}^{(2)} + \bar{\phi}_{2,1}\bar{n} + \bar{\phi}_{2,2}\bar{n}^2\Big) \times \big((1-\bar{r}(0,\theta))\cos\theta + \bar{r}(0,\theta)\sin\theta\big)^2 - \bar{\lambda}_1^{(0,2)}\bar{r}(0,\theta)(1-\bar{r}(0,\theta))(\cos\theta - \sin\theta)^2,$$

Substituting the expression for $\bar{r}(0,\theta)$ from Table 4.2, we finally obtain the expression in Table 4.3, i.e.,

$$\bar{\lambda}_2^{(2,0,0)} = \cos\theta \sin\theta\, \bar{\lambda}_1^{(0,2)}.$$

4.2.3.3 Derivatives of the fast-equilibrium manifold

The derivatives w.r.t. (r,ε) of the fast-equilibrium manifold $s_f(r,\varepsilon,\theta)$ are obtained by differentiating the definition (4.22) and by applying property P1–P4. For notation convenience, we omit functions' arguments and denote by $g(1)$ and $g(2)$ the evaluations

$$g\big((1-r)s_f(r,\varepsilon,\theta), r\,s_f(r,\varepsilon,\theta), \bar{x}+\varepsilon\cos\theta, \bar{x}+\varepsilon\sin\theta, \bar{x}+\varepsilon\cos\theta\big)$$

and

$$g\big((1-r)s_f(r,\varepsilon,\theta), r\,s_f(r,\varepsilon,\theta), \bar{x}+\varepsilon\cos\theta, \bar{x}+\varepsilon\sin\theta, \bar{x}+\varepsilon\sin\theta\big)$$

appearing in the definition (4.22) (and differing only in the last argument equal to x_1 and x_2, respectively).

First note that the evaluation at $\varepsilon = 0$ of equation (4.22) and P2 give

$$g(s_f(r,0,\theta), 0, \bar{x}, \bar{x}, \bar{x}) = 0, \tag{4.44}$$

that compared with the definition (4.2) of the resident equilibrium gives the zero-order term $s_f(r,0,\theta) = \bar{n}(\bar{x})$ in Table 4.1.

The r-derivative of equation (4.22), i.e.,

$$\Big[(1-r)\Big(g^{(1,0,0,0,0)}(1)\big(-s_f+(1-r)s_f^{(1,0,0)}\big)+g^{(0,1,0,0,0)}(1)\big(s_f+rs_f^{(1,0,0)}\big)\Big)-g(1)+ r\Big(g^{(1,0,0,0,0)}(2)\big(-s_f+(1-r)s_f^{(1,0,0)}\big)+g^{(0,1,0,0,0)}(2)\big(s_f+rs_f^{(1,0,0)}\big)\Big)+g(2)\Big]\Big|_{\varepsilon=0}=0,$$

simplifies to

$$\bar{g}^{(1,0,0,0,0)}s_f^{(1,0,0)}(r,0,\theta) = 0$$

using P2 (i.e., taking (4.35) into account) and noting that

$$g(1)|_{\varepsilon=0} = g(2)|_{\varepsilon=0} = g(s_f(r,0,\theta),0,\bar{x},\bar{x},\bar{x}) = 0$$

by equation (4.44). Being $\bar{g}^{(1,0,0,0,0)} < 0$ by the hyperbolic stability of the resident equilibrium $\bar{n}(\bar{x})$, we conclude $s_f^{(1,0,0)}(r,0,\theta) = 0$ (as in Table 4.1).

The ε-derivative of equation (4.22), i.e.,

$$\Big[(1-r)\Big(g^{(1,0,0,0,0)}(1)(1-r)s_f^{(0,1,0)} + g^{(0,1,0,0,0)}(1)rs_f^{(0,1,0)} + g^{(0,0,1,0,0)}(1)\cos\theta + g^{(0,0,0,1,0)}(1)\sin\theta + g^{(0,0,0,0,1)}(1)\cos\theta\Big) + r\Big(g^{(1,0,0,0,0)}(2)(1-r)s_f^{(0,1,0)} + g^{(0,1,0,0,0)}(2)rs_f^{(0,1,0)} + g^{(0,0,1,0,0)}(2)\cos\theta + g^{(0,0,0,1,0)}\sin\theta + g^{(0,0,0,0,1)}(2)\sin\theta\Big)\Big]\Big|_{\varepsilon=0} = 0,$$

simplifies to

$$\bar{g}^{(1,0,0,0,0)}s_f^{(0,1,0)}(r,0,\theta) + \big(\bar{\phi}_{1,1}\bar{n} + \bar{g}^{(0,0,0,0,1)}\big)\big((1-r)\cos\theta + r\sin\theta\big) = 0$$

using P2 (i.e., taking (4.35) into account), P4, and P3,4. Then, using equation (4.43), we obtain

$$s_f^{(0,1,0)}(r,0,\theta) = \big((1-r)\cos\theta + r\sin\theta\big)\bar{n}^{(1)}$$

(as in Table 4.1).

The computation of the derivatives $s_f^{(1,1,0)}(r,0,\theta)$ and $s_f^{(0,2,0)}(r,0,\theta)$ that appear in equation (4.41) can be found in Dercole et al. [2014].

4.2.3.4 Derivatives of the slow equilibrium

The derivatives w.r.t. ε of the slow equilibrium $r(\varepsilon,\theta)$ are obtained by ε-differentiating the definition (4.23) and by applying property P1–P4. For notation convenience, we omit functions' arguments and denote by $g(1)$ and $g(2)$ the evaluations

$$g\big((1-\bar{r}(\varepsilon,\theta))s_f(\bar{r}(\varepsilon,\theta),\varepsilon,\theta), \bar{r}(\varepsilon,\theta)s_f(\bar{r}(\varepsilon,\theta),\varepsilon,\theta), \bar{x}+\varepsilon\cos\theta, \bar{x}+\varepsilon\sin\theta, \bar{x}+\varepsilon\cos\theta\big)$$

and

$$g\big((1-\bar{r}(\varepsilon,\theta))s_f(\bar{r}(\varepsilon,\theta),\varepsilon,\theta), \bar{r}(\varepsilon,\theta)s_f(\bar{r}(\varepsilon,\theta),\varepsilon,\theta), \bar{x}+\varepsilon\cos\theta, \bar{x}+\varepsilon\sin\theta, \bar{x}+\varepsilon\sin\theta\big)$$

appearing in the definition (4.23) (and differing only in the last argument equal to x_1 and x_2, respectively).

The ε-derivative of (4.23) simply gives

$$g^{(0,0,0,0,1)}(2)\Big|_{\varepsilon=0}\sin\theta - g^{(0,0,0,0,1)}(1)\Big|_{\varepsilon=0}\cos\theta \overset{\text{P2}}{=} \bar{g}^{(0,0,0,0,1)}(\sin\theta-\cos\theta)=0, \quad (4.45)$$

as all derivatives not involving the last argument cancel in the difference $g(2) - g(1)$. equation (4.45) is however an identity, being $\bar{g}^{(0,0,0,0,1)} = \bar{\lambda}_1^{(0,1)} = 0$ (see equation (4.12) and the singularity condition (4.5)).

We therefore need to take the second ε-derivative of (4.23), i.e.,

$$\Big[\sin\theta\Big(2g^{(1,0,0,0,1)}(2)\big(-\bar{r}^{(1,0)}s_f + (1-\bar{r})\big(s_f^{(1,0,0)}\,\bar{r}^{(1,0)} + s_f^{(0,1,0)}\big)\big) + 2g^{(0,1,0,0,1)}(2)\big(\bar{r}^{(1,0)}s_f + \bar{r}\big(s_f^{(1,0,0)}\,\bar{r}^{(1,0)} + s_f^{(0,1,0)}\big)\big) + 2g^{(0,0,1,0,1)}(2)\cos\theta + 2g^{(0,0,0,1,1)}(2)\sin\theta + g^{(0,0,0,0,2)}(2)\sin\theta\Big) + -\cos\theta\Big(2g^{(1,0,0,0,1)}(1)\big(-\bar{r}^{(1,0)}s_f + (1-\bar{r})\big(s_f^{(1,0,0)}\,\bar{r}^{(1,0)} + s_f^{(0,1,0)}\big)\big) + 2g^{(0,1,0,0,1)}(1)\big(\bar{r}^{(1,0)}s_f + \bar{r}\big(s_f^{(1,0,0)}\,\bar{r}^{(1,0)} + s_f^{(0,1,0)}\big)\big) + 2g^{(0,0,1,0,1)}(1)\cos\theta + 2g^{(0,0,0,1,1)}(1)\sin\theta + g^{(0,0,0,0,2)}(1)\cos\theta\Big)\Big]\Big|_{\varepsilon=0} = 0,$$

that simplifies into

$$2\,\bar{g}^{(1,0,0,0,1)}\big(s_f^{(1,0,0)}(\bar{r}(0,\theta),0,\theta)\,\bar{r}^{(1,0)}(0,\theta) + s_f^{(0,1,0)}(\bar{r}(0,\theta),0,\theta)\big) + 2\,\bar{\phi}_{1,1}^{(0,0,1)}s_f(\bar{r}(0,\theta),0,\theta)\big((1-\bar{r}(0,\theta))\cos\theta + \bar{r}(0,\theta)\sin\theta\big) + \bar{g}^{(0,0,0,0,2)}(\sin\theta+\cos\theta) = 0 \quad (4.46)$$

using P2, P4, and P3,4 (i.e., taking (4.35) and (4.36) into account) and removing the factor $(\sin\theta - \cos\theta) \neq 0$ (see equation (4.19b)). Substituting in (4.46) the expressions in Table 4.1 for the fast-equilibrium manifold $s_f(\bar{r}(0,\theta),0,\theta)$ and for the derivatives $s_f^{(1,0,0)}(\bar{r}(0,\theta),0,\theta)$ and $s_f^{(0,1,0)}(\bar{r}(0,\theta),0,\theta)$ (computed in section 4.2.3.3), we obtain

$$2\big(\bar{g}^{(1,0,0,0,1)}\bar{n}^{(1)} + \bar{\phi}_{1,1}^{(0,0,1)}\bar{n}\big)\big((1-\bar{r}(0,\theta))\cos\theta + \bar{r}(0,\theta)\sin\theta\big) + \bar{g}^{(0,0,0,0,2)}(\sin\theta+\cos\theta) = 0, \quad (4.47)$$

from which, taking equations (4.12) into account, we conclude

$$\bar{r}(0,\theta) = \frac{(\cos\theta+\sin\theta)\bar{\lambda}_1^{(0,2)} + 2\cos\theta\bar{\lambda}_1^{(1,1)}}{2(\cos\theta-\sin\theta)\bar{\lambda}^{(1,1)}}$$

(as in Table 4.2).

The computation of the first derivative $r^{(1,0)}(0,\theta)$, needed for the third-order in the expansion (4.26), can be found in Dercole et al. [2014].

4.2.3.5 The case of polymorphic and/or multispecies coevolution

We allow in this appendix the resident and mutant populations 1 and 2 to interact and coevolve with P other populations of the same or different species, with densities packed in vector $N(t) \in \mathbb{R}^P$ and corresponding strategies (finitely different from x_1 and x_2 in the case of conspecifics) packed in vector X (multiple, mutationally independent, traits per population are also allowed Dercole and Rinaldi [2008]).

The resident-mutant model (4.1) then becomes

$$\begin{aligned} \dot{n}_1 &= n_1\, g(n_1, n_2, N, x_1, x_2, X, x_1), && \text{(4.48a)} \\ \dot{n}_2 &= n_2\, g(n_1, n_2, N, x_1, x_2, X, x_2), && \text{(4.48b)} \\ \dot{N} &= F(n_1, n_2, N, x_1, x_2, X), && \text{(4.48c)} \end{aligned}$$

where the function vector F collects the population growth rates of the P other populations (each component given by the density N_p multiplied by the per-capita growth rate $f_p(n_1, n_2, N, x_1, x_2, X)$ of population p, $p = 1, \ldots, P$) and $g(n_1, n_2, N, x_1, x_2, X, x')$ is the new g-function. Properties P1–P4 easily extend to the new g and also apply to vector F. E.g., property P1 defines the functions

$$\begin{aligned} g_1(n_1, N, x_1, X, x') &:= g(n_1, 0, N, x_1, x_2, X, x'), \\ F_1(n_1, N, x_1, X) &:= F(n_1, 0, N, x_1, x_2, X), \end{aligned}$$

and P4 reads

$$g^{(0,0,0,d_1,0,0,0)}(n_1,n_2,N,x,x,X,x') = \sum_{i_1=1}^{d_1} \phi_{d_1,i_1}(n_1+n_2,N,x,X,x')\, n_1^{i_1},$$

$$g^{(0,0,0,d_1,d_2,0,0)}(n_1,n_2,N,x,x,X,x') = \sum_{i_1=1}^{d_1} \sum_{i_2=1}^{d_2} \phi_{d_1,d_2,i_1,i_2}(n_1+n_2,N,x,X,x')\, n_1^{i_1} n_2^{i_2},$$

$$F^{(0,0,0,d_1,0,0)}(n_1,n_2,N,x,x,X) = \sum_{i_1=1}^{d_1} \psi_{d_1,i_1}(n_1+n_2,N,x,X)\, n_1^{i_1},$$

$$F^{(0,0,0,d_1,d_2,0)}(n_1,n_2,N,x,x,X) = \sum_{i_1=1}^{d_1} \sum_{i_2=1}^{d_2} \psi_{d_1,d_2,i_1,i_2}(n_1+n_2,N,x,X)\, n_1^{i_1} n_2^{i_2},$$

for suitable new functions ϕ_{d_1,i_1} and ϕ_{d_1,d_2,i_1,i_2} and suitable function vectors ψ_{d_1,i_1} and ψ_{d_1,d_2,i_1,i_2} (with relations $\psi_{1,1,1,1} = \psi_{2,2}$, $\psi_{2,1,1,1} = \psi_{1,2,1,1} = \frac{1}{3}\psi_{3,2}$, $\psi_{2,1,2,1} = \psi_{1,2,1,2} = \psi_{3,3}$, analogous to P1–4), $d_1, d_2 \geq 1$ [Dercole, 2014].

We assume that for all values of the strategies x_1 and X that we consider, population 1 stationarily coexists with the other P interacting populations at a strictly positive and (hyperbolically) stable equilibrium of model (4.48a,c) with $n_2 = 0$. The resident equilibrium densities, denoted with functions $\bar{n}(x_1, X)$ and $\bar{N}(x_1, X)$, are

implicitly defined by

$$\begin{aligned} g_1(\bar{n}(x_1,X),\bar{N}(x_1,X),x_1,X,x_1) &= 0, \\ F_1(\bar{n}(x_1,X),\bar{N}(x_1,X),x_1,X) &= 0. \end{aligned}$$

The hyperbolic stability of the resident equilibrium is given by the negative real part of the eigenvalues of the Jacobian matrix

$$J(x_1,X) = \left[\begin{matrix} ng_1^{(1,0,0,0,0)} & ng_1^{(0,1,0,0,0)} \\ F_1^{(1,0,0,0)} & F_1^{(0,1,0,0)} \end{matrix}\right]\Bigg|_{\substack{n=\bar{n}(x_1,X),\\ N=\bar{N}(x_1,X)}}$$

and guarantees that also population 2 is able to coexist with the other P interacting populations at a strictly positive (and hyperbolically stable) equilibrium $(\bar{n}(x_2,X),\bar{N}(x_2,X))$ of model (4.48 b, c) with $n_1 = 0$ and $x_1 \simeq x_2$. Thus, the resident-mutant model (4.48) admits the two monomorphic equilibria $(\bar{n}(x_1,X),0,\bar{N}(x_1,X))$ and $(0,\bar{n}(x_2,X),\bar{N}(x_2,X))$ for all x_1, x_2, and X that we consider.

The invasion fitness for a mutant strategy $x' \simeq x$ is given by

$$\lambda_1(x,X,x') := g_1(\bar{n}(x,X),\bar{N}(x,X),x,X,x').$$

Analogously, to characterize the joint evolution of strategies (x,X), one has to write the invasion fitnesses for the mutants of each of the resident strategies in X, that are each based on the corresponding resident-mutant model Dercole and Rinaldi [2008]. The result is the AD canonical equation

$$\dot{x} = \tfrac{1}{2}\mu(x)\sigma(x)^2\bar{n}(x,X)\lambda_1^{(0,0,1)}(x,X,x), \tag{4.49a}$$

$$\dot{X} = \cdots \tag{4.49b}$$

Here we do not explicitly consider the evolution of the strategies in X, but rather treat X as a vector of constant parameters. We assume that $(\bar{x},\bar{X})$ is a stable equilibrium of the canonical equation (4.49) (a convergence-stable *singular coalition* of strategies, in the AD jargon), i.e., $\bar{\lambda}_1^{(0,0,1)} = 0$ holds together with similar relations for the selection gradients associated to the strategies in X (over-bars here denote evaluations at the singular coalition). For any given X sufficiently close to $\bar{X}$, we define the function $\bar{x}(X)$ as the singular value for the strategy x at the given X, i.e.,

$$\lambda_1^{(0,0,1)}(\bar{x}(X),X,\bar{x}(X)) = 0, \quad \bar{x}(\bar{X}) = \bar{x}, \tag{4.50}$$

as if the strategies in X were not subject to the mutation-selection process. Note that $\bar{x}(X)$ is uniquely defined by (4.50) locally to $X = \bar{X}$ (by the implicit function theorem) under

$$\bar{\lambda}_1^{(1,0,1)} + \bar{\lambda}_1^{(0,0,2)} \neq 0, \tag{4.51}$$

which is granted by the resident-mutant coexistence condition (G1), now rewritten as

$$\bar{\lambda}_1^{(1,0,1)} < 0, \tag{C.G1}$$

and by the proximity to the branching bifurcation at which $\bar{\lambda}_1^{(0,0,2)} = 0$. The quantity in (4.51) is hence negative and excludes that a saddle-node bifurcation between two solutions for $\bar{x}(X)$ could occur for X close to $\bar{X}$ (see also the comment below equation (4.18)).

Then, our analysis in Sects. 4.2.2 and 4.2.3 goes through (with the complicacy of the P extra coexisting populations, see Dercole et al. [2014] for the details). Specifically, under (C.G1), a locally conical resident-mutant coexistence region is rooted at $(\bar{x}(X), \bar{x}(X))$ in the strategy plane (x_1, x_2) and, for each point of the region, the coexistence equilibrium densities $\bar{n}_1(x_1, x_2, X)$, $\bar{n}_2(x_1, x_2, X)$, and $\bar{N}(x_1, x_2, X)$ are positive and defined by

$$\begin{aligned} g(\bar{n}_1(x_1,x_2,X), \bar{n}_2(x_1,x_2,X), \bar{N}(x_1,x_2,X), x_1, x_2, X, x_1) &= 0, \\ g(\bar{n}_1(x_1,x_2,X), \bar{n}_2(x_1,x_2,X), \bar{N}(x_1,x_2,X), x_1, x_2, X, x_2) &= 0, \\ F(\bar{n}_1(x_1,x_2,X), \bar{n}_2(x_1,x_2,X), \bar{N}(x_1,x_2,X), x_1, x_2, X) &= 0. \end{aligned}$$

The coexistence region boundaries can be approximated as in section 4.2.2, where now

$$x_1 := \bar{x}(X) + \varepsilon \cos\theta \quad \text{and} \quad x_2 := \bar{x}(X) + \varepsilon \sin\theta. \tag{4.52}$$

The tangent direction and the curvature of the boundaries at $(\bar{x}(X), \bar{x}(X))$ are given by formulas that are formally analogous to those in equations (4.17), (4.20), and (4.21), with the difference that the derivatives of $\lambda_1(x, X, x')$ are now evaluated at $(\bar{x}(X), X, \bar{x}(X))$ and not at $(\bar{x}, \bar{X}, \bar{x})$. For this, we use over-hats (evaluation at the singular strategy $\bar{x}(X)$) instead of over-bars (evaluation at the singular coalition $(\bar{x}, \bar{X})$):

$$\tan\theta_{\mathrm{T}0}(0) = \frac{1}{\tan\theta_{\mathrm{T}1}(0)} = -\frac{2\hat{\lambda}^{(1,0,1)} + \hat{\lambda}^{(0,0,2)}}{\hat{\lambda}^{(0,0,2)}} \overset{(4.11\mathrm{b})}{=} \frac{\hat{\lambda}^{(2,0,0)}}{\hat{\lambda}^{(0,0,2)}}$$

and

$$\theta^{(1)}_{\mathrm{T}0}(0)=\theta^{(1)}_{\mathrm{T}1}(0):=$$
$$-\frac{4\left(\hat\lambda^{(1,0,1)}\right)^2\hat\lambda^{(0,0,3)}-2\hat\lambda^{(1,0,1)}\hat\lambda^{(0,0,2)}\left(3\hat\lambda^{(1,0,2)}-\hat\lambda^{(0,0,3)}\right)+\left(\hat\lambda^{(0,0,2)}\right)^2\left(3\hat\lambda^{(2,0,1)}+\hat\lambda^{(0,0,3)}\right)}{6\sqrt{2}\left(2\left(\hat\lambda^{(1,0,1)}\right)^2+2\hat\lambda^{(1,0,1)}\hat\lambda^{(0,0,2)}+\left(\hat\lambda^{(0,0,2)}\right)^2\right)^{3/2}}$$

(recall that $\theta_{\mathrm{T}i^*}(\varepsilon)=\theta_{\mathrm{T}i^*}(0)+\theta^{(1)}_{\mathrm{T}i^*}(0)\varepsilon$, $i^*:=2-i$, $i=1,2$, approximates for small $|\varepsilon|$ the boundary i on which $n_i(x_1,x_2,X)=0$).

For (x_1,x_2) in the resident-mutant coexistence region and $X\simeq\bar X$, the dimorphic fitness reads:

$$\lambda_2(x_1,x_2,X,x'):=g(\bar n_1(x_1,x_2,X),\bar n_2(x_1,x_2,X),\bar N(x_1,x_2,X),x_1,x_2,X,x')$$

(we keep using "monomorphic" and "dimorphic" to denote the situations before and after resident-mutant coexistence, though evolution could be polymorphic due to the presence of other conspecifics). Analogously to what done in section 4.2.3, it can be rewritten in terms of $(\varepsilon,\theta,\Delta X,\Delta x')$, with $\Delta X:=X-\bar X$ and $\Delta x':=x'-\bar x(X)$, as

$$\lambda_2(\varepsilon,\theta,\Delta X,\Delta x'):=$$
$$g\big((1-\bar r(\varepsilon,\theta,X))s_f(\bar r(\varepsilon,\theta,X),\varepsilon,\theta,X),\bar r(\varepsilon,\theta,X)s_f(\bar r(\varepsilon,\theta,X),\varepsilon,\theta,X),N_f(\bar r(\varepsilon,\theta,X),\varepsilon,\theta,X),$$
$$\bar x(X)+\varepsilon\cos\theta,\bar x(X)+\varepsilon\sin\theta,X,\bar x(X)+\Delta x'\big),\quad(4.53)$$

where $\{s_f(r,\varepsilon,\theta,X),N_f(r,\varepsilon,\theta,X),\ r\in[0,1]\}$ is the fast-equilibrium manifold of model (4.48) at which $s:=n_1+n_2$ and N converge at constant r, defined by

$$\begin{aligned}0&=\dot n_1+\dot n_2\\&=(1-r)g((1-r)s_f(r,\varepsilon,\theta),rs_f(r,\varepsilon,\theta),N_f(r,\varepsilon,\theta,X),\bar x+\varepsilon\cos\theta,\bar x+\varepsilon\sin\theta,\bar x+\varepsilon\cos\theta)\\&\quad+rg((1-r)s_f(r,\varepsilon,\theta),rs_f(r,\varepsilon,\theta),N_f(r,\varepsilon,\theta,X),\bar x+\varepsilon\cos\theta,\bar x+\varepsilon\sin\theta,\bar x+\varepsilon\sin\theta),\\0&=\dot N=F((1-r)s_f(r,\varepsilon,\theta),rs_f(r,\varepsilon,\theta),N_f(r,\varepsilon,\theta,X),\bar x+\varepsilon\cos\theta,\bar x+\varepsilon\sin\theta),\end{aligned}$$

and $\bar r(\varepsilon,\theta,X)$ is the equilibrium of the slow variable r (see Dercole et al. [2014]).

The right-hand side of equation (4.53) can be Taylor expanded around $(\varepsilon,\Delta X,\Delta x')=(0,0,0)$ at given θ. However, we exploit again the parametric definition of the singular strategy $\bar x(X)$ in (4.50) and expand equation (4.53) w.r.t. $(\varepsilon,\Delta x')$ around $(0,0)$ at given (X,θ). Then, the analysis of section 4.2.3 applies, so we can write (back in the

variables $\Delta x_1 := x_1 - \bar{x}(X) = \varepsilon\cos\theta$ and $\Delta x_2 := x_2 - \bar{x}(X) = \varepsilon\sin\theta$, see (4.52))

$$\lambda_2(\varepsilon, \theta, \Delta X, \Delta x') = \tilde{\lambda}_2(\Delta x_1, \Delta x_2, \Delta X, \Delta x') + O(\|(\varepsilon, \Delta x')\|^4),$$

with

$$\tilde{\lambda}_2(\Delta x_1, \Delta x_2, \Delta X, \Delta x') :=$$
$$\left(\tfrac{1}{2}\hat{\lambda}_1^{(0,0,2)} + \tfrac{1}{6}\hat{\lambda}_1^{(0,0,3)}(\Delta x_1 + \Delta x_2 + \Delta x') - \tfrac{1}{4}\frac{\hat{\lambda}_1^{(0,0,2)}\hat{\lambda}_1^{(1,0,2)}}{\hat{\lambda}_1^{(1,0,1)}}(\Delta x_1 + \Delta x_2)\right)$$
$$(\Delta x' - \Delta x_1)(\Delta x' - \Delta x_2), \quad (4.54)$$

formally obtained from equation (4.27) replacing the over-bar evaluations with over-hat ones (in Dercole et al. [2014] we have checked that the third-order ΔX-expansion of (4.54) at $\Delta X = 0$ coincides with the third-order expansion of equation (4.53) around $(\varepsilon, \Delta X, \Delta x') = (0, 0, 0)$). Note the new definitions of variables Δx_1 and Δx_2. They respectively measure the horizontal and vertical deviations of x_1 and x_2 from the singular point $(\bar{x}(X), \bar{x}(X))$ in the strategy plane (x_1, x_2). A change in ΔX at constant $(\Delta x_1, \Delta x_2)$ (to be seen in the right-hand side of (4.54) as a change in the over-hat evaluations of λ_1) hence implies a change in (x_1, x_2).

Under

$$\bar{\lambda}_1^{(0,0,3)} \neq 0, \quad \text{(C.G2)}$$

the two canonical models presented in section 4.3, and their unfolding as $\bar{\lambda}_1^{(0,0,2)}$ moves across zero, are also formally valid for any X sufficiently close to $\bar{X}$, provided over-bars are replaced with over-hats and $\bar{x}$ in Figs. 3–5 is interpreted as $\bar{x}(X)$. Note, in particular, that the central panel in the figures occurs when $\hat{\lambda}_1^{(0,0,2)} = 0$ and the discriminant between the top and bottom panels is $\hat{\lambda}_1^{(0,0,3)} \gtrless 0$.

We are now ready to take into account that the strategies in X are coevolving with x according to the canonical equation (4.49) in the monomorphic phase, and with x_1 and x_2 according to the normal

form

$$\begin{aligned}
\dot{x}_1 &= \left(\hat{\lambda}_1^{(1,0,1)}\Delta x_2 + \tfrac{1}{2}\,\hat{\lambda}_1^{(0,0,2)}(\Delta x_1+\Delta x_2)\right)\\
&\quad\left(\tfrac{1}{2}\,\hat{\lambda}_1^{(0,0,2)}+\tfrac{1}{6}\,\hat{\lambda}_1^{(0,0,3)}(2\Delta x_1+\Delta x_2)-\tfrac{1}{4}\,\frac{\hat{\lambda}_1^{(0,0,2)}\hat{\lambda}_1^{(1,0,2)}}{\hat{\lambda}_1^{(1,0,1)}}(\Delta x_1+\Delta x_2)\right)\\
\dot{x}_2 &= \left(\hat{\lambda}_1^{(1,0,1)}\Delta x_1 + \tfrac{1}{2}\,\hat{\lambda}_1^{(0,0,2)}(\Delta x_1+\Delta x_2)\right)\\
&\quad\left(\tfrac{1}{2}\,\hat{\lambda}_1^{(0,0,2)}+\tfrac{1}{6}\,\hat{\lambda}_1^{(0,0,3)}(\Delta x_1+2\Delta x_2)-\tfrac{1}{4}\,\frac{\hat{\lambda}_1^{(0,0,2)}\hat{\lambda}_1^{(1,0,2)}}{\hat{\lambda}_1^{(1,0,1)}}(\Delta x_1+\Delta x_2)\right)\\
\dot{X} &= \cdots
\end{aligned}$$

(see equations (4.60), (4.61), (4.63)) in the dimorphic phase.

If $\bar{\lambda}_1^{(0,0,2)} < 0$ and X is initially sufficiently close to $\bar{X}$, the situation is that of the left panels in Figs. 3–5, so the singular coalition is a terminal point w.r.t. strategy x (possible branching in the strategies in X can be similarly discussed, simply separately focusing on each component of X as "the small x"). Note that if X is not sufficiently close to $\bar{X}$, it might be that $\bar{\lambda}_1^{(0,0,2)} < 0$ and $\hat{\lambda}_1^{(0,0,2)} > 0$, so the right panels apply. An incipient branching is therefore possible in strategy x, but the evolution of X is much faster (X being far from equilibrium) and turns the situation to the left panels before branching could actually develop (thanks to the assumed convergence stability of the singular coalition).

A similar scenario of *missed branching* Kisdi [1999] (see also Paragraph 5.2.3.2 and Landi et al. [2013]) occurs when point $(x_1(t), x_2(t))$, moving in the strategy plane in accordance with the canonical equation (4.55) along an incipient branching, hits the boundaries of the resident-mutant coexistence region, which are moving themselves along with the strategies in X. This is however (generically) not possible if $\bar{\lambda}_1^{(0,0,2)} > 0$ with $X(0)$ sufficiently close to $\bar{X}$. In fact, look at the right panels in Figs. 3–5 and consider an initial condition for the incipient branching that is above the diagonal and on the anti-diagonal $\Delta x_1 + \Delta x_2 = 0$ (i.e., $\Delta x_1(0) = -\varepsilon$, $\Delta x_2(0) = \varepsilon$, $\varepsilon > 0$ small). From equations (4.55a,b) we then see that $\dot{x}_1 < 0$ and $\dot{x}_2 > 0$ have opposite leading terms ($-\dot{x}_1 = \dot{x}_2 = -\frac{1}{2}\,\hat{\lambda}_1^{(1,0,1)}\hat{\lambda}_1^{(0,0,2)}\varepsilon > 0$), so the diversification initially points in the direction of the anti-diagonal. Moreover, the branching population remains initially split into two halves, as we

see from the scaled approximation

$$\tilde{n}_1(\Delta x_1, \Delta x_2) := \frac{\hat{\lambda}_1^{(1,0,1)} \Delta x_2 + \frac{1}{2} \hat{\lambda}_1^{(0,0,2)} (\Delta x_1 + \Delta x_2)}{\Delta x_1 - \Delta x_2}, \quad (4.55a)$$

$$\tilde{n}_2(\Delta x_1, \Delta x_2) := \frac{\hat{\lambda}_1^{(1,0,1)} \Delta x_1 + \frac{1}{2} \hat{\lambda}_1^{(0,0,2)} (\Delta x_1 + \Delta x_2)}{\Delta x_2 - \Delta x_1}, \quad (4.55b)$$

that we have from (4.62), with $\Delta x_1 + \Delta x_2 \simeq 0$ during the initial phase of branching. As a consequence, the strategies in X initially remain under (nearly) neutral selection, the corresponding populations facing half of the x-resident with a trait increased by ε and the other half with the same trait decreased by the same ε. Since the strategies in X were close to equilibrium ($(x, X) \simeq (\bar{x}, \bar{X})$) before the splitting, the same condition is maintained during the initial phase of branching (i.e., X stays close to the null-surface $\dot{X} = 0$). The result is that the evolution of X according to the canonical equation (4.55) is initially slower than the divergence of x_1 from x_2, as it is typically observed in the numerical simulations (see figure 4.7(A)), and slow is also the corresponding movement of the coexistence region boundaries in the plane (x_1, x_2). This prevents missing the branching.

If the initial condition for (x_1, x_2) is not taken on the anti-diagonal (figure 4.7(B)) and/or that for X is not taken at $\bar{X}$ (figure 4.7(C)), the convergence stability of the singular coalition $(\bar{x}, \bar{X})$ and the initial evolution of (x_1, x_2) toward the anti-diagonal (see the right panels in Figs. 3 and 4, where the diagonal and the anti-diagonal respectively are the stable and unstable eigenvectors of the equilibrium $(\bar{x}, \bar{x})$) make branching in strategy x possible from many initial conditions close to $(\bar{x}, \bar{X})$.

4.3 Normal form of the bifurcation

From (4.7) and from the analyses of Paragraphs 4.2.2 and 4.2.3, we now derive two simplified models that approximate the dimorphic evolutionary dynamics locally to a branching point. In the first model, we take into account the curvature of the boundaries of the resident-mutant coexistence region, to preserve the geometric features relating evolutionary trajectories with the boundaries themselves. The curvature of the boundaries is however irrelevant for the branching bifurcation ($\bar{\lambda}^{(0,2)} = 0$ under (G1)), so we ignore it in the second model, that we propose as the "normal form" for the canonical equation at the incipient branching.

First we get rid of the scaling $\frac{1}{2}\,\mu(x_i)\sigma(x_i)^2$, $i=1,2$. Locally to $(\bar{x},\bar{x})$ this can be done by (i) a near-identity coordinate transformation, $z_{1,2}=z_{1,2}(x_1,x_2)$ ($\partial z_i/\partial x_j=1$ if $i=j$, 0 otherwise), whose expansion can be set to eliminate all the derivatives of μ and σ in the expansion of the scaling terms around $x_1=x_2=\bar{x}$; (ii) a time-scaling $\tau=\frac{1}{2}\,\mu(\bar{x})\sigma(\bar{x})^2 t$, τ being the new time. For simplicity, we keep on using variables x_i, actually Δx_i, $i=1,2$, and t for the new variables and time.

Second, we use our radial expansion to approximate the coexistence equilibrium (4.24). The expansion up to first order (in ε), i.e.,

$$\tilde{n}_1(\varepsilon,\theta):=(1-\bar{r}(0,\theta))\bar{n}(\bar{x})+$$
$$\varepsilon\Big((1-\bar{r}(0,\theta))\big((1-\bar{r}(0,\theta)\cos\theta+\bar{r}(0,\theta)\sin\theta)\bar{n}^{(1)}(\bar{x})\big)-\bar{r}^{(1)}(0,\theta)\bar{n}(\bar{x})\Big)=$$
$$\tilde{n}_1(\Delta x_1,\Delta x_2):=-\frac{\bar{\lambda}_1^{(1,1)}\Delta x_2+\frac{1}{2}\,\bar{\lambda}_1^{(0,2)}(\Delta x_1+\Delta x_2)}{(\Delta x_1-\Delta x_2)\bar{\lambda}_1^{(1,1)}}\,\bar{n}(\bar{x})+$$
$$-\frac{1}{24(\Delta x_1-\Delta x_2)\big(\bar{\lambda}_1^{(1,1)}\big)^3}\Bigg(4\bar{\lambda}_1^{(0,3)}\big(\bar{\lambda}_1^{(1,1)}\big)^2\bar{n}(\bar{x})(\Delta x_1^2+\Delta x_1\Delta x_2+\Delta x_2^2)+$$
$$-6\bar{\lambda}^{(0,2)}\bar{\lambda}^{(1,1)}\bar{n}^{(1)}(\bar{x})(\Delta x_1+\Delta x_2)\big(2\bar{\lambda}_1^{(1,1)}\Delta x_2+\bar{\lambda}_1^{(0,2)}(\Delta x_1+\Delta x_2)\big)+$$
$$3\bar{n}(\bar{x})\bar{\lambda}_1^{(0,2)}(-2\bar{\lambda}_1^{(1,1)}\bar{\lambda}_1^{(1,2)}+\bar{\lambda}_1^{(0,2)}\bar{\lambda}_1^{(2,1)})(\Delta x_1+\Delta x_2)^2$$
$$+3\bar{n}(\bar{x})\big(2\bar{\lambda}_1^{(1,1)}\Delta x_1+\bar{\lambda}_1^{(0,2)}(\Delta x_1+\Delta x_2)\big)\big(2\bar{\lambda}_1^{(1,1)}\Delta x_2+\bar{\lambda}_1^{(0,2)}(\Delta x_1+\Delta x_2)\big)$$
$$\Big(\bar{\phi}_{2,1}^{(1,0,0)}\bar{n}(\bar{x})+\frac{\bar{g}^{(1,0,0,0,1)}}{\bar{g}^{(1,0,0,0,0)}}(\bar{\lambda}_1^{(0,2)}-\bar{\phi}_{2,1}\bar{n}(\bar{x}))\Big)\Bigg),\quad(4.56a)$$

$$\tilde{n}_2(\varepsilon,\theta) := \bar{r}(0,\theta)\bar{n}(\bar{x}) + \varepsilon\Big(\bar{r}(0,\theta)\big((1-\bar{r}(0,\theta)\cos\theta+\bar{r}(0,\theta)\sin\theta)\bar{n}^{(1)}(\bar{x})\big)+\bar{r}^{(1)}(0,\theta)\bar{n}(\bar{x})\Big) =$$

$$\tilde{n}_2(\Delta x_1,\Delta x_2) := -\frac{\bar{\lambda}_1^{(1,1)}\Delta x_1+\frac{1}{2}\bar{\lambda}_1^{(0,2)}(\Delta x_1+\Delta x_2)}{(\Delta x_2-\Delta x_1)\bar{\lambda}_1^{(1,1)}}\,\bar{n}(\bar{x}) +$$

$$-\frac{1}{24(\Delta x_2-\Delta x_1)\big(\bar{\lambda}_1^{(1,1)}\big)^3}\Bigg(4\bar{\lambda}_1^{(0,3)}\big(\bar{\lambda}_1^{(1,1)}\big)^2\bar{n}(\bar{x})(\Delta x_1^2+\Delta x_1\Delta x_2+\Delta x_2^2)+$$

$$-6\bar{\lambda}^{(0,2)}\bar{\lambda}^{(1,1)}\bar{n}^{(1)}(\bar{x})(\Delta x_1+\Delta x_2)\big(2\bar{\lambda}_1^{(1,1)}\Delta x_1+\bar{\lambda}_1^{(0,2)}(\Delta x_1+\Delta x_2)\big)+$$

$$3\bar{n}(\bar{x})\bar{\lambda}_1^{(0,2)}(-2\bar{\lambda}_1^{(1,1)}\bar{\lambda}_1^{(1,2)}+\bar{\lambda}_1^{(0,2)}\bar{\lambda}_1^{(2,1)})(\Delta x_1+\Delta x_2)^2$$

$$+3\bar{n}(\bar{x})\big(2\bar{\lambda}_1^{(1,1)}\Delta x_1+\bar{\lambda}_1^{(0,2)}(\Delta x_1+\Delta x_2)\big)\big(2\bar{\lambda}_1^{(1,1)}\Delta x_2+\bar{\lambda}_1^{(0,2)}(\Delta x_1+\Delta x_2)\big)$$

$$\Big(\bar{\phi}_{2,1}^{(1,0,0)}\bar{n}(\bar{x})+\frac{\bar{g}^{(1,0,0,0,1)}}{\bar{g}^{(1,0,0,0,0)}}(\bar{\lambda}_1^{(0,2)}-\bar{\phi}_{2,1}\bar{n}(\bar{x}))\Big)\Bigg), \quad (4.56b)$$

is consistent with our approximation, locally to $(\bar{x},\bar{x})$, of the resident-mutant coexistence region (Paragraph 4.2.2), where, indeed, up to third-order derivatives of the monomorphic fitness are involved. Moreover, by defining the cone boundaries by $\tilde{n}_1(\varepsilon,\theta_{\mathrm{T}1}(\varepsilon))=0$ and $\tilde{n}_2(\varepsilon,\theta_{\mathrm{T}2}(\varepsilon))=0$, we checked that one obtains for $\theta_{\mathrm{T}i}(0)$ and $\theta_{\mathrm{T}i}^{(1)}(0)$ the same results derived in Paragraph 4.2.2 (see equations (4.17) and (4.20)). Note that the symmetry $\tilde{n}_1(\Delta x_2,\Delta x_1)=\tilde{n}_2(\Delta x_1,\Delta x_2)$ is respected by the approximation. Also note the term $(\Delta x_i-\Delta x_j)$, $i\neq j$, at denominator of $\tilde{n}_i(\Delta x_1,\Delta x_2)$, which makes evident the nonsmoothness of functions $\bar{n}_1(x_1,x_2)=0$ and $\bar{n}_2(x_1,x_2)=0$ at $(\bar{x},\bar{x})$.

Instead of using the complicated expressions at numerator in (4.56), we note that the following expressions share the same linear terms:

$$\eta_1(\Delta x_1,\Delta x_2) := \bar{\lambda}_1^{(1,1)}\Delta x_2+\tfrac{1}{2}\bar{\lambda}_1^{(0,2)}(\Delta x_1+\Delta x_2)+$$
$$\tfrac{1}{2}\bar{\lambda}_1^{(1,2)}\Delta x_2(\Delta x_1+\Delta x_2)+\tfrac{1}{2}\bar{\lambda}_1^{(2,1)}\Delta x_2^2+\tfrac{1}{6}\bar{\lambda}_1^{(0,3)}(\Delta x_1^2+\Delta x_1\Delta x_2+\Delta x_2^2), \quad (4.57a)$$

$$\eta_2(\Delta x_1,\Delta x_2) := \bar{\lambda}_1^{(1,1)}\Delta x_1+\tfrac{1}{2}\bar{\lambda}_1^{(0,2)}(\Delta x_1+\Delta x_2)+$$
$$\tfrac{1}{2}\bar{\lambda}_1^{(1,2)}\Delta x_1(\Delta x_1+\Delta x_2)+\tfrac{1}{2}\bar{\lambda}_1^{(2,1)}\Delta x_1^2+\tfrac{1}{6}\bar{\lambda}_1^{(0,3)}(\Delta x_1^2+\Delta x_1\Delta x_2+\Delta x_2^2). \quad (4.57b)$$

The expressions in (4.57) come from a cubic expansion w.r.t. (x_1,x_2)

of $\lambda_1(x_2, x_1)$ and $\lambda_1(x_1, x_2)$, respectively. Specifically,

$$\lambda_1(\bar{x} + \Delta x_2, \bar{x} + \Delta x_1) = \eta_1(\Delta x_1, \Delta x_2)(\Delta x_1 - \Delta x_2) + O(\|(\Delta x_1, \Delta x_2)\|^4),$$
$$\lambda_1(\bar{x} + \Delta x_1, \bar{x} + \Delta x_2) = \eta_2(\Delta x_1, \Delta x_2)(\Delta x_2 - \Delta x_1) + O(\|(\Delta x_1, \Delta x_2)\|^4),$$

so $\eta_i(\Delta x_1, \Delta x_2) = 0$ is a quadratic approximation (in $(\Delta x_1, \Delta x_2)$) of the boundary i of the coexistence region (the one on which $\bar{n}_i(x_1, x_2) = 0$). It is a different approximation w.r.t. $\theta_{\mathrm{T}i}(\varepsilon) = \theta_{\mathrm{T}i}(0) + \theta^{(1)}_{\mathrm{T}i}(0)\varepsilon$, derived in Paragraph 4.2.2, and $\tilde{n}_i(\varepsilon, \theta_{\mathrm{T}i}(\varepsilon)) = 0$, $i = 1, 2$, proposed above. But again, defining function $\theta_{\mathrm{T}i}(\varepsilon)$ by $\eta_i(\varepsilon \cos\theta_{\mathrm{T}i}(\varepsilon), \varepsilon \sin\theta_{\mathrm{T}i}(\varepsilon)) = 0$, we checked that one obtains for $\theta_{\mathrm{T}i}(0)$ and $\theta^{(1)}_{\mathrm{T}i}(0)$ the results derived in Paragraph 4.2.2.

By means of a near-identity coordinate transformation, we can then use

$$\tilde{n}_i(\Delta x_1, \Delta x_2) := \frac{\eta_i(\Delta x_1, \Delta x_2)}{\Delta x_i - \Delta x_j}, \quad i = 1, 2,\ i \neq j, \tag{4.58}$$

as an approximation of $\bar{n}_i(x_1, x_2)$ in the canonical equation (4.7), and $\eta_i(\Delta x_1, \Delta x_2) = 0$ as an approximation of the coexistence region boundaries. Note that the new $\tilde{n}_i(\Delta x_1, \Delta x_2)$, $i = 1, 2$, are positive, by construction, inside the approximated coexistence region (easy to check, e.g., for $0 < \Delta x_2 = -\Delta x_1$).

Third step, we approximate $\lambda_2^{(0,0,1)}(x_1, x_2, x_i)$ using our approximation (4.27), thus obtaining

$$\tilde{\lambda}_2^{(0,0,1)}(\Delta x_1, \Delta x_2, \Delta x_i) := s_i(\Delta x_1, \Delta x_2)(\Delta x_i - \Delta x_j), \quad i = 1, 2,\ i \neq j, \tag{4.59}$$

with

$$s_1(\Delta x_1, \Delta x_2) := \left(\tfrac{1}{2}\,\bar{\lambda}_1^{(0,2)} + \tfrac{1}{6}\,\bar{\lambda}_1^{(0,3)}(2\Delta x_1 + \Delta x_2) - \tfrac{1}{4}\,\frac{\bar{\lambda}_1^{(0,2)}\bar{\lambda}_1^{(1,2)}}{\bar{\lambda}_1^{(1,1)}}(\Delta x_1 + \Delta x_2)\right) \tag{4.60a}$$

$$s_2(\Delta x_1, \Delta x_2) := \left(\tfrac{1}{2}\,\bar{\lambda}_1^{(0,2)} + \tfrac{1}{6}\,\bar{\lambda}_1^{(0,3)}(\Delta x_1 + 2\Delta x_2) - \tfrac{1}{4}\,\frac{\bar{\lambda}_1^{(0,2)}\bar{\lambda}_1^{(1,2)}}{\bar{\lambda}_1^{(1,1)}}(\Delta x_1 + \Delta x_2)\right). \tag{4.60b}$$

Our first simplified model—the one taking the curvature $\theta_{\mathrm{T}i}^{(1)}(0)$ into account—then reads

$$\dot{x}_i = \tilde{n}_i(\Delta x_1, \Delta x_2)\tilde{\lambda}_2^{(0,0,1)}(\Delta x_1, \Delta x_2, \Delta x_i) = \eta_i(\Delta x_1, \Delta x_2)s_i(\Delta x_1, \Delta x_2), \tag{4.61}$$

with $i = 1, 2$. Note the simplification of the differences $(\Delta x_i - \Delta x_j)$ at denominator in equation (4.58) and at numerator in equation (4.59), that makes the model equations polynomial (and therefore smooth!).

Our second model is the most simple form showing the bifurcation, so we call it the "normal form" (though we do not provide a formal proof of the topological equivalence between the truncated normal form and the dimorphic canonical equation (4.7)). It considers only a conical coexistence region $\theta \in [\theta_{\mathrm{T}2}(0), \theta_{\mathrm{T}1}(0)]$ and, consistently, a zero-order approximation (in ε) of the coexistence equilibrium (4.24), i.e.,

$$\begin{aligned} \tilde{n}_1(\varepsilon, \theta) &:= (1 - \bar{r}(0,\theta))\bar{n}(\bar{x}) = \\ \tilde{n}_1(\Delta x_1, \Delta x_2) &:= \frac{\eta_1(\Delta x_1, \Delta x_2)}{\Delta x_1 - \Delta x_2}, \qquad (4.62a) \\ \tilde{n}_2(\varepsilon, \theta) &:= \bar{r}(0,\theta)\bar{n}(\bar{x}) = \\ \tilde{n}_2(\Delta x_1, \Delta x_2) &:= \frac{\eta_2(\Delta x_1, \Delta x_2)}{\Delta x_2 - \Delta x_1}, \qquad (4.62b) \end{aligned}$$

with

$$\begin{aligned} \eta_1(\Delta x_1, \Delta x_2) &:= \bar{\lambda}_1^{(1,1)}\Delta x_2 + \tfrac{1}{2}\bar{\lambda}_1^{(0,2)}(\Delta x_1 + \Delta x_2), \quad (4.63a) \\ \eta_2(\Delta x_1, \Delta x_2) &:= \bar{\lambda}_1^{(1,1)}\Delta x_1 + \tfrac{1}{2}\bar{\lambda}_1^{(0,2)}(\Delta x_1 + \Delta x_2). \quad (4.63b) \end{aligned}$$

The model equations are formally those in (4.61), but with the new definitions of $\tilde{n}_i(\Delta x_1, \Delta x_2)$ and $\eta_i(\Delta x_1, \Delta x_2)$, $i = 1, 2$, in equations (4.62) and (4.63).

The unfolding parameter—that we move across zero—is $\bar{\lambda}^{(0,2)}$. Three other parameters are left in the normal form (4.60, 4.61, 4.63): $\bar{\lambda}^{(1,1)}$, $\bar{\lambda}^{(0,3)}$, and $\bar{\lambda}^{(1,2)}$. The first two are constrained by the genericity conditions (G1) and (G2), whereas $\bar{\lambda}^{(1,2)}$ plays no role in the bifurcation, as it only appears multiplied by $\bar{\lambda}^{(0,2)}$ in $s_i(\Delta x_1, \Delta x_2)$ (equation (4.60)). Only the product $\bar{\lambda}^{(1,1)}\bar{\lambda}^{(0,3)}$ is relevant at the bifurcation ($\bar{\lambda}^{(0,2)} = 0$). Being $\bar{\lambda}^{(1,1)}$ constrained in sign, $\bar{\lambda}^{(0,3)}$ is the only relevant coefficient of the normal form (as already anticipated by Kisdi [1999], without, however, a formal derivation).

Finally, it is important to note that none of the two models (4.57, 4.60, 4.61) and (4.60, 4.61, 4.63) correspond to an ε-expansion of the dimor-

phic canonical equation (4.7). E.g., the first model includes cubic ε-terms—composed of the product of a quadratic terms in $\tilde{\lambda}_2^{(0,0,1)}(\varepsilon,\theta,\Delta x_i)$ and a linear term in $\tilde{n}_1(\varepsilon,\theta)$—but misses others. This is due to the choice of separately ε-expanding $\bar{n}_i(x_1,x_2)$ and $\lambda_2^{(0,0,1)}(x_1,x_2,x_i)$ in equation (4.7), with the advantage of preserving some structural features of the canonical equation, e.g., the presence of boundary equilibria when $\bar{n}_i(x_1,x_2)$ and $\lambda_2^{(0,0,1)}(x_1,x_2,x_j)$ vanish with $i\neq j$.

4.4 Unfolding of the bifurcation

Under the genericity conditions (G1) and (G2), we analyze in this Paragraph the dynamics of model (4.60, 4.61, 4.63), restricted to the resident-mutant coexistence region $\tilde{n}_i(\Delta x_1,\Delta x_2)\geq 0$, $i=1,2$, defined in (4.62, 4.63) (i.e., $\theta\in[\theta_{\mathrm{T}2}(0),\theta_{\mathrm{T}1}(0)]$ see equations (4.17) and (4.21)), by varying the parameter $\bar{\lambda}^{(0,2)}$ across zero.

By inspection of equations (4.60, 4.61, 4.63), it is straightforward to check that there are four equilibria:

E0: $(\Delta\bar{x}_1,\Delta\bar{x}_2)=(0,0)$, at which $\eta_1(\Delta\bar{x}_1,\Delta\bar{x}_2)=\eta_2(\Delta\bar{x}_1,\Delta\bar{x}_2)=0$.

E1: $(\Delta\bar{x}_1,\Delta\bar{x}_2)=-\frac{1}{\bar{\lambda}^{(0,2)}\bar{\lambda}^{(0,3)}-2\bar{\lambda}^{(1,1)}\bar{\lambda}^{(0,3)}+3\bar{\lambda}^{(0,2)}\bar{\lambda}^{(1,2)}}$
$\left(3\left(\bar{\lambda}^{(0,2)}\right)^2,3\bar{\lambda}^{(0,2)}\left(2\bar{\lambda}^{(1,1)}+\bar{\lambda}^{(0,2)}\right)\right)$,
annihilating $\eta_1(\Delta\bar{x}_1,\Delta\bar{x}_2)$ and $s_2(\Delta\bar{x}_1,\Delta\bar{x}_2)$.

E2: $(\Delta\bar{x}_1,\Delta\bar{x}_2)=-\frac{1}{\bar{\lambda}^{(0,2)}\bar{\lambda}^{(0,3)}-2\bar{\lambda}^{(1,1)}\bar{\lambda}^{(0,3)}+3\bar{\lambda}^{(0,2)}\bar{\lambda}^{(1,2)}}$
$\left(3\bar{\lambda}^{(0,2)}\left(2\bar{\lambda}^{(1,1)}+\bar{\lambda}^{(0,2)}\right),3\left(\bar{\lambda}^{(0,2)}\right)^2\right)$,
annihilating $\eta_1(\Delta\bar{x}_1,\Delta\bar{x}_2)$ and $s_2(\Delta\bar{x}_1,\Delta\bar{x}_2)$.

E3: $(\Delta\bar{x}_1,\Delta\bar{x}_2)=\left(-\frac{\bar{\lambda}^{(1,1)}\bar{\lambda}^{(0,2)}}{\bar{\lambda}^{(1,1)}\bar{\lambda}^{(0,3)}-\bar{\lambda}^{(0,2)}\bar{\lambda}^{(1,2)}},\ \Delta\bar{x}_1\right)$, at which $s_1(\Delta\bar{x}_1,\Delta\bar{x}_2)=s_2(\Delta\bar{x}_1,\Delta\bar{x}_2)=0$.

Note that E1 and E2 are symmetric boundary equilibria lying on the coexistence cone boundary on which $\tilde{n}_1(\Delta x_1,\Delta x_2)$ and $\tilde{n}_2(\Delta x_1,\Delta x_2)$ vanish, respectively. E3 lies on the diagonal $\Delta x_1=\Delta x_2$ and is therefore not feasible for the dimorphic canonical equation (4.7).

The four equilibria are all involved in the bifurcation occurring at $\bar{\lambda}^{(0,2)}=0$, as they collide at $(0,0)$ at the bifurcation. Under the genericity conditions (G1) and (G2), equilibria E1–3 intersect transversely as $\bar{\lambda}^{(0,2)}$ moves across zero (transversality of the bifurcation

[Kuznetsov, 2004, Meijer et al., 2009]). The bifurcation classifies as a *non-simple branch point* [Govaerts, 2000, Meijer et al., 2009] (not to be confused with the branching point of AD!), i.e., the transversal intersection of more than two equilibrium branches. This requires the continuation problem [Allgower and Georg, 2003] defining each of the four $\bar{\lambda}^{(0,2)}$-parameterized equilibrium branches in the space $(\Delta\bar{x}_1, \Delta\bar{x}_2, \bar{\lambda}^{(0,2)})$, i.e.,

$$C_i(\Delta x, \bar{\lambda}^{(0,2)}) := \eta_i(\Delta x_1, \Delta x_2, \bar{\lambda}^{(0,2)}) s_i(\Delta x_1, \Delta x_2, \bar{\lambda}^{(0,2)}) = 0, \quad i = 1, 2$$

(where $\Delta x := (\Delta x_1, \Delta x_2)$ and $\bar{\lambda}^{(0,2)}$ is explicitly mentioned as an argument of functions η_i and s_i), to have a null-space with dimension larger than two at the bifurcation. The Jacobian of function $C(\Delta x, \bar{\lambda}^{(0,2)}) := \big(C_1(\Delta x, \bar{\lambda}^{(0,2)}), C_2(\Delta x, \bar{\lambda}^{(0,2)})\big)$ is indeed a (2×3) null matrix at the bifurcation, i.e., the null-space is three-dimensional. Due to the symmetries of the dimorphic canonical equation, this bifurcation can occur as a *codimension-one*, i.e., as a single model parameter is moved (see Govaerts [2000], section 8.2).

Two cases must be distinguished, namely $\bar{\lambda}_1^{(0,3)} > 0$ and $\bar{\lambda}_1^{(0,3)} < 0$, whose unfoldings are pictured in Figure 4.3 (top and bottom panels, respectively). The movements and stability of the four equilibria as $\bar{\lambda}^{(0,2)}$ goes from negative to positive are evident from the graphics. In particular, the flow of model (4.60, 4.61, 4.63) is drawn also outside the resident-mutant coexistence cone to make stability easily readable. Note that the stability for the unrestricted model (4.60, 4.61, 4.63) is different from the stability for the dimorphic canonical equation. E.g., equilibrium E0 is always unstable (saddle type) for model (4.60, 4.61, 4.63), though is stable/unstable for the dimorphic canonical equation when $\bar{\lambda}^{(0,2)} \lessgtr 0$ (evolutionary stability/branching).

Also note that the two cases ($\bar{\lambda}_1^{(0,3)} \gtrless 0$) are topologically equivalent (at the bifurcation there is a symmetry w.r.t. the anti-diagonal $x_1 = -x_2$), so their distinction is not mathematically relevant. However, the distinction is biologically relevant and becomes evident if one considers the curvature of the boundaries of the resident-mutant coexistence region, as we do in model (4.57, 4.60, 4.61). The unfolding of model (4.57, 4.60, 4.61) are show in Figure 4.4 together with the coexistence region $\tilde{n}_i(\Delta x_1, \Delta x_2) \geq 0$, $i = 1, 2$, defined in (4.57, 4.58). Note the different curvatures of the coexistence region boundaries in the two cases (see equation (4.20) that gives the curvature of the locally vertical boundary, $\lessgtr 0$ for $\bar{\lambda}_1^{(0,3)} \gtrless 0$). Then $\bar{\lambda}_1^{(0,3)} \gtrless 0$ makes branching possible at the bifurcation only for mutants with larger/smaller trait values (as already anticipated, without

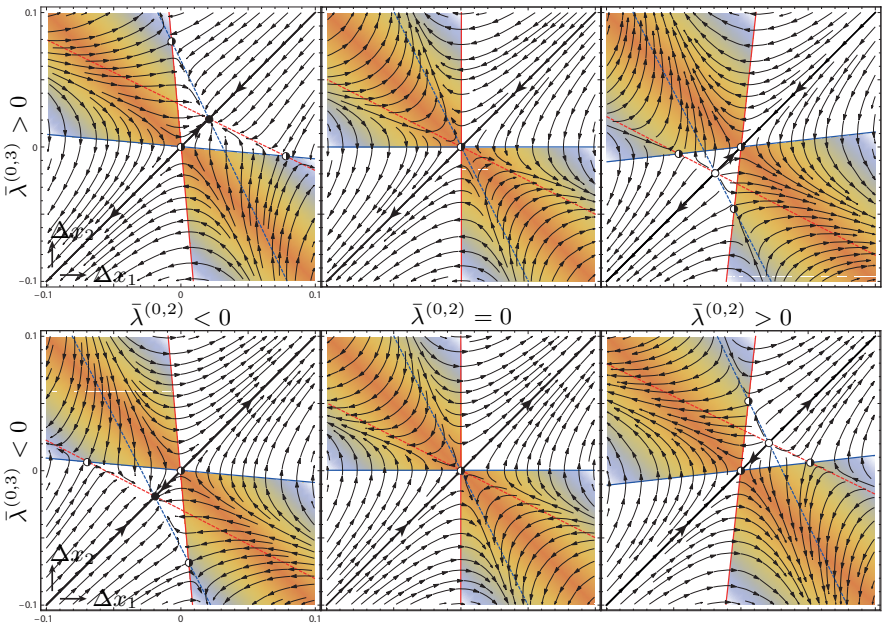

Figure 4.3: Unfolding of the branching bifurcation using model (4.60, 4.61, 4.63). The unfolding parameter $\bar{\lambda}^{(0,2)}$ increases from left to right, and vanishes in the central panels, in which all equilibria E0–4 collide. Top (resp., bottom) row: $\bar{\lambda}^{(0,3)} > 0$ (resp., $\bar{\lambda}^{(0,3)} < 0$). Shaded colored (orange: high total abundance, blue: low total abundance) area: region of resident-mutant coexistence. Blue line: $\eta_1(\Delta x_1, \Delta x_2) = 0$. Red line: $\eta_2(\Delta x_1, \Delta x_2) = 0$. Blue dashed line: $s_1(\Delta x_1, \Delta x_2) = 0$. Red dashed line: $s_1(\Delta x_1, \Delta x_2) = 0$. Full points: stable equilibria. Half-filled points: saddles. Empty points: unstable equilibria.

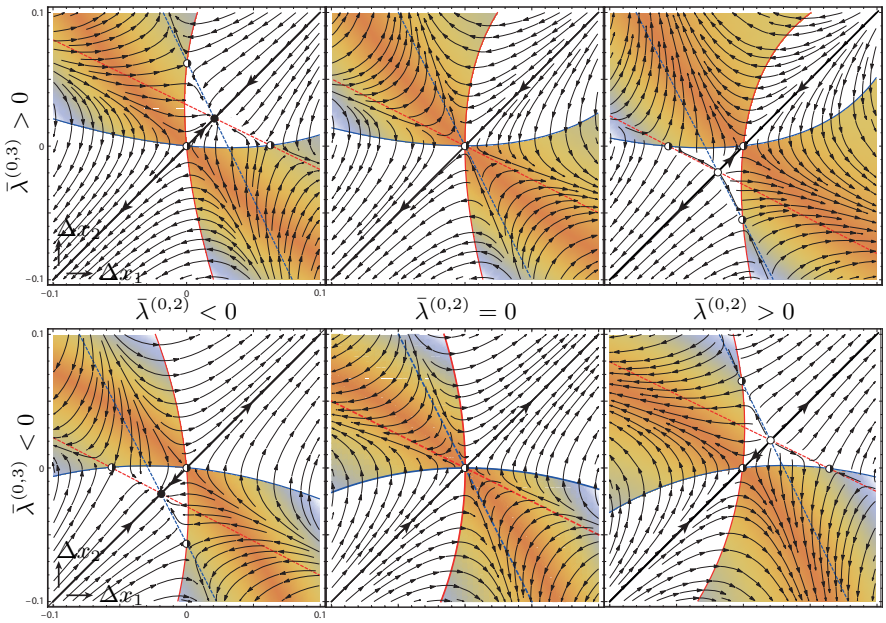

Figure 4.4: Unfolding of the branching bifurcation using model (4.57, 4.60, 4.61). The unfolding parameter $\bar{\lambda}^{(0,2)}$ increases from left to right, and vanishes in the central panels, in which all equilibria E0–4 collide. Top (resp., bottom) row: $\bar{\lambda}^{(0,3)} > 0$ (resp., $\bar{\lambda}^{(0,3)} < 0$). Shaded colored (orange: high total abundance, blue: low total abundance) area: region of resident-mutant coexistence. Blue line: $\eta_1(\Delta x_1, \Delta x_2) = 0$. Red line: $\eta_2(\Delta x_1, \Delta x_2) = 0$. Blue dashed line: $s_1(\Delta x_1, \Delta x_2) = 0$. Red dashed line: $s_1(\Delta x_1, \Delta x_2) = 0$. Full points: stable equilibria. Half-filled points: saddles. Empty points: unstable equilibria.

a formal derivation, in Kisdi [1999]). In any case, under (G2), the singular strategy is a branching point at the bifurcation.

4.5 Examples

4.5.1 Branching in a single species model of asymmetric competition

We first consider the single species AD model of asymmetric competition described in Kisdi [1999]. The resident-mutant model (4.1)

reads:

$$\dot{n}_1 = n_1\big(\rho(x_1) - \alpha(0)n_1 - \alpha(x_1-x_2)n_2\big), \qquad (4.64a)$$
$$\dot{n}_2 = n_2\big(\rho(x_2) - \alpha(x_2-x_1)n_1 - \alpha(0)n_2\big), \qquad (4.64b)$$

with Gaussian $\rho(x) = \exp(-x^2/2\sigma^2)$ and sigmoidal $\alpha(x) = 1 - \frac{1}{1+\nu\exp(-x)}$, $\sigma, \nu > 0$, that is built on the g-function

$$g(n_1, n_2, x_1, x_2, x') = \rho(x') - \alpha(x'-x_1)n_1 - \alpha(x'-x_2)n_2.$$

Model (4.64) is simple enough (Lotka-Volterra competition) that we can solve analytically for all the relevant quantities. That is, the monomorphic and dimorphic resident equilibrium densities

$$\bar{n}(x) = \rho(x)/\alpha(0),$$
$$\bar{n}_1(x_1, x_2) = \frac{\rho(x_1)\alpha(0) - \rho(x_2)\alpha(x_1-x_2)}{\alpha(0)^2 - \alpha(x_1-x_2)\alpha(x_2-x_1)}, \quad \bar{n}_2(x_1, x_2) = n_1(x_2, x_1),$$

the monomorphic and dimorphic fitnesses

$$\lambda_1(x, x') = g(\bar{n}(x), 0, x, x, x') = \rho(x') - \alpha(x'-x)\bar{n}(x),$$
$$\lambda_2(x_1, x_2, x') = g(\bar{n}_1(x_1, x_2), \bar{n}_2(x_1, x_2), x_1, x_2, x') =$$
$$\rho(x') - \alpha(x'-x_1)\bar{n}_1(x_1, x_2) - \alpha(x'-x_2)\bar{n}_2(x_1, x_2),$$

the monomorphic and dimorphic selection gradients

$$\lambda_1^{(0,1)}(x, x) = \rho^{(1)}(x) - \frac{\alpha^{(1)}(0)}{\alpha(0)}\rho(x) = \frac{\sigma^2 - \nu x - x}{\sigma^2(1+\nu)\exp(x^2/2\sigma^2)},$$
$$\lambda_2^{(0,0,1)}(x_1,x_2,x_i) = \rho^{(1)}(x_i) - \alpha^{(1)}(x_i-x_1)\bar{n}_1(x_1,x_2) - \alpha^{(1)}(x_i-x_2)\bar{n}_2(x_1,x_2), \quad i=1,2,$$

the singular strategy

$$\bar{x} = \sigma^2/(1+\nu),$$

annihilating $\lambda_1^{(0,1)}(x, x)$, the fitness second derivatives ruling branching at $\bar{x}$

$$\bar{\lambda}_1^{(1,1)} = \frac{\alpha^{(2)}(0)}{\alpha(0)}\rho(\bar{x}) - \frac{\alpha^{(1)}(0)}{\alpha(0)}\rho^{(1)}(\bar{x}) = -\frac{\nu}{(1+\nu)^2\exp(\sigma^2/2(1+\nu)^2)},$$
$$\bar{\lambda}_1^{(0,2)} = \rho^{(2)}(\bar{x}) - \frac{\alpha^{(2)}(0)}{\alpha(0)}\rho(\bar{x}) = -\frac{(1+\nu)^2 - \nu\sigma^2}{\sigma^2(1+\nu)^2\exp(\sigma^2/2(1+\nu)^2)},$$

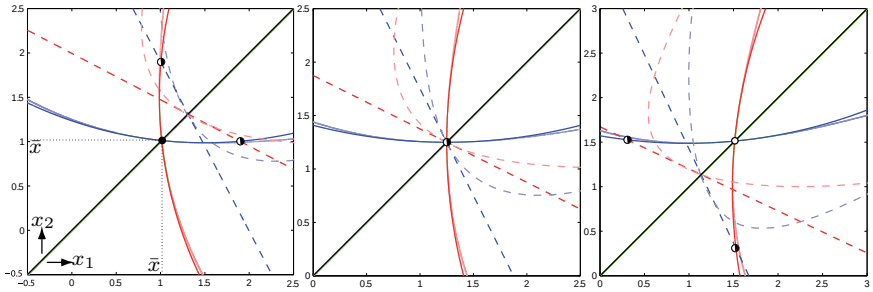

Figure 4.5: Unfolding of the branching bifurcation in the AD model in Kisdi [1999]. The model parameter σ increases from left to right turning the singular strategy $\bar{x}$ from a terminal ($\bar{\lambda}_1^{(0,2)} < 0$) to a branching ($\bar{\lambda}_1^{(0,2)} > 0$) point (other parameter: $\nu = 4$). The approximations $\eta_i(\Delta x_1, \Delta x_2) = 0$ (4.57) and $s_i(\Delta x_1, \Delta x_2) = 0$ (4.60) of the coexistence region boundaries and of the internal x_i-nullcline, $i = 1, 2$, are shown around $(\bar{x}, \bar{x})$ using the same graphical and color codes of figures 4.3–4.4. Lighter colors are used for the fully nonlinear versions: boundary 1, $\lambda_1(x_2, x_1) = 0$; boundary 2, $\lambda_1(x_1, x_2) = 0$; and x_i-nullcline, $\lambda_2^{(0,0,1)}(x_1, x_2, x_i) = 0$.

and the third derivatives entering our approximations

$$\bar{\lambda}_1^{(2,1)} = -\frac{\alpha^{(3)}(0)}{\alpha(0)}\rho(\bar{x}) + 2\frac{\alpha^{(2)}(0)}{\alpha(0)}\rho^{(1)}(\bar{x}) - \frac{\alpha^{(1)}(0)}{\alpha(0)}\rho^{(2)}(\bar{x}) = \frac{\nu^2\sigma^2 - \nu^2 - 2\nu\sigma^2 - 2\nu - 1}{\sigma^2(1+\nu)^3\exp(\sigma^2/2(1+\nu)^2)},$$

$$\bar{\lambda}_1^{(1,2)} = \frac{\alpha^{(3)}(0)}{\alpha(0)}\rho(\bar{x}) - \frac{\alpha^{(2)}(0)}{\alpha(0)}\rho^{(1)}(\bar{x}) = \frac{\nu(3-\nu)}{(1+\nu)^3\exp(\sigma^2/2(1+\nu)^2)},$$

$$\bar{\lambda}_1^{(0,3)} = \rho^{(3)}(\bar{x}) - \frac{\alpha^{(3)}(0)}{\alpha(0)}\rho(\bar{x}) = \frac{\nu^2\sigma^2 + 3\nu^2 - 4\nu\sigma^2 + 6\nu + 3}{\sigma^2(1+\nu)^3\exp(\sigma^2/2(1+\nu)^2)}.$$

It is easy to verify that the singular strategy $\bar{x}$ is attracting the monomorphic evolutionary dynamics for any positive (σ, ν) (eigenvalue $\bar{\lambda}_1^{(1,1)} + \bar{\lambda}_1^{(0,2)} = -(\sigma^2\exp(\sigma^2/2(1+\nu)^2))^{-1} < 0$), that coexistence in its vicinity is always possible ($\bar{\lambda}_1^{(1,1)} < 0$ for $\nu > 0$), and that branching ($\bar{\lambda}_1^{(0,2)} > 0$) occurs for $\sigma^2 > (1+\nu)^2/\nu$. At $\sigma^2 = (1+\nu)^2/\nu$ the system undergoes the branching bifurcation. Increasing the value of σ, we pass from a terminal (figure 4.5 left) to a branching point (figure 4.5 right).

Figure 4.5 compares our approximated model (4.57, 4.60, 4.61) and coexistence region boundaries $\eta_i(\Delta x_1, \Delta x_2) = 0$, $i = 1, 2$ (4.57), with the fully nonlinear versions. As in figures 4.3 and 4.4, the boundary 1 of the coexistence region and the internal x_1-nullcline of the dimorphic evolutionary dynamics are plotted in blue (solid and dashed); red for boundary 2 and the internal x_2-nullcline. Lighter colors are used for the fully nonlinear versions. The values of the model parameters are reported in the caption and those of the genericity conditions left-hand sides, $\bar{\lambda}_1^{(1,1)}$ (G1) and $\bar{\lambda}_1^{(0,3)}$ (G2) can be checked below each figure panel.

4.5.2 Prey branching in a prey-predator community

As a second example, we consider the multi-species prey-predator AD model described in Landi et al. [2013]. Using the notation introduced in Appendix 4.2.3.5, the resident-mutant model (4.1) after a mutation in the prey population reads:

$$\begin{aligned}
\dot{n}_1 &= n_1\Big(r - c(x_1,x_1)n_1 - c(x_1,x_2)n_2 + \\
&- \frac{a(x_1,X)}{1 + a(x_1,X)h(x_1,X)n_1 + a(x_2,X)h(x_2,X)n_2}N\Big), \\
\dot{n}_2 &= n_2\Big(r - c(x_2,x_1)n_1 - c(x_2,x_2)n_2 + \\
&- \frac{a(x_2,X)}{1 + a(x_1,X)h(x_1,X)n_1 + a(x_2,X)h(x_2,X)n_2}N\Big), \\
\dot{N} &= N\Big(e\frac{a(x_1,X)n_1 + a(x_2,X)n_2}{1 + a(x_1,X)h(x_1,X)n_1 + a(x_2,X)h(x_2,X)n_2} - d\Big),
\end{aligned} \tag{4.65}$$

with valley-shaped prey intra-specific competition

$$c(x_1,x_2) = \frac{\gamma_1 + \gamma_2 x_1^2}{1 + \gamma_0(\gamma_1 + \gamma_2 x_1^2)} \exp\big(-\tfrac{1}{4}(x_1 - x_2)^2\big),$$

bell-shaped predator attack rate

$$a(x_1,X) = \alpha_0 + \exp\big(-(x_1 - X)^2\big),$$

and sigmoidal predator handling time

$$h(x_1,X) = \theta\Big(\tfrac{3}{2} - \frac{1}{1 + \exp(\theta_3 x_1)}\Big)\Big(\tfrac{3}{2} - \frac{1}{1 + \exp(-\theta_4 X)}\Big).$$

It is built on the g-function

$$g(n_1, n_2, N, x_1, x_2, X, x') = r - c(x', x_1)n_1 - c(x', x_2)n_2 + \\ - \frac{a(x', X)}{1 + a(x_1, X)h(x_1, X)n_1 + a(x_2, X)h(x_2, X)n_2} N.$$

Analytically, we can only compute the monomorphic resident equilibrium

$$\bar{n}(x, X) = \frac{d}{a(x, X)(e - dh(x, X))},$$
$$\bar{N}(x, X) = \left(\frac{r - c(x, x)\bar{n}(x, X)}{a(x, X)}\right)\big(1 + a(x, X)h(x, X)\bar{n}(x, X)\big),$$

the prey monomorphic fitness

$$\lambda_1(x, X, x') = g(\bar{n}(x, X), 0, \bar{N}(x, X), x, x, X, x') = r - c(x', x)\bar{n}(x, X) \\ - \frac{a(x', X)}{1 + a(x, X)h(x_1, X)\bar{n}(x, X)} \bar{N}(x, X),$$

the selection gradient

$$\lambda_1^{(0,0,1)}(x, X, x) = -c^{(1,0)}(x, x)\bar{n}(x, X) + \\ - \frac{a^{(1,0)}(x, X)}{1 + a(x, X)h(x_1, X)\bar{n}(x, X)} \bar{N}(x, X),$$

and the fitness second and third derivatives, $\lambda_1^{(1,0,1)}$ and $\lambda_1^{(0,0,2)}$ ruling prey branching, and $\lambda_1^{(2,0,1)}$, $\lambda_1^{(1,0,2)}$, and $\lambda_1^{(0,0,3)}$ entering our approximations.

All other relevant quantities must be computed numerically. That is,

- the singular coalition $(\bar{x}, \bar{X})$, by simulating the coevolution of both prey and predator (see Landi et al. [2013] for the modeling of predator mutations),
- the prey singular strategy $\bar{x}(X)$ at frozen predator trait, by solving $\lambda_1^{(0,0,1)}(x, X, x) = 0$ at given X,
- the fitness second and third derivatives $\bar{\lambda}_1^{(1,0,1)}$, $\bar{\lambda}_1^{(0,0,2)}$, $\bar{\lambda}_1^{(2,0,1)}$, $\bar{\lambda}_1^{(1,0,2)}$, and $\bar{\lambda}_1^{(0,0,3)}$, simply evaluating the corresponding analytical expressions at $(\bar{x}, \bar{X})$,

- the boundaries 1 and 2 of the resident-mutant coexistence region rooted at $(\bar{x}(X), \bar{x}(X))$ in the plane (x_1, x_2), by continuing the contour-lines $\lambda_1(x_2, X, x_1) = 0$ and $\lambda_1(x_1, X, x_2) = 0$, respectively,
- the dimorphic resident equilibrium densities $\bar{n}_1(x_1, x_2, X)$, $\bar{n}_2(x_1, x_2, X)$, and $\bar{N}(x_1, x_2, X)$, by continuing the nontrivial equilibrium solution of model (4.65) w.r.t. (x_1, x_2) treated as model parameters,
- the x_i-nullcline of the dimorphic coevolutionary dynamics, by continuing the contour-line

$$\lambda_2^{(0,0,0,1)}(x_1,x_2,X,x_i) = -c^{(1,0)}(x_i,x_1)\bar{n}_1(x_1,x_2,X) - c^{(1,0)}(x_i,x_2)\bar{n}_2(x_1,x_2,X) + \\ - \frac{a^{(1,0)}(x_i,X)}{1+a(x_1,X)h(x_1,X)\bar{n}_1(x_1,x_2,X)+a(x_2,X)h(x_2,X)\bar{n}_2(x_1,x_2,X)}\bar{N}(x_1,x_2,X) = 0,$$

  $i = 1, 2$, together with the equilibrium densities $\bar{n}_1(x_1, x_2, X)$, $\bar{n}_2(x_1, x_2, X)$, and $\bar{N}(x_1, x_2, X)$.

From the analysis in Landi et al. [2013], we know that an attracting singular coalition $(\bar{x}, \bar{X})$ exists for broad ranges of the model parameters and a prey-branching bifurcation occurs by increasing the predator efficiency e (see equation (4.65)). Fixing the model parameters to the values reported in the caption, figure 4.6 compares our approximated model (4.57, 4.60, 4.61) and coexistence region boundaries $\eta_i(\Delta x_1, \Delta x_2) = 0$, $i = 1, 2$ (4.57), with the fully nonlinear versions. As in figures 4.3 and 4.4, the boundary 1 of the coexistence region and the internal x_1-nullcline of the dimorphic coevolutionary dynamics are plotted in blue (solid and dashed); red for boundary 2 and the internal x_2-nullcline. Lighter colors are used for the fully nonlinear versions. The genericity of the bifurcation is granted by the values of $\bar{\lambda}_1^{(1,0,1)}$ (C.G1) and $\bar{\lambda}_1^{(0,0,3)}$ (C.G2) reported below each figure panel.

Figure 4.7 shows three cases of dimorphic coevolutionary dynamics at incipient branching. In case (A), the prey traits are initialized along the anti-diagonal of the coexistence region, i.e.,

$$x_1(0) = \bar{x}(X) + \varepsilon\cos\theta \quad \text{and} \quad x_2(0) = \bar{x}(X) + \varepsilon\sin\theta, \tag{4.66}$$

with $\theta = \frac{3}{4}\pi$, and the predator trait X is initially set at its singular value $\bar{X}$. As predicted by our analysis in Appendix 4.2.3.5 (by the leading terms of the dimorphic normal form (4.55) and by the scaled approximations (4.55a,b) of the coexistence equilibrium densities $\bar{n}_1(x_1, x_2, X)$ and $\bar{n}_2(x_1, x_2, X)$), the prey traits x_1 and x_2 initially

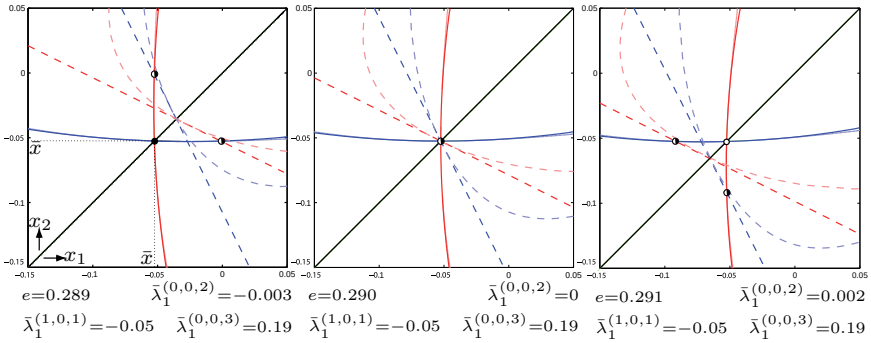

Figure 4.6: Unfolding of the branching bifurcation in the AD model in Landi et al. [2013]. The model parameter e increases from left to right turning the singular coalition $(\bar{x}, \bar{X})$ from a terminal ($\bar{\lambda}_1^{(0,0,2)} < 0$) to a branching ($\bar{\lambda}_1^{(0,0,2)} > 0$) point (other parameters: $r = 0.5$, $d = 0.05$, $\gamma_0 = 0.01$, $\gamma_1 = 0.5$, $\gamma_2 = 2.3$, $\alpha_0 = 0.01$, $\theta = 0.5$, $\theta_3 = \theta_4 = 5$). The approximations $\eta_i(\Delta x_1, \Delta x_2) = 0$ (4.57) and $s_i(\Delta x_1, \Delta x_2) = 0$ (4.60) of the coexistence region boundaries and of the internal x_i-nullcline, $i = 1, 2$, are shown around $(\bar{x}, \bar{x})$ in the (x_1, x_2) plane, using the same graphical and color codes of figures 4.3–4.4. Lighter colors are used for the fully nonlinear versions: boundary 1, $\lambda_1(x_2, \bar{X}, x_1) = 0$; boundary 2, $\lambda_1(x_1, \bar{X}, x_2) = 0$; and x_i-nullcline, $\lambda_2^{(0,0,0,1)}(x_1, x_2, \bar{X}, x_i) = 0$, $i = 1, 2$. Numerical continuation performed with the software package Matcont Dhooge et al. [2002].

diverge symmetrically w.r.t. the singular value $\bar{x}$ (dashed), while the population remains split into two halves (same gray scale) and the predator trait is under neutral selection.

In case (B), the prey traits are initialized close to the boundary 2 of the coexistence region (as in (4.66) with $\theta = \frac{1}{2}\pi$), and the predator trait still at the singular value $\bar{X}$. Close to boundary 2 the prey population is almost monomorphic and mainly composed of x_1-individuals (see the gray scale, initially darker in trait x_1), so (x_1, X) initially are almost at equilibrium at the singular coalition $(\bar{x}, \bar{X})$. However, in accordance with our analysis of sections 4.3 and 4.4 and of Appendix 4.2.3.5, the branching dynamics of (x_1, x_2) point toward the anti-diagonal and this, at the same time, equilibrate the equilibrium densities $\bar{n}_1(x_1, x_2, X)$ and $\bar{n}_2(x_1, x_2, X)$. Note that in the very initial phase of branching, as soon as x_1 moves away from $\bar{x}$, evolution is still basically monomorphic and (x_1, X) tend to quickly converge to $(\bar{x}, \bar{X})$. Being the singular coalition a stable focus, this induces fast dumped oscillations in (x_1, X) (only those in X are just barely

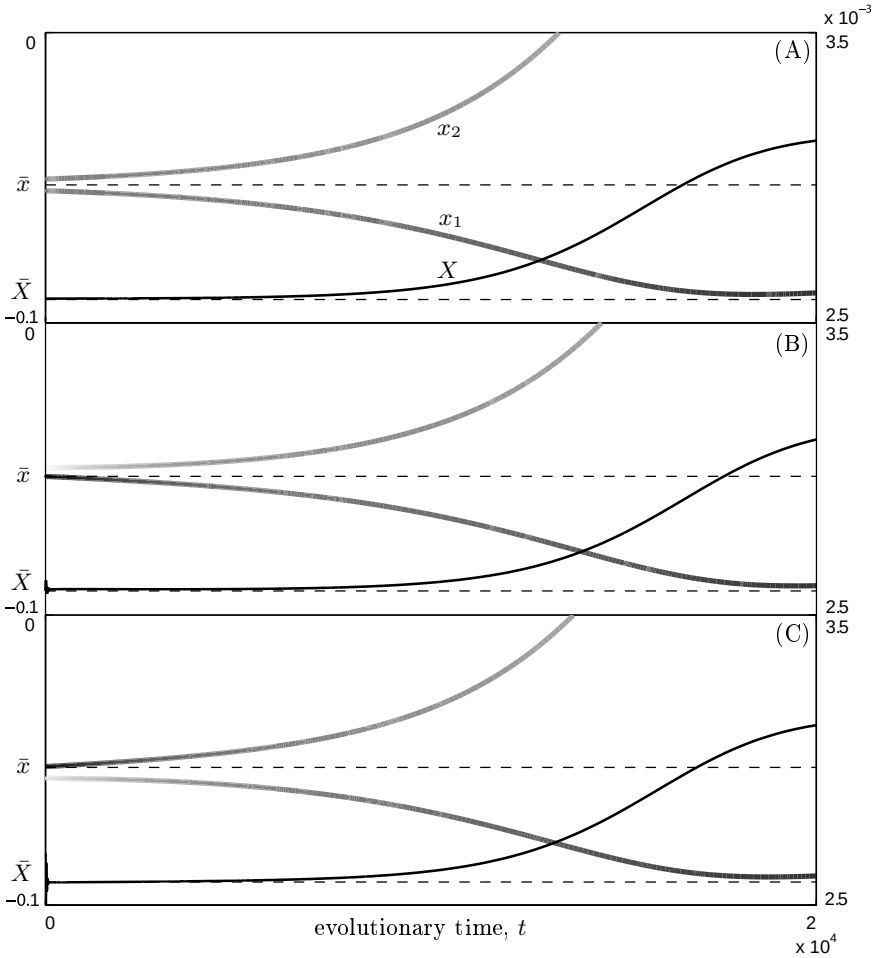

Figure 4.7: Three examples of dimorphic coevolutionary dynamics at incipient branching in the AD model in Landi et al. [2013]. Case (A): $x_1(0) = \bar{x} - \frac{\sqrt{2}}{2}\varepsilon$, $x_2(0) = \bar{x} + \frac{\sqrt{2}}{2}\varepsilon$, $X(0) = \bar{X}$. Case (B): $x_1(0) = \bar{x}$, $x_2(0) = \bar{x} + \varepsilon$, $X(0) = \bar{X}$. Case (C): $x_1(0) = \bar{x}(\bar{X}+\delta) - \frac{\sqrt{2}}{2}\varepsilon$, $x_2(0) = \bar{x}(\bar{X}+\delta) + \frac{\sqrt{2}}{2}\varepsilon$, $X(0) = \bar{X}+\delta$. Parameter values as in figure 4.6 (right), $\varepsilon = 0.003$, $\delta = 0.0001$. The gray scale in the x_i-time-series indicates the relative density $\bar{n}_i(x_1, x_2, X)/(\bar{n}_1(x_1, x_2, X) + \bar{n}_2(x_1, x_2, X))$, $i = 1, 2$.

visible at the scale of the figure). As the density of x_2-individuals grows in detriment of x_1-individuals, the slower branching dynamics take over. As long as x_1-individuals are still predominant, predator trait is not under neutral selection, but actually under a negative selection pressure due to adaptation to the decreasing trait x_1. This

is scarcely visible in the figure, where the eventual increase of X is slightly delayed w.r.t. case (A).

In case (C), the prey traits are initialized along the anti-diagonal (as in case (A), according to (4.66) with $\theta = \frac{3}{4}\pi$), but the predator trait is perturbed from singularity ($X(0) = \bar{X} + \delta$). In this case, the predator trait X is initially out of equilibrium and quickly evolves toward $\bar{X}$ (the barely visible X-oscillations are wider than in case (B), whereas the corresponding oscillations in the prey traits are not visible). The evolution of the predator trait induces a corresponding movement of the prey coexistence region in the (x_1, x_2) plane, that however avoids missing the branching ((x_1, x_2) touching the region boundaries) if the initial perturbation δ of X from $\bar{X}$ is sufficiently small. Once X is close to $\bar{X}$, the prey coexistence region is rooted at $x \simeq \bar{x} > \bar{x}(\bar{X} + \delta)$, so that the initial point (x_1, x_2) is not anymore on the anti-diagonal, but actually close to boundary 1. Then, after the first quick transient, the situation is symmetric w.r.t. case (B), with the prey population mainly composed of x_2-individuals.

4.6 Discussion and conclusions

The main theoretical contribution of this chapter is a general method of approximating the dimorphic fitness (4.8). It is based on a radial expansion (w.r.t. ε) on a given ray (identified by the angle θ) in the plane (x_1, x_2) of the two similar coexisting strategies. It exploits the fact (observed in Durinx [2008] and Dercole and Geritz [2014]) that the equilibrium densities $\bar{n}_1(x_1, x_2)$ and $\bar{n}_2(x_1, x_2)$, at which the two strategies can coexist (under (G1)) for (x_1, x_2) close to the singular strategy $\bar{x}$, are well defined and smooth along each given ray in the cone of coexistence rooted at $(\bar{x}, \bar{x})$, though nonsmooth at $(\bar{x}, \bar{x})$. As a consequence, the ε-expansions of the densities $\bar{n}_1(\varepsilon, \theta)$ and $\bar{n}_2(\varepsilon, \theta)$ and of the dimorphic fitness $\lambda_2(\varepsilon, \theta, \Delta x')$ (redefined in polar coordinates, $\Delta x' := x' - \bar{x}$) are θ-dependent but, interestingly, they can be written back in terms of rational ($\bar{n}_1$ and $\bar{n}_2$) and polynomial (λ_2) expressions of (x_1, x_2). The resulting expressions are not expansions w.r.t. (x_1, x_2)—such expansions cannot be defined, contrary to what originally done in Geritz et al. [1997, 1998] (see Geritz et al. [1998] Appendix 1 in particular)—but can be nevertheless used as approximations in the resident-mutant coexistence region locally to the singular point $(\bar{x}, \bar{x})$.

Our approach is quite general. Other non-similar resident populations (of the same of different species) can be considered (see Para-

graph 4.2.3.5) and the approximation can be taken up to any order (in ε). Thanks to a structural property assumed for the dimorphic fitness (property P4 in Paragraph 4.2.1, recently introduced in Dercole [2014]), the $\bar{n}_1$, $\bar{n}_2$, and λ_2 ε-expansions can be written in terms of the geometry of the monomorphic fitness (4.3) (in contrast to what preliminarily found in Durinx [2008], in the special case of Lotka-Volterra models).

We have used the developed approach to unfold the *branching bifurcation*, at which a stable equilibrium of the monomorphic AD canonical equation (4.4) loses evolutionary stability. Specifically, assuming (G1)—allowing resident-mutant coexistence—and (G2)—ensuring the transversality and genericity of the bifurcation—we have unfolded the transition of $\bar{\lambda}^{(0,2)}$ across zero—the evolutionary equilibrium turning from a terminal ($\bar{\lambda}^{(0,2)} < 0$) to a branching ($\bar{\lambda}^{(0,2)} > 0$) point of AD.

At the bifurcation, the evolutionary dynamics ruled by the dimorphic canonical equation (4.7) are dominated by the third-order terms in the ε-expansion of the dimorphic fitness (4.8). Interestingly, the second-order terms coincide with those Geritz et al. [1997, 1998] obtained by assuming smoothness, though nongeneric constraints on the monomorphic fitness come along at second- as well as at higher-orders (see Paragraph 4.2.3.1). Thus the (second-order) branching condition (4.9) of Geritz et al. [1997, 1998] is correct and our approach becomes essential only at third-order.

By means of a smooth coordinate change and time-scaling, and assuming (G1) and (G2), we have identified the most simple model, locally equivalent to the dimorphic canonical equation (4.7), showing the bifurcation. We claim this is the normal form for the branching bifurcation: model (4.60, 4.61, 4.63) restricted to the resident-mutant coexistence region $\tilde{n}_i(\Delta x_1, \Delta x_2) \geq 0$, $i = 1, 2$, defined in (4.62, 4.63), locally to $(\Delta x_1, \Delta x_2) = (0, 0)$. The model depends on four parameters that are all monomorphic fitness derivatives: the unfolding parameter $\bar{\lambda}^{(0,2)}$, the fitness cross-derivative $\bar{\lambda}^{(1,1)}$ constrained by (G1), the normal form coefficient $\bar{\lambda}^{(0,3)}$, and $\bar{\lambda}^{(1,2)}$ that plays no role and could be eliminated by a further coordinate change (in that sense the normal form could be further simplified, though losing the geometric matching with the dimorphic canonical equation). The only genericity (and transversality) condition required by the bifurcation (other than resident-mutant coexistence under (G1)), is then (G2).

Keeping into account the curvature of the boundaries of the resident-mutant coexistence region, we have proposed a second (though in-

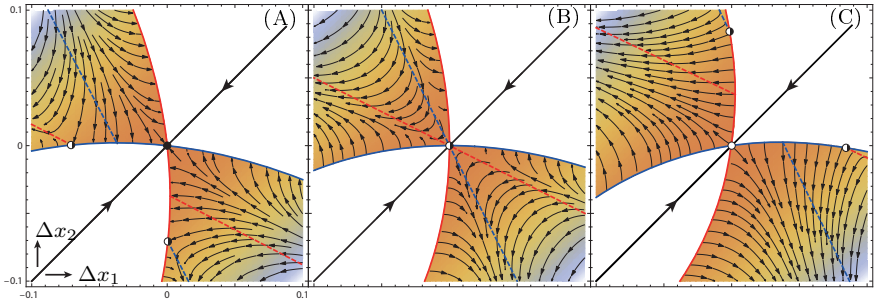

Figure 4.8: Monomorphic and dimorphic evolutionary dynamics around the branching bifurcation restricted to the area of coexistence. The region of resident-mutant coexistence is the shaded colored region, where orange means a high total abundance and blue a low total abundance. The singular strategy (the dot at the center of each panel) is always convergence stable (it attracts the monomorphic dynamics along the diagonal), while it is evolutionarily stable (terminal point, full dot) in panel (A), an evolutionary saddle in panel (B) (branching point, half-filled dot), and evolutionarily unstable in panel (C) (branching point, empty dot). Other lines and colors as in Figures 4.3 and 4.4.

troduced as first in Paragraph 4.3), necessarily less simple, model locally equivalent to the dimorphic canonical equation at the incipient branching: model (4.57, 4.60, 4.61) restricted to the coexistence region $\tilde{n}_i(\Delta x_1, \Delta x_2) \geq 0$, $i = 1, 2$, defined in (4.57, 4.58). The quadratic approximation of the coexistence region boundaries also depends on $\bar{\lambda}^{(2,1)}$, which is the last independent third-derivative of the monomorphic fitness to be involved ($\bar{\lambda}^{(3,0)}$ is dependent of the others, recall equation (4.11c)). The boundaries quadratic approximation has the advantage of showing some geometric features relating the trajectories of the dimorphic canonical equation with the boundaries themselves. Specifically, the internal x_1-isocline ($s_1((\Delta x_1, \Delta x_2)) = 0$; dashed blue in Figure 4.8) connects to an horizontal fold of boundary 1 ($\tilde{n}_1(\Delta x_1, \Delta x_2) = 0$, solid blue)—smaller/larger x_1-mutants invade at the right/left of the fold; and to boundary 2 ($\tilde{n}_2(\Delta x_1, \Delta x_2) = 0$, solid red) at a boundary saddle with $x_1 = \bar{x}$—strategy x_1 is alone and at equilibrium at the singular strategy; symmetrically for the internal x_2-isocline (see Geritz et al. [1999], the Paragraph in particular, for more details).

The analysis of our simplified models as $\bar{\lambda}^{(0,2)}$ moves across zero unravels the dynamical phenomena turning a terminal point of AD into a branching point. Restricting the model dynamics into the re-

gion of coexistence for the strategies pair (x_1, x_2), we see (Figure 4.8) that the singular point $(\Delta x_1, \Delta x_2) = (0, 0)$ is always a "corner" equilibrium that is attracting nearby trajectories for $\bar{\lambda}^{(0,2)} < 0$ and repelling for $\bar{\lambda}^{(0,2)} > 0$. The basin of attraction for $\bar{\lambda}^{(0,2)} < 0$ is limited by the stable manifold of two boundary saddles (the trajectories going into the boundary saddles), the convergence being composed of a dimorphic phase up to the extinction of one of the two similar strategies, followed by a monomorphic phase to the singular strategy. As $\bar{\lambda}^{(0,2)}$ moves across zero, the two saddles move along the boundaries and cross the diagonal at $(0, 0)$ at the bifurcation. The three equilibria collide and exchange stability (both eigenvalues do change sign, see Paragraph 4.4). For $\bar{\lambda}^{(0,2)} > 0$ the trajectories originating close to $(0, 0)$ go away from the singularity and reach an evolutionary attractor that is not local to the singularity [Geritz et al., 1999] (and not involved in the bifurcation). The same attractor is generically viable even for $\bar{\lambda}^{(0,2)} < 0$, but it cannot be reached from a neighborhood of the singularity, unless the mutational step is large enough to escape the basin of attraction. The branching bifurcation is therefore catastrophic, in the sense that a small change in $\bar{\lambda}^{(0,2)}$ triggers a large evolutionary transient leading to a new attractor.

Finally, by considering the curvature of the boundaries of the resident-mutant coexistence region at the bifurcation ($\bar{\lambda}^{(0,2)} = 0$), we can extend (under (G2)) the branching condition (4.9) as

$$\lambda_1^{(0,2)}(\bar{x}, \bar{x}) \geq 0,$$

as already anticipated by Kisdi [1999], without, however, a formal derivation.

The natural follow-up to this work is the analysis of the other codimension-one branching bifurcation—the one at which the fitness cross-derivative $\bar{\lambda}^{(1,1)}$ vanishes with positive $\bar{\lambda}^{(0,2)}$. The resident-mutant coexistence region is locally a cusp rooted at the singular point $(\bar{x}, \bar{x})$ (see Dercole and Geritz [2014]), and though there might generically be up to two coexistence equilibria, only one is stable and should be considered for developing a proper expansion of the dimorphic fitness. Further research could investigate the codimension-two bifurcation at which both fitness second-derivatives vanish (the type of coexistence is already available in Dercole and Geritz [2014]), or the cases at which $\bar{\lambda}^{(0,3)} = 0$ together with one of the fitness second-derivatives; or, as well, higher codimensions that do occur in applications (see, e.g., Doebeli and Ispolatov [2010]). The mathematical

approach developed in this chapter is readily applicable and convenient to pursue the above projects.

Chapter 5

The evolution of biodiversity

We show in this chapter how simulations of ODEs and continuations of systems of algebraic equations can be combined to study the evolution of biodiversity in multi-species systems where phenotypic traits are genetically transmitted. We follow the AD approach, that provides a deterministic approximation of the evolutionary dynamics of stationary coexisting populations in terms of an ODE system, the so-called AD canonical equation. AD also provides explicit conditions to test whether a stable evolutionary equilibrium of the canonical equation is a branching point—resident and mutant morphs coexist and further differentiate thus increasing biodiversity—or not. We analyze a standard parameterized family of prey-predator communities, described by the most standard ecological model, and propose an iterative procedure to obtain the branching portrait, explaining the dependence of branching scenarios on two (demographic, environmental or control) parameters. Among a number of interesting results, in line with field studies and known ecological principles, we find that prey branching is induced by the predation pressure, and is favored when prey intraspecific competition is highly sensitive to the resident-mutant phenotypic mismatch; while predator branching is not possible when prey and predators are present in equal number of morphs. This results in alternate prey-predator branching sequences with possible phases of prey unilateral branching. We also find that predator handling time limits branching sequences, as harvesting saturation limits the predation pressures thus restraining prey from branching; and the same occurs if predator are too generalist, while specialists may generate long branching sequences, but also non-stationary evolutionary regimes preventing further branching. The guidelines for deriving a general method for analyzing the evolution of biodiversity are also dis-

cussed. The proposed approach could be readily applied to different prey-predator and host-parasite communities, as well as to communities regulated by other ecological interactions. The indications that can be obtained typically have qualitative nature, but can be of help for the long-term conservation and management of biodiversity. More details can be found in Landi et al. [2013].

5.1 Introduction

Explaining why there are so many similar populations in Nature is one of the major questions in ecology [Hutchinson, 1959]. Classical competition theory can provide some answers; for example, it can explain why self-organized patterns of groups of similar populations emerge in rich communities [Scheffer and van Nes, 2006]. Perhaps the most difficult problem in need of explanation is this: under the assumption that life started from a common ancestor, how is it that we obverse so much biodiversity today? For this, we can combine two independent mechanisms. One is genetic mutation that rarely and randomly diversifies the phenotypic trait (x) of some individual from that (x') of its offspring, thus creating a mutant population similar to the resident one, though initially with very low abundance. The second is natural selection, i.e., the competition between resident and mutant populations, that generically leads to the extinction of one of the two populations [Geritz, 2005, Dercole and Rinaldi, 2008]. If mutants go extinct, nothing changes because x remains the resident trait, while if residents go extinct, the mutant population becomes the new resident, endowed, however, of a new trait x'. Only in exceptional cases, called evolutionary branchings [Geritz et al., 1997, 1998, Dercole and Rinaldi, 2008], can the mutant and resident populations coexist under disruptive selection, i.e., competition favors further differentiation between the two similar residents. Evolutionary branching thus explains why the number of distinct morphs of a species, that is, biodiversity, can increase. Biodiversity can also decrease, not only accidentally, but as the result of evolution toward the boundary of the viability region in trait space (evolutionary extinction, see Paragraphs 1.2.5, 2.7 and Gyllenberg and Parvinen [2001], Dercole and Rinaldi [2008]). Evolutionary branchings and extinctions can also alternate [Doebeli and Dieckmann, 2000, Kisdi et al., 2001, Dercole, 2003, Dercole and Rinaldi, 2008], making the problem more complex.

Among the many quantitative approaches to evolutionary dynamics introduced in Paragraph 1.3 only two of them, that is, Individual-

Based Modeling (IBM) and Adaptive Dynamics (AD) are suitable for predicting branching scenarios. IBM [De Angelis and Gross, 1992, Dieckmann and Doebeli, 1999] is a stochastic simulation approach which requires little in the way of mathematical analysis and skill, but which can be quite attractive because it allows any sort of detail to be included in the model (e.g. age, size, stage and spatial structures, sexual reproduction, and seasonalities). In contrast, AD [Metz et al., 1996, Geritz et al., 1997, 1998, Dercole and Rinaldi, 2008, Geritz and Dercole, 2011] is population-based, focused on the long-term evolution of the adaptive traits (it assumes rare mutations of small phenotypic effect), and provides a deterministic approximation of the evolutionary dynamics in terms of ODEs, one for each trait, known as the AD canonical equation [Dieckmann and Law, 1996, Champagnat et al., 2006, Dercole and Rinaldi, 2008]. Evolutionary branching is possible only in the vicinity of evolutionary equilibria (far from equilibria the extinction of either the resident or the mutant population is the generic outcome of competition [Geritz, 2005, Dercole and Rinaldi, 2008]), and explicit branching conditions are available [Geritz et al., 1997, 1998, Dercole and Rinaldi, 2008]. Here we consider the simplest setting in which the AD canonical equation can be derived, i.e., the case of unstructured, asexual populations, characterized by a single trait each, and stationary coexisting in an isolated homogeneous and constant abiotic environment (see Dieckmann and Law [1996], Durinx et al. [2008], Kisdi and Geritz [1999] for extensions).

Most branching scenarios produced until now have been obtained either analytically (for relatively simple models or limited to primary branchings, see e.g. Metz et al. [1996], Geritz et al. [1998], Kisdi [1999], Doebeli and Dieckmann [2000], Ferriére et al. [2002], Dercole et al. [2008], Best et al. [2010]) or by means of stochastic simulations (with the IBM approach [Dieckmann and Doebeli, 1999, Doebeli and Dieckmann, 2000, Ferriére et al., 2002] or stochastically simulating the mutation process of an AD model [Metz et al., 1996, Geritz et al., 1998, Kisdi, 1999, Best et al., 2010]), starting from an ancestral community composed of a single population or two populations of different species. In some studies concerning prey-predator systems the scenarios are extremely simple, ranging from no branching due to periodic evolutionary attractors in Dieckmann et al. [1995], to a primary prey branching followed by predator branching in Doebeli and Dieckmann [2000] (a primary predator branching has been identified in Geritz et al. [2007], but relying on cyclically coexisting predators). By contrast, in studies on the coevolution of mutualism, richer scenarios

characterized by alternate branching and extinction (in facultative or opportunistic mutualisms [Doebeli and Dieckmann, 2000]) and by very long series of evolutionary branchings (in obligate mutualisms [Ferriére et al., 2002]) have been discovered. In Ferriére et al. [2002] branching is unilateral in some regions of parameter space, that is, it concerns always populations of the same species, while in other regions it is bilateral and alternate between the two species. Alternate branchings have also been obtained in a study of a host-parasite model [Best et al., 2010], while bilateral but not alternate branchings have been discovered in a study of evolution of cannibalistic populations toward complex food webs [Ito and Ikegami, 2006].

The above mentioned studies show that branching scenarios depend not only on the ancestral community but also on the parameter values characterizing some demographic processes (like efficiency or death rate) or their dependence on evolving traits. To find out the full catalog of branching scenarios, say in a two-dimensional parameter space, one cannot rely on simulation approaches, as this would be computationally impracticable. Instead, one could use the AD canonical equation and the branching conditions to generate a point on each curve separating regions of parameter space with different branching scenarios, and, then, produce the entire curve through numerical continuation techniques [Allgower and Georg, 2003]. Until now, this has been done only a few times up to the first branching (in a study of seed size and competitive ability [Geritz et al., 1999], in a study of prey-predator coevolution [Dercole et al., 2003], in a model for the evolution of cannibalism [Dercole and Rinaldi, 2002, Dercole, 2003], and in modeling the host-parasite range [Best et al., 2010]).

The aim of this chapter is to show how the analysis of evolutionary branching can be organized through continuation in a case of complex scenarios. For this, we study the coevolution of a resource-consumer system starting from an ancestral prey-predator pair, the building block of complex food webs [Martinez, 2006]. The model we consider is based on the prey-predator model most frequently used in ecology, for which all properties, except branching scenarios, have already been studied in detail (the primary prey branching has been studied in Dercole et al. [2003], while the primary branching of cycling predators in Geritz et al. [2007]). This choice allows this chapter to be considered as the natural follow-up of the work in Dercole et al. [2003]. We feel our results are of interest because they both support ecological properties that emerge from field studies and suggest new theoretical insights on prey-predator coevolution that might be of help for the

conservation and management of biodiversity. In Paragraph 5.5, we also describe how our approach can be made general and applied to study the evolution of biodiversity in different communities.

5.2 Coevolution of prey-predator systems

Evolving systems are in general composed of M interacting plant and/or animal populations characterizable by two features: the number n_i of individuals of each population or, equivalently, the density of the population (a positive real number), and an adaptive phenotypic trait x_i (e.g., body size, typically measured by a real number on a suitable scale, see Paragraph 2.2 and Dercole et al. [2003], Dercole and Rinaldi [2008]). Both features vary in time, but densities can vary at a much faster rate than traits. This means that an evolving system has two distinct timescales called ecological and evolutionary (see Paragraph 1.2.3). The first is fast and concerns only the densities, while traits remain practically constant if mutations are assumed to be extremely rare events on the ecological timescale; the second concerns the slow variation of the traits, due to sequences of mutations and resident substitutions, and entrains the slow variations of the equilibrium densities attained after each substitution.

From now on we restrict our attention to the coevolution of populations belonging to two different species (prey and predator), so that, in general, the community is composed of M_1 prey populations and M_2 predator populations, with $M_1 + M_2 = M$. In particular, $n_1, \ldots, n_{M_1}$ and $x_1 \leq \cdots \leq x_{M_1}$ are densities and traits of the M_1 prey populations, while $n_{M_1+1}, \ldots, n_{M_1+M_2}$ and $x_{M_1+1} \leq \cdots \leq x_{M_1+M_2}$ are densities and traits of the M_2 predator populations, respectively. Assume that initially $M_1 = M_2 = 1$, so that n_1 and x_1 are prey density and trait while n_2 and x_2 are predator density and trait. At ecological timescale, the traits remain constant while the densities vary according to two ODEs of the form:

$$\begin{aligned} \dot{n}_1 &= n_1 f_1^{\mathrm{R}}(n_1, n_2, x_1, x_2) \\ \dot{n}_2 &= n_2 f_2^{\mathrm{R}}(n_1, n_2, x_1, x_2), \end{aligned} \tag{5.1}$$

where f_i is the per capita growth rate of the i-th population. In the following, model (5.1), called resident model, is assumed to have one strictly positive and globally stable equilibrium $(\bar{n}_1(x_1, x_2), \bar{n}_2(x_1, x_2))$ for each (x_1, x_2) belonging to a set of the trait space called the evolution set of model (5.1).

At evolutionary timescale (slow dynamics), the traits vary according to two ODEs called evolutionary model of the form:

$$\begin{aligned} \dot{x}_1 &= k_1 H_1(x_1, x_2) \\ \dot{x}_2 &= k_2 H_2(x_1, x_2), \end{aligned} \tag{5.2}$$

where k_1 and k_2 are suitable parameters (here assumed constant) scaling the speed of evolution in the coevolving species determined by size and frequency of mutations. As mentioned above, population densities vary slowly with the traits, as model (5.1) is always at the equilibrium $(\bar{n}_1(x_1, x_2), \bar{n}_2(x_1, x_2))$ at evolutionary timescale.

The most transparent approach for deriving the evolutionary model (5.2) is the AD canonical equation [Dieckmann and Law, 1996, Champagnat et al., 2006, Dercole and Rinaldi, 2008]. It is based on the resident-mutant models, which describe the interactions among three populations, namely the two resident populations, and a mutant population with trait x_1' or x_2'. When the mutation occurs in the prey, the prey population is split into two sub-populations (resident and mutant) with densities n_1 and n_1' and traits x_1 and x_1', so the model is:

$$\begin{aligned} \dot{n}_1 &= n_1 f_1(n_1, n_1', n_2, x_1, x_1', x_2) \\ \dot{n}_1' &= n_1' f_1(n_1', n_1, n_2, x_1', x_1, x_2) \\ \dot{n}_2 &= F_2(n_1, n_1', n_2, x_1, x_1', x_2). \end{aligned} \tag{5.3}$$

A similar three-dimensional model involving the mutant trait x_2' and the density n_2' describes the case in which the mutant is a predator, namely

$$\begin{aligned} \dot{n}_1 &= F_1(n_2, n_2', n_1, x_2, x_2', x_1) \\ \dot{n}_2 &= n_2 f_2(n_2, n_2', n_1, x_2, x_2', x_1) \\ \dot{n}_2' &= n_2' f_2(n_2', n_2, n_1, x_2', x_2, x_1), \end{aligned} \tag{5.4}$$

where functions f_i and F_i, $i = 1, 2$, are consistently related to functions $f_i^{\mathrm{R}}(n_1, n_2, x_1, x_2)$, $i = 1, 2$, in the resident model (5.1), i.e.,

$$\begin{aligned} f_1(n_1, 0, n_2, x_1, \cdot, x_2) &= f_1^{\mathrm{R}}(n_1, n_2, x_1, x_2) \\ F_2(n_1, 0, n_2, x_1, \cdot, x_2) &= n_2 f_2^{\mathrm{R}}(n_1, n_2, x_1, x_2) \end{aligned}$$

and

$$\begin{aligned} F_1(n_2, 0, n_1, x_2, \cdot, x_1) &= n_1 f_1^{\mathrm{R}}(n_1, n_2, x_1, x_2) \\ f_2(n_2, 0, n_1, x_2, \cdot, x_1) &= f_2^{\mathrm{R}}(n_1, n_2, x_1, x_2) \end{aligned}$$

(see Paragraphs 2.3 and 5.2.1). The values of n_1' and n_2' immediately after the mutation are very small because a mutant population is initially composed of one or a few individuals. In words, each mutation brings a new trait into the system, but competition between

resident and mutant populations selects the trait that remains in the system in the long term. As long as mutants either disappear or substitute the corresponding residents, the evolutionary process is called monomorphic—each species is present in a single morph—whereas dimorphic and polymorphic evolution phases follow after sequences of evolutionary branchings.

5.2.1 A specific ecological model

The ecological model we consider is the Rosenzweig-MacArthur prey-predator model [Rosenzweig and MacArthur, 1963]:

$$\begin{aligned} \dot{n}_1 &= n_1\left(r - cn_1 - \frac{a}{1+ahn_1}n_2\right) \\ \dot{n}_2 &= n_2\left(e\frac{an_1}{1+ahn_1} - d\right), \end{aligned} \tag{5.5}$$

where r is prey per capita growth rate, c is prey intraspecific competition, a is predator attack rate, h is predator handling time, namely the time needed by each predator to handle and digest one unit of prey, e is predator efficiency, namely a conversion factor transforming each unit of predated biomass into predator newborns, and d is predator death rate. The six positive parameters of the model (r, c, a, h, e, d) could be reduced to three through rescaling. However, we do not follow this option because the biological interpretation of the dependence of the parameters on prey and predator traits would become less transparent.

In order to have a meaningful problem one must assume $e > dh$, because, otherwise, the predator population cannot grow even in the presence of an infinitely abundant prey population. For any meaningful parameter setting, model (5.5) has a global attractor in $\mathbb{R}^2_+$ [Hsu et al., 1978], namely

(a) the trivial equilibrium $(r/c, 0)$ if $d/a(e-dh) \geq r/c$,

(b) a strictly positive equilibrium if $\dfrac{rah-c}{2ahc} \leq \dfrac{d}{a(e-dh)} < \dfrac{r}{c}$,

(c) a strictly positive limit cycle if $d/a(e-dh) < (rah-c)/(2ahc)$.

The transition from (a) to (b) is a transcritical bifurcation (which is generic in the class of positive systems of the form (5.5) [Kuznetsov, 2004]), while the transition from (b) to (c) is a supercritical Hopf bifurcation (see Kuznetsov [2004] for a proof). In the following, the

functional dependencies of the parameters on the traits and the parameter values will be chosen to satisfy condition (b) for stationary coexistence. In particular, we limit the value of the handling time h.

If we now imagine that a mutant population is also present, we can enlarge the resident model (5.5) by adding a third ODE and by modifying the equations of the resident populations in order to take the mutant population into account. Of course we also need to specify how the parameters depend upon the traits x_1, x_2, x_1', x_2'. The number of possibilities is practically unlimited, because even for well identified prey and predator species there are many meaningful options. Thus, at this level of abstraction, it is reasonable to limit the number of parameters sensitive to the traits and avoid trait dependencies that could give rise to biologically unrealistic evolutionary dynamics, like the unlimited growth of a trait. Our choice has been to assume that the parameters r, e, and d are independent on the traits, because this will allow us to compare our results with those obtained in Dieckmann et al. [1995] and Dercole et al. [2003]. Thus, in the case of a mutation in the prey population, the resident-mutant model is

$$\begin{aligned}
\dot{n}_1 &= n_1\Bigg(r - c(x_1,x_1)n_1 - c(x_1,x_1')n_1' + \\
&- \frac{a(x_1,x_2)}{1 + a(x_1,x_2)h(x_1,x_2)n_1 + a(x_1',x_2)h(x_1',x_2)n_1'}n_2\Bigg) \\
\dot{n}_1' &= n_1'\Bigg(r - c(x_1',x_1)n_1 - c(x_1',x_1')n_1' + \\
&- \frac{a(x_1',x_2)}{1 + a(x_1,x_2)h(x_1,x_2)n_1 + a(x_1',x_2)h(x_1',x_2)n_1'}n_2\Bigg) \\
\dot{n}_2 &= n_2\left(e\frac{a(x_1,x_2)n_1 + a(x_1',x_2)n_1'}{1 + a(x_1,x_2)h(x_1,x_2)n_1 + a(x_1',x_2)h(x_1',x_2)n_1'} - d\right).
\end{aligned} \tag{5.6}$$

Otherwise, if the mutation occurs in the predator population, the

resident-mutant model is

$$\begin{aligned}
\dot{n}_1 &= n_1\Bigg(r - c(x_1,x_1)n_1 + \\
&- \frac{a(x_1,x_2)}{1+a(x_1,x_2)h(x_1,x_2)n_1}n_2 - \frac{a(x_1,x_2')}{1+a(x_1,x_2')h(x_1,x_2')n_1}n_2'\Bigg) \\
\dot{n}_2 &= n_2\left(e\frac{a(x_1,x_2)n_1}{1+a(x_1,x_2)h(x_1,x_2)n_1} - d\right) \\
\dot{n}_2' &= n_2'\left(e\frac{a(x_1,x_2')n_1}{1+a(x_1,x_2')h(x_1,x_2')n_1} - d\right).
\end{aligned} \tag{5.7}$$

5.2.1.1 g-function

We here show that the resident-mutant models (5.3) and (5.3) can also be expressed in terms of g-functions (see Paragraph 3.1). Indeed,

$$\begin{aligned}
f_1(n_1,n_1',n_2,x_1,x_1',x_2) &= g_1(n_1,n_1',n_2,x_1,x_1',x_2,x_1) \\
f_1(n_1',n_1,n_2,x_1',x_1,x_2) &= g_1(n_1,n_1',n_2,x_1,x_1',x_2,x_1')
\end{aligned}$$

and

$$\begin{aligned}
f_2(n_2,n_2',n_1,x_2,x_2',x_1) &= g_2(n_2,n_2',n_1,x_2,x_2',x_1,x_2) \\
f_2(n_2',n_2,n_1,x_2',x_2,x_1) &= g_2(n_2,n_2',n_1,x_2,x_2',x_1,x_2')
\end{aligned}$$

with g_1 and g_2 as specified below. Notice that here the numeric subscript of g stands for population 1 (prey) and population 2 (predator), thus having a different meaning with respect to the previous chapters. In particular, the g-function for the prey is given by

$$\begin{aligned}
g_1(n_1,n_1',n_2,x_1,x_1',x_2,y) &= r - c(y,x_1)n_1 - c(y,x_1')n_1' + \\
&- \frac{a(y,x_2)}{1+a(x_1,x_2)h(x_1,x_2)n_1 + a(x_1',x_2)h(x_1',x_2)n_1'}n_2,
\end{aligned}$$

where y is a "virtual" strategy with vanishing abundance in an environment set by strategies x_1, x_1', and x_2 with abundances n_1, n_1', and n_2. Evaluating $g_1(n_1,n_1',n_2,x_1,x_1',x_2,y)$ at $y = x_1$ (resp., $y = x_1'$) we obtain $f_1(n_1,n_1',n_2,x_1,x_1',x_2)$ (resp., $f_1(n_1',n_1,n_2,x_1',x_1,x_2)$); see equation (5.6).

The g-function for the predator is

$$g_2(n_2,n_2',n_1,x_2,x_2',x_1,y) = e\frac{a(x_1,y)n_1}{1+a(x_1,y)h(x_1,y)n_1} - d,$$

that suitably evaluated at $y = x_2$ and $y = x_2'$ allows to obtain the predator per-capita growth rates in the resident-mutant model (5.7).

In general, for M-morphic communities (with $M = M_1 + M_2$), the g-function for the prey species is

$$g_1(n_{1:M_1}, n_{M_1+1:M_1+M_2}, x_{1:M_1}, x_{M_1+1:M_1+M_2}, y) = \\ r - \sum_{i=1}^{M_1} c(y, x_i) n_i - \sum_{j=M_1+1}^{M_1+M_2} \frac{a(y, x_j)}{1 + \sum_{i=1}^{M_1} a(x_i, x_j) h(x_i, x_j) n_i} n_j,$$

where the notation $n_{1:M_1}$ stands for $n_1, \ldots, n_{M_1}$, while the g-function for the predator species is

$$g_2(n_{M_1+1:M_1+M_2}, n_{1:M_1}, x_{M_1+1:M_1+M_2}, x_{1:M_1}, y) = \\ e \frac{\sum_{i=1}^{M_1} a(x_i, y) n_i}{1 + \sum_{i=1}^{M_1} a(x_i, y) h(x_i, y) n_i} - d.$$

5.2.2 Trait-dependent parameters

We must now specify how the three remaining parameters, namely the prey intraspecific competition c, the predator attack rate a, and the predator handling time h, appearing in the resident-mutant models, depend on the resident and mutant traits. Due to our definition of the traits, which are scaled measures of the phenotypes, c, a, and h are bounded functions. Unless otherwise stated, the parameters appearing in these functions are positive.

Prey intraspecific competition c is given by

$$c(x_1, x_1') = \frac{\gamma_1 + \gamma_2 (x_1 - \gamma)^2}{1 + \gamma_0 \left(\gamma_1 + \gamma_2 (x_1 - \gamma)^2 \right)} \exp\left(- \left(\frac{x_1 - x_1'}{\gamma_3} \right)^2 \right). \quad (5.8)$$

It is the product of two terms. The first defines the extra-mortality within groups of identical prey, that has a quadratic minimum at $x_1 = \gamma$ and saturates at $1/\gamma_0$ as x_1 diverges from γ (the minimum competition and the local curvature are controlled by parameters γ_1 and γ_2, respectively). Parameter γ (positive or negative) therefore describes a fixed characteristic of the environment, and is henceforth called *optimum prey trait*. The second term in (5.8) describes resident-mutant competition. Both resident and mutant prey suffer the highest (yet different) competition when they face identical individuals, as the exponential factor is maximum for $x_1 = x_1'$. The width γ_3 of this gaussian bell is inversely proportional to the sensitivity of competition to

the resident-mutant phenotypic mismatch. High (resp. low) sensitivity yields significant (resp. mild) drops in competition as resident and mutant differentiate in phenotype. Intuitively, this suggests that prey branching might be favored by lowering γ_3, because the individuals of the less abundant prey population, whether resident or mutant, are more likely opposed to different rather than identical individuals, so they suffer a lower competition.

The predator attack rate a is the bell-shaped function

$$a(x_1, x_2) = \alpha_0 + \alpha \exp\left(-\left|\frac{x_1 - x_2}{\alpha_1}\right|^{2-\alpha_2}\right), \tag{5.9}$$

where α_1 and α_2 are the width and the kurtosis of the function, respectively. In particular, if $0 < \alpha_2 < 2$ the function is leptokurtic, if $\alpha_2 < 0$ the function is platykurtic, while $\alpha_2 = 0$ corresponds to the normokurtic function, i.e., a gaussian bell. Predator with pronounced $\alpha_2 > 0$ (resp. $\alpha_2 < 0$) are called specialist (resp. generalist) because they exploit a narrow (resp. large) spectrum of prey. If prey and predator traits are tuned, that is, if $x_1 = x_2$, the predator attack rate is maximum (and equal to $\alpha_0 + \alpha$). When prey and predator traits are far from being tuned, the predator attack rate drops to α_0. This supports the idea that in a system with one predator and two prey populations with diversified traits, the predator might be prone to branch into two different predator sub-populations with traits tuned with those of the two prey.

The predator handling time h is the product of an increasing sigmoidal function of the prey trait x_1 and of a decreasing sigmoidal function of the predator trait x_2

$$h(x_1, x_2) = \theta\left[1 + \theta_1 - \frac{2\theta_1}{1 + \exp(\theta_3 x_1)}\right]\left[1 + \theta_2 - \frac{2\theta_2}{1 + \exp(-\theta_4 x_2)}\right], \tag{5.10}$$

where θ is the handling time corresponding to the tuned situation $x_1 = x_2 = 0$.

The graphs of functions $c(x_1, x_1')$, $a(x_1 - x_2)$, and $h(x_1, x_2)$ are shown in Figure 5.1 for the parameter values indicated in the caption. Only the third of these functions, namely, the handling time h, coincides with those used in Dercole et al. [2003]. The reason for this change is that the functions proposed in this thesis are biologically sound, while one of those used in Dercole et al. [2003], though fully appropriate for the purposes of that paper, was particularly extreme. In fact, in Dercole et al. [2003], the prey intraspecific competition

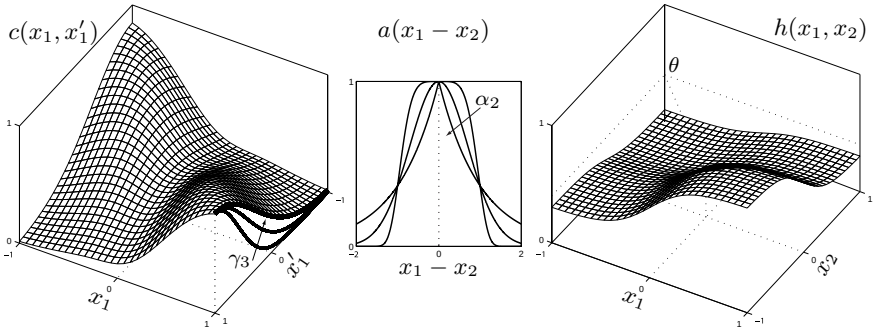

Figure 5.1: Prey intraspecific competition c, predator attack rate a, and predator handling time h. The graphs correspond to the following parameter values: $\gamma = 0$, $\gamma_0 = 1$, $\gamma_1 = 0.5$, $\gamma_2 = 5$, $\gamma_3 = 0.6, 0.8, 1$, $\alpha = 1$, $\alpha_0 = 0$, $\alpha_1 = 1$, $\alpha_2 = -3, 0, 1$, $\theta = 0.4$, $\theta_1 = \theta_2 = 0.5$, $\theta_3 = \theta_4 = 5$.

corresponds to equation (5.8) for $\gamma_3 \to \infty$, which means that the competition suffered by an individual only depends on its own trait and not on that of the opponent, a rather disputable biological assumption. Moreover, the shape of the attack rate in Dercole et al. [2003] assumes some environmental constrain on the predator body size, while the function used here does not.

5.2.3 Evolutionary dynamics

The mutation-competition process can be further specified by making suitable assumptions on the frequency and distribution of small mutations [Dieckmann and Law, 1996, Champagnat et al., 2006, Dercole and Rinaldi, 2008], and the conclusion is that the rate at which the trait x_i varies at evolutionary timescale is given by the following ODE, called the AD canonical equation:

$$\dot{x}_i = k_i \bar{n}_i(x_1, x_2) \left. \frac{\partial \lambda_i(x_1, x_2, x_i')}{\partial x_i'} \right|_{x_i' = x_i}, \tag{5.11}$$

$i = 1, 2$, where k_i is proportional to the frequency and size of mutations, $\bar{n}_i(x_1, x_2)$ is the equilibrium density of the resident model, while

$$\begin{array}{rcl} \lambda_1(x_1, x_2, x_1') & = & f_1(0, \bar{n}_1(x_1, x_2), \bar{n}_2(x_1, x_2), x_1', x_1, x_2) \\ \lambda_2(x_1, x_2, x_2') & = & f_2(0, \bar{n}_2(x_1, x_2), \bar{n}_1(x_1, x_2), x_2', x_2, x_1), \end{array} \tag{5.12}$$

or, equivalently,

$$\begin{aligned}\lambda_1(x_1, x_2, x_1') &= g_1(\bar{n}_1(x_1, x_2), 0, \bar{n}_2(x_1, x_2), x_1, \cdot, x_2, x_1') \\ \lambda_2(x_1, x_2, x_2') &= g_2(\bar{n}_2(x_1, x_2), 0, \bar{n}_1(x_1, x_2), x_2, \cdot, x_1, x_2'),\end{aligned}$$

are the invasion fitness functions of the mutations (the initial exponential rate of increase of the mutant populations). Equation (5.11), written for the prey and for the predator, gives the two ODEs that form the evolutionary model (5.2) with

$$H_i(x_1, x_2) = \bar{n}_i(x_1, x_2) \left. \frac{\partial \lambda_i(x_1, x_2, x_i')}{\partial x_i'} \right|_{x_i' = x_i}. \tag{5.13}$$

Once the monomorphic dynamics has found a halt at a stable evolutionary equilibrium $\bar{x} = (\bar{x}_1, \bar{x}_2)$ of model (5.2), one can look at the second-order terms in the Taylor expansion of the mutant per capita growth rate to establish if the equilibrium is a branching point (see Paragraph 3.3 and Geritz et al. [1997, 1998], Dercole and Rinaldi [2008]) or not. More precisely, a stable equilibrium $\bar{x}$ of (5.2) is a branching point for the i-th population if

$$B_i' = \left. \frac{\partial^2 \lambda_i(x_1, x_2, x_i')}{\partial x_i \partial x_i'} \right|_{\substack{x_1 = \bar{x}_1,\ x_2 = \bar{x}_2 \\ x_i' = \bar{x}_i}} < 0 \tag{5.14}$$

and

$$B_i'' = \left. \frac{\partial^2 \lambda_i(x_1, x_2, x_i')}{\partial x_i'^2} \right|_{\substack{x_1 = \bar{x}_1,\ x_2 = \bar{x}_2 \\ x_i' = \bar{x}_i}} > 0. \tag{5.15}$$

Under condition (5.14), there exist a region in the plane (x_i, x_i') (with the shape, locally to point $(\bar{x}, \bar{x})$, of a cone symmetrically opened with respect to the anti-diagonal, see Paragraph 3.2.1) for which small mutations in the i-th population invade and coexist, at a stable ecological equilibrium, with the former residents. The ecological equilibrium exists but is unstable if the condition is reversed; it does not exist if $B_i' = 0$.

Note that the computation of B_i' requires the derivatives of the ecological equilibrium $\bar{n}(x)$, for which typically there is no analytical expression. These derivatives can however be computed by solving suitable systems of algebraic linear equations, as explained in Paragraph 5.2.3.1.

Under condition (5.15), the two similar traits x_i and x_i' further differentiate in accordance with the higher-dimensional canonical equation, where x_i' plays the role of a new resident trait.

Finally, if conditions (5.14) or (5.15) are not satisfied neither for $i = 1$ nor $i = 2$, no branching is possible and the equilibrium $\bar{x}$ is a terminal point (see Paragraph 3.3) of the evolutionary dynamics, among which the evolutionarily stable coalitions of game theory when B_i'' is negative for all populations.

After a first branching has occurred, there are three resident populations, and one can repeat the analysis by considering the three corresponding resident-mutant models and by deriving from them the corresponding canonical equation. If the evolutionary trajectory originating at the branching point of the new canonical equation converges toward an equilibrium point, three different branchings are possible since there are three resident populations in the system. But the branching conditions are still based on the signs of B_i' and B_i'' (similarly specified as in (5.14) and (5.15)), where i is the index spanning the resident populations ($i = 1, 2, 3$) and $\lambda_i(x_1, x_2, x_3, x_i')$ is the fitness of the mutants of the i-th population.

And the story continues like so through a sequence of successive evolutionary branchings (and possible evolutionary extinctions) until a terminal point is reached or the evolutionary trajectory tends toward a non-stationary (cyclic or chaotic) regime (called *Red Queen* behavior after Van Valen [1973], see also Marrow et al. [1992], Dieckmann et al. [1995], Marrow et al. [1996], Dercole et al. [2006], Dercole and Rinaldi [2010], Dercole et al. [2010a]). In principle infinite branching sequences are possible, but have been shown to be structurally unstable, meaning that the region in parameter space associated to a possible sequence should shrink with the length of the sequence and vanish as the length diverges to infinity [Gyllenberg and Meszéna, 2005, Meszéna et al., 2006].

5.2.3.1 Computation of B_i'

We show in this paragraph how the branching condition (5.15) can be numerically computed, with reference to the simplest community composed of $M = 2$ populations. Generalization to the case with $M > 2$ is straightforward.

The invasion fitness λ_i is a function of the resident and mutant traits (x_1, x_2, x_i'), $i = 1, 2$, that is obtained by evaluating the mutant per-capita growth rate (the initial exponential rate of increase of the mutant population) at the resident equilibrium of model (5.1), i.e.,

$$\lambda_1(x_1, x_2, x_1') = f_1(0, \bar{n}_1(x_1, x_2), \bar{n}_2(x_1, x_2), x_1', x_1, x_2)$$

for the prey and similarly for the predator population. When taking the fitness derivative with respect to x_j, $j = 1, 2$, one obtains

$$\begin{aligned}\frac{\partial}{\partial x_j}\lambda_1(x_1, x_2, x_1') &= \Bigg[\frac{\partial}{\partial n_1} f_1(0, n_1, n_2, x_1', x_1, x_2) \frac{\partial}{\partial x_j}\bar{n}_1(x_1, x_2) + \\ &\quad \frac{\partial}{\partial n_2} f_1(0, n_1, n_2, x_1', x_1, x_2) \frac{\partial}{\partial x_j}\bar{n}_2(x_1, x_2) + \\ &\quad \frac{\partial}{\partial x_j} f_1(0, n_1, n_2, x_1', x_1, x_2)\Bigg]\Bigg|_{n_{1,2}=\bar{n}_{1,2}(x_1,x_2)},\end{aligned}$$

where the explicit expressions for the derivatives of the resident equilibrium with respect to the traits are typically not available.

They can however be computed recalling the definition of $\bar{n}(x)$, i.e.,

$$\begin{aligned} f_1^{\mathrm{R}}(\bar{n}_1(x_1, x_2), \bar{n}_2(x_1, x_2), x_1, x_2) &= 0 \\ f_2^{\mathrm{R}}(\bar{n}_1(x_1, x_2), \bar{n}_2(x_1, x_2), x_1, x_2) &= 0 \end{aligned} \tag{5.16}$$

(see model (5.1)). In fact, taking the derivative of (5.16) with respect to x_j gives

$$\begin{aligned} \frac{\partial f_1^{\mathrm{R}}}{\partial n_1}\frac{\partial \bar{n}_1}{\partial x_j} + \frac{\partial f_1^{\mathrm{R}}}{\partial n_2}\frac{\partial \bar{n}_2}{\partial x_j} + \frac{\partial f_1^{\mathrm{R}}}{\partial x_j} &= 0 \\ \frac{\partial f_2^{\mathrm{R}}}{\partial n_1}\frac{\partial \bar{n}_1}{\partial x_j} + \frac{\partial f_2^{\mathrm{R}}}{\partial n_2}\frac{\partial \bar{n}_2}{\partial x_j} + \frac{\partial f_2^{\mathrm{R}}}{\partial x_j} &= 0, \end{aligned} \tag{5.17}$$

where the functions' arguments have been omitted for simplicity, but note that $\partial f_{1,2}^{\mathrm{R}}/\partial x_j = \partial f_{1,2}^{\mathrm{R}}(n_1, n_2, x_1, x_2)/\partial x_j|_{n_{1,2}=\bar{n}_{1,2}(x_1,x_2)}$.

The equations in (5.17) form a linear system in the unknowns $\partial\bar{n}_1/\partial x_j$ and $\partial\bar{n}_2/\partial x_j$. In matrix form, it is

$$J \begin{bmatrix} \dfrac{\partial \bar{n}_1}{\partial x_j} \\ \dfrac{\partial \bar{n}_2}{\partial x_j} \end{bmatrix} = - \begin{bmatrix} \dfrac{\partial f_1^{\mathrm{R}}}{\partial x_j} \\ \dfrac{\partial f_2^{\mathrm{R}}}{\partial x_j} \end{bmatrix},$$

where J is the Jacobian matrix of the demographic model associated with the resident equilibrium, that is hyperbolic (and therefore invertible) by assumption. Same approach also holds for the x_j-derivatives ($j = 1, 2$) of $\lambda_2(x_1, x_2, x_2')$ of the predator population.

5.2.3.2 Missed or simultaneous branching?

If conditions (5.14) and (5.15) are satisfied for both populations, i.e., for i equal to 1 and 2, each one will initially become dimorphic, but

generically only one of the two nascent branchings survives. The reason is that the speed of divergence $|\dot{x}_i' - \dot{x}_i|$ between the two branching morphs is given by $k_i \bar{n}_i B_i'' |x_i' - x_i| + O(|x_i' - x_i|^2)$ and (generically) differs among the two populations. Thus, as branching takes off (according to the four-dimensional canonical equation) in the population i with largest exponential rate of divergence

$$D_i = k_i \bar{n}_i B_i'', \tag{5.18}$$

the evolution of x_i and x_i' (generically) change the equilibrium trait $\bar{x}_j$, $j \neq i$, so that the pair (x_j, x_j') falls outside the resident-mutant coexistence region that is present locally to point $(\bar{x}_j, \bar{x}_j)$ in the plane (x_j, x_j') for the current values of (x_i, x_i'). Either the x_j- or the x_j'-population therefore goes extinct on the ecological timescale, so the population turns back monomorphic and branching does not develop (this phenomenon has been called missed branching in Kisdi [1999], see Paragraph 3.3).

In nongeneric cases, that is, for critical parameter combinations (e.g. on curves in parameter planes) or in models characterized by particular symmetries (see e.g. Metz et al. [1996], Dieckmann and Doebeli [1999], Doebeli and Dieckmann [2000]), branching can develop simultaneously in more than one population. For example, if we set $h(x_1, x_2) = 0$ in our model, we are considering a Holling-type I functional response for the predator (instead of a Holling-type II). In this case the resident model (5.5) becomes

$$\begin{aligned} \dot{n}_1 &= n_1 (r - c n_1 - a n_2) \\ \dot{n}_2 &= n_2 (e a n_1 - d) , \end{aligned}$$

while the fitness functions are

$$\begin{aligned} \lambda_1(x_1, x_2, x_1') &= r - c(x_1', x_1) n_1 - a(x_1', x_2) n_2 \\ \lambda_2(x_1, x_2, x_2') &= e a(x_1, x_2') n_1 - d \end{aligned}$$

(see equations (5.12), (5.6), and (5.7) with $h(x_1, x_2) = 0$). It is now possible to compute the selections gradients for the prey and the predator traits. Recalling the shapes of functions $c(x_1, x_1')$ and $a(x_1, x_2)$ (see equations (5.8) and (5.9) and Figure 5.1), it is easy to see that the evolution of the prey will try to minimize intra-specific competition evolving toward the valley of function $c(x_1, x_1')$, while the predator will chase the prey climbing the peak of function $a(x_1, x_2)$. As a result, the evolutionary equilibrium is attained at the optimum prey trait (γ, γ), where the prey is at the competition minimum and

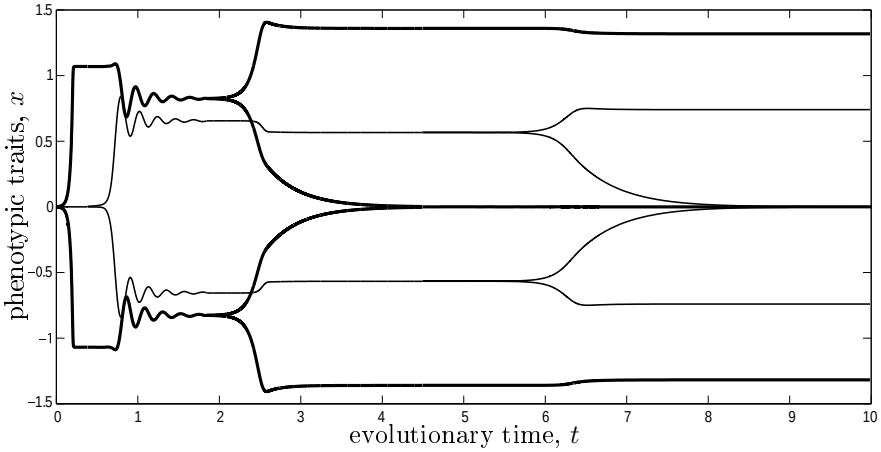

Figure 5.2: Simulation of successive AD canonical equations in the model without predator functional response. Simultaneous branchings are possible both for the prey and the predator species. Thick (resp. normal) line: prey (resp. predator) traits. Parameter values are as in Figure 5.6. Branching instants are chosen when $\dot{x}_i < 10^{-9}$ for each i.

the predator is tuned to the prey and at its predation maximum. It is easy to see that the eco-evolutionary model is perfectly symmetric around this equilibrium point (as in Metz et al. [1996], Dieckmann and Doebeli [1999], Doebeli and Dieckmann [2000]), and the same symmetry holds for enlarged models. So in this particular models branching can develop simultaneously in more than one population.

Figure 5.2 shows a simulation of the eco-evolutionary model without predator functional response ($h(x_1, x_2) = 0$)—see Paragraphs 5.4.1 and 5.4.2 for the simulation technique and the choice of the initial conditions after each branching. The structural symmetries in this model allow simultaneous branchings, that does not happen in the model with the functional response (compare with Figure 5.6). Notice that such symmetries also imply that conditions (5.14) are structurally critical ($B_i' = 0$ for all i), thus these branchings are non-generic and would require a deeper study.

Since no symmetry is present in the specific eco-evolutionary model introduced in the previous paragraphs, we restrain our attention to the branching scenarios that occur generically in parameter space.

5.3 Branching scenarios and sequences

So far, we have seen that the AD canonical equation (5.11) and the branching conditions (5.14) and (5.15) allow one to fully predict the evolution of biodiversity starting from a given ancestral community. Since the analysis presented in the next paragraphs shows that evolutionary extinctions play no role in the coevolutionary model introduced in the previous paragraphs, we now focus our attention only on evolutionary branching.

Each branching scenario identifies a branching sequence, that is a sequence of symbols (1 and 2 in the case of two species), that specify in which species the branchings occur. It is important to notice that two different branching scenarios can be associated to the same branching sequence. For example, suppose that in a system initially composed of monomorphic prey and predator, a first branching occurs in the prey. If, after that, branching is again possible in both prey populations, we have two possible branching scenarios depending upon which one of the two prey does branch. However, the two branching scenarios identify the same branching sequence, namely the sequence $s = 11$. In other words, branching sequences do not contain the full information on branching scenarios, but summarize the relevant information to study the evolution of biodiversity, namely the change in the number of coevolving prey and predator populations.

All branching sequences that can potentially occur in all eco-evolutionary models can be represented as paths from the root of the infinite binary tree T shown in Figure 5.3. The root node $(1, 1)$ represents the ancestral community composed of two populations, one for each coevolving species, and the nodes of each layer $k = 0, 1, 2, \ldots$ refer to communities with $k + 2$ populations. Notice that finite sequences can be represented by the last node of the corresponding path in T, i.e., finite branching sequences and nodes of T are interchangeable.

The aim of our analysis is to identify the branching sequences that develop from given ancestral conditions for different parameter values. Fixing the ancestral conditions means that we start from a given community (one prey, one predator in our case), characterized by given phenotypic traits (x_1, x_2) and coexisting on a given ecological equilibrium $\bar{n}(x)$. Specifically, we analyze a compact domain P of a parameter plane (p_1, p_2).

For a transparent description of our approach we now give some definitions. Let s be a finite branching sequence, which could be

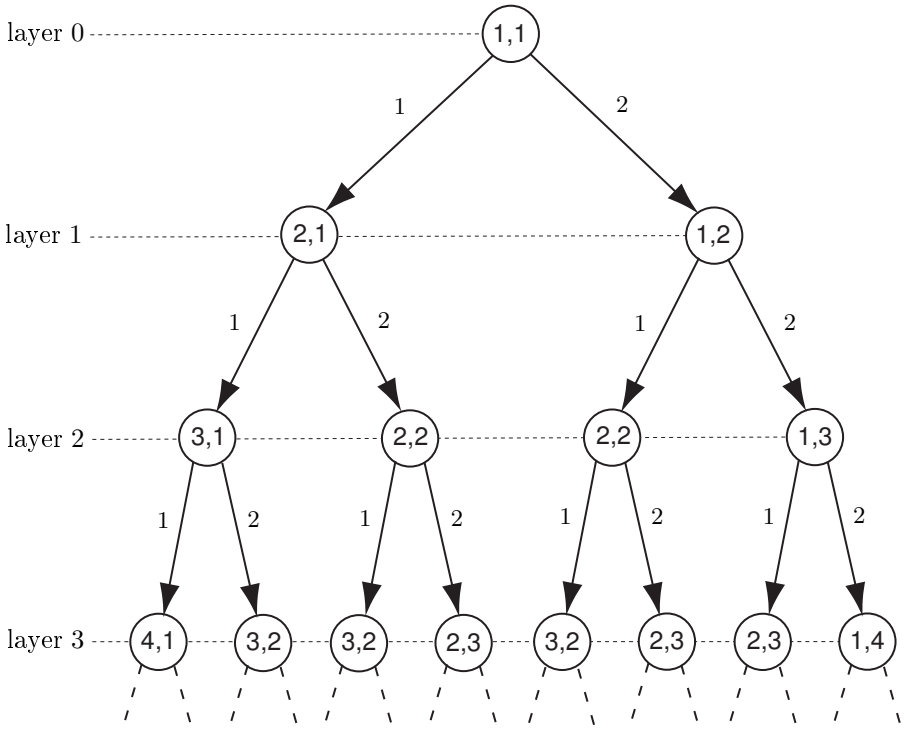

Figure 5.3: The tree T representing all potential branching sequences of a two-species community. Each node (M_1, M_2) represents a community composed of M_1 prey populations and M_2 predator populations and belongs to the layer $k = M_1+M_2-2$, $k = 0, 1, 2, \ldots$. Edges 1 and 2 represent prey and predator branching, respectively.

the first part of a longer sequence (called s-extension). A branching sequence s is called *observable* iff there exists $p = (p_1, p_2) \in P$ that produces a branching scenario associated to s or to an s-extension. The subset of P giving rise to an observable branching sequence s is indicated by $O(s)$.

An observable sequence s is called *complete* iff there exists $p \in O(s)$ that does not produce an s-extension; *incomplete* otherwise. The subset of $O(s)$ giving rise to a complete branching sequence s is indicated with $C(s)$.

By definition, given a branching sequence s, we have

$$\varnothing \subseteq C(s) \subseteq O(s) \subseteq P. \tag{5.19}$$

If $O(s) = \varnothing$ the branching sequence s cannot occur and the corre-

sponding node in T can be eliminated together with all its successors.

If $O(s) \neq \varnothing$ and $C(s) = \varnothing$ the branching sequence s is incomplete and the corresponding node in the tree can be identified with a particular color (grey). In this case, s-extensions can be of any type because through extension one can obtain completeness or not, or even lose observability.

If $C(s) \neq \varnothing$ the branching sequence s is complete and the corresponding node in the tree can be identified with a second color (white). Again, the successors of a white node in the tree can be of any type.

When all nodes of T are eliminated or colored in the way just described, a new tree BT, called *branching tree*, is obtained. Notice that the tree BT can be infinite (but recall that infinite sequences require some criticality in the choice of the model functions and parameters [Gyllenberg and Meszéna, 2005, Meszéna et al., 2006]). Moreover, a non empty subset of P can be associated to each node of the branching tree: the set $O(s)$ to each gray node identifying the incomplete sequence s; the set $C(s)$ to each white node identifying the complete sequence s. The sets $C(s)$ are all disjoint, whereas given two sequences s' and s'', $O(s'') \subseteq O(s')$ iff s'' extends s'. The collection C of all sets $C(s)$ obviously defines a partition of the parametric domain P, though some of the sets $C(s)$ may have zero measure in P (those corresponding to non-generic sequences, e.g. sequences where several branching occur simultaneously).

Finally, we call *branching portrait* (BP) the diagram of the collection C. This parametric portrait graphically summarizes the analysis of branching scenarios and can be used as a control chart in deriving managerial policies. It can be composed of infinite regions, though shrinking with the length of the sequence, so that an iterative procedure for its construction, that considers sequences with increasing length, is proposed in the next paragraph.

5.4 Iterative procedure

In this paragraph we show how the branching portrait BP can be progressively approximated by applying an iterative procedure involving simulations and continuations. The procedure is illustrated by applying it to the prey-predator eco-evolutionary model described above. The two parameters p_1 and p_2, belonging to two given intervals, are e and γ_3, i.e., predator efficiency (see (5.5)) and the parameter specifying the sensitivity of prey intraspecific competition to resident-mutant

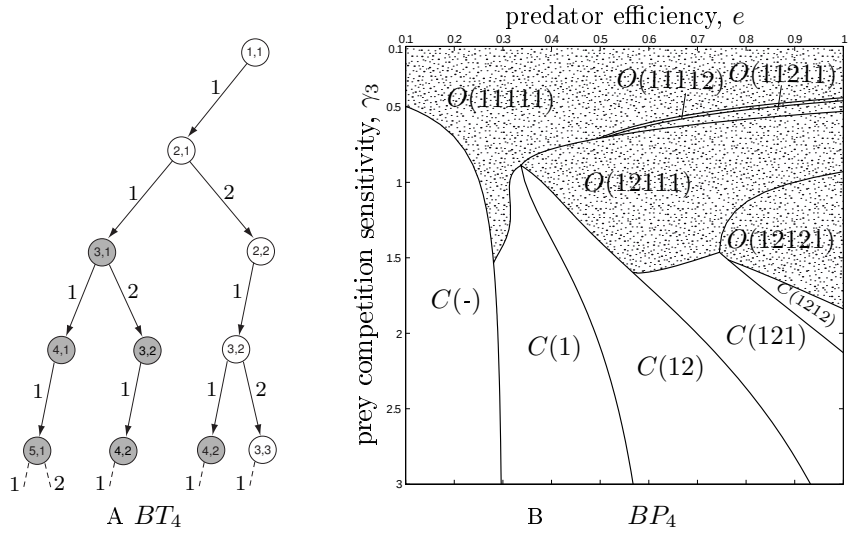

Figure 5.4: The tree BT_4, where white and grey nodes represent complete and incomplete branching sequences. The approximation BP_4 of the branching portrait, where a complete branching sequence of length smaller or equal to 4 is associated to each white region, whereas a sequence of length equal to 5 is associated to each dotted region. All parameters, except e and γ_3, are at their reference values: $r = 0.5$, $d = 0.05$, $\gamma = 0$, $\gamma_0 = 0.01$, $\gamma_1 = 0.5$, $\gamma_2 = 2.3$, $\alpha = 1$, $\alpha_0 = 0.01$, $\alpha_1 = 1$, $\alpha_2 = 0$, $\theta = \theta_1 = \theta_2 = 0.5$, $\theta_3 = \theta_4 = 1$, $k_1 = k_2 = 1$. The considered ancestral condition is $x_1(0) = 0$, $x_2(0) = 0$.

phenotypic mismatch (see (5.8)).

The procedures generates at iteration k the tree BT_k, composed of layers $0, \ldots, k$ of the branching tree BT, and an approximation BP_k of the branching portrait BP. Specifically, BP_k includes the sets $C(s)$ associated to branching sequences s of length smaller or equal to k, while the remaining area of the parameter domain P is divided into the sets $O(s)$ associated to sequences of length equal to $k+1$. All this information can be obtained by analyzing the canonical equation describing the communities corresponding to the nodes at layer k of BT_k. In particular, the branching points in these communities identify the observable sequences of length $k+1$ and define the nodes at layer $k+1$ of BT_{k+1}, their color to be determined at the next iteration.

For example, in the case of our prey-predator model, for $k = 4$, the tree BT_4 and the portrait BP_4 are as in Figure 5.4. The white region $C_4 = C(\text{-}) \cup C(1) \cup C(12) \cup C(121) \cup C(1212)$ in BP_4 is the

collection of the sets $C(s)$ of the white nodes of BT_4, i.e., the sets $C(s)$ of all complete branching sequences of length smaller or equal to $k = 4$. Hence, $C_4 \subseteq C$. The dotted region is the union of the sets $O(s)$ of sequences of length $k + 1 = 5$, so five branchings are observable in this region. Obviously, the dotted region shrinks and eventually disappears as k is increased. In conclusion, smaller dotted regions in BP_k correspond to better approximations of BP.

5.4.1 Iteration 0

We start with $k = 0$, i.e., with a degenerate tree composed of the root node $(1, 1)$ corresponding to the empty sequence $s =$ -, and the target is to determine BT_0 and BP_0. As for BT_0, we must establish the nature (complete or not) of the root node, whereas for BP_0, we must determine the set $C_0 = C(\text{-})$, i.e., the parameter values for which no branching is possible, and the sets $O(1)$ and $O(2)$ where sequences of length $k + 1 = 1$ are observable.

For this, we start our analysis from a given point in the parameter domain P (we start from $p = (e, \gamma_3) = (0.1, 2)$) and determine the stable equilibrium $(\bar{x}_1,\bar{x}_2)$ of the corresponding AD canonical equation (5.11) reached from the considered ancestral condition. This can be easily accomplished in a standard way, because the non-trivial equilibrium $(\bar{n}_1(x_1, x_2), \bar{n}_2(x_1, x_2))$ of the ecological model (5.5) is known in closed form (see Dercole et al. [2003]). However, this is not true for the nodes of all larger trees, because the equilibrium $\bar{n}(x)$ of the resident model cannot be derived analytically when the populations are three or more. Thus, we systematically determine the stable equilibrium of any AD canonical equation through the simulation of an eco-evolutionary model characterized by two different time scales. In the case $k = 0$ the slow-fast ODE system is

$$\begin{aligned} \dot{n}_1 &= n_1 f_1^{\mathrm{R}}(n_1, n_2, x_1, x_2, e, \gamma_3) \\ \dot{n}_2 &= n_2 f_2^{\mathrm{R}}(n_1, n_2, x_1, x_2, e, \gamma_3) \\ \dot{x}_1 &= \epsilon k_1 H_1(x_1, x_2, e, \gamma_3) \\ \dot{x}_2 &= \epsilon k_2 H_2(x_1, x_2, e, \gamma_3), \end{aligned} \tag{5.20}$$

where ϵ is a small positive parameter used to tune the slow evolutionary dynamics with respect to the fast ecological dynamics (in our application the value $\epsilon = 10^{-3}$ has given satisfactory results).

For $p = (e, \gamma_3) = (0.1, 2)$ and the ancestral condition we consider $(x_1(0) = 0,\ x_2(0) = 0)$, system (5.20) tends toward the stable equilibrium $(\bar{n}_1, \bar{n}_2, \bar{x}_1, \bar{x}_2) = (0.6589, 0.2269, -0.0048, 0.0371)$, thus

characterized by

$$f_1^{\mathrm{R}} = f_2^{\mathrm{R}} = H_1 = H_2 = 0. \tag{5.21}$$

Once this equilibrium has been found, it is possible to continue it by varying e [γ_3]. The aim is to continue it until a point where $B_1'' = 0$ is obtained, that is, until a solution of the system with five equations

$$f_1^{\mathrm{R}} = f_2^{\mathrm{R}} = H_1 = H_2 = B_1'' = 0 \tag{5.22}$$

is found. Since the unknowns in this system are six (n_1, n_2, x_1, x_2, e, γ_3), the solution of (5.22) can in turn be continued by varying both e and γ_3, thus finding a curve $e(\gamma_3)$ (resp. $\gamma_3(e)$) in parameter space. On this curve, shown in BP_0 in Figure 5.5, the first branching function of the prey B_1'' annihilates. Therefore, at one side of the curve the first branching condition for the prey ((5.14) with $i = 1$) is satisfied.

In principle, analogous operations should be done for the other three branching functions B_1', B_2' and B_2'' to possibly obtain other three curves in parameter space. The region in which population i does branch would then be the one in which $B_i' < 0$ and $B_i'' > 0$, provided population i has the largest resident-mutant trait divergence (see (5.18)) where both prey and predator satisfy the branching conditions (5.14) and (5.15). However, it is possible to numerically verify that B_1' is always negative (see Paragraph 5.2.3.1). This property is valid in general, that is, also in systems with many populations of prey and predator, and is due to the exponential term in the competition function (5.8) which favors resident-mutant coexistence. Hence, the branching condition of the i-th prey population is $B_i'' > 0$.

Instead, for the predator, the function B_2' is identically null, so that the predator branching is not possible. Also this property is valid in general, when the number of predator populations (M_2) is equal to the number of prey populations (M_1). As already noticed in Dercole et al. [2003], this is a direct consequence of the well known *competitive exclusion* principle [Hardin, 1960, MacArthur and Levins, 1964, 1967, MacArthur, 1969] and its more recent generalizations [Diekmann et al., 2003, Diekmann and Metz, 2006, Gyllenberg and Meszéna, 2005, Meszéna et al., 2006]. If, otherwise, $M_1 > M_2$, then B_i' is negative for all predator populations (numerically checked), so that, the branching condition for the i-th predator population reduces to $B_i'' > 0$. Using the terminology introduced in Diekmann et al. [2003], the number of stationary coexisting morphs of a species is limited by the number of biotic environmental factors affecting the

ecological dynamics of the species. For the predator, these factors are simply the prey densities, i.e., M_1 factors.

While monitoring functions B_1'' and B_2'' during continuation, we must also check whether the equilibrium of system (5.20) undergoes a bifurcation [Kuznetsov, 2004, Meijer et al., 2009], e.g., it might disappear through a saddle-node (or fold) bifurcation or lose stability through a Hopf bifurcation. This is easy and automatically done by standard continuation softwares. In the first case, the evolutionary trajectory originated from the considered ancestral condition will converge to another evolutionary attractor, possibly an evolutionary equilibrium that might generate a different branching sequence, whereas evolutionary cycling prevents further branching in the second case. Recall that our choice of the model parameters guarantees the stationary coexistence of the demographic model (5.1), so that bifurcations can only involve the slow dynamics of system (5.20). Moreover, while moving parameters in the presence of multiple evolutionary attractors, different branching sequences might also arise without bifurcations, simply because the considered ancestral condition switches from the basin of attraction of one attractor to that of another. Multi-stability is related to the presence of saddle equilibria, whose stable manifolds are the boundaries of the different basins of attraction. Since attractors themselves, saddles, and their manifolds move in the state space when changing parameters, it could happen that the considered ancestral condition (which is fixed and does not change with parameters) passes, at a critical parameter value, from the basin of attraction of one attractor to that of another. Technically, this is not a bifurcation, but implies a qualitatively different evolutionary dynamics.

None of the above possibilities occurred in system (5.20), whereas saddle-node bifurcations will be found in the further iterations of the procedure, though with no effect on the branching portraits. For this reason, they will no more be discussed in the next iterations. Otherwise, Hopf bifurcations will be found and will affect the branching portraits with respect to other parameter pairs that will be presented in the Discussion.

In conclusion, the iteration $k = 0$ of the procedure shows that the empty branching sequence $s =$ - is complete, because region C(-) (where no branching is possible) is not empty, so that the color of the root of the tree BT_0 (the first node of BT_4 in Figure 5.4) is white. The first approximation BP_0 of the branching portrait BP is shown in Figure 5.5, where the dotted region is nothing but $O(1)$, since $O(2)$ is empty because the predator cannot branch (so that $O(1) = P - C$(-)).

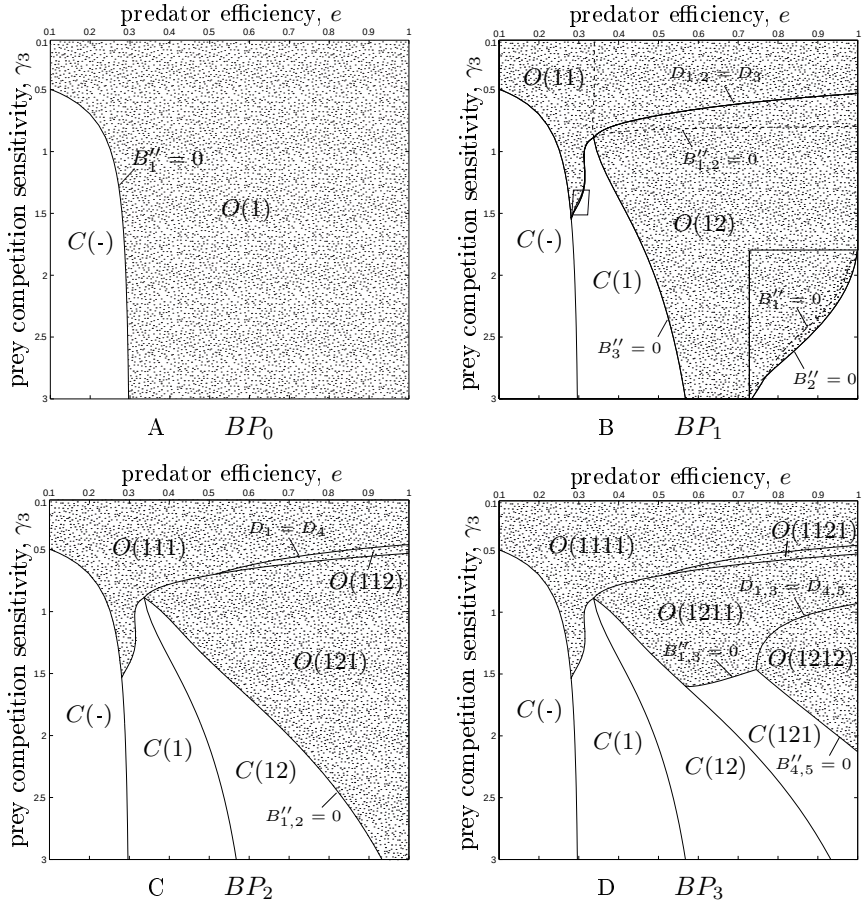

Figure 5.5: The approximated branching portraits BP_0–BP_3 produced at the iterations $k = 0, 1, 2, 3$ of our procedure. At each iteration the boundaries added to the diagram are curves of the type $B_i'' = 0$ or $D_i = D_j$ and are accordingly labeled (recall that at iteration k we analyze communities with $M_1 + M_2 = k + 2$ populations and that $i = 1, \ldots, M_1$ and $i = M_1+1, \ldots, M_1+M_2$ are prey and predator indexes, respectively). As shown in BP_1 (see also enlarged box), the region boundaries (solid lines) might concatenate segments of different curves. Parameter values as in Figure 5.4.

5.4.2 Iteration 1

At the iteration $k = 1$ the community has two prey populations ($M_1 = 2$) and one predator population ($M_2 = 1$) and the target is to determine BT_1 and BP_1. BT_1 has only node $(2, 1)$ at level 1

(because predator branching is not possible at the root node), so we must establish its nature. As for BP_1, we must determine the set $C(1)$, i.e., the parameter values for which no branching is possible at node $(2,1)$, and the sets $O(11)$ and $O(12)$ where sequences of length $k+1=2$ are observable. Of course, such sets are contained in $O(1)$, i.e., in the dotted region of BP_0 (see Figure 5.5).

For this, first we write the AD canonical equation (composed of three ODEs, one for each population), and then determine its stable equilibrium ($\bar{x}_1$,$\bar{x}_2$,$\bar{x}_3$). Similarly to what was done in the previous paragraphs, we simulate a slow-fast eco-evolutionary system with six variables: n_1, n_2, n_3 and x_1, x_2, x_3, where n_3 and x_3 are predator density and trait. This system is analogous to (5.20) and must be simulated starting from initial conditions that represent the state of the system just after a prey branching has occurred in the system with $M_1 = M_2 = 1$. This links this iteration with the previous one. For producing the six required initial conditions we select any point on the curve $B_1'' = 0$ in BP_0, which corresponds to a stable equilibrium of system (5.20) and we continue it by increasing e in order to enter into the dotted region $O(1)$ where prey branching occurs. Since close to the branching point the two similar traits coexist and evolve in opposite directions, we define the initial condition as follows: $n_1(0) = n_2(0) = \bar{n}_1/2$, $n_3(0) = \bar{n}_2$, $x_1(0) = \bar{x}_1 - \delta$, $x_2(0) = \bar{x}_1 + \delta$, $x_3(0) = \bar{x}_2$, where $(\bar{n}_1, \bar{n}_2, \bar{x}_1, \bar{x}_2)$ is the obtained equilibrium of system (5.20) (we used $\delta = 10^{-3}$). Once a stable equilibrium $(\bar{n}_1, \bar{n}_2, \bar{n}_3, \bar{x}_1, \bar{x}_2, \bar{x}_3)$ has been obtained by simulating the six-dimensional eco-evolutionary system, the parameter e and/or γ_3 are varied until three points in parameter space are obtained where $B_1'' = 0$, $B_2'' = 0$, $B_3'' = 0$, respectively. These three points belong to the boundaries of the regions where populations $1, 2, 3$ can branch, so that the three boundaries can be produced through continuation of the solution of the algebraic systems

$$f_1^{\mathrm{R}} = f_2^{\mathrm{R}} = f_3^{\mathrm{R}} = H_1 = H_2 = H_3 = B_i'' = 0 \tag{5.23}$$

with $i = 1, 2, 3$.

The result allows one to determine, by simply looking at the signs of all B_i'' in the vicinity of the curves, the tree BT_1 (the first two layers in BT_4 in Figure 5.4) and the approximation BP_1 of the branching portrait (see Figure 5.5). Node $(2,1)$ is white because region $C(1)$ (where one and only one prey branching occurs) is not empty. The dotted region of BP_1, to be further investigated, is the union of the sets $O(11)$ and $O(12)$, where prey or predator branching occurs at node $(2,1)$. Note that the curves $B_1'' = 0$ and $B_2'' = 0$ are very close

one to the other and not distinguishable at the scale of the figure. The enlargement in BP_1 shows that $O(11)$ is the region where at least one of the two prey can branch. Where both prey can branch, it does not matter which one does it—the one with faster resident-mutant divergence (see (5.18))—since further branchings produce the same sequences. Where also the predator acquires a positive B_3'', the population that branches is again the one with faster resident-mutant divergence, and in this case the lines along which $D_1 = D_3$ and $D_2 = D_3$ (again not distinguishable at the scale of the figure) matter in the branching portrait.

5.4.3 Successive iterations

The successive iterations proceed along the same lines we have described in detail in the two previous paragraphs. We now briefly summarize seven sequential steps in which each iteration can be subdivided. We recall that the target of iteration k is the determination of the tree BT_k and of the approximation BP_k of the branching portrait BP.

1. Write the AD canonical equation associated to each of the sets $O(s)$, with s of length k, composing the dotted region of the approximation BP_{k-1} of the branching portrait determined at the previous iteration. In each of these regions, after the first k branchings, the community is composed of M_1 prey and M_2 predator (with $M_1 + M_2 = k+2$). For example, at the iteration 2, we consider the sets $O(11)$ with $M_1 = 3$ and $M_2 = 1$ and $O(12)$ with $M_1 = 2$ and $M_2 = 2$ (see BP_1 in Figure 5.5).

2. For each considered canonical equation, write the corresponding $2(k+2)$-dimensional slow-fast eco-evolutionary system.

3. Determine the stable equilibrium of the eco-evolutionary system through simulation. The initial conditions of the simulation must represent the density and the trait of the populations just after the k-th branching. Note that if the boundary of the set $O(s)$ is composed of several segments corresponding to branching of different populations, an initial condition for each branching must be considered.

4. Continue the stable equilibria of the eco-evolutionary systems varying e or γ_3 until a point on each possible curve where $B_i'' = 0$ is found. If no such point is found, B_i'' never changes sign. If B_i''

is negative, no branching is possible for population i, whereas if it is positive branching is possible in the whole region.

5. Produce the curves on which $B_i'' = 0$ through continuation of the points determined at step 4.

6. In the regions where B_i'' and B_j'' are positive for $i \neq j$, produce through continuation the curves on which $D_i = D_j$.

7. Determine (through a simple inspection of the signs of B_i'' near the curves) the tree BT_k and the approximation BP_k of the branching portrait BP. In particular, C_k is obtained by adding to C_{k-1} the parameter combinations for which no further branching has been detected, whereas the new dotted region is the union of the identified sets $O(s)$, with s of length $k+1$. The boundary of such sets are obtained by suitable concatenating segments of the obtained curves $B_i'' = 0$ and $D_i = D_j$.

Figure 5.5 shows the approximations BP_k of the branching portrait obtained for $k = 0, 1, 2, 3$ while BP_4 was already reported in Figure 5.4. The comparison of these approximations clearly points out that our procedure is rather efficient since the dotted region (that must be further analyzed at iteration $k+1$) shrinks significantly at each iteration.

Figure 5.6 shows an example of simulation of successive canonical equations corresponding to a complete sequence with four alternate branchings.

5.5 Discussion

In the first part of this paragraph we discuss the main biological consequences of the analysis performed so far, while in the second part we show how, with a marginal extra computational effort, the scope of the analysis can be substantially enlarged. Finally, we describe the steps that are required to abstract from our analysis and propose a general method for investigating branching scenarios in coevolving species.

Before discussing the approximation of the branching portrait in Figure 5.4, let us notice that the parameter γ_3 on the vertical axis of that figure is increasing from top to bottom. Since decreasing values of γ_3 correspond (see (5.8)) to increasing sensitivities of prey intraspecific competition to the resident-mutant phenotypic mismatch,

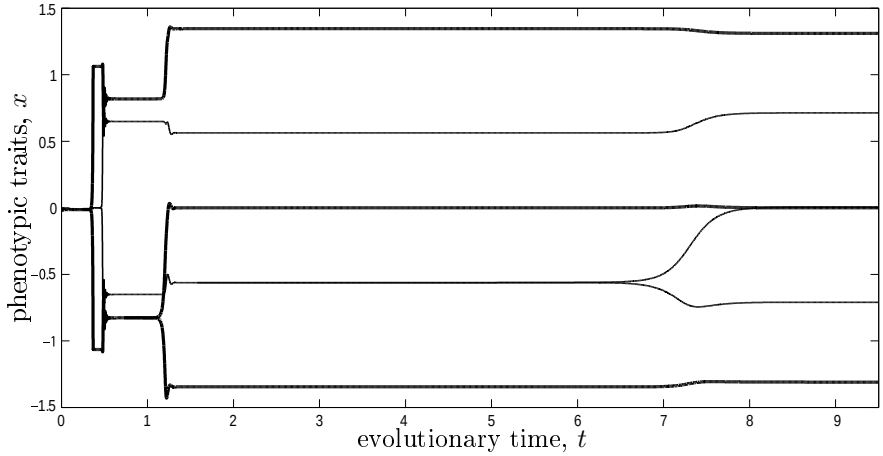

Figure 5.6: Simulation of successive AD canonical equations for the alternate branching sequence $s = 1212$. Thick (resp. normal) line: prey (resp. predator) traits. Parameter values are as in Figure 5.4, $e = 0.98$ and $\gamma_3 = 2$. Branching instants are chosen when $\dot{x}_i < 10^{-9}$ for each i.

in interpreting Figure 5.4 we must take into account that its left lower corner represents prey with low sensitivity of competition and predator with low efficiency, whereas highly sensitive competing prey and very efficient predator are located at the right upper corner.

The first property emerging from Figure 5.4 is that the region $C(\text{-})$ where branching is not possible is in the left lower corner. This is quite intuitive from a biological point of view, because prey with low sensitivity of competition has no relevant advantages in splitting when the predation pressure is limited by a low predator efficiency. For the same reason, at the right upper corner, long branching sequences are possible.

A second interesting property pointed out by Figure 5.4 is that both alternate (prey and predator) and unilateral (only prey) branching sequences are possible. More precisely, long alternate branching sequences are favored by high predator efficiency, while long unilateral prey branching sequences (see for example the set $O(11111)$) occur for low predator efficiency and high prey sensitivity of competition. Also this property can be intuitively understood because when prey competition is highly sensitive prey have an advantage in splitting in order to reduce the negative consequences of being too similar.

Notice that also long branching sequences composed of a first phase of alternate branching concatenated with a long sequence of

prey branching are possible (see e.g. region $O(12111)$ in Figure 5.4), but require a few more iterations of our procedure in order to be clearly pointed out in better approximations of the branching portrait (e.g. observable prey branchings are added to $O(12121)$ in BP_k for $k > 4$).

Finally, a third property that is worth mentioning is that branching scenarios can be highly sensitive to parameter perturbations. This is clearly visible close to the points in parameter space where two or more region boundaries merge. Also the boundary separating set $C(-)$ from $O(11111)$ in BP_4 shows that as soon as prey branching becomes possible at node $(1, 1)$, branching is possible also at nodes $(M_1, 1)$, with $M_1 \geq 2$, so that a small parameter perturbation can discriminate between very poor and extremely rich prey biodiversity. This latter property has also been observed in the Lotka-Volterra competition model [Kisdi, 1999, Dercole et al., 2008].

In conclusion, in coevolving prey-predator systems not only the number of prey populations (i.e., biodiversity) is higher than the number of predator populations (as implied by the principle of competitive exclusion) but often this difference is remarkable, in particular when prey intraspecific competition is highly sensitive to the resident-mutant phenotypic mismatch. This conclusion is in good agreement with many studies based on field observations of aquatic and terrestrial food chains like phytoplankton-zooplankton in shallow lakes [Scheffer, 1998], rodents and their predators in boreal and arctic regions [Turchin, 2003, King and Schaffer, 2001], and many others [Briand and Cohen, 1984].

We now show how the analysis described so far, concerning the influence of two parameters p_1 and p_2 on branching scenarios, can be extended to study the influence of any other parameter p_3. The idea, suggested by the power and flexibility of continuation methods, is very simple. Suppose an approximation of the branching portrait BP, like that shown in Figure 5.4, has already been produced. Except for p_1 and p_2, this approximated portrait has been computed for fixed reference values

$$p_i = p_i^* \qquad i = 3, 4, 5, \ldots$$

of all other parameters (see the caption of Figure 5.4). We can therefore fix p_2 at a particular reference value p_2^* and read from BP_4 in Figure 5.4 the p_1-coordinates of all points of the boundaries of the various regions with $p_2 = p_2^*$. Obviously, these p_1-coordinates allow one to determine in the space (p_1,p_3) a series of points with $p_3 = p_3^*$ belonging to the boundaries of the various regions of the approximated

branching portrait obtainable for

$$p_i = p_i^* \qquad i = 2, 4, 5, \ldots$$

Then, with a limited computational effort, we can produce through continuation of this series of points a new approximated branching portrait in the space (p_1,p_3). This means that, with almost the same computational burden necessary for discussing the influence of a pair of parameters, we can, in reality, discuss the influence of any other parameter pair.

Six examples of new branching portraits obtained from Figure 5.4 by fixing $\gamma_3 = 2$ are shown in Figure 5.7. Since the branching sequences obtained for $\gamma_3 = 2$ are all complete in BP_4, it was reasonable to expect exact branching portraits in the space (p_1, p_3) (no dotted regions) characterized by complete sequences, at least for small deviations of p_3 from p_3^*. All branching portraits have predator efficiency on their horizontal axis (as BP_4 in Figure 5.4) while the new parameter on the vertical axis is

A the ratio k_1/k_2 of the evolution speed of prey and predator (see (5.2)),

B the predator handling time θ (see (5.10)),

C the optimum prey trait γ (see (5.8)),

D the curvature of prey competition γ_2 around the optimum prey trait (see (5.8)),

E the predator maximum attack rate α (see (5.9)),

F the kurtosis of predator attack rate α_2 (see (5.9)).

The first five new parameters have been selected in order to obtain results comparable with those reported in Dercole et al. [2003], while the sixth choice has been suggested by the interest in discussing the role played by generalist vs. specialist predator on evolution (see Sasaki [1997], Hernández-García et al. [2009], Pigolotti et al. [2010]).

Figure 5.7A shows that the ratio of evolution speed has no influence on branching scenarios. This might seem obvious a priori, since k_1 and k_2 do not modify the evolutionary equilibria and the branching conditions (5.14) and (5.15). However, the ratio k_1/k_2 affects the stability of the evolutionary equilibria (recall that branching points have been defined as stable equilibria of the canonical equation satisfying

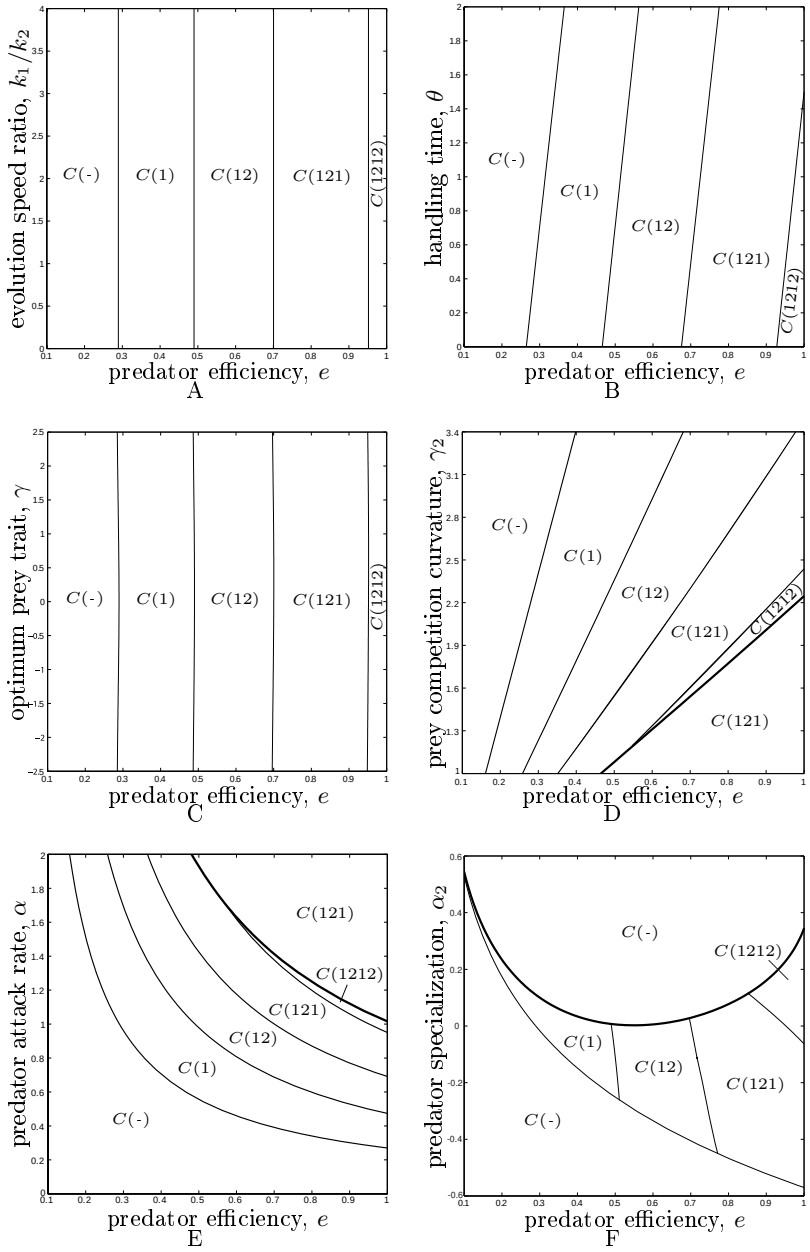

Figure 5.7: Six examples of branching portraits obtained from Figure 5.4 through continuation. Parameter values as in Figure 5.4 and $\gamma_3 = 2$. Thick line: Hopf bifurcation curve.

conditions (5.14) and (5.15)), though no change in stability occurs in

Figure 5.7A.

Figure 5.7B shows that the predator handling time θ has a detectable impact on branching scenarios. In particular, for fixed predator efficiency, the number of alternate branchings decreases if θ is increased. As far as we know, this property has never been discussed in the literature, though it is biologically sensible: predators with longer handling times exert a limited predation pressure and therefore do not turn selection disruptive on prey with relatively low sensitivity of competition.

Figure 5.7C shows that the optimum prey trait γ has almost no influence on branching scenarios. This is perhaps intuitive because a variation of γ essentially introduces a shift in the body size of the prey (and hence of the predator). In our model, however, the handling time is sensitive to such a shift, so that there is an influence (branching being slightly favored by nonzero values of γ), though not clearly visible at the scale of the figure.

In contrast, the influence of the prey competition curvature γ_2 (Figure 5.7D) is significant. This property seems also to have gone unnoticed in the literature and is less intuitive. A smaller curvature implies a larger valley of the competition function around the optimum prey trait γ, i.e. a larger trait interval that prey can exploit through branching for escaping the predation pressure; and predator branching is favored after each prey diversification. This mechanism however does not work if competition is too mild, as the evolutionary dynamics in the system with three prey and two predator populations get destabilized. The five coevolving traits start to oscillate on a Red Queen evolutionary cycle, along which the two predators alternate between harvesting the prey with smaller (resp. larger) trait and the intermediate prey. Technically, evolutionary cycling is due to a Hopf bifurcation in the system at node (3,2) (the thick curve in the figure) through which the evolutionary equilibrium becomes unstable and surrounded by a stable limit cycle. Recall that evolutionary cycling prevents further branching, as branching requires evolution to settle down at an evolutionary equilibrium, so the sequence $s = 121$ is complete below the Hopf curve (see the lower set $C(121)$).

Also the influence of the predator maximum attack rate is relevant (Figure 5.7E). Increasing the predation pressure favors prey branching, which in turn makes selection disruptive on the predator. Again increasing the attack rate destabilizes the evolutionary dynamics and prevents further branching (see the Hopf bifurcation in the system at node $(3, 2)$). Red Queen evolutionary cycles of the kind just described

for Figure 5.7D develop in the upper set $C(121)$.

Finally, Figure 5.7F shows that a predator with given efficiency promotes alternate branchings only if the kurtosis of the attack rate has intermediate values. If the kurtosis is decreased, i.e., if predator become more generalist, branching sequences become shorter until no branching is possible anymore (lower set $C(\text{-})$). In contrast, if kurtosis increases, i.e., if predator become more specialist, longer branching sequences are first promoted but then made impossible by a Hopf bifurcation involving the monomorphic equilibrium of the ancestral community at the root node $(1, 1)$ (see the upper set $C(\text{-})$). As far as we know, this latter property was not discovered until now, while the former is in agreement with the literature (see Hernández-García et al. [2009], Pigolotti et al. [2010]).

We close this discussion by describing how a general method for investigating branching scenarios in two (or more) coevolving species could be derived from our analysis. First of all, evolutionary extinction should be considered by allowing sequences of four (instead of two) different events, namely branching and extinction of one or the other species, and extinctions events would be represented by backwards links in the graph of Figure 5.3, which would no longer be a tree. This would allow the study of interesting systems, e.g. the evolution of cannibalism [Dercole and Rinaldi, 2002], where the existence of branching-extinction cycles has already been established [Dercole, 2003]. Technically, evolutionary extinctions can be detected during continuation and simulation of the slow-fast system (5.20) as the collision of evolutionary trajectories with bifurcation boundaries of the ecological system (the fast compartment). Two types of bifurcations are responsible of evolutionary extinctions: the saddle-node bifurcation at which the ecological equilibrium (the node) collides with a saddle equilibrium and disappear; the transcritical bifurcation at which the density of a population vanishes. In the first case, the coevolution drives the community toward the loss of the ecological equilibrium of coexistence, after which the ecological system switches (on the fast ecological timescale) to another attractor, typically to another equilibrium at which some (or even all) populations are no longer present (evolutionary suicide [Gyllenberg and Parvinen, 2001, Dercole and Rinaldi, 2008]). In the second case, the density of a population is driven to zero by the evolution of the others (evolutionary murder [Dercole and Rinaldi, 2008]).

Another aspect not highlighted by our application is the possibility that the fitness derivative B_i' changes sign while moving the model

parameters. The points in parameter space where this occurs can be detected during continuation (see Paragraph 5.2.3.1 for the details on the computation of B_i') and the curves along which $B_i' = 0$ accordingly traced.

Worth to be mentioned is the choice of the ancestral condition of interest. The ancestral community for a case with two species should not necessarily be the $(1, 1)$-community. Interesting cases where no branching is possible in the simplest community, whereas long branching sequences are observable starting from richer communities have indeed been discussed [Kisdi, 1999].

Moreover, rich and interesting branching scenarios for the selected ancestral community can be observable starting from some initial conditions and not starting from others. Multiple attractors in the fast (ecological) and in the slow (evolutionary) compartments can in fact be present [Dercole et al., 2002, 2003]. Keeping track of all possible observable branching sequences is possible, but the description of a method greatly simplifies if one focuses on a specific initial condition.

Of course the bifurcations involving the selected ecological and evolutionary equilibria may force the community to switch (on the ecological or evolutionary timescale) to other attractors. In our analysis we always had coexistence at stable ecological equilibria (numerically checked), even though the AD canonical equation can be (heuristically) generalized to the case of nonstationary ecological attractors [Dieckmann and Law, 1996, Dercole et al., 2006].

But attractor switchings can also occur without involving bifurcations. In fact, in cases with multiple evolutionary attractors, the boundaries of the various basins of attraction (which are the stable manifold of saddle equilibria) do change along with the model parameters, so that the selected ancestral condition, or the initial condition imposed by a branching point on the next canonical equation, can pass from one basin of attraction to another at a critical parameter combination. Technically, this is not a bifurcation, but involves a qualitative change in the evolutionary dynamics, and therefore in the branching scenario produced from the initial condition under consideration. In some cases, the boundaries of the attraction basins can be continued, as suitable heteroclinic trajectories connecting saddle equilibria [Kuznetsov, 2004, Meijer et al., 2009], but most often basins of attraction are estimated by means of systematic simulations.

Keeping track of all the above possibilities in the formal description of a general method of analysis is quite involved and not among the aims of this paper. In our analysis we have emphasized only the

aspects that were relevant for the considered application. Of course, of each computed curve (along which a branching condition vanishes, a bifurcation of the slow-fast system occurs, or the ancestral condition changes basin of attraction), only the segments for which the corresponding evolutionary equilibrium is reached from the considered ancestral condition matter in the branching portrait. Such segments are part of the branching portrait only if the change produced in the evolutionary dynamics induces a change in the branching sequence. This can be noticed, e.g., in Figure 5.7(d,e), where the curve $B''_{4,5} = 0$ separating regions $C(121)$ and $C(1212)$ (on which the two predators acquire branching) merges with the Hopf bifurcation of the slow-fast system corresponding to node $(3, 2)$. Moving right-to-left, the curve $B''_{4,5} = 0$ is part of the branching portrait only up to the contact with the Hopf curve.

5.6 Concluding remarks

We have analyzed the evolution of biodiversity in a prey-predator coevolutionary model based on the standard Rosenzweig-MacArthur ecological model [Rosenzweig and MacArthur, 1963]. Neglecting the introduction of alien species and accidental or artificial extinctions, we consider evolutionary branching [Geritz et al., 1997, 1998, Dercole and Rinaldi, 2008]—the coexistence and further differentiation of resident-mutant phenotypes—and evolutionary extinction [Gyllenberg and Parvinen, 2001, Dercole and Rinaldi, 2008]—evolution toward self- or other-distruction—as the major drivers of biodiversity. Adaptive dynamics (AD [Metz et al., 1996, Geritz et al., 1997, 1998, Dercole and Rinaldi, 2008, Geritz and Dercole, 2011]) is the most suited modeling approach to investigate evolutionary branching and extinction in coevolutionary models, and the AD canonical equation makes it possible on a deterministic ground [Dieckmann and Law, 1996, Dercole and Rinaldi, 2008].

We opted for measuring biodiversity with the number of phenotypically different prey and predator populations, thus losing information on the actual phenotypic values, but acquiring simplicity and compactness of representation. In particular, we have not found extinction events in the analyzed model, so that biodiversity evolves according to branching sequences, namely sequences of symbols 1 and 2 identifying branching in the prey and predator species, respectively.

We have discovered that long alternate (prey and predator) as well as unilateral (prey) branching sequences can occur. But we have

also discovered that long sequences composed of a first phase of alternate branching concatenated with a long unilateral sequence of prey branchings are possible in some regions of parameter space. This explains why prey populations can be much more numerous than predator populations, a fact that is often mentioned in field studies and is in agreement with traditional [Hardin, 1960, MacArthur and Levins, 1964, 1967, MacArthur, 1969] and modern [Diekmann et al., 2003, Diekmann and Metz, 2006, Gyllenberg and Meszéna, 2005, Meszéna et al., 2006] theories of competitive exclusion.

Another interesting result is that branching sequences become longer if predator become more and more specialist, until a critical point is reached at which never ending Red Queen ups and downs of the coevolving traits prevent a halt at evolutionary equilibria and therefore evolutionary branching. This discontinuity occurs at the birth of a stable evolutionary cycle due to a Hopf bifurcation of the evolutionary system.

Finally, critical parameter combinations for which branching scenarios are highly sensitive to parameter perturbations have been identified. This knowledge is of strategic importance for the conservation and management of biodiversity.

Our iterative procedure is based on simulations of ODEs (the AD canonical equation and the underlying ecological models) and continuations of algebraic systems of equations [Allgower and Georg, 2003] and explores, at each iteration, the nature of longer and longer branching sequences. At each iteration, a better approximation of a two-dimensional branching portrait (explaining the dependence of branching scenarios on two parameters) becomes available. Our approach is more interesting, both computationally and conceptually, than the stochastic individual- or population-based simulations mainly used until now when analytical tractability is unfeasible. Each simulation, even the deterministic one shown in Figure 5.6, can only reveal an observable branching sequence, whereas our systematic analysis extracts information on all possible sequences including their nature, whether complete, incomplete or not observable. A particularly attractive feature is that, after a first branching portrait has been produced, the dependence of the branching scenarios on other parameters can be discussed without significantly increase the computational burden.

In principle, our approach can be made more general in view of investigating branching and extinction scenarios in AD models with two (or more) coevolving species, e.g., different prey-predator and host-parasite communities (see, e.g., Best et al. [2010]), as well as

communities regulated by other ecological interactions (e.g., mutualistic [Ferriére et al., 2002] and competitive [Kisdi, 1999] communities). Although the rigorous formulation of an iterative algorithm is basically impossible—exactly for the same reasons why bifurcation analysis cannot be made fully automatic [Kuznetsov, 2004, Meijer et al., 2009]—we have discussed, partly in light of the specific model we have analyzed, the guidelines of a general method. In particular, evolutionary extinctions could be taken into account by considering sequences of different events, identifying branching and extinction in each of the coevolving species.

The indications that can be obtained by the proposed approach typically have qualitative nature, as those we have drawn for prey-predator coevolution, and should be checked not to be too specific for the considered model. However, dealing with rather complex long-term dynamics, we believe that this type of analysis can be of great help and should be considered for the long-term conservation and management of biodiversity.

Chapter 6

Fisheries-induced diversification

Commercial harvesting is recognized to induce adaptive responses of life-history traits in fish populations, in particular by shifting the age and size at maturation through directional selection. In addition to such evolution of a target stock, the corresponding fishery itself may adapt, in terms of fishing policy, technological progress, fleet dynamics, and adaptive harvest. The aim of this chapter is to assess how the interplay between natural and artificial selection, in the simplest setting in which a fishery and a target stock coevolve, can lead to disruptive selection, which in turn may cause trait diversification. To this end, we build an eco-evolutionary model for a size-structured population, in which both the stock's maturation schedule and the fishery's harvest rate are adaptive, while fishing may be subject to a selective policy based on fish size and/or maturity stage. Using numerical bifurcation analysis, we study how the potential for disruptive selection changes with fishing policy, fishing mortality, harvest specialization, life-history tradeoffs associated with early maturation, and other demographic and environmental parameters. We report the following findings. First, fisheries-induced disruptive selection is readily caused by commonly used fishing policies, and occurs even for policies that are not specific for fish size or maturity, provided that the harvest is sufficiently adaptive and large individuals are targeted intensively. Second, disruptive selection is more likely in stocks in which the selective pressure for early maturation is naturally strong, provided life-history tradeoffs are sufficiently consequential. Third, when a fish stock is overexploited, fisheries targeting only large individuals might slightly increase sustainable yield by causing trait

diversification (even though the resultant yield always remains lower than the maximum sustainable yield that could be obtained under low fishing mortality, without causing disruptive selection). We discuss the broader implications of our results and highlight how these can be taken into account for designing evolutionarily informed fisheries-management regimes. More details can be found in Landi et al. [2014].

This work has been developed in collaboration with Professor Cang Hui (Stellenbosch University and African Institute for Mathematical Sciences) and Doctor Ulf Dieckmann (International Institute for Applied Systems Analysis) during the Southern African Young Scientists Summer Program (SA-YSSP), for the organization and funding of which we thank the Department of Science and Technology (DST, South Africa), the National Research Foundation (NRF, South Africa), the University of the Free State (UFS, South Africa), and the International Institute for Applied Systems Analysis (IIASA, Austria).

6.1 Introduction

The exploitation of renewable resources is a major source of mortality, which can trigger population collapse [Stokes et al., 1993, Hutchings and Reynolds, 2004] and adaptive changes in the life history of harvested species [Palumbi, 2001, Ashley et al., 2003]. Indeed, in commercially exploited fish stocks harvest has been recognized a driver of evolutionary adaptations [Law, 2000, Heino and Godø, 2002, Jørgensen et al., 2007, Dieckmann et al., 2009]. To date, most studies considering the genetic and phenotypic responses of fish stock to fishing have focused on fisheries-induced directional selection on life-history traits such as age and size at maturation [Barot et al., 2004, Ernande et al., 2004, de Roos et al., 2006, Gårdmark and Dieckmann, 2006, Dunlop et al., 2009, Poos et al., 2011].

In addition, a fishery itself can adapt, in terms of fishing policy, technological progress, fleet dynamics, and adaptive harvest [Salthaug, 2001, Hannesson, 2002, Walters and Martell, 2004]. Fishing policies can be selective for both size and maturity stage of individuals in the stock: size selectivity results from mesh-size and gear regulation or from size-specific incentives [Hart and Reynolds, 2002, Fromentin and Powers, 2005], while maturity selectivity may arise when a stock's juveniles and adults are spatially segregated during spawning [Sinclair, 1992, Swain and Wade, 1993, Engelhard and Heino, 2004, Opdal, 2010]. Harvest is readily adaptive, because fishers constantly tune

their effort and selectivity for maximum profit, targeting stock components that are most profitable to harvest. Such adaptation is relatively fast, leading to a continuously changing selective pressure on the exploited stock. Accordingly, the effect of technological progress on a fishery's sustainability is often assessed while neglecting adaptive responses of the targeted stock (e.g., Dercole et al. [2010b]).

The coupled dynamics of adaptations in a stock and its fishery can be interpreted as a coevolutionary process, in which one component of the system is biological (the exploited stock) while the other component is economic (the exploiting fishery). In his pioneering work, Heino [1998] approached the stock-fishery system from this coevolutionary perspective: individuals in the considered stock could adapt their age at maturation in response to the selective pressure imposed by harvesting, while fishers adapted their strategy to maximize the sustainable yield on a slower timescale, causing directional selection on the age at maturation.

The interaction between adaptive harvest imposed by a fishery and biological evolution could possibly result in disruptive selection, as suggested by Carlson et al. [2007] and Edeline et al. [2007] and supported by statistical analysis of field data by Edeline et al. [2009]. The objective of this chapter is to provide a first model-based investigation of this phenomenon. For this, we approach the stock-fishery system from the coevolutionary perspective, allowing harvest to adapt on the timescale of population dynamics, thus improving on Heino's (1998) corresponding assumption, and studying both directional and disruptive selective pressure. Disruptive selection increase the genetic and/or phenotypic variance of adaptive traits [Gross, 1985, Edeline et al., 2009, Keller et al., 2013], and under some circumstances may even lead to evolutionary branching and dimorphic trait diversification [Maynard Smith, 1966, Geritz et al., 1998]. Either impact may increase a stock's capacity to respond to directional selective pressures [Roff, 1997], and may raise the stock's abundance and yield. By contrast, such impacts could also have negative effects on the ecosystem in which the fish stock is embedded [Jennings and Kaiser, 1998], which are notoriously difficult to predict in general. We conclude our investigation by discussing such broad implications of our findings, which might be taken into account for the evolutionarily informed management of fisheries and the design of sustainable fishery policies.

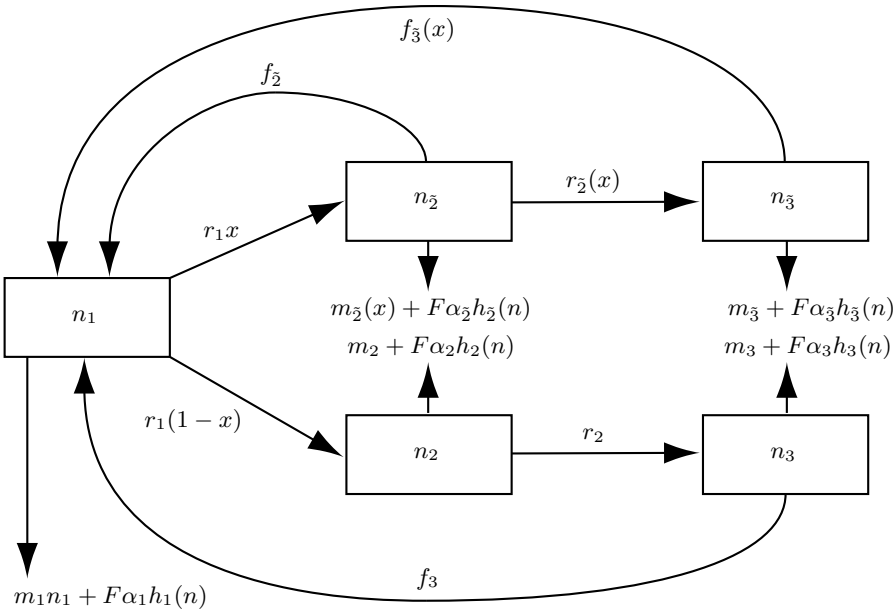

Figure 6.1: Schematic representation of the life-history model. The harvested population is divided into juveniles (with density n_1), small individuals (with densities $n_{\tilde{2}}$ and n_2), and large individuals (with densities $n_{\tilde{3}}$ and n_3), where tilde-subscripts refer to early-maturing individuals. Individuals can either mature early (with probability x, top row) or late (with probability $1-x$, bottom row). The probability of early maturation is the adaptive trait considered in this chapter. Table 6.1 and Paragraph 6.2 provide further details.

6.2 Model and methods

We use a discretely size-structured life-history model, similar to that employed in Poos et al. [2011] and Bodin et al. [2012], to describe an adaptively harvested fish population divided into three size classes (Figure 6.1). Individuals can mature either in the second or in the third size class, and accordingly differ in their sizes at maturation. We refer to the probability of maturing in the second size class as the probability of early maturation, and consider it an adaptive trait constrained by life-history tradeoffs [Roff, 1983, Stearns, 1992]. From this stock-fishery model, we derive the stock's basic reproduction ratio in dependence of the adaptive trait, and from this, the evolutionary dynamics of maturation. Using bifurcation analysis [Kuznetsov, 2004] and numerical continuation techniques [Allgower and Georg, 2003], we

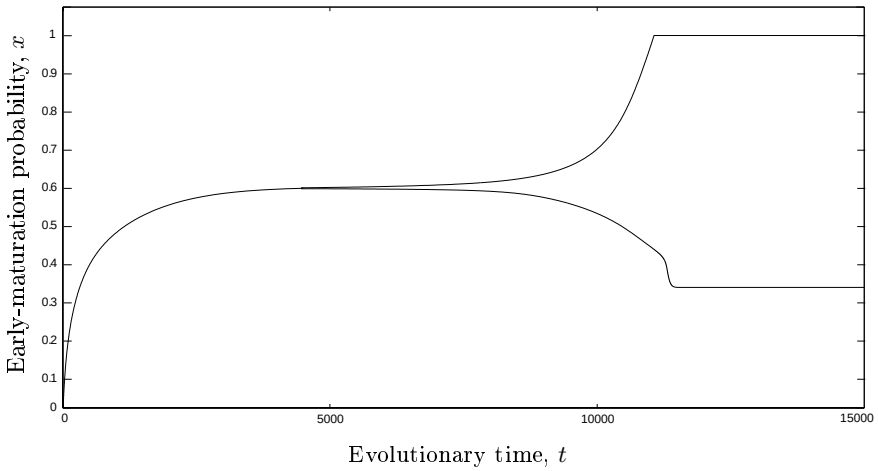

Figure 6.2: Model-based illustration of maturation diversification in response to fisheries-induced disruptive selection. The probability of early maturation, initially set at 0, gradually converges to a monomorphic evolutionary equilibrium at which selection turns disruptive and evolutionary branching takes place. The resultant two coexisting morphs, which initially are very similar, then diversify, eventually converging to a dimorphic evolutionary equilibrium. Parameters as in Figure 6.3, with $F = 1.1$ yr^{-1}.

study the selective pressures exerted on the stock by different levels of fishing mortality and by different levels of selectivity for size and/or maturity. In this way, we assess the potential for fish stocks to experience disruptive selection and thus potentially undergo maturation diversification (Figure 6.2).

6.2.1 Population dynamics

We consider a stock in which individuals are classified into three size classes—juveniles, small, and large. An individual can become mature at small size (early maturation) with probability x or at large size with probability $1-x$ [Gross, 1985]. The probability of early maturation is analyzed as an adaptive life-history trait under selection. Specifically, we denote by $n(t) = (n_i(t))$ the vector of fish abundances at time t, with $i = 1, \tilde{2}, 2, \tilde{3}$, or 3 ranging over all stock components (where tilde-subscripts refer to early-maturing individuals). Figure 6.1 provides a schematic representation of the considered stock structure.

Newborn juvenile individuals grow into the second size class at rate r_1. With probability x, they are early-maturing, thus grow-

ing into stock component $\tilde{2}$, whereas with probability $1-x$ they are late-maturing, thus growing into stock component 2. Small individuals grow into the third size class at rates $r_{\tilde{2}}$ or r_2, depending on whether they are early-maturing or late-maturing, respectively. Early-maturing individuals give birth to juveniles in the second and third size classes, at rates $f_{\tilde{2}}$ and $f_{\tilde{3}}$, respectively, while late-maturing individuals produce offspring only once they reach the third size class, at rate f_3. The natural mortality of juveniles is considered to be density-dependent, at rate $m_1 n_1$, while small and large individuals experience density-independent mortality, at rates $m_{\tilde{2}}$ and m_2 in the small size class and at rates $m_{\tilde{3}}$ and m_3 in the large size class, depending on whether they are early-maturing or late-maturing, respectively.

Following an energy-budget approach, we assume that early-maturing individuals face several life-history tradeoffs, since energy allocation to maturation reduces the energy available for other life-history processes, including growth, survival, and reproduction [Poos et al., 2011, Bodin et al., 2012]. We make the simplest possible assumptions for these three tradeoffs, by considering the mortality of small early-maturing individuals to be increased relative to small late-maturing individuals according to $m_{\tilde{2}}(x) = m_2(1+\beta_{\mathrm{m}}x)$, the growth rate of small early-maturing individuals to be decreased relative to small late-maturing individuals according to $r_{\tilde{2}}(x) = r_2(1-\beta_{\mathrm{r}}x)_+$, and the fecundity of large early-maturing individuals to be decreased relative to large late-maturing individuals according to $f_{\tilde{3}}(x) = f_3(1-\beta_{\mathrm{f}}x)_+$. In each case, the considered costs of early maturation are thus proportional to the probability x of early maturation, with proportionality constants β_{m}, β_{r}, and β_{f} measuring the strengths of the respective tradeoffs. The subscript $(\dots)_+$ means that negative values in the parenthesis are mapped to 0, while positive values remain unchanged. This means that for values of $\beta_{\mathrm{r}} > 1$ and $\beta_{\mathrm{f}} > 1$ the growth rate $r_{\tilde{2}}(x)$ and the fecundity rate $f_{\tilde{3}}(x)$, respectively, may become zero as x increases, but can never become negative.

Based on these considerations, we obtain the following stock-fishery model

$$\begin{aligned}
\dot{n}_1 &= f_{\tilde{2}} n_{\tilde{2}} + f_{\tilde{3}}(x) n_{\tilde{3}} + f_3 n_3 - m_1 n_1^2 - r_1 n_1 - F\alpha_1 h_1(n) n_1,\\
\dot{n}_{\tilde{2}} &= x r_1 n_1 - m_{\tilde{2}}(x) n_{\tilde{2}} - r_{\tilde{2}}(x) n_{\tilde{2}} - F\alpha_{\tilde{2}} h_{\tilde{2}}(n) n_{\tilde{2}},\\
\dot{n}_2 &= (1-x) r_1 n_1 - m_2 n_2 - r_2 n_2 - F\alpha_2 h_2(n) n_2,\\
\dot{n}_{\tilde{3}} &= r_{\tilde{2}}(x) n_{\tilde{2}} - m_{\tilde{3}} n_{\tilde{3}} - F\alpha_{\tilde{3}} h_{\tilde{3}}(n) n_{\tilde{3}},\\
\dot{n}_3 &= r_2 n_2 - m_3 n_3 - F\alpha_3 h_3(n) n_3,
\end{aligned} \tag{6.1}$$

where $\dot{n}_i$ is the time derivative of the abundance n_i of each component

Notation	Description [Unit]
	Variables
x	Early-maturation probability
n_1	Density of juvenile individuals [km^{-2}]
$n_{\tilde{2}}$	Density of early-maturing small individuals [km^{-2}]
n_2	Density of late-maturing small individuals [km^{-2}]
$n_{\tilde{3}}$	Density of early-maturing large individuals [km^{-2}]
n_3	Density of late-maturing large individuals [km^{-2}]
$r_{\tilde{2}}(x)$	Growth rate of early-maturing small individuals [yr^{-1}]
$f_{\tilde{3}}(x)$	Fecundity rate of early-maturing large individuals [yr^{-1}]
$m_{\tilde{2}}(x)$	Mortality rate of early-maturing small individuals [yr^{-1}]
$h_i(n)$	Relative adaptive harvest of component i
	Parameters
r_1	Growth rate of juvenile individuals [yr^{-1}]
r_2	Growth rate of late-maturing small individuals [yr^{-1}]
$f_{\tilde{2}}$	Fecundity rate of early-maturing small individuals [yr^{-1}]
f_3	Fecundity rate of late-maturing large individuals [yr^{-1}]
m_1	Mortality rate of juvenile individuals [yr^{-1}]
m_2	Mortality rate of late-maturing small individuals [yr^{-1}]
$m_{\tilde{3}}$	Mortality rate of early-maturing large individuals [yr^{-1}]
m_3	Mortality rate of late-maturing large individuals [yr^{-1}]
β_r	Strength of growth tradeoff
β_f	Strength of fecundity tradeoff
β_m	Strength of mortality tradeoff
s_i	Size of individuals in component i [m]
w_i	Weight of individuals in component i [tonnes]
k	Allometric coefficient relating size to weight [tonnes $\mathrm{m}^{-\theta}$]
θ	Allometric exponent relating size to weight
$\boldsymbol{\alpha} = (\alpha_i)$	Fishing policy
F	Fishing-mortality rate [yr^{-1}]
γ	Degree of harvest specialization

Table 6.1: Variables and parameters of the stock-fishery model in Equations (6.1). The index i refers to the five stock components, $i = 1$, $\tilde{2}$, 2, $\tilde{3}$, or 3. First block: trait and densities. Second block: trait-dependent and density-dependent functions. Third block: stock parameters. Fourth block: fishery parameters.

of the fish stock, while the last terms in each equation describes harvest, as explained in the next paragraph. All variables and parameters

of our stock-fishery model are summarized in Table 6.1.

6.2.2 Fishery dynamics

Fishing activities imply an extra mortality in each stock component of the form $F\alpha_i h_i(n) n_i$, where i ranges over all five stock components, $i = 1$, $\tilde{2}$, 2, $\tilde{3}$, or 3, F denotes the fishing-mortality rate, the binary vector $\boldsymbol{\alpha} = (\alpha_i)$ characterizes the selective fishing policy according to fish size and maturity, and $h_i(n)$ is the relative adaptive harvest of stock component i.

We consider ten different fishing policies, with different selectivity according to size and maturity [Ajiad et al., 1999, Law, 2000, Poos et al., 2011, Bodin et al., 2012]. These are detailed in Table 6.2. For example, fishing with no restrictions on size and maturity translates into the vector $\boldsymbol{\alpha} = (1, 1, 1, 1, 1)$, while a policy that allows fishing only of mature individuals is represented by the vector $\boldsymbol{\alpha} = (0, 1, 0, 1, 1)$. The relative adaptive harvest $h_i(n)$ of stock component i is described by a power law [Egas et al., 2005],

$$h_i(n) = \frac{[\alpha_i w_i n_i]^\gamma}{\sum_j [\alpha_j w_j n_j]^\gamma}, \tag{6.2}$$

with the sum extending over all five stock components $j = 1$, 2, $\tilde{2}$, 3, or $\tilde{3}$. In this equation, w_i is the weight of a fish in stock component i, which is given by the allometric scaling relation $w_i = k s_i^\theta$, where k and θ are the allometric coefficient and allometric exponent, respectively, and s_i is the size of a fish in stock component i. Notice that the allometric coefficient cancels in Equation (6.2); its only effect is that of scaling the yield, see Equations (6.3) and (6.9). The multiplication with fish weights translates the density of individuals into their biomass density. Therefore, the product $w_i n_i$ is the catch obtained from harvesting stock component i. The parameter γ measures the degree of harvest specialization and ranges from 0 to ∞. When $\gamma = 0$, the harvest is not adaptive and is randomly distributed over all five stock components (in analogy to random foraging). When $\gamma = 1$, the relative harvest for each stock component equals the relative catch from that compartment (in analogy to foraging according to the ideal free distribution). When γ tends to ∞, the harvest is completely focused on the stock component yielding maximum catch (in analogy to optimal foraging).

The total sustainable yield of the fishery for a monomorphic stock

	Selectivity	Juvenile	Early-maturing small	Late-maturing small	Early-maturing large	Late-maturing large
No regulation	None	✓	✓	✓	✓	✓
Only juvenile	Size	✓	X	X	X	X
Only small	Size	X	✓	✓	X	X
Only large	Size	X	X	X	✓	✓
Juvenile or small	Size	✓	✓	✓	X	X
Small or large	Size	X	✓	✓	✓	✓
Only immature	Maturity	✓	X	✓	X	X
Only mature	Maturity	X	✓	X	✓	✓
Only immature and small	Size and maturity	X	X	✓	X	X
Only mature and small	Size and maturity	X	✓	X	X	X

Table 6.2: Overview of the ten fishing policies examined in this chapter. Entries in the five rightmost columns indicate whether harvesting the corresponding stock component is allowed by the considered fishing policy.

with trait value $\bar{x}$ is given by

$$Y_{\mathrm{M}} = \sum_i F\alpha_i h_i(\bar{n})\bar{n}_i w_i\Big|_{x=\bar{x}} [\text{tonnes km}^{-2}\text{yr}^{-1}], \tag{6.3}$$

with the sum extending over all the five stock components $i = 1$, $\tilde{2}$, 2, $\tilde{3}$, or 3, and $\bar{n}$ indicating the values of the demographic equilibrium. A very similar expression gives the total sustainable yield for a dimorphic stock, see Equation (6.9).

6.2.3 Evolutionary dynamics

Following Poos et al. [2011] and Bodin et al. [2012], we derive the basic reproduction ratio R_0, measuring an individual's expected reproductive success in terms of offspring produced during its lifetime. This reproductive success depends both on the trait value of the focal individual and on the other trait values represented in the population. When an individual with trait value x' experiences a resident population with trait value x at its demographic equilibrium $\bar{n}(x)$, the focal individual's basic reproduction ratio is given by

$$R_0(x,x') = r_1 D_1\{(1-x')r_2 D_2 D_3 f_3 + x'[D_{\tilde{2}} f_{\tilde{2}} + r_{\tilde{2}}(x') D_{\tilde{2}} D_{\tilde{3}} f_{\tilde{3}}(x')]\}, \tag{6.4}$$

where $D_1 = [m_1\bar{n}_1 + r_1 + F\alpha_1 h_1(\bar{n})]^{-1}$, $D_{\tilde{2}} = [m_{\tilde{2}}(x') + r_{\tilde{2}}(x') + F\alpha_{\tilde{2}} h_{\tilde{2}}(\bar{n})]^{-1}$, $D_2 = [m_2 + r_2 + F\alpha_2 h_2(\bar{n})]^{-1}$, $D_{\tilde{3}} = [m_{\tilde{3}} + F\alpha_{\tilde{3}} h_{\tilde{3}}(\bar{n})]^{-1}$, and $D_3 = [m_3 + F\alpha_3 h_3(\bar{n})]^{-1}$ are the average durations spent by individuals in each of the five stock components. These are inversely related to the exit rate from those stock components, see Figure 6.1 and Equations (6.1). Thus, the product $r_i D_i$ is the probability that an individual in component i reaches the next size class, while the product $D_i f_i$ is the expected number of offsprings produced by the individual while being in component i. The focal individual's basic reproduction ratio $R_0(x,x')$ is a fitness proxy and can be used for evolutionary invasion analysis. Specifically, if $R_0(x,x') > 1$, individuals with trait values x' can invade and, generically, substitute individuals of a population with resident trait value x; otherwise, such invasion is not possible.

The so-called selection gradient

$$S(x) = \frac{\partial R_0(x,x')}{\partial x'}\bigg|_{x'=x} \tag{6.5}$$

is the slope of the fitness landscape $R_0(x,x')$ around x, and measures the strength of the directional selection on x. The rate of evolutionary change is proportional to this selection gradient, independent of

whether one considers the gradual reshaping of a polymorphic resident trait distribution through selection (as in quantitative genetics theory) or changes in a monomorphic trait distribution through mutation and selection (as in adaptive dynamics theory) [Dieckmann et al., 2006].

Using the selection gradient, we can apply the canonical equation of adaptive dynamics theory [Dieckmann and Law, 1996, Champagnat et al., 2006, Dercole and Rinaldi, 2008], an ordinary differential equation that deterministically approximates the evolutionary dynamics of the adaptive trait x. Specifically, the rate of change $\dot{x}$ in the trait value x is proportional to $S(x)$,

$$\dot{x} \propto S(x), \tag{6.6}$$

multiplied with half the product of population density, mutation probability, and mutation variance; since the latter three factors are positive, they play no role in monomorphic evolutionary dynamics in adaptive dynamics theory. Trait values $0 < \bar{x} < 1$ for which $S(\bar{x}) = 0$ are equilibria of the adaptive dynamics, and hence are called evolutionarily singular points. The boundaries $\bar{x} = 0$ and $\bar{x} = 1$ are also evolutionary equilibria, even if, generically, the selection gradient $S(x)$ do not vanish at such points [Bodin et al., 2012]. Internal equilibria ($0 < \bar{x} < 1$) and boundary equilibria ($\bar{x} = 0$ or $\bar{x} = 1$) represent mixed strategies and pure strategies, respectively (see Gross [1996] for a review).

If the dynamics of the adaptive trait x described by the canonical equation (6.6) converges to an evolutionary equilibrium $\bar{x}$, that trait value is said to be convergence stable. For internal equilibria, the slope of the fitness landscape then vanishes, and the curvature of the fitness landscape $R_0(\bar{x}, x')$ in x' determines whether $\bar{x}$ is evolutionarily stable or not. If the fitness landscape has a maximum at $\bar{x}$ (negative curvature), no mutants can invade and $\bar{x}$ is evolutionarily stable: since it is also convergence stable, it is a so-called continuously stable strategy (CSS, see Eshel [1983], Geritz et al. [1998] and Paragraph 3.3), characterizing an endpoint of the evolutionary dynamics. Otherwise, if the adaptive dynamics converge to a fitness minimum, it is evolutionarily unstable. Thus, the condition for evolutionary instability is given by

$$\left.\frac{\partial^2 R_0(\bar{x}, x')}{\partial x'^2}\right|_{x' = \bar{x}} > 0. \tag{6.7}$$

If Condition (6.7) is satisfied, $\bar{x}$ is a fitness minimum, so mutants on both sides of $\bar{x}$ can invade. Such mutants and the former residents

then coexist on the ecological timescale, forming a new dimorphic resident population. Their traits will experience further disruptive selection and, in the case of asexual populations, are expected to diversify on the evolutionary timescale (Figure 6.2). Such diversification can occur also in sexual populations, provided reproductive isolation between the incipient species arises concomitantly (e.g., Keller et al. [2013]): here we do not dwell on such complications, which would deserve and require a dedicated separate study. Monomorphic convergence stable singular points satisfying condition (6.7) are called evolutionary branching points (see Geritz et al. [1997, 1998], Dercole and Rinaldi [2008] and Paragraph 3.3). In our analysis below, we will thus test Condition (6.7) at monomorphic evolutionary equilibria $\bar{x}$ under different fishing policies, as well as for different levels of fishing mortality and different degrees of harvest specialization.

6.2.4 Dimorphic dynamics

In this paragraph, we specify the population dynamics and the evolutionary dynamics of a dimorphic stock, with population densities $n_x = (n_{ix})$ for individuals with an early-maturation probability x and of $n_y = (n_{iy})$ for individuals with an early-maturation probability y. The dimorphic population dynamics are given by

$$
\begin{aligned}
\dot{n}_{1x} &= f_{\tilde{2}} n_{\tilde{2}x} + f_{\tilde{3}}(x) n_{\tilde{3}x} + f_3 n_{3x} - m_1 n_{1x}(n_{1x} + n_{1y}) - r_1 n_{1x} + \\
&- F\alpha_1 h_1(n_x, n_y) n_{1x}, \\
\dot{n}_{\tilde{2}x} &= x r_1 n_{1x} - m_{\tilde{2}}(x) n_{\tilde{2}x} - r_{\tilde{2}}(x) n_{\tilde{2}x} - F\alpha_{\tilde{2}} h_{\tilde{2}}(n_x, n_y) n_{\tilde{2}x}, \\
\dot{n}_{2x} &= (1-x) r_1 n_{1x} - m_2 n_{2x} - r_2 n_{2x} - F\alpha_2 h_2(n_x, n_y) n_{2x}, \\
\dot{n}_{\tilde{3}x} &= r_{\tilde{2}}(x) n_{\tilde{2}x} - m_{\tilde{3}} n_{\tilde{3}x} - F\alpha_{\tilde{3}} h_{\tilde{3}}(n_x, n_y) n_{\tilde{3}x}, \\
\dot{n}_{3x} &= r_2 n_{2x} - m_3 n_{3x} - F\alpha_3 h_3(n_x, n_y) n_{3x}, \\
\dot{n}_{1y} &= f_{\tilde{2}} n_{\tilde{2}y} + f_{\tilde{3}}(y) n_{\tilde{3}y} + f_3 n_{3y} - m_1 n_{1y}(n_{1x} + n_{1y}) - r_1 n_{1y} + \\
&- F\alpha_1 h_1(n_x, n_y) n_{1y}, \\
\dot{n}_{\tilde{2}y} &= y r_1 n_{1y} - m_{\tilde{2}}(y) n_{\tilde{2}y} - r_{\tilde{2}}(y) n_{\tilde{2}y} - F\alpha_{\tilde{2}} h_{\tilde{2}}(n_x, n_y) n_{\tilde{2}y}, \\
\dot{n}_{2y} &= (1-y) r_1 n_{1y} - m_2 n_{2y} - r_2 n_{2y} - F\alpha_2 h_2(n_x, n_y) n_{2y}, \\
\dot{n}_{\tilde{3}y} &= r_{\tilde{2}}(y) n_{\tilde{2}y} - m_{\tilde{3}} n_{\tilde{3}y} - F\alpha_{\tilde{3}} h_{\tilde{3}}(n_x, n_y) n_{\tilde{3}y}, \\
\dot{n}_{3y} &= r_2 n_{2y} - m_3 n_{3y} - F\alpha_3 h_3(n_x, n_y) n_{3y},
\end{aligned}
$$

where

$$
h_i(n_x, n_y) = \frac{[\alpha_i w_i (n_{ix} + n_{iy})]^\gamma}{\sum_j [\alpha_j w_j (n_{jx} + n_{jy})]^\gamma},
$$

with the sum extending over all five stock components $j = 1$, 2, $\tilde{2}$, 3, or $\tilde{3}$.

Indicating by x' and y' the trait values of mutants appearing in a population with resident trait values x and y we obtain the basic reproduction ratios of such mutants as

$$R_0(x,y,x') = r_1 D_1\{(1-x')r_2 D_2 D_3 f_3 + x'[D_{\tilde{2}x} f_{\tilde{2}} + r_{\tilde{2}}(x') D_{\tilde{2}x} D_{\tilde{3}} f_{\tilde{3}}(x')]\},$$
$$R_0(x,y,y') = r_1 D_1\{(1-y')r_2 D_2 D_3 f_3 + y'[D_{\tilde{2}y} f_{\tilde{2}} + r_{\tilde{2}}(y') D_{\tilde{2}y} D_{\tilde{3}} f_{\tilde{3}}(y')]\},$$

where $D_1 = [m_1(\bar{n}_{1x}+\bar{n}_{1y}) + r_1 + F\alpha_1 h_1(\bar{n}_x,\bar{n}_y)]^{-1}$, $D_{\tilde{2}x} = [m_{\tilde{2}}(x') + r_{\tilde{2}}(x') + F\alpha_{\tilde{2}} h_{\tilde{2}}(\bar{n}_x,\bar{n}_y)]^{-1}$, $D_{\tilde{2}y} = [m_{\tilde{2}}(y') + r_{\tilde{2}}(y') + F\alpha_{\tilde{2}} h_{\tilde{2}}(\bar{n}_x,\bar{n}_y)]^{-1}$, $D_2 = [m_2 + r_2 + F\alpha_2 h_2(\bar{n}_x,\bar{n}_y)]^{-1}$, $D_{\tilde{3}} = [m_{\tilde{3}} + F\alpha_{\tilde{3}} h_{\tilde{3}}(\bar{n}_x,\bar{n}_y)]^{-1}$, $D_3 = [m_3 + F\alpha_3 h_3(\bar{n}_x,\bar{n}_y)]^{-1}$, and $(\bar{n}_x,\bar{n}_y)$ are the values of the dimorphic demographic equilibrium.

On the evolutionary timescale, the traits x and y evolve following a two-dimensional canonical equation

$$\dot{x} = k_x \sum_i n^*_{ix} \frac{\partial R_0(x,y,x')}{\partial x'}\bigg|_{x'=x}, \quad \dot{y} = k_y \sum_i n^*_{iy} \frac{\partial R_0(x,y,y')}{\partial y'}\bigg|_{y'=y}, \tag{6.8}$$

where k_x and k_y are half the product of probability and variance of mutations in x and y, respectively, and scale the speed of evolutionary dynamics in x and y, and the sum extending over all five stock components $i = 1$, 2, $\tilde{2}$, 3, or $\tilde{3}$. These dimorphic dynamics converges to the evolutionary equilibrium $(x^*_{\mathrm{D}}, y^*_{\mathrm{D}})$.

Finally, the sustainable yield of the dimorphic stock with trait values $(\bar{x}_{\mathrm{D}}, \bar{y}_{\mathrm{D}})$ is given by

$$Y_{\mathrm{D}} = \sum_i F\alpha_i h_i(\bar{n}_x,\bar{n}_y)(\bar{n}_{ix}+\bar{n}_{iy}) w_i\Big|_{x=\bar{x}_{\mathrm{D}}, y=\bar{y}_{\mathrm{D}}}, \tag{6.9}$$

with the sum extending over all five stock components $i = 1$, 2, $\tilde{2}$, 3, or $\tilde{3}$.

6.2.5 Outline of analysis

In our further analysis, we use numerical bifurcation analysis and continuation techniques, in an approach similar to that in Landi et al. [2013] and Chapter 5, to which interested readers are invited to refer for more detailed explanations and discussions.

As the fishing-mortality rate F is the driver of fisheries-induced selection on the stock, we use it as our primary bifurcation parameter. We then extend the analysis by adding a secondary bifurcation parameter, for which we choose γ, measuring the degree of harvest

specialization. In this way, we can assess the effects of fishing, in terms of fishing mortality and fishing specialization, on the occurrence of disruptive selection. To evaluate the generality of results, we also consider as alternative secondary bifurcation parameters the tradeoff strengths β_{r}, β_{f}, and β_{m}. Eventually, we consider all other demographic and environmental parameters as secondary bifurcation parameters. This procedure will pinpoint the characteristics of stocks that are more likely to experience fisheries-induced disruptive selection, as well as the characteristics of fishing regimes there are more likely to cause such selection. To conclude, we evaluate the effect of fisheries-induced diversification on sustainable yield.

As the analytic form of the demographic equilibrium $\bar{n}(x)$ is unknown for calculating $R_0(x, x')$ in Equation (6.4), we numerically integrate a fast-slow eco-evolutionary dynamics according to Equations (6.1) and (6.5), using a small parameter ϵ to regulate the relative speed of the (slow) evolutionary dynamics $\dot{x} = \epsilon S(x)$ relative to the speed of the (fast) demographic dynamics [Abrams, 2000, Landi et al., 2013]. Extensive and systematic numerical analyses of Equations (6.1) reveal that there can only be one nontrivial stable equilibrium $\bar{n}(x)$ for all $0 \leq x \leq 1$. This simplifies the analysis of the adaptive dynamics by ruling out possible bifurcations of the demographic dynamics that could complicate the evolutionary dynamics [Dercole et al., 2002].

We first consider the case without fishing mortality ($F = 0$), with all other parameters set as in Figure 6.3; those parameter values are chosen for convenient illustration, and other values have been found to produce qualitatively similar results. We start the fast-slow eco-evolutionary dynamics from the demographic initial condition $n(0)$ and the evolutionary initial condition $x(0)$ and integrate these dynamics until they converge to the unique eco-evolutionary equilibrium $(\bar{n}, \bar{x})$. This equilibrium turns out to be a CSS, suggesting that the unharvested stock never experiences disruptive selection and at evolutionary equilibrium has a low probability of early maturation. We then successively consider each of the ten fishing policies listed in Table 6.2 and examine how the eco-evolutionary equilibrium responds to increasing fishing-mortality rate F (Figure 6.3). While doing so, we continuously monitor Condition (6.7), which is not satisfied at $F = 0$. Depending on the fishing policy, the fishing mortality may reach a threshold $F = F_{\mathrm{B}}$ at which a branching bifurcation occurs, i.e., selection turns disruptive. This means that the initial CSS turns into an evolutionary branching point. We continue to follow this branching bifurcation point while changing both the fishing-mortality rate

F and the degree of specialization γ, obtaining the bifurcation curve in the bivariate (F, γ) space that separates regions of disruptive and stabilizing selection (Figure 6.4).

6.3 Results

We first examine which fishing policies can cause disruptive selection, then investigate which kinds of fish stocks are susceptible to fisheries-induced disruptive selection, and finally, analyze the effects of fisheries-induced diversification on sustainable yield.

6.3.1 Which fishing policies can cause fisheries-induced disruptive selection?

Figure 6.3 shows three qualitatively different routes to fisheries-induced disruptive selection revealed by our model. As fishing mortality is increased in each scenario, the globally convergence stable evolutionarily stable equilibrium at low early-maturation probability shifts to higher early-maturation probabilities before losing its stability: in scenario (A), it loses its evolutionary stability, while in scenarios (B) and (C), it first loses its global convergence stability and then its evolutionary stability.

Scenario (A). At all levels of fishing mortality, only a single internal equilibrium ($0 < \bar{x} < 1$) is present, which is always globally convergence stable. Both boundary equilibria ($\bar{x} = 0$ and $\bar{x} = 1$) are convergence unstable. The early-maturation probability increases with fishing mortality. At high levels of fishing mortality ($F > F_{\mathrm{B}}$; dark gray region), the equilibrium loses its evolutionary stability, so selection becomes disruptive. This scenario occurs for four of the ten studied fishing policies: it applies to the no-regulation, small-or-large, and only-mature fishing policies, as well as to the only-large fishing policy when $\beta_{\mathrm{r}} < 1$ (see below).

Scenario (B). At intermediate levels of fishing mortality ($F_{\mathrm{S1}} < F < F_{\mathrm{S2}}$), two alternative convergence stable internal equilibria are present. At either end of the interval, two different saddle-node bifurcations occur ($F = F_{\mathrm{S1}}$ and $F = F_{\mathrm{S2}}$, with $F_{\mathrm{S2}} < F_{\mathrm{S1}}$), annihilating one of the convergence stable internal equilibria. The upper internal convergence stable equilibrium is always an evolutionary branching point, whereas the lower internal convergence stable equilibrium is an evolutionary branching point only for $F > F_{\mathrm{B}}$. In this scenario, selection is conditionally disruptive, depending on the ancestral condition

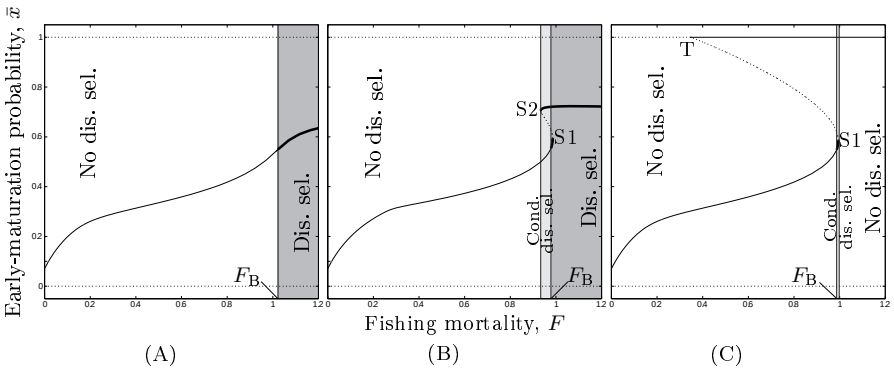

Figure 6.3: Three qualitatively different routes to fisheries-induced disruptive selection on the probability of early maturation as fishing mortality is increased. In panel (A) there is only a single internal equilibrium for any value of the fishing mortality. In panel (B) there is bistability between two internal equilibria for a range of fishing mortalities. In panel (C), there is bistability between an internal equilibrium and a boundary equilibrium. Panels (A) and (B) show results for the no-regulation fishing policy; results are qualitatively equivalent for the small-or-large and the only-mature fishing policies, as well as for the only-large fishing policy when $\beta_r < 1$. Panel (C) shows results for the only-large fishing policy when $\beta_r \geq 1$. Throughout the panels, convergence stable and evolutionarily stable equilibria (continuously stable strategies or CSSs) are represented by a thin line, convergence stable but evolutionarily unstable equilibria (evolutionary branching points) are represented by a thick line, and convergence unstable equilibria (evolutionary repellors) are represented by a dotted line. The fishing mortality at the bifurcation point at which selection turns disruptive, and thus can cause evolutionary branching, is indicated by F_B. Saddle-node bifurcations, at which a convergence stable internal equilibrium collides with a convergence unstable internal equilibrium, are indicated by S1 and S2. A transcritical bifurcation, at which a convergence stable boundary equilibrium collides with a convergence unstable internal equilibrium, is indicated by T. Light gray and dark gray regions represent intervals of fishing mortality causing conditional disruptive selection and disruptive selection, respectively. In the former case, two convergence stable equilibria coexist, but only one of them is evolutionarily unstable: it thus depends on the ancestral condition whether or not disruptive selection will occur. Initial conditions: $n(0) = (1, 1, 1, 1, 1)$ km^{-2}, $x(0) = 0.5$. Parameters: $\epsilon = 10^{-3}$ yr^{-1}, $r_1 = 1$ yr^{-1}, $r_2 = 0.8$ yr^{-1}, $f_{\tilde{2}} = 0.8$ yr^{-1}, $f_3 = 1$ yr^{-1}, $m_1 = 0.4$ yr^{-1}, $m_2 = 0.3$ yr^{-1}, $m_3 = m_{\tilde{3}} = 0.2$ yr^{-1}, $\beta_r = \beta_f = \beta_m = 1$, $s_1 = 0.3$ m, $s_{\tilde{2}} = s_2 = 0.6$ m, $s_{\tilde{3}} = s_3 = 0.9$ m, $k = 0.01$ tonnes m$^{-\theta}$, $\theta = 3$, and $\gamma = 5$ (A, C) or $\gamma = 25$ (B).

$x(0)$, when $F_{S2} < F < F_B$ (light gray region), as the early-maturation probability can either converge to the upper internal convergence stable equilibrium (which is an evolutionary branching point; thick line) or to the lower internal convergence stable equilibrium (which is a CSS; thin line). Selection is always disruptive for $F > F_B$ (dark gray region), no matter which one of the two internal convergence stable equilibria is reached from the ancestral condition. This scenario occurs for four of the ten studied fishing policies: it applies to the no-regulation, small-or-large, and only-mature fishing policies, as well as to the only-large fishing policy when $\beta_r < 1$ (see below). Notice that this set of fishing policies is the same as for scenario (A), highlighting that it depends on model parameters other than fishing mortality which of the two scenarios applies. It is worth pointing out that the evolutionary bistability was not detected in earlier analyses of similar models [Poos et al., 2011, Bodin et al., 2012], because tradeoffs were not trait-dependent in those studies. However, evolutionary bistability has been found in other studies on fisheries-induced evolution considering different models and traits [Gårdmark and Dieckmann, 2006, de Roos et al., 2006, Boukal et al., 2008]. This study appears to be the first in which evolutionary bistability is found to co-occur with disruptive selection, making evolutionary dynamics more complex and interesting.

Scenario (C). At intermediate levels of fishing mortality ($F_T < F < F_{S1}$), a convergence stable internal equilibrium coexists with a convergence stable boundary equilibrium. At either end of the interval, two different bifurcations occur, annihilating one of the convergence stable equilibria. First, a transcritical bifurcation happens at $F = F_T$, when the convergence unstable internal equilibrium (dotted line) collides with the convergence stable boundary equilibrium $\bar{x} = 1$ (thin line), exchanging their convergence stability. Second, a saddle-node bifurcation happens at $F = F_{S1}$ when the same convergence unstable internal equilibrium (dotted line) collides with the the internal evolutionary branching point (thick line). In this scenario, selection is conditionally disruptive, depending on the ancestral condition, when $F_B < F < F_{S1}$ (light gray region): if the ancestral condition $x(0)$ lies below the convergence unstable internal equilibrium (dotted line), the early-maturation probability converges to the convergence stable internal equilibrium (which is an evolutionary branching point; thick line), so selection becomes disruptive. In contrast, if the ancestral condition lies above the convergence unstable internal equilibrium, the early-maturation probability converges to the boundary equilib-

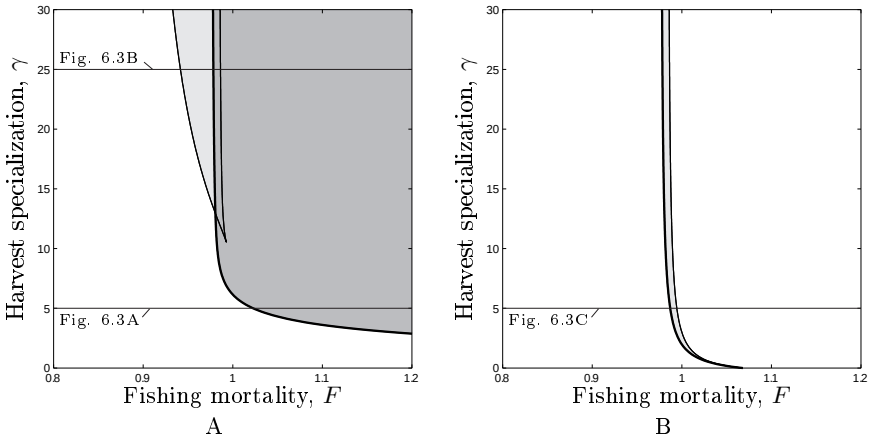

Figure 6.4: Two qualitatively different routes to fisheries-induced disruptive selection on the probability of early maturation as fishing mortality and harvest specialization are varied together. White, light gray, and dark gray regions indicate parameter combinations for which selection is not disruptive, conditionally disruptive (depending on the ancestral evolutionary condition), and disruptive, respectively. The bifurcation curves along which evolutionary branching starts to be possible are represented as thick lines, while saddle-node bifurcation curves are represented as thin lines. The univariate scenarios shown in Figure 6.3 are slices of the bivariate scenarios shown here, as indicated by labeled horizontal lines in both panels. Panel A shows results for the no-regulation fishing policy; results are qualitatively equivalent for the small-or-large and only-mature fishing policies, as well as for the only-large fishing policy when $\beta_r < 1$. Panel B shows results for the only-large fishing policy when $\beta_r \geq 1$. Parameters as in Figure 6.3.

rium $\bar{x} = 1$, where selection cannot be disruptive, as trait values $x > 1$ are unfeasible. This scenario occurs for only one fishing policy: it applies to the only-large fishing policy when $\beta_r \geq 1$ (see below).

These results imply that scenarios (A) to (C) cannot occur for six of the ten studied fishing policies: this applies to the only-juvenile, only-small, juvenile-or-small, only-immature, only-immature-and-small, and only-mature-and-small fishing policies. Consequently, these six types of fisheries can ever cause fisheries-induced disruptive selection.

We can now expand our analysis by considering the effect of harvest specialization on disruptive selection. For this, we need to continue the aforementioned bifurcations in the bivariate (F, γ) space,

obtaining the bivariate disruptive-selection scenarios shown in Figure 6.4. These plots provide a full qualitative characterization of the effects of fishing—in terms of policy, fishing mortality, and the degree of harvest specialization—on disruptive selection. Notice that the univariate scenarios shown in Figure 6.3 can be understood as slices, for fixed degree of harvest specialization γ, of the bivariate scenarios shown in Figure 6.4. In particular, Figures 6.3A and 6.3B are slices of Figure 6.4A for two different degrees of harvest specialization, while Figure 6.3C is a slice of Figure 6.4B. For this reason, we only have two bivariate scenarios, one applying to the no-regulation, small-or-large, and only-mature fishing policies, as well as to the only-large fishing policy when $\beta_\mathrm{r} < 1$ (Figure 6.4A) and the other one applying to the only-large fishing policy when $\beta_\mathrm{r} \geq 1$ (Figure 6.4B).

From these bivariate scenarios we obtain the following results. First, disruptive selection occurs only for high levels of fishing mortality. Second, harvest specialization promotes disruptive selection: at high values of γ, selection turns disruptive already for lower fishing mortalities (this effect becomes saturated as harvest specialization is increased). Third, random, and thus non-adaptive, harvest ($\gamma = 0$) prohibits disruptive selection, demonstrating that adaptive harvest is a necessary condition for the occurrence of fisheries-induced disruptive selection. Fourth, all four fishing policies causing disruptive selection target large individuals, which therefore is a second necessary condition for the occurrence of fisheries-induced disruptive selection.

6.3.2 Which kinds of fish stocks are susceptible to fisheries-induced disruptive selection?

To find out which kinds of stocks are susceptible to fisheries-induced disruptive selection, we carry out a sensitivity analysis for the two fisheries-induced disruptive selection scenarios in Figure 6.4 with respect to the tradeoff strengths β_m, β_r, and β_f (Figures 6.5 and 6.6), continuing all detected bifurcations in the (F, β_j) spaces, with j spanning all three tradeoffs, $j = \mathrm{m}$, r, or f.

We find that the univariate and bivariate scenarios for disruptive selection under the only-large fishing policy (Figures 6.3C and 6.4B, respectively) occur only when $\beta_\mathrm{r} \geq 1$ (Figure 6.5), that is, when the growth tradeoff is very strong. Figure 6.3C shows that for $\beta_\mathrm{r} = 1$ and large fishing mortality F only the boundary equilibrium $x = 1$ exists: at that evolutionary equilibrium, $r_{\bar{2}} = 0$, i.e., early-maturing individuals stop growing. The stock will then be composed of only juveniles

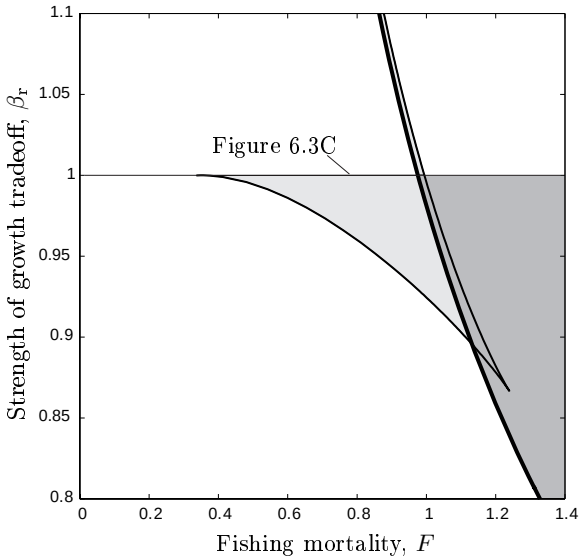

Figure 6.5: Limited realism and generality of the fisheries-induced disruptive selection scenario for the only-large fishing policy with $\beta_r \geq 1$. As explained in the text, this scenario unrealistically allows the stock to escape all fishing by maturing early. Also, it can never cause unconditional fisheries-induced disruptive selection, and can cause conditional fisheries-induced disruptive selection only for the restrictive conditions in the narrow light gray band in the upper part of the figure. Hence, the more realistic and general scenario is that in Figure 6.4A. Colors and lines as in Figure 6.4. Parameters as in Figure 6.3, with $\gamma = 5$.

and early-maturing small individuals, so that, under the considered only-large fishing policy, it escapes all fishing. Such a complete escape from fishing seems clearly unrealistic: at the very least, it would trigger a switch to a different fishing policy. Figure 6.5 shows that, when $\beta_r \geq 1$, this unrealistic situation occurs for even smaller fishing mortalities F. We therefore discard the scenarios in Figures 6.3C and 6.4B as unrealistic for larger fishing mortalities F. In addition, these scenarios can never cause unconditional fisheries-induced disruptive selection, while the conditions under which they cause conditional fisheries-induced disruptive selection are very restrictive, as the narrowness of the light gray regions in Figures 6.3C, 6.4B, and 6.5 documents. For these reasons, we focus our further analyses on the scenarios in Figures 6.3A, 6.3B, and 6.4A, which also cover the only-large fishing policy for $\beta_r < 1$. For the purpose of illustration, we consider the no-regulation fishing policy, as all effects shown in

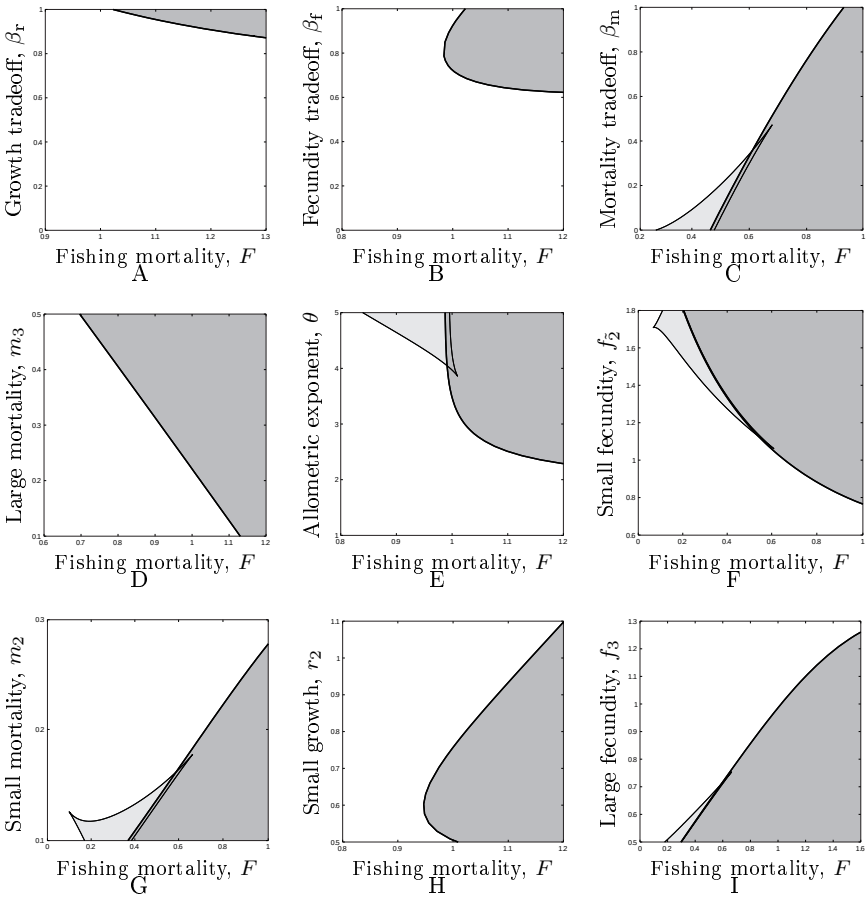

Figure 6.6: Effects of tradeoff strengths, demographic parameters, and environmental parameters on fisheries-induced disruptive selection. (A, B) Tradeoffs in growth and fecundity promote disruptive selection: the presence of both tradeoffs is a necessary condition for disruptive selection. C Tradeoffs in mortality restrain disruptive selection. (D, E, F) parameters that promote disruptive selection. (G, H, I) other parameters that restrain disruptive selection. All shown effects are discussed in Paragraph 6.3.2. Parameter ranges along the axes are chosen so as to exclude parameter combinations for which the stock would go extinct on the evolutionary timescale. Colors and lines as in Figure 6.4. Parameters as in Figure 6.3, with $\gamma = 5$.

Figure 6.6 are qualitatively equivalent for all four fishing policies that can cause disruptive selection in the scenarios in Figures 6.3A, 6.3B, and 6.4A (no-regulation, small-or-large, only-mature fishing policies,

as well as only-large fishing policy when $\beta_r < 1$).

Relaxing the tradeoffs in growth and fecundity restrains disruptive selection (Figures 6.6A and 6.6B). Disruptive selection is impossible when either one of these tradeoffs is absent (i.e., when $\beta_r = 0$ or $\beta_f = 0$; Figures 6.6A and 6.6B): this means that the joint presence of growth and fecundity tradeoffs of early maturation is a necessary condition for the occurrence of disruptive selection. In contrast, relaxing the tradeoff in mortality promotes disruptive selection (Figure 6.6C), and disruptive selection is still possible even when this tradeoff is absent (i.e., when $\beta_m = 0$; Figure 6.6C).

To identify other characteristics of fish stocks that are susceptible to fisheries-induced disruptive selection, we now analyze the effects of all demographic and environmental parameters. In this way, we obtain the following findings. First, the juvenile growth rate r_1 and the juvenile mortality rate m_1 do not have any effect on disruptive selection (not illustrated). This is because all individuals have to pass through the juvenile stage in a way that cannot be affected by their adaptive trait. Second, disruptive selection is promoted by increasing the mortality rate m_3 of large individuals (Figure 6.6D), the allometric exponent θ relating size to weight (Figure 6.6E), and the fecundity rate $f_{\tilde{2}}$ of early-maturing small individuals (Figure 6.6F). Increasing the first two parameters can reduce the time individuals spend in the large size class, lowering that class' contribution to fitness according to Equation 6.4. Equivalently, increasing the last parameter increases the contribution of small individuals to fitness. Hence, all three cases select for earlier maturation: this, in turn, strengthens the impacts of the considered tradeoffs and thereby promotes disruptive selection. Third, by contrast, disruptive selection is restrained by increasing the mortality rate m_2 of late-maturing individuals (Figure 6.6G), the growth rate r_2 of late-maturing small individuals (Figure 6.6H), and the fecundity rate f_3 of late-maturing large individuals (Figure 6.6I). Hence, all three cases select for later maturation; this, in turn, weakens the impacts of the considered tradeoffs and thereby restrain disruptive selection.

In general, therefore, selection is more likely to be disruptive if large individuals make a smaller contribution to fitness according to Equation (6.4), that is, when selection for early maturation is naturally strong. Then the resultant high early-maturation probability will strengthen the impact of life-history tradeoffs in growth and fecundity so as to promote fisheries-induced disruptive selection.

6.3.3 What are the effects of diversification on sustainable yield?

We now analyze the situation in which, after diversification, two coexisting resident populations exhibit alternative trait values x and y close to the evolutionary equilibrium $\bar{x}$ of the monomorphic stock. These two coexisting resident traits then diverge on the evolutionary timescale, under the continuous influence of disruptive selection, and eventually settle onto a dimorphic evolutionary equilibrium $(\bar{x}_{\mathrm{D}}, \bar{y}_{\mathrm{D}})$ (Figure 6.2). The corresponding dimorphic evolutionary dynamics are specified in Paragraph 6.2.4. In principle, a dimorphic evolutionary equilibrium might be an evolutionary branching point for one or both of the diverged populations. However, in our case, $\bar{y}_{\mathrm{D}}$ always equals 1, i.e., individuals of one resident population are always maturing as early as possible; as highlighted above, such a boundary equilibrium cannot be an evolutionary branching point. By contrast, $\bar{x}_{\mathrm{D}}$ is evolutionarily stable. Therefore, no further diversification is possible at the dimorphic evolutionary equilibrium.

Once the dimorphic evolutionary equilibrium is attained, the stock's density, and thus its sustainable yield, change relative to the monomorphic evolutionary equilibrium. Using Equations (6.3) and (6.9), we can evaluate the sustainable yield for different fishing-mortality rates F (Figure 6.7), again using numerical continuation. We thereby find that, for $0 < F < F_{\mathrm{B}}$ (where F_{B} again denotes the fishing mortality rate at the branching bifurcation) the stock stays at its monomorphic evolutionary equilibrium $\bar{x}$, while for $F > F_{\mathrm{B}}$ the monomorphic evolutionary equilibrium becomes evolutionarily unstable, and the stock, following a two-dimensional canonical equation, Equation (6.8), converges to $(\bar{x}_{\mathrm{D}}, \bar{y}_{\mathrm{D}})$. Note that discontinuities in yield at $F = F_{\mathrm{B}}$ shown in Figures 6.7A and 6.7B are not surprising, as the outcome of the evolutionary dynamics does not vary continuously with the fishing mortality F across the branching bifurcation.

After diversification, the sustainable yield can slightly increase, but only for the only-large fishing policy when $\beta_{\mathrm{r}} < 1$. Even then, it remains far below the maximum sustainable yield (MSY), defined by the peaks in Figures 6.7A and 6.7B. When the fishing-mortality rate F is increased beyond F_{B}, the sustainable yield continuously declines toward zero for the no-regulation, small-or-large and only-mature fishing policies, but remains practically constant (after slightly increasing) for the only-large fishing policy when $\beta_{\mathrm{r}} < 1$. This is because the only-large fishing policy, in contrast to the other three

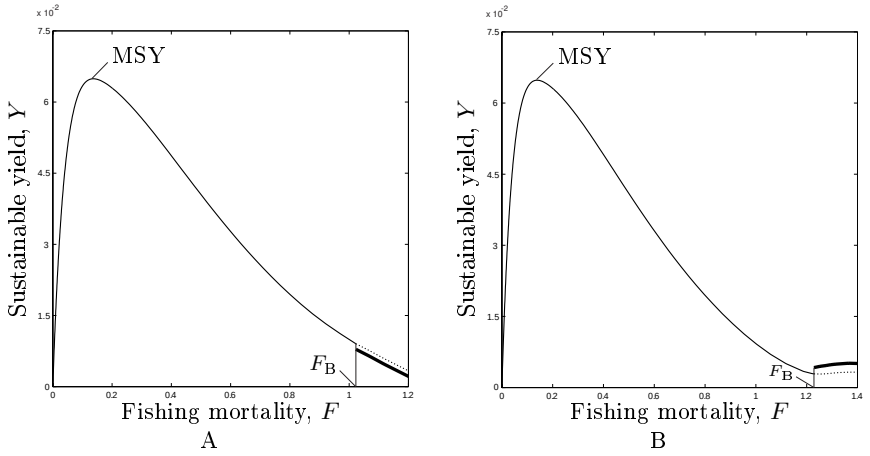

Figure 6.7: Effects of fisheries-induced diversification on sustainable yield. Panel A shows results for the no-regulation fishing policy; results are qualitatively equivalent for the small-or-large and the only-mature fishing policies. Panel B shows results for the only-large fishing policy when $\beta_r < 1$. Selection is not disruptive for low fishing mortality rates ($F < F_B$), including those resulting in maximum sustainable yield (MSY). By contrast, when the stock is heavily exploited ($F > F_B$), diversification may occur. The sustainable yield is represented by thin lines for the monomorphic stock when selection is not disruptive, by dashed lines for the monomorphic stock when selection is disruptive, and by thick lines for the dimorphic stock. As shown in A and B, diversification can cause either a decrease or an increase in yield, respectively, depending on the fishing policy. Parameters as in Figure 6.3, with $\gamma = 5$, except for $\beta_r = 0.85$ in B.

fishing policies, does not allow fishing on the early-maturing small individuals in stock component $\tilde{2}$, which are vital for sustaining the stock under very high exploitation rates.

6.4 Discussion

Human exploitation of fish stocks as renewable resources often causes massive excess mortality. This alters the fitness landscapes of the exploited fish stocks, which in turn may cause adaptive responses of the stocks' phenotypic and genotypic variability [Hutchings and Fraser, 2008]. In general, coexisting life-history strategies and corresponding polymorphism can be induced and maintained by negatively frequency-dependent selection (as, for example, in the size at matu-

ration of male coho salmon; Gross [1985]). In this chapter, we have considered a life-history trait given by a discrete probabilistic reaction norm for the size at maturation [Dieckmann and Heino, 2007], representing the amount of energy allocated to early maturation. For this reason, we introduced trait-dependent tradeoffs: the more energy is allocated to early maturation, the higher the resultant costs in terms of reduced growth, survival, and reproduction. Here we have demonstrated that fisheries-induced selection on such a trait can be disruptive: this means not only that dimorphism in fish populations can be maintained, but also that such dimorphism may evolve *de novo* [Keller et al., 2013], thereby giving rise to a coexistence of maturation strategies [Gross, 1996]. Several empirical studies have argued the possibility of disruptive selection in fish populations through the interplay of natural selection and adaptive harvesting [Carlson et al., 2007, Edeline et al., 2007, 2009]: here we have systematically analyzed, for the first time, under which specific conditions such disruptive selection may arise.

Fishing imposes a strong selective pressure for early maturation, even though this is accompanied by increased physiological costs via life-history tradeoffs. In our model, such selection forces first give rise to a convergence stable mixed strategy, consistent with the argument by Carlson et al. [2007] that natural selection and fisheries-induced selection often act in opposite directions and hence produce strongly stabilizing selection. We have found that, however, with sufficiently strong tradeoffs in growth and fecundity, this convergence stable mixed strategy can become evolutionarily unstable, implying disruptive selection and enabling the coexistence of two maturation strategies, consistent with the argument by Edeline et al. [2009] that fisheries-induced disruptive selection tends to increase trait variance. Specifically, a harvested stock may split into two life-history types: one exploits the advantages of early maturation, while the other reduces the losses imposed by growth and fecundity tradeoffs. By contrast, an analogous life-history tradeoff in mortality has the opposite effect: disruptive selection is enhanced when this tradeoff is relaxed. Moreover, we have shown that strong growth and fecundity tradeoffs both act as indispensable prerequisites for disruptive selection (Figures 6.6A and 6.6B), while a weak mortality tradeoff merely serves as a dispensable promotor of disruptive selection (Figure 6.6C).

In addition to strong life-history tradeoffs in both growth and fecundity, we have identified two other necessary conditions for a stock-fishery system to experience disruptive selection: (i) fishing policies

that target large individuals, and (ii) adaptive harvesting that adjusts the harvest distribution for optimal benefit (Figure 6.4). Ultimately, these two conditions emerge from the same mechanism described in the previous paragraph. For selection to turn disruptive, the impact of growth and fecundity tradeoffs must become large, and this happens more readily when the probability of early maturation becomes high. Harvesting a stock's large individuals, as happens through many widely adopted fishing policies (Table 6.2), increases the directional selection pressure toward early maturation, as recurrently highlighted by earlier studies (e.g., Law [1979], Law and Grey [1989], Abrams and Rowe [1996]). Moreover, when harvesting is adaptive, a fishery behaves similar to an optimally foraging predator that maximizes its intake rate (e.g., Egas et al. [2005]): this tends to increase the mortality of large individuals, as these are more profitable to harvest. Therefore, adaptive harvesting under policies that allow the targeting of large individuals alters natural adaptive landscapes in a way that selects for increased reproductive investment early in life. This, in turn, reduces somatic growth and fecundity later in life through life-history tradeoffs [Edeline et al., 2007], and thereby strengthens the mechanism that leads to disruptive selection. Poos et al. [2011] and Bodin et al. [2012] have considered a rather similar model, yet without considering adaptive harvesting and trait-dependent tradeoffs: this explains why disruptive selection was not found in their analyses.

In line with these findings and explanations, our results have also shown that populations with demographic conditions that penalize large individuals and/or favor small individuals are more sensitive to disruptive selection. This is because such populations are naturally prone to early maturation, strengthening the impacts of the tradeoffs in growth and fecundity that turn selection disruptive. Therefore, there are three different ways to promote the mechanism that turns selection disruptive via growth and fecundity tradeoffs: first, the tradeoffs themselves may be strong due to physiological reasons; second, fishing mortality may select for early maturation, making the impacts of those tradeoffs strong; and third, a stock's other demographic and environmental conditions may predispose it to early maturation. Overall, this pattern of chasing the benefits of early maturation while avoiding the costs in growth and fecundity can be considered as an important general mechanism for the origin of dimorphism in exploited fish populations and other coevolving systems (e.g., Zhang et al. [2013]).

Naturally, our study can be extended in a number of interesting directions. For example, fishing fleets in many regions of the world are composed of high-technology large commercial boats and low-technology small private boats. This suggests that the fishery component in a coevolving stock-fishery system can also experience selective pressures promoting the coexistence of different fleet segments. In other words, the fleet can experience an analogous disruptive selection and adaptive diversification, as suggested by Dercole et al. [2010b] and illustrated by standard eco-evolutionary predator-prey models [Doebeli and Dieckmann, 2000, Landi et al., 2013]; this warrants future research and model extensions. Specifically, fishery dynamics could happen at many levels: at the level of the fleet (adaptive harvesting on a short timescale, fleet size and structure on an intermediate timescale, and technological adaptation on a longer timescale; Egas et al. [2005]), at the level of fishing strategy (constant effort, fixed quota, or fixed stock size; Hilborn and Walters [1992]), and/or at the level of fishing regulations (limitations on the size and maturity of target individuals; Cole and Ward [1994], Matsumura et al. [2011]). Here we have examined only the simplest setting, that is, adaptive harvesting with a constant-effort strategy. To detect disruptive selection on the fishery, adjustments in fleet size, fleet structure, and fleet technology must be explicitly modeled. As a starting point, the degree of harvest specialization in our model, Equation (6.2), could be interpreted as characterizing the technological level of the fleet (affecting, e.g., the probability of locating aggregations of fish, catchability, and/or the efficiency of handling and transporting the catch). On this basis, this parameter could be used as an adaptive trait of the fishery using the framework of adaptive dynamics theory [Dercole et al., 2008, 2010b].

An ultimate target of fishery management is to increase sustainable yield (e.g., Heino [1998]). This raises the question of whether fisheries-induced disruptive selection could, and should, be managed: as such selection pressures result from the interplay between natural selection and fishing mortality [Carlson et al., 2007, Edeline et al., 2007, 2009], they are human-induced and may arguably be controlled by fishing policies and fleet and harvest regulations. In practice, this can be achieved through legal limitations and incentives. Our results show that sustainable yield can slightly increase after diversification when only large individuals are targeted (Figure 6.7B), even though it still remains far below the maximum sustainable yield obtained at low fishing mortality when the stock is monomorphic. As many

fish stocks are still overexploited, being managed considerably below their maximum sustainable yield, our findings imply that diversification triggered by fisheries-induced disruptive selection under high fishing mortality might slightly increase the yield from its level before diversification, if only large individuals are targeted. However, our results also suggest that such a population dimorphism can be taken as a sign of extreme harvesting pressure, as trait diversification is a way for species to escape from severe selection pressures resulting from human exploitation. Hence, when such a pattern is observed, our analysis suggests that sustainable yield can usually be improved by reducing fishing mortality.

Fisheries-induced disruptive selection could also increase phenotypic variability [Edeline et al., 2009], without promoting life-history dimorphism: favoring extreme phenotypes may just widen an existing population polymorphism. This could have positive consequences beyond those analyzed in this chapter, since higher variability makes a population more reactive to future adaptation needs. This means that the population can react more promptly to any rapid changes in its environmental conditions, both for natural and anthropogenic causes. In other words, fisheries-induced disruptive selection could lead to a better capacity of an exploited stock to cope with environmental disturbances and changes [Roff, 1997].

In summary, fisheries-induced disruptive selection can indicate overexploitation, can slightly increase or decrease the yield depending on the adopted fishing policy, and can enhance a stock's resilience to abrupt changes in its environmental conditions. Weighting these three aspects, decision makers can manage a fishery in pursuit of their economic, social, and conservation objectives.

Chapter 7

Diversification of fashion traits

We propose a model to investigate the dynamics of fashion traits. We consider pure social interactions between people that adapt their style to maximize social success. People play a repeated group game in which the payoff reflects the social norms dictated by fashion: on one hand, the tendency to imitate the trendy stereotypes opposed to the tendency to diverge from them to proclaim identity; on the other hand, the tendency to exploit sex appeal in dating success opposed to the moral judgment of the society. This opposing forces result in the promotion of diversity in fashion traits, as predicted by the Adaptive Dynamics framework. More details can be found in Landi and Dercole [2014b] and Landi and Dercole [2014a].

7.1 Introduction

The dynamics of fashion traits has attracted much attention in the last centuries [Veblen, 1894, Simmel, 1904, Blumer, 1969, Sproles, 1979, 1985]. The several driving forces of fashion are best described by Sproles [1985]: "*Psychologists speak of fashion as the seeking of individuality; sociologists see class competition and social conformity to norms of dress; economists see a pursuit of the scarce; aestheticians view the artistic components and ideals of beauty; historians offer evolutionary explanations for changes in design. Literally hundreds of viewpoints unfold, from a literature more immense than for any phenomenon of consumer behavior.*" Changes in fashion traits have been documented since the XVIII century [Young, 1937, Richardson and

Kroeber, 1940, Robinson, 1976, Weeden, 1977, Sproles, 1981, Lowe and Lowe, 1990] and many studies tried to formally interpret and model fashion dynamics [Lowe and Lowe, 1982, 1983, Lowe, 1993, Miller et al., 1993, Pesendorfer, 1995, Caulkins et al., 2007]. But "*The current state of fashion theory includes a loosely organized array of descriptive principles and propositions but is not formalized in that it does not specify a detailed structure of concepts, variables, and relations*" [Sproles, 1981].

We are interested in the evolution of fashion traits that emerges from pure personal choice driven by social interactions, the so-called *horizontal dynamics* in the trickle-across theory [Simmel, 1904, Field, 1970, Robinson, 1976] and in the trickle-up theory—"*It now appears that some fashions, as well as some analogous nonfashion phenomena, climb the status pyramid from below, trickling up, as it were*" [Field, 1970]. We thus do not consider the external drivers of marketing, business, and other economic and production aspects in this study, as well as the tendency to emulate stereotypes from higher social classes, the *vertical dynamics* often investigated in the trickle-down theory [Veblen, 1894, Simmel, 1904]. This is in line with the view of Blumer [1969], who considers intra-class social interactions (the horizontal dynamics) dominant with respect to business and inter-class (vertical) drivers. "*The fashion mechanism appears not in response to a need of class differentiation and class emulation but in response to a wish to be in fashion, to be abreast of what has good standing, to express new tastes which are emerging in a changing world.*" [Blumer, 1969]. Blumer again argues that the change in fashion traits is the result of "*the gradual formation and refinement of collective tastes, which occur through social interaction among people with similar interests and social experience, with the result that many people develop tastes in common*".

Specifically, we want to assess whether the social interactions between common-class people can alone be responsible of the emergence of diversity in fashion traits. We see Evolutionary Game Theory and Adaptive Dynamics (mathematical approaches borrowed from evolutionary biology, see Paragraph 1.3) as the promising frameworks to model the evolution of social traits, fashion traits in particular. Although the context is different, innovation and competition play the role that genetic mutations and natural selection have in biological evolution [Ziman, 2000, Dercole et al., 2008, Dercole and Rinaldi, 2008]: when a new style is introduced in the market, people can try it and the style will be selected it if it gives some better performance

in terms of social score.

The aim of this chapter is to use the AD tools to assess if fashion can diversify in society starting from a unique clothing style and without any external influence, but only considering its inner social mechanisms. Moreover, the resident-innovative competition model will be based on a Replicator Equation of Evolutionary Game Theory derived from an underlying N-players game, in which the strategy is the clothing style chosen and the performance criteria is the social success in everyday life.

7.2 Methods

We study a (technically infinite and well-mixed) population in which each individual has initially the same style, that we represent with a one-dimensional continuous trait or *strategy* x assumed to be positively related with the sex appeal exerted by adopting that style. This is supported by many authors [Veblen, 1894, Laver, 1937, Lurie, 1981, Steele, 1985]. E.g., Steele [1985] argues: "*Because clothing is so intimately connected to the physical self, it automatically carries an erotic charge*", while Lurie [1981] applies psychoanalytic theory in the description of what is communicated by one's handbag, walking sticks, umbrellas, men's hats, and men's tie. For example, x could measure the sizes of clothes (as in Lowe and Lowe [1990], where the skirt length of women's evening dresses was recorded over two centuries). For simplicity, x is assumed unbounded and can be interpreted as a physical measure through a suitable transformation. If an innovative style x' similar to x is introduced by one or a few individual into the population, people can then either choose x or x'. The presence of only one innovation at a time is a simplification of AD, justified if innovations are sufficiently rare w.r.t. the timescale of the social interaction. While assuming that innovations are small ensures a gradual (mathematically continuous) evolution of the trait, as also envisaged in the context of fashion. For example, Blumer [1969] supports the idea of the historical continuity of fashion change, in which new fashions evolve from those previously established by the society. And, again, in Lowe and Lowe [1983] the following assumptions on fashion dynamics are made: inertia operates (e.g., if skirts have been progressively rising for the last few years, they tend to continue to rise until they reach an extreme) and resistance to that motion occurs (large year-to-year jumps in one direction create force back the other way).

The fraction (or *frequency*) of people adopting x (resp. x') is indicated with n (resp. $n' = 1 - n$). Individuals with different strategies will compete in their everyday life for their social success [Lowe and Lowe, 1983], here mainly related to their dating success [Barber, 1999]. We assume that people repeatedly meet at social events involving N randomly selected individuals and we indicate with n_x (resp $n_{x'} = N - n_x$) the number of x- (resp. x'-) strategists among them. We evaluate their dating success as the expected payoff of an underlying N-players game, indicating with P_x and $P_{x'}$ the expected payoff of the two competing strategies. The population dynamics is then ruled by the Replicator Equation [Taylor and Jonker, 1978, Schuster and Sigmund, 1983]

$$\begin{aligned} \dot{n}(t) &= n(P_x - \bar{P}) \\ \dot{n}'(t) &= n'(P_{x'} - \bar{P}), \end{aligned} \tag{7.1}$$

where $\bar{P} = nP_x + n'P_{x'}$ is the average payoff in the population. The Replicator Equation express the competition between agents with different strategies, and can thus be used as the resident-mutant model in the framework of AD.

The per-capita growth rate $\dot{n}'/n'$ of the innovative style evaluated at the resident equilibrium ($\bar{n} = 1$) is the invasion fitness, that we indicate with

$$\lambda(x, x') = P_{x'} - \bar{P}\big|_{n=\bar{n}=1} = P_{x'} - P_x|_{n=\bar{n}=1}\,. \tag{7.2}$$

The evolution of the strategy x proceeds by a sequence of successful innovations, characterized by a positive fitness, that replace the current resident strategy. In the limit of infinitesimally small innovations, x evolves in the direction of the selection gradient

$$S(x) = \left.\frac{\partial \lambda(x, x')}{\partial x'}\right|_{x'=x}, \tag{7.3}$$

namely, $\dot{x} = S(x)$, where the time derivative is taken on a slower evolutionary timescale. Once the strategy has reached an equilibrium $\bar{x}$ (i.e., $S(\bar{x}) = 0$), the second-order fitness derivative

$$B'' = \left.\frac{\partial^2 \lambda(x, x')}{\partial x'^2}\right|_{x'=x=\bar{x}} \tag{7.4}$$

tells if diversification is possible. If positive, the innovative style now coexists with the resident one, thus forming a second resident population, and the two coexisting strategies diversify under disruptive

selection by following distinct evolutionary branches [Geritz et al., 1997, 1998]. And again, when diversification has reached an equilibrium, another branching phenomenon can occur, thus increasing diversity on and on (see also Chapter 5).

7.3 Model

We assume the social payoff to be the sum of four terms. Each of them is expressed w.r.t. a strategy y, to be thought as x, x', or a virtual strategy with vanishing frequency (in analogy with the g-function notation, see Paragraph 3.1). In this way, their expression can be also used (with some slight adjustment) for the two-style resident community (see Paragraph 7.3.1).

- The payoff for being trendy. It is the absolute advantage to conform to one of the established styles. It is formulated as

$$P_\varepsilon(y) = \varepsilon n \exp[-\alpha(y-x)^2] + \varepsilon n' \exp[-\alpha(y-x')^2]. \qquad (7.5)$$

  It is proportional, through the *trendy payoff* ε, to the fraction of people adopting a style similar to y (the more people wear a style the more trendy it is), where similarity is weighted by the exponential terms. For example, if everyone is wearing x, then $n = 1$ and $n' = 0$, so that x-strategists receive $P_\varepsilon(x) = \varepsilon$, while x'-strategists receive $P_\varepsilon(x') = 0$. Notice that, if $y = x = x'$ (that means that individuals are identical), the payoff is consistently ε for all strategies.

- The payoff for being sexy. It is a relative advantage for sexy vs. austere styles when competing for dating in a social event. For the virtual strategy y, it is expressed as

$$P_\sigma(y) = \sigma(y-x)\frac{n_x}{N-1} + \sigma(y-x')\frac{n_{x'}}{N-1}. \qquad (7.6)$$

  It is proportional, through the *sexy payoff* σ, to the difference in strategy w.r.t. possible competitors (recall that the strategy is proportional to the sex appeal), weighted by the probability of meeting such a competitor at the social event, while it is 0 if strategies are all identical.

- The payoff for respecting morality. It is an absolute judgment on style, given by the morality codes uniformly accepted by the

society. It therefore solely depends on the strategy adopted by an individual, and for the virtual strategy y it is expressed as

$$P_\mu(y) = \mu\{1 - \exp[\beta(y - x_0)]\}, \tag{7.7}$$

where μ is the *morality payoff* and x_0 represents a *morality threshold* somehow separating austere from immoral styles, that reflects the morality codes accepted by the whole society. It is positive (resp., negative) for austere (resp., immoral) styles $y < x_0$ (resp., $y > x_0$).

- The payoff for originality. It is the advantage to be minority at the social event. For the virtual strategy y, it is expressed as

$$P_\varphi(y) = \varphi \exp[-\gamma(y-x_0)]\left(\frac{1}{2} - \frac{n_x}{N}\exp[-\delta(y-x)^2] - \frac{n_{x'}}{N}\exp[-\delta(y-x')^2]\right), \tag{7.8}$$

where the first exponential term modulates the *originality payoff* φ that vanishes for highly immoral styles, whereas the second term goes from $\frac{1}{2}$ to $-\frac{1}{2}$ as the strategy y goes from extreme minority (y largely differs from the established styles with similarity measured by the exponential terms) to absolute majority ($y = x$ with $n = 1$ or $y = x'$ with $n' = 1$).

The expected payoffs P_x and $P_{x'}$ are then given by (recall that $n' = 1 - n$ and $n_{x'} = N - n_x$)

$$P_x = \sum_{n_x=1}^{N} [P_\varepsilon(x) + P_\sigma(x) + P_\mu(x) + P_\varphi(x)]\binom{N-1}{n_x - 1} n^{n_x - 1}(1-n)^{N-n_x}$$

and

$$P_{x'} = \sum_{n_x=0}^{N-1} [P_\varepsilon(x') + P_\sigma(x') + P_\mu(x') + P_\varphi(x')]\binom{N-1}{n_x} n^{n_x}(1-n)^{N-n_x-1},$$

that is,

$$P_x = \sum_{n_x=1}^{N} \Bigg[\varepsilon n + \varepsilon(1-n)\exp[-\alpha(x-x')^2] + \\ \sigma(x-x')\frac{N-n_x}{N-1} + \mu\{1-\exp[\beta(x-x_0)]\} + \\ \varphi\exp[-\gamma(x-x_0)]\left(\frac{1}{2} - \frac{n_x}{N} - \frac{N-n_x}{N}\exp[-\delta(x-x')^2]\right)\Bigg] \\ \binom{N-1}{n_x-1} n^{n_x-1}(1-n)^{N-n_x}$$

and

$$P_{x'} = \sum_{n_x=0}^{N-1} \Bigg[\varepsilon n\exp[-\alpha(x'-x)^2] + \varepsilon(1-n) + \\ \sigma(x'-x)\frac{n_x}{N-1} + \mu\{1-\exp[\beta(x'-x_0)]\} + \\ \varphi\exp[-\gamma(x'-x_0)]\left(\frac{1}{2} - \frac{n_x}{N}\exp[-\delta(x'-x)^2 - \frac{N-n_x}{N}]\right)\Bigg] \\ \binom{N-1}{n_x} n^{n_x}(1-n)^{N-n_x-1}.$$

Collecting n_x and computing the summations of the probabilities (see Paragraph 7.3.2) we obtain

$$P_x = \varepsilon n + \varepsilon(1-n)\exp[-\alpha(x-x')^2] + \sigma(x-x')\frac{N}{N-1} + \\ \mu\{1-\exp[\beta(x-x_0)]\} + \varphi\exp[-\gamma(x-x_0)]\left(\frac{1}{2} - \exp[-\delta(x-x')^2]\right) + \\ \left[-\sigma(x-x')\frac{1}{N-1} + \varphi\exp[-\gamma(x-x_0)]\left(\frac{1}{N}\exp[-\delta(x-x')^2] - \frac{1}{N}\right)\right] \\ \Big[1+n(N-1)\Big]$$

and

$$P_{x'} = \varepsilon n \exp[-\alpha(x'-x)^2] + \varepsilon(1-n) + \mu\{1-\exp[\beta(x'-x_0)]\} + \varphi\exp[-\gamma(x'-x_0)]\left(\frac{1}{2}-1\right) + \left[\sigma(x'-x)\frac{1}{N-1} + \varphi\exp[-\gamma(x'-x_0)]\left(\frac{1}{N} - \frac{1}{N}\exp[-\delta(x'-x)^2]\right)\right] \Bigg[n(N-1)\Bigg].$$

Recalling its definition (7.2), it is now possible to compute the invasion fitness $\lambda(x, x')$, that is

$$\lambda(x,x') = \varepsilon\Big(\exp[-\alpha(x'-x)^2] - 1\Big) + \sigma(x'-x) + \mu\Big(\exp[\beta(x-x_0)] - \exp[\beta(x'-x_0)]\Big) + \frac{1}{2}\varphi\exp[-\gamma(x-x_0)] + \varphi\exp[-\gamma(x'-x_0)]\left(\frac{N-1}{N} - \frac{N-1}{N}\exp[-\delta(x'-x)^2] - \frac{1}{2}\right).$$

The strategy evolves according to (7.3), that is,

$$\dot{x} = \sigma - \beta\mu\exp[\beta(x-x_0)] + \frac{1}{2}\gamma\varphi\exp[-\gamma(x-x_0)].$$

Notice that the advantage of the sex appeal σ and of the originality φ lead the strategy to increase and become more and more sex appealing, while the morality μ leads it to decrease (notice that the advantage of wearing the trendy style ϵ is not playing any role here). These two opposed forces keep the strategy bounded and make it converge to the equilibrium $\bar{x}$, defined by $S(\bar{x}) = 0$ (but notice that the analytical expression of the evolutionary equilibrium $\bar{x}$ cannot be obtained explicitly).

Finally, it is possible to assess if $\bar{x}$ is a branching point, i.e., if the innovative strategy coexists with the resident one and then diverge under disruptive selection, giving rise to two different style, that is, diversification. Evaluating equation (7.4) we obtain the condition for diversification, that is

$$B'' = -2\alpha\varepsilon - \beta^2\mu\exp[\beta(\bar{x}-x_0)] + 2\frac{N-1}{N}\delta\varphi\exp[-\gamma(\bar{x}-x_0)] > 0.$$

As done in Landi et al. [2013] and Chapters 5 and 6, the evolutionary equilibrium and the divergence condition are continued w.r.t. parameter pairs, to obtain the branching portraits reported in Figure 7.2.

7.3.1 Two-style community

After diversification, it is possible to study the evolution of the two resident strategies. For this, we must consider a resident population split into two different sub-populations n_1 and n_2 with strategies x_1 and x_2, whose resident dynamics are given by

$$\dot{n}_1(t) = n_1(P^R_{x_1} - \bar{P}^R)$$
$$\dot{n}_2(t) = n_2(P^R_{x_2} - \bar{P}^R),$$

where $\bar{P}^R = n_1 P^R_{x_1} + n_2 P^R_{x_2}$ is the average payoff in the resident population. Notice that this two-style resident model is nothing but model (7.1) with $n = n_1$, $n' = n_2$, $x = x_1$, and $x' = x_2$.

When innovative agents with abundance n' and strategy x' appear in the population, the resident-innovative model now is

$$\dot{n}_1(t) = n_1(P_{x_1} - \bar{P})$$
$$\dot{n}_2(t) = n_2(P_{x_2} - \bar{P})$$
$$\dot{n}'(t) = n'(P_{x'} - \bar{P})$$

with $\bar{P} = n_1 P_{x_1} + n_2 P_{x_2} + n' P_{x'}$. The per-capita growth rate $\dot{n}'/n'$ of the innovative agents evaluated at the resident equilibrium $(\bar{n}_1(x_1, x_2), \bar{n}_2(x_1, x_2))$ gives the two-style fitness function $\lambda(x_1, x_2, x')$. Recall that at the resident equilibrium the frequencies of the innovative agents are null, so that $\bar{n}_2 = 1 - \bar{n}_1$. The definition of the resident equilibrium is

$$0 = n_1(P^R_{x_1} - \bar{P}^R)\big|_{n_1=\bar{n}_1, n_2=1-\bar{n}_1}$$
$$0 = n_2(P^R_{x_2} - \bar{P}^R)\big|_{n_1=\bar{n}_1, n_2=1-\bar{n}_1},$$

from which the condition for the coexistence equilibrium is consistently $P^R_{x_1}\big|_{n_1=\bar{n}_1, n_2=1-\bar{n}_1} = P^R_{x_2}\big|_{n_1=\bar{n}_1, n_2=1-\bar{n}_1}$. This can be solved in order to obtain $\bar{n}_1$ (and $\bar{n}_2 = 1 - \bar{n}_1$). Thus, the fitness function is

$$\lambda(x_1, x_2, x') = (P_{x'} - \bar{P})\big|_{n_1=\bar{n}_1, n_2=1-\bar{n}_1}. \tag{7.9}$$

Strategies x_1 and x_2 evolve proportionally to the selection gradient

$$S_i(x_1, x_2) = \left.\frac{\partial \lambda(x_1, x_2, x')}{\partial x'}\right|_{x'=x_i}, \tag{7.10}$$

with $i = 1, 2$, multiplied by half the mutational rate and the demographic equilibrium density. If a two-style evolutionary equilibrium $(\bar{x}_1, \bar{x}_2)$ is reached, the branching conditions

$$B'_i = \left.\frac{\partial^2 \lambda(x_1, x_2, x')}{\partial x_i \partial x'}\right|_{\substack{x_1=\bar{x}_1,\ x_2=\bar{x}_2 \\ x'=\bar{x}_i}} < 0,$$

and

$$B_i'' = \left.\frac{\partial^2 \lambda(x_1, x_2, x')}{\partial x'^2}\right|_{\substack{x_1=\bar{x}_1,\ x_2=\bar{x}_2 \\ x'=\bar{x}_i}} > 0$$

with $i = 1, 2$, can be tested to assess if another diversification in style is possible or not.

Indicating with n_{x_1}, n_{x_2}, and $n_{x'} = N - n_{x_1} - n_{x_2}$ the number of x_1-, x_2-, and x'-strategists at the social event, we can use equations (7.5), (7.6), (7.7), and (7.8)—replacing n with n_1, n' with n_2, x with x_1, x' with x_2 and y with x'—to compute the expected payoffs P_{x_1}, P_{x_2}, and $P_{x'}$. Thus, they are given by (recall that $n_1 + n_2 + n' = 1$)

$$\begin{aligned} P_{x_1} = \sum_{n_{x_1}=1}^{N} \sum_{n_{x_2}=0}^{N-n_{x_1}} & [P_\varepsilon(x_1) + P_\sigma(x_1) + P_\mu(x_1) + P_\varphi(x_1)] \\ & \binom{N-1}{n_{x_1}-1} n_1^{n_{x_1}-1} (1-n_1)^{N-n_{x_1}} \\ & \binom{N-n_{x_1}}{n_{x_2}} \left(\frac{n_2}{1-n_1}\right)^{n_{x_2}} \left(\frac{1-n_1-n_2}{1-n_1}\right)^{N-n_{x_1}-n_{x_2}}, \end{aligned}$$

$$\begin{aligned} P_{x_2} = \sum_{n_{x_2}=1}^{N} \sum_{n_{x_1}=0}^{N-n_{x_2}} & [P_\varepsilon(x_2) + P_\sigma(x_2) + P_\mu(x_2) + P_\varphi(x_2)] \\ & \binom{N-1}{n_{x_2}-1} n_2^{n_{x_2}-1} (1-n_2)^{N-n_{x_2}} \\ & \binom{N-n_{x_2}}{n_{x_1}} \left(\frac{n_1}{1-n_2}\right)^{n_{x_1}} \left(\frac{1-n_1-n_2}{1-n_2}\right)^{N-n_{x_1}-n_{x_2}}, \end{aligned}$$

and

$$\begin{aligned} P_{x'} = \sum_{n_{x_1}=0}^{N-1} \sum_{n_{x_2}=0}^{N-n_{x_1}-1} & [P_\varepsilon(x') + P_\sigma(x') + P_\mu(x') + P_\varphi(x')] \\ & \binom{N-1}{n_{x_1}} n_1^{n_{x_1}} (1-n_1)^{N-n_{x_1}-1} \\ & \binom{N-n_{x_1}-1}{n_{x_2}} \left(\frac{n_2}{1-n_1}\right)^{n_{x_2}} \left(\frac{1-n_1-n_2}{1-n_1}\right)^{N-n_{x_1}-n_{x_2}}. \end{aligned}$$

Collecting n_{x_1} and n_{x_2} and computing the probabilities (see Para-

graph 7.3.2) we obtain

$$P_{x_1} = \varepsilon n_1 + \varepsilon n_2 \exp[-\alpha(x_1 - x_2)^2] + \sigma(x_1 - x')\frac{N}{N-1} +$$
$$\mu\{1 - \exp[\beta(x_1 - x_0)]\} + \varphi \exp[-\gamma(x_1 - x_0)]\left(\frac{1}{2} - \exp[-\delta(x_1 - x')^2]\right) +$$
$$\left[-\sigma(x_1 - x')\frac{1}{N-1} + \varphi \exp[-\gamma(x_1 - x_0)]\left(\frac{1}{N}\exp[-\delta(x_1 - x')^2] - \frac{1}{N}\right)\right]$$
$$\left[1 + n_1(N-1)\right] +$$
$$\left[-\sigma(x_1 - x')\frac{1}{N-1} + \sigma(x_1 - x_2)\frac{1}{N-1} +\right.$$
$$\left.\varphi \exp[-\gamma(x_1 - x_0)]\left(\frac{1}{N}\exp[-\delta(x_1 - x')^2] - \frac{1}{N}\exp[-\delta(x_1 - x_2)^2]\right)\right]$$
$$\left[n_2(N-1)\right],$$

$$P_{x_2} = \varepsilon n_1 \exp[-\alpha(x_2 - x_1)^2] + \varepsilon n_2 + \sigma(x_2 - x')\frac{N}{N-1} +$$
$$\mu\{1 - \exp[\beta(x_2 - x_0)]\} + \varphi \exp[-\gamma(x_2 - x_0)]\left(\frac{1}{2} - \exp[-\delta(x_2 - x')^2]\right) +$$
$$\left[-\sigma(x_2 - x')\frac{1}{N-1} + \varphi \exp[-\gamma(x_2 - x_0)]\left(\frac{1}{N}\exp[-\delta(x_2 - x')^2] - \frac{1}{N}\right)\right]$$
$$\left[1 + n_2(N-1)\right] +$$
$$\left[-\sigma(x_2 - x')\frac{1}{N-1} + \sigma(x_2 - x_1)\frac{1}{N-1} +\right.$$
$$\left.\varphi \exp[-\gamma(x_2 - x_0)]\left(\frac{1}{N}\exp[-\delta(x_2 - x')^2] - \frac{1}{N}\exp[-\delta(x_2 - x_1)^2]\right)\right]$$
$$\left[n_1(N-1)\right],$$

and

$$P_{x'} = \varepsilon n_1 \exp[-\alpha(x' - x_1)^2] + \varepsilon n_2 \exp[-\alpha(x' - x_2)^2] + \mu\{1 - \exp[\beta(x' - x_0)]\} + \varphi \exp[-\gamma(x' - x_0)]\left(\frac{1}{2} - 1\right) + \left[\sigma(x' - x_1)\frac{1}{N-1} + \varphi \exp[-\gamma(x' - x_0)]\left(\frac{1}{N} - \frac{1}{N}\exp[-\delta(x' - x_1)^2]\right)\right] \left[n_1(N-1)\right] + \left[\sigma(x' - x_2)\frac{1}{N-1} + \varphi \exp[-\gamma(x' - x_0)]\left(\frac{1}{N} - \frac{1}{N}\exp[-\delta(x' - x_2)^2]\right)\right] \left[n_2(N-1)\right].$$

From these terms it is possible to compute the two-style fitness (7.9) to be used for the analysis of the evolutionary dynamics of the two-style community.

7.3.2 Probabilities computation

We here show how to compute the probability terms in the fitness functions expressions. As for the computation of $P_{x'}$ in the single-style community, it is easy to see that

$$\sum_{n_x=0}^{N-1} \binom{N-1}{n_x} n^{n_x}(1-n)^{N-n_x-1} = 1$$

and

$$\sum_{n_x=0}^{N-1} n_x \binom{N-1}{n_x} n^{n_x}(1-n)^{N-n_x-1} = n(N-1)\sum_{n_x=1}^{N-1} \binom{N-2}{n_x-1} n^{n_x-1}(1-n)^{N-n_x-1} = n(N-1).$$

As for P_x we have

$$\sum_{n_x=1}^{N} \binom{N-1}{n_x-1} n^{n_x-1}(1-n)^{N-n_x} = 1,$$

while

$$\sum_{n_x=1}^{N} n_x \binom{N-1}{n_x-1} n^{n_x-1}(1-n)^{N-n_x} =$$
$$\sum_{n_x=1}^{N} (1+n_x-1)\binom{N-1}{n_x-1} n^{n_x-1}(1-n)^{N-n_x} =$$
$$1+n(N-1)\sum_{n_x=2}^{N} \binom{N-2}{n_x-2} n^{n_x-2}(1-n)^{N-n_x} =$$
$$1+n(N-1).$$

As for P_{x_1} in the two-style community, we need

$$\sum_{n_{x_2}=0}^{N-n_{x_1}} n_{x_2} \binom{N-n_{x_1}}{n_{x_2}} \left(\frac{n_2}{1-n_1}\right)^{n_{x_2}} \left(\frac{1-n_1-n_2}{1-n_1}\right)^{N-n_{x_1}-n_{x_2}} =$$
$$\frac{n_2}{1-n_1}(N-n_{x_1})$$
$$\sum_{n_{x_2}=1}^{N-n_{x_1}} \binom{N-n_{x_1}-1}{n_{x_2}-1} \left(\frac{n_2}{1-n_1}\right)^{n_{x_2}-1} \left(\frac{1-n_1-n_2}{1-n_1}\right)^{N-n_{x_1}-n_{x_2}} =$$
$$\frac{n_2}{1-n_1}(N-n_{x_1})$$

to be used in

$$\sum_{n_{x_1}=1}^{N} \frac{n_2}{1-n_1}(N-n_{x_1}) \binom{N-1}{n_{x_1}-1} n_1^{n_{x_1}-1}(1-n_1)^{N-n_{x_1}} =$$
$$\frac{n_2}{1-n_1}\left[N - \sum_{n_x=1}^{N} n_{x_1} \binom{N-1}{n_{x_1}-1} n_1^{n_{x_1}-1}(1-n_1)^{N-n_{x_1}}\right] =$$
$$\frac{n_2}{1-n_1}\Big[(1-n_1)(N-1)\Big] = n_2(N-1),$$

and similarly for P_{x_2}.

As for $P_{x'}$, we need

$$\sum_{n_{x_2}=0}^{N-n_{x_1}-1} n_{x_2}\binom{N-n_{x_1}-1}{n_{x_2}}\left(\frac{n_2}{1-n_1}\right)^{n_{x_2}}\left(\frac{1-n_1-n_2}{1-n_1}\right)^{N-n_{x_1}-n_{x_2}-1} = \frac{n_2}{1-n_1}(N-n_{x_1}-1)$$

$$\sum_{n_{x_2}=1}^{N-n_{x_1}-1}\binom{N-n_{x_1}-2}{n_{x_2}-1}\left(\frac{n_2}{1-n_1}\right)^{n_{x_2}-1}\left(\frac{1-n_1-n_2}{1-n_1}\right)^{N-n_{x_1}-n_{x_2}-1} = \frac{n_2}{1-n_1}(N-n_{x_1}-1)$$

to be used in

$$\sum_{n_{x_1}=0}^{N-1}\frac{n_2}{1-n_1}(N-n_{x_1}-1)\binom{N-1}{n_{x_1}}n_1^{n_{x_1}}(1-n_1)^{N-n_{x_1}-1} =$$

$$\frac{n_2}{1-n_1}\left[N-1-\sum_{n_{x_1}=0}^{N-1} n_{x_1}\binom{N-1}{n_{x_1}}n_1^{n_{x_1}}(1-n_1)^{N-n_{x_1}-1}\right] =$$

$$\frac{n_2}{1-n_1}\Big[(1-n_1)(N-1)\Big] = n_2(N-1)$$

7.4 Results

We carry out the analysis of the model with the same spirit of Landi et al. [2013] (see also Chapter 5). Figure 7.1 shows the evolution, according to our model for the parameter setting indicated in the caption, of an initially uniform and neutrally moral style. After reaching the equilibrium $\bar{x}$ close to x_0 a first evolutionary branching occurs: it is now possible to study the evolution of the two resident strategies x_1 and x_2 with frequencies n_1 and n_2 by considering that innovative styles can originate as slight modifications of both of them, i.e., x' is close to either x_1 or x_2 (see Paragraph 7.3.1). This because two populations with very similar strategies coexist on the (fast) social timescale, so that two different selection gradients (7.10) $S_1(x_1, x_2)$ and $S_2(x_1, x_2)$ can be derived and from them the evolution of the two traits. These selection gradients have opposite sign, so that strategies diverge on the (slow) fashion timescale, one becoming austere while the other immoral. When divergence reaches the two-style equilibrium $(\bar{x}_1, \bar{x}_2)$, both strategy can branch in principle,

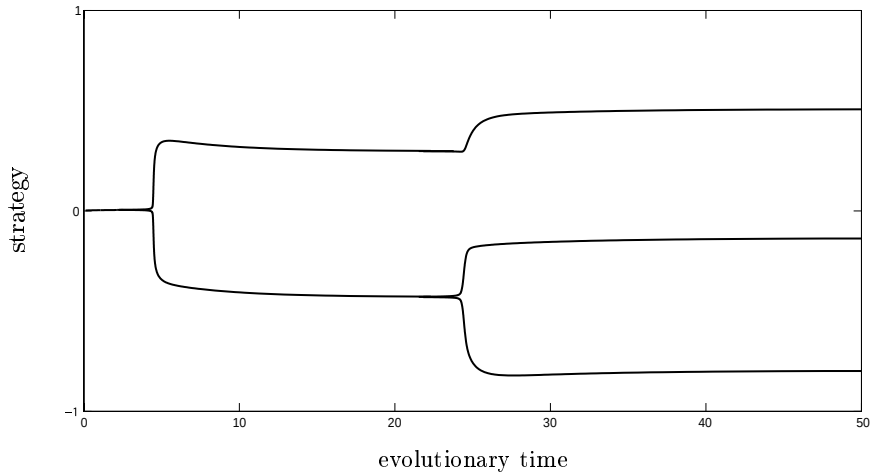

Figure 7.1: Simulation of the model showing the evolution and branching of the fashion trait. Parameters: $\varepsilon = 0.01$, $\alpha = \delta = \varphi = 10$, $\beta = \sigma = \mu = 1$, $\gamma = 0.001$, $x_0 = 0$.

but generically only one of the two nascent branchings survives (see Paragraph 5.2.3.2). In this case, another diversification phenomenon occurs in the austere population. These two new austere populations diverge, one becoming more and more austere, the other increasing its sex appeal approaching the neutral strategy x_0. Also the three-style equilibrium $(\bar{x}_1, \bar{x}_2, \bar{x}_3)$ shown at the righthand side of Figure 7.1 is a branching point for all populations, thus diversification continues to emerge in the system. Notice that strategies close to x_0 return in fashion during the three-style evolution after a long period of two-style evolution in which no one was wearing it anymore. Thus, recurrent diversification also explain the cyclical recurrence of fashion traits and the revival of old-fashioned and vintage styles.

Figure 7.2 shows the effect of the different social mechanisms underlying fashion dynamics on style diversification. Figures 7.2A and 7.2B focus on the need of conforming to established styles (the trendy payoff ε, see equation (7.5)) vs. the need to proclaim identity and individual affirmation (the originality payoff φ and the originality exponent γ, see equation (7.8)). In particular, diversification is promoted when the originality payoff φ is sufficiently larger than the trendy payoff ε (Figure 7.2A) and when the originality payoff tends to be uniformly distributed between austere and immoral styles (low values of γ, Figure 7.2B).

Figures 7.2C and 7.2D show the effect of the need for being sexy

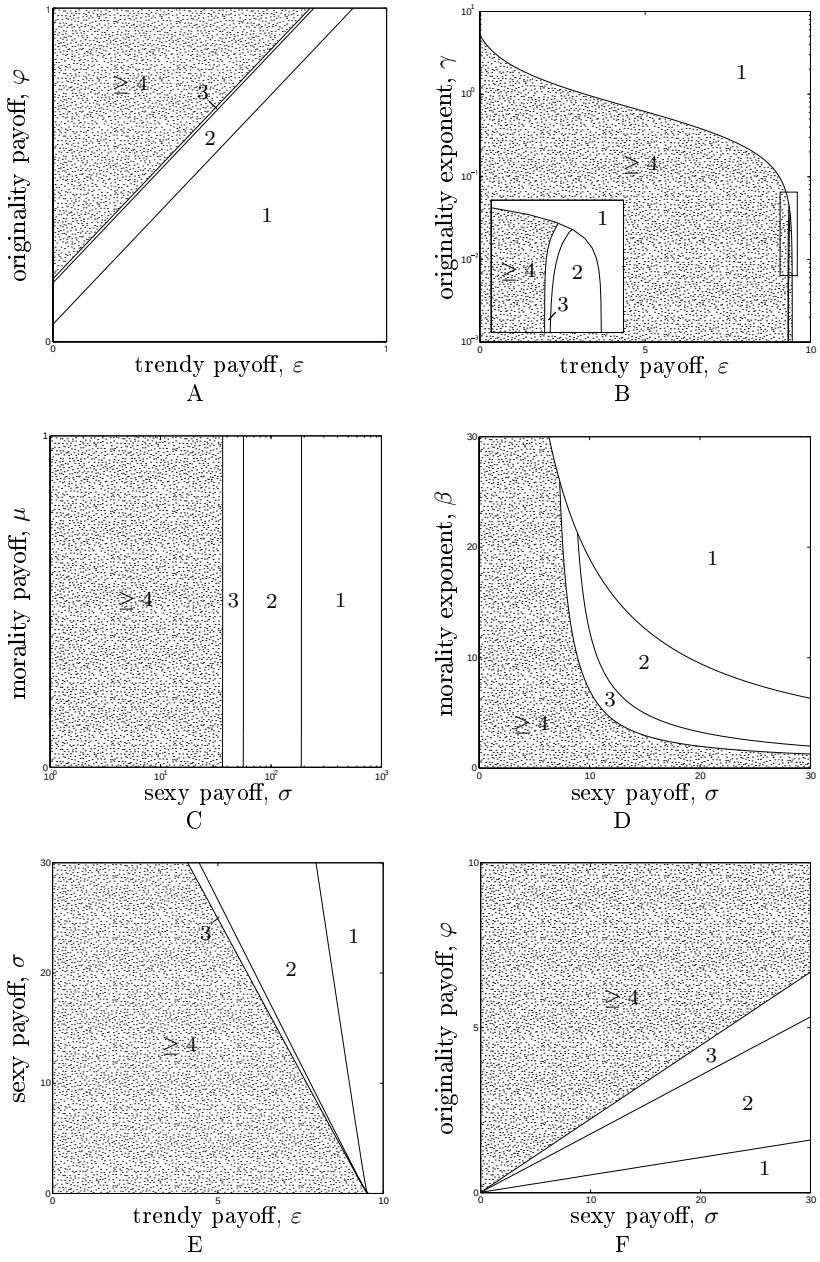

Figure 7.2: Regions of the parameter spaces allowing the coexistence of 1, 2, 3, ≥ 4 different styles, starting from a single-style community. In the dotted region at least three successive branchings take place, but the analysis can be furthered. Parameters as in Figure 7.1.

(the sexy payoff σ, see equation (7.6)) vs. the morality code of the society (the morality payoff μ and the morality exponent β, see equation (7.7)). In particular, the absolute value of morality μ does not play a significant role (Figure 7.2C, the same holds for the morality threshold x_0, results not shown), while diversification is again promoted when the relative moral judgement between austere and immoral styles tend to be uniform (low values of β, Figure 7.2D). As for the sexy payoff σ, it must be limited to promote style diversity (see also Figures 7.2E and 7.2F).

Figure 7.2E compares the need to be trendy (ε) and the need to be sexy (σ). They must both be limited to promote diversification, even if the sexy payoff is less restrictive.

Figure 7.2F focus on the effect of sex appeal (σ) and originality (φ). Fashion diversity is promoted whenever the need for individual affirmation and identity display φ is high and the need to be sex appealing σ is low.

7.5 Discussion

We showed that social interactions alone are capable of generating fashion diversification in society. This is in agreement with the view of Blumer [1969], who argues that the change in fashion traits is the result of "*the gradual formation and refinement of collective tastes, which occur through social interaction among people with similar interests and social experience, with the result that many people develop tastes in common*". The model is based on a Replicator Equation and on Adaptive Dynamics, and its assumptions are in agreement with the classical hypothesis on fashion dynamics. For example, the idea of Blumer [1969] on the historical continuity of fashion change, for which new fashions evolve from those previously established by the society, is in good agreement with the AD assumptions of rare and small mutations and with the smooth approximation of the canonical equation. Moreover, the idea that the clothing style is strictly related to the sex appeal is supported by manu authors in the fashion literature [Veblen, 1894, Laver, 1937, Lurie, 1981, Steele, 1985]. And, again, mechanisms that drive fashion change, i.e., the need for being trendy ("*... a wish to be in fashion ...*") opposed to the need for originality ("*... [a wish] to express new tastes ...*" [Blumer, 1969]), and the need to be sexy opposed to the need for respecting morality (skirts continue to rise until they reach an extreme in Lowe and Lowe [1983]; "*... [a wish]to be abreast of what has good standing ...*"

[Blumer, 1969]), seems to be in line with the ideas of the theorists of fashion.

Our analysis points out (see Figure 7.2) that the main mechanism promoting fashion diversification is the need to proclaim identity and to be original φ, especially when its advantage is uniformly distributed between the austere and immoral styles (low values of γ), whereas the need to conform to the trendy style ε and the need to be sexy σ reduce the emergence of style diversity. The effect of morality is a bit more subtle: diversity is promoted when the relative judgement between austere and immoral styles tends to be uniform (low values of β), while there is no effect of the absolute moral judgement μ and the morality threshold x_0.

As already noticed in Paragraph 5.5, there exist particular parameter regions where diversification scenarios are very sensitive to parameter perturbations. E.g., see the line segment in Figure 7.2B where a small perturbation in the originality exponent γ can switch from a low (region 1, where only a single style can coexist) to a high diversity scenario (region ≥ 4, where at least four different styles can coexist). And the same can occur varying the morality exponent β in Figure 7.2D.

The social norms dictated by fashion in the horizontal dynamics approach can generate a rich variety of coexisting styles, starting from an initial situation of conformity. This diversification dynamics can also be responsible of the periodic recurrence of some clothing style [Young, 1937, Lowe and Lowe, 1990, Pesendorfer, 1995, Caulkins et al., 2007], as we can see from Figure 7.1 and briefly discussed in the previous paragraph. Moreover, the presence of more than one style could lead to a periodic, quasi-periodic, or even chaotic fashion regimes, where the styles oscillates continuously without ever reaching a stationary equilibrium [Marrow et al., 1992, Dieckmann et al., 1995, Dercole et al., 2006, 2010a]. The simplest of such never-ending dynamics would be a two-style limit cycle: for this to happen, a Hopf bifurcation should be identified in the two-style community. A more subtle and evolutionarily intriguing periodic dynamics are the branching-extinction cycles [Doebeli and Dieckmann, 2000, Kisdi et al., 2001, Dercole, 2003, Dercole and Rinaldi, 2008]. This happens when evolution first leads to an evolutionary branching point, and then drives one of the morphs to extinction. If the dynamics goes back again to the branching point, this leads to a never-ending evolutionary dynamics of increase and successive loss of diversity. In this case, the sexy style after diversification could become so immoral

to bring disadvantages to who adopts it, leading to its extinction. The austere style would then converge back to the neutral style, thus undergoing again diversification, and so on. However, such periodic dynamics was not detected in the present model. These extensions are left for future research.

Chapter 8

Conclusions

Innovation and competition processes are ubiquitous in our world. They drive evolutionary dynamics by innovative changes in the characteristics of individual agents and by competitive interactions that promote better performing ones. This evolution paradigm can be applied also outside biology, for example to social, economic, information sciences and engineering. Adaptive Dynamics represents a flexible modelling framework, based on the hypothesis of rare and small mutations, for the formal description of evolution of the characteristics of the system in terms of ordinary differential equations. Diversity reduce when evolution brings groups of agents to extinction, and increases through evolutionary branching: in appropriate conditions, innovative agents can coexist with resident ones and their strategies, initially very similar, can then diverge giving rise to the presence of two resident forms with different characteristics. The evolution of this enlarged system can still bring to the situation in which evolutionary branching is possible for one or both forms of agents present in the system. Thus, this succession of evolutionary branchings brings simple systems (with few resident forms) toward more complex and diversified configurations. The study of the possible branching scenarios is then very interesting in biology (where it gives an interpretation of the diversification of species from a common ancestor), but also in social sciences, economics, technology, engineering, etcetera. Moreover, some theoretical aspects of branching are still unstudied. For example, mathematical conditions under which branching occurs are not yet available in critical cases.

After introducing the theory of evolution, its history, its main processes (mutation and selection), and the mathematical approaches available for its study, we focus on the Adaptive Dynamics approach

(the resident-mutant competition model, the computation of the invasion fitness, and the AD canonical equation), with particular emphasis on evolutionary branching. We recover the classification of the evolutionary equilibria with respect to their convergence and evolutionary stability and the classical branching conditions in terms of second derivatives of the invasion fitness, under which the system becomes dimorphic and experience disruptive selection thus increasing its diversity. We then focus on the branching bifurcation, namely, the transition from evolutionary stability to evolutionary instability along with the change in a model parameter. This bifurcation occurs when the sign of the branching condition ruling evolutionary stability changes from negative to positive. To study such critical case, a particular third order approximation of the invasion fitness must be computed, and a novel property of the resident-mutant competition model must be exploited in order to obtain simple and general results. The study of this critical case extends the theory of evolutionary branching, expands our knowledge on the phenomenon and provides more general conditions under which it occurs. Moreover, our approach is general and remains valid also in the case in which the other branching condition is critical, as well as for the study of further degenerate cases (e.g., when both branching conditions are critical). These extensions are left for future research. As for the applications, we develop a general methodology to study the evolution of diversity, with an application to eco-evolutionary two-species communities. We then use such methodology also in two fields of science different from biology. First, we study the evolutionary consequences of fisheries on exploited fish stocks, finding out that the interplay of artificial and natural selection can lead to disruptive selection on the stock's maturation schedule. Finally, we study the evolution of fashion traits purely driven by social interactions and discover that a cascade of style diversification phenomena is possible starting from a single style society.

In particular, in chapter 4 we unfold the bifurcation concerning the loss of evolutionary stability of an equilibrium of the canonical equation of Adaptive Dynamics. In the vicinity of a stable equilibrium of the AD canonical equation, a mutant type can invade and coexist with the present resident types, whereas resident-mutant coexistence is generically impossible far from equilibrium—the fittest always win. After coexistence, residents and mutants effectively diversify, according to the enlarged canonical equation, only if natural selection favors outer rather than intermediate traits. Though the conditions for evo-

lutionary branching have been known for long, the unfolding of the bifurcation remained a missing tile of AD, the reason being related to the nonsmoothness of the mutant invasion fitness at the branching point. We develop a methodology that allows the approximation of the invasion fitness after branching in terms of the expansion of the (smooth) fitness before branching. We then derive a canonical model for the branching bifurcation and perform its unfolding around the loss of evolutionary stability, finding out more general conditions under which evolutionary branching occurs. Moreover, our theoretical approach is general and remains valid also for the case in which the other branching condition is critical, as well as for the study of further degenerate cases (e.g., when both the branching conditions are critical, or when also third and higher order derivatives annihilate).

The main theoretical contribution of this chapter is a general method of approximating the dimorphic fitness. It is based on a radial expansion on a given ray in the plane of the two similar coexisting strategies. It exploits the fact (observed in Durinx [2008] and Dercole and Geritz [2014]) that the equilibrium densities at which the two strategies can coexist are nonsmooth at the monomorphic singular strategy, but are well defined and smooth along each given ray in the cone of coexistence. As a consequence, the radial expansions of the dimorphic equilibrium densities and of the dimorphic fitness depend on the chosen ray, but, interestingly, they can be written back in terms of rational and polynomial expressions of the two strategies. The resulting expressions are not expansions w.r.t. the coexisting strategies—such expansions cannot be defined, contrary to what originally done in Geritz et al. [1997, 1998]—but can be nevertheless used as approximations in the resident-mutant coexistence region locally to the singular point.

Our approach is quite general. Other non-similar resident populations (of the same of different species) can be considered and the approximation can be taken up to any order. Thanks to a structural property assumed for the dimorphic fitness, recently introduced in Dercole [2014]), the radial expansions can be written in terms of the geometry of the monomorphic fitness (in contrast to what preliminarily found in Durinx [2008], in the special case of Lotka-Volterra models).

We have used the developed approach to unfold the branching bifurcation, at which a stable equilibrium of the monomorphic AD canonical equation loses evolutionary stability. Specifically, allowing resident-mutant coexistence and ensuring the transversality and

genericity of the bifurcation, we have unfolded the transition of the evolutionary equilibrium turning from a terminal to a branching point of AD.

At the bifurcation, the evolutionary dynamics ruled by the dimorphic canonical equation are dominated by the third-order terms in the radial expansion of the dimorphic fitness. Interestingly, the second-order terms coincide with those Geritz et al. [1997, 1998] obtained by assuming smoothness, though nongeneric constraints on the monomorphic fitness come along at second- as well as at higher-orders. Thus the (second-order) branching condition of Geritz et al. [1997, 1998] is correct and our approach becomes essential only at third-order.

By means of a smooth coordinate change and time-scaling, we have identified the most simple model, locally equivalent to the dimorphic canonical equation, showing the bifurcation. We claim this is the normal form for the branching bifurcation. The model depends on four parameters that are all monomorphic fitness derivatives: the unfolding parameter, the fitness cross-derivative (constrained by one of the two genericity conditions), the normal form coefficient, and a third mixed-derivative that plays no role and could be eliminated by a further coordinate change (in that sense the normal form could be further simplified, though losing the geometric matching with the dimorphic canonical equation). The only genericity (and transversality) condition required by the bifurcation (other than resident-mutant coexistence), is then that the normal form coefficient is not vanishing.

Keeping into account the curvature of the boundaries of the resident-mutant coexistence region, we have proposed a second, necessarily less simple, model locally equivalent to the dimorphic canonical equation at the incipient branching. The boundaries quadratic approximation has the advantage of showing some geometric features relating the trajectories of the dimorphic canonical equation with the boundaries themselves (see Geritz et al. [1999] for more details).

The analysis of our simplified models as the unfolding parameter moves across zero unravels the dynamical phenomena turning a terminal point of AD into a branching point. Restricting the model dynamics into the region of coexistence, we see that the singular point is always a "corner" equilibrium that is attracting or repelling nearby trajectories, depending on the sign of the unfolding parameter, that is, its evolutionary stability/instability. The basin of attraction in the case of evolutionary stability is limited by the stable manifold of two boundary saddles, the convergence being composed of a dimor-

phic phase up to the extinction of one of the two similar strategies, followed by a monomorphic phase to the singular strategy. As the evolutionary stability condition moves across zero, the two saddles move along the boundaries and cross the diagonal at the singular strategy at the bifurcation. The three equilibria collide and exchange stability (both eigenvalues do change sign). In the case of evolutionary instability, the trajectories go away from the singularity and reach an evolutionary attractor that is not local to the singularity (and not involved in the bifurcation). The same attractor is generically viable even in the case of evolutionary stability, but it cannot be reached from a neighborhood of the singularity, unless the mutational step is large enough to escape the basin of attraction. The branching bifurcation is therefore catastrophic, in the sense that a small change in the unfolding parameter triggers a large evolutionary transient leading to a new attractor.

Finally, by considering the curvature of the boundaries of the resident-mutant coexistence region at the bifurcation, we can extend the branching condition as $\lambda_1^{(0,2)}(\bar{x},\bar{x}) \geq 0$, as already anticipated by Kisdi [1999], without, however, a formal derivation.

The natural follow-up to this work is the analysis of the other codimension-one branching bifurcation—the one at which the fitness cross-derivative vanishes and the singular strategy is evolutionary unstable. The resident-mutant coexistence region is locally a cusp rooted at the singular point (see Dercole and Geritz [2014]), and though there might generically be up to two coexistence equilibria, only one is stable and should be considered for developing a proper expansion of the dimorphic fitness. Further research could investigate the codimension-two bifurcation at which both fitness second-derivatives vanish (the type of coexistence is already available in Dercole and Geritz [2014]), or the cases at which the normal form coefficient vanishes together with one of the fitness second-derivatives; or, as well, higher codimensions that do occur in applications (see, e.g., Doebeli and Ispolatov [2010]). The mathematical approach developed in this chapter is readily applicable and convenient to pursue the above projects.

In chapter 5 we show how simulations of ODEs and continuations of systems of algebraic equations can be combined to study the evolution of biodiversity in multi-species systems where phenotypic traits are genetically transmitted. We analyze a standard parameterized family of prey-predator communities and propose an iterative procedure to obtain the branching portrait, explaining the dependence of branching scenarios on two parameters. We have discovered that

prey branching, that is induced by the predation pressure, is favored when prey intraspecific competition is highly sensitive to the resident-mutant phenotypic mismatch; while predator branching is not possible when prey and predators are present in equal number of morphs. Therefore, long alternate (prey and predator) as well as unilateral (prey) branching sequences can occur. But we have also discovered that long sequences composed of a first phase of alternate branching concatenated with a long unilateral sequence of prey branchings are possible in some regions of parameter space. This explains why prey populations can be much more numerous than predator populations, a fact that is often mentioned in field studies and is in agreement with traditional [Hardin, 1960, MacArthur and Levins, 1964, 1967, MacArthur, 1969] and modern [Diekmann et al., 2003, Diekmann and Metz, 2006, Gyllenberg and Meszéna, 2005, Meszéna et al., 2006] theories of competitive exclusion. We also find that predator handling time limits branching sequences, as harvesting saturation limits the predation pressures thus restraining prey from branching; and the same occurs if predator are too generalist, while specialists may generate long branching sequences, until a critical point is reached at which never ending Red Queen ups and downs of the coevolving traits prevent a halt at evolutionary equilibria and therefore evolutionary branching. Finally, critical parameter combinations for which branching scenarios are highly sensitive to parameter perturbations have been identified. This knowledge is of strategic importance for the conservation and management of biodiversity.

Our iterative procedure explores, at each iteration, the nature of longer and longer branching sequences. At each iteration, a better approximation of a two-dimensional branching portrait becomes available. Our approach is more interesting, both computationally and conceptually, than the stochastic individual- or population-based simulations mainly used until now when analytical tractability is unfeasible. Each simulation can only reveal an observable branching sequence, whereas our systematic analysis extracts information on all possible sequences including their nature, whether complete, incomplete or not observable. A particularly attractive feature is that, after a first branching portrait has been produced, the dependence of the branching scenarios on other parameters can be discussed without significantly increase the computational burden.

In principle, our approach can be made more general in view of investigating branching and extinction scenarios in AD models with two (or more) coevolving species, e.g., different prey-predator and host-

parasite communities (see, e.g., Best et al. [2010]), as well as communities regulated by other ecological interactions (e.g., mutualistic [Ferriére et al., 2002] and competitive [Kisdi, 1999] communities). Although the rigorous formulation of an iterative algorithm is basically impossible, we have discussed, partly in light of the specific model we have analyzed, the guidelines of a general method. In particular, evolutionary extinctions could be taken into account by considering sequences of different events, identifying branching and extinction in each of the coevolving species. This methodology has also been used outside ecology in the following chapters.

In chapter 6, we study fisheries-induced diversification resulting from the interplay of natural and artificial selection, in the simplest setting in which a fishery and a target stock coevolve. Several empirical studies have argued this possibility [Carlson et al., 2007, Edeline et al., 2007, 2009]: here we have systematically analyzed under which specific conditions such disruptive selection may arise.

Fishing imposes a strong selective pressure for early maturation, even though this is accompanied by increased physiological costs via life-history tradeoffs. Therefore, a harvested stock may split into two life-history types: one exploits the advantages of early maturation, while the other reduces the losses imposed by early-maturation tradeoffs. Indeed, we have shown that strong life-history tradeoffs of early-maturation act as indispensable prerequisites for disruptive selection. In addition, we have identified two other necessary conditions for a stock-fishery system to experience disruptive selection: (i) fishing policies that target large individuals, and (ii) adaptive harvesting that adjusts the harvest distribution for optimal benefit. Ultimately, these two conditions emerge from the same mechanism described above. Harvesting a stock's large individuals increases the directional selection pressure toward early maturation, as recurrently highlighted by earlier studies (e.g., Law [1979], Law and Grey [1989], Abrams and Rowe [1996]). Moreover, when harvesting is adaptive, a fishery behaves similar to an optimally foraging predator that maximizes its intake rate: this tends to increase the mortality of large individuals, as these are more profitable to harvest. Therefore, adaptive harvesting of large individuals selects for increased reproductive investment early in life. This, in turn, increases life-history tradeoffs and thereby strengthens the mechanism that leads to disruptive selection.

In line with these findings and explanations, populations with demographic conditions that penalize large individuals and/or favor small individuals are more sensitive to disruptive selection. This is

because such populations are naturally prone to early maturation, strengthening the impacts of the tradeoffs that turn selection disruptive. Therefore, there are three different ways to promote the mechanism that turns selection disruptive: first, the tradeoffs themselves may be strong due to physiological reasons; second, fishing mortality may select for early maturation, making the impacts of those tradeoffs strong; and third, a stock's other demographic and environmental conditions may predispose it to early maturation. Overall, this pattern of chasing the benefits of early maturation while avoiding its costs can be considered as an important general mechanism for the origin of dimorphism in exploited fish populations and other coevolving systems (e.g., Zhang et al. [2013]).

An ultimate target of fishery management is to increase sustainable yield. This raises the question of whether fisheries-induced disruptive selection should be managed. Our results show that sustainable yield can slightly increase after diversification when only large individuals are targeted, even though it still remains far below the maximum sustainable yield obtained at low fishing mortality when the stock is monomorphic. As many fish stocks are still overexploited, being managed considerably below their maximum sustainable yield, our findings imply that diversification triggered by fisheries-induced disruptive selection under high fishing mortality might slightly increase the yield from its level before diversification, if only large individuals are targeted. However, our results also suggest that such a population dimorphism can be taken as a sign of extreme harvesting pressure, as trait diversification is a way for species to escape from severe selection pressures resulting from human exploitation. Hence, when such a pattern is observed, our analysis suggests that sustainable yield can usually be improved by reducing fishing mortality.

Fisheries-induced disruptive selection could also increase phenotypic variability, without promoting life-history dimorphism: favoring extreme phenotypes may just widen an existing population polymorphism. This could have positive consequences beyond those analyzed in this chapter, since higher variability makes a population more reactive to future adaptation needs. This means that the population can react more promptly to any rapid changes in its environmental conditions, both for natural and anthropogenic causes. In other words, fisheries-induced disruptive selection could lead to a better capacity of an exploited stock to cope with environmental disturbances and changes.

In summary, fisheries-induced disruptive selection can indicate

overexploitation, can slightly increase or decrease the yield depending on the adopted fishing policy, and can enhance a stock's resilience to abrupt changes in its environmental conditions. Weighting these three aspects, decision makers can manage a fishery in pursuit of their economic, social, and conservation objectives.

Naturally, this study can be extended in a number of interesting directions. For example, fishing fleets in many regions of the world are composed of high-technology large commercial boats and low-technology small private boats. This suggests that the fishery component in a coevolving stock-fishery system can also experience selective pressures promoting the coexistence of different fleet segments. In other words, the fleet can experience an analogous disruptive selection and adaptive diversification, as suggested by Dercole et al. [2010b] and illustrated by standard eco-evolutionary predator-prey models [Doebeli and Dieckmann, 2000, Landi et al., 2013]; this warrants future research and model extensions. Specifically, fishery dynamics could happen at many levels: at the level of the fleet (adaptive harvesting on a short timescale, fleet size and structure on an intermediate timescale, and technological adaptation on a longer timescale), at the level of fishing strategy (constant effort, fixed quota, or fixed stock size), and/or at the level of fishing regulations (limitations on the size and maturity of target individuals). Here we have examined only the simplest setting, that is, adaptive harvesting with a constant-effort strategy. To detect disruptive selection on the fishery, adjustments in fleet size, fleet structure, and fleet technology must be explicitly modeled. As a starting point, the degree of harvest specialization in our model could be interpreted as characterizing the technological level of the fleet (affecting, e.g., the probability of locating aggregations of fish, catchability, and/or the efficiency of handling and transporting the catch). On this basis, this parameter could be used as an adaptive trait of the fishery using the framework of Adaptive Dynamics [Dercole et al., 2008, 2010b].

Finally, in chapter 7, we propose a model to investigate the dynamics of fashion traits. We consider pure social interactions between people that adapt their style to maximize social success. We thus do not consider the external drivers of marketing, business, and other economic and production aspects in this study, as well as the tendency to emulate stereotypes from higher social classes. This is in line with the view of Blumer [1969], who considers intra-class social interactions (the horizontal dynamics) dominant with respect to business and inter-class (vertical) drivers, and argues that the change in

fashion traits is the result of "*the gradual formation and refinement of collective tastes, which occur through social interaction among people with similar interests and social experience, with the result that many people develop tastes in common*".

People play a repeated group game in which the payoff reflects the social norms dictated by fashion: on one hand, the tendency to imitate the trendy stereotypes ("*... a wish to be in fashion ...*") opposed to the tendency to diverge from them to proclaim identity ("*...* [*a wish*] *to express new tastes ...*" [Blumer, 1969]); on the other hand, the tendency to exploit sex appeal in dating success [Veblen, 1894, Laver, 1937, Lurie, 1981, Steele, 1985] opposed to the moral judgment of the society (skirts continue to rise until they reach an extreme in Lowe and Lowe [1983]; "*...* [*a wish*]*to be abreast of what has good standing ...*" [Blumer, 1969]). The model is based on a Replicator Equation and on Adaptive Dynamics, and its assumptions are in agreement with the classical hypothesis on fashion dynamics: the idea of Blumer [1969] on the historical continuity of fashion change, for which new fashions evolve from those previously established by the society, is in good agreement with the AD assumptions of rare and small mutations and with the smooth approximation of the AD canonical equation.

Our study points out that the main mechanism promoting fashion diversification is the need to proclaim identity and to be original, especially when its advantage is uniformly distributed between the austere and immoral styles, whereas the need to conform to the trendy style and the need to be sexy reduce the emergence of style diversity. The effect of morality is a bit more subtle: diversity is promoted when the relative judgement between austere and immoral styles is weak, while there is no effect of the absolute moral judgement and the morality threshold of society.

The social norms dictated by fashion in the horizontal dynamics approach can generate a rich variety of coexisting styles, starting from an initial situation of conformity. This diversification can also be responsible of the periodic recurrence of some clothing style [Young, 1937, Lowe and Lowe, 1990, Pesendorfer, 1995, Caulkins et al., 2007]. Moreover, the presence of more than one style could lead to periodic, quasi-periodic, or even chaotic fashion regimes, where the styles oscillates continuously without ever reaching a stationary equilibrium (the so-called Red Queen dynamics, see, e.g., Marrow et al. [1992], Dieckmann et al. [1995], Dercole et al. [2006, 2010a]). The simplest of such never-ending dynamics would be a two-style limit cycle: for this to happen, a Hopf bifurcation should be identified in the two-style

community. A more subtle and evolutionarily intriguing periodic dynamics are the branching-extinction cycles. This happens when evolution first leads to an evolutionary branching point, and then drives one of the morphs to extinction [Doebeli and Dieckmann, 2000, Kisdi et al., 2001, Dercole, 2003, Dercole and Rinaldi, 2008]. If the dynamics goes back again to the branching point, this leads to a never-ending evolutionary dynamics of increase and successive loss of diversity. In this case, the sexy style after diversification could become so immoral to bring disadvantages to who adopts it, leading to its extinction. The austere style would then converge back to the neutral style, thus undergoing again diversification, and so on. However, such periodic dynamics was not detected in the present model. These extensions are left for future research.

Bibliography

P. A. Abrams. The evolution of predator-prey interactions: theory and evidence. *Annual Review of Ecological Systems*, 31:79–105, 2000.

P. A. Abrams and L. Rowe. The effects of predation on the age and size of maturity of prey. *Evolution*, 50:1052–1061, 1996.

P. A. Abrams, H. Matsuda, and Y. Harada. Evolutionary unstable fitness maxima and stable fitness minima of continuous traits. *Evolutionary Ecology*, 7:465–487, 1993.

A. Ajiad, T. Jakobsen, and O. Nakken. Sexual difference in maturation of Northeast Arctic cod. *Journal of Northwest Atlantic Fishery Science*, 25:1–15, 1999.

E. L. Allgower and K. Georg. *Introduction to Numerical Continuation Methods*. SIAM Classics in Applied Mathematics, 2003.

M. V. Ashley, M. F. Willson, O. R. W. Pergams, D. J. O'Dowd, S. M. Gende, and J. S. Brown. Evolutionarily enlightened management. *Biological Conservation*, 111:115–123, 2003.

N. Barber. Women's dress fashions as a function of reproductive strategy. *Sex Roles*, 40:459–471, 1999.

S. Barot, M. Heino, L. O'Brien, and U. Dieckmann. Long-term trend in the maturation reaction norm of two cod stocks. *Ecological Applications*, 14:1257–1271, 2004.

A. Best, A. White, E. Kisdi, J. Antonovics, M. A. Brockhurst, and M. Boots. The evolution of host-parasite range. *The American Naturalist*, 176:63–71, 2010.

H. Blumer. Fashion: from class differentiation to collective selection. *The Sociological Quarterly*, 10:275–291, 1969.

M. Bodin, Å. Brännström, and U. Dieckmann. A systematic overview of harvesting-induced maturation evolution in predator-prey systems with three different life-history tradeoffs. *Bulletin of Mathematical Biology*, 74:2842–2860, 2012.

B. Bolker and S. W. Pacala. Using moment equations to understand stochastically driven spatial pattern formation in ecological systems. *Theoretical Population Biology*, 52:179–197, 1997.

D. S. Boukal, E. S. Dunlop, M. Heino, and U. Dieckmann. Fisheries-induced evolution of body size and other life history traits: the impact of gear selectivity. In *ICES CM/F:07*, 2008.

F. Briand and J. E. Cohen. Community food webs have scale-invariant structure. *Nature*, 307:264–267, 1984.

J. S. Brown and T. L. Vincent. Coevolution as an evolutionary game. *Evolution*, 41:66–79, 1987.

J. S. Brown and T. L. Vincent. Organization of predator-prey communities as an evolutionary game. *Evolution*, 46:1269–1283, 1992.

M. G. Bulmer. *The Mathematical Theory of Quantitative Genetics*. Oxford University Press, 1980.

S. M. Carlson, E. Edeline, L. A. Vøllestad, T. O. Haugen, I. J. Winfield, J. M. Fletcher, J. B. James, and N. C. Stenseth. Four decades of opposing natural and human-induced artificial selection acting on Windermere pike (*Esox lucius*). *Ecology Letters*, 10:512–521, 2007.

J. P. Caulkins, R. F. Hart, P. M. Kort, and G. Feichtinger. Explaining fashion cycles: imitators chasing innovators in product space. *Journal of Economic Dynamics and Control*, 31:1535–1556, 2007.

N. Champagnat, R. Ferrière, and S. Méléard. Unifying evolutionary dynamics: From individual stochastic processes to macroscopic models. *Theoretical Population Biology*, 69:297–321, 2006.

F. B. Christiansen. On conditions for evolutionary stability for a continuously varying character. *The American Naturalist*, 138:37–50, 1991.

Y. Cohen, T. L. Vincent, and J. S. Brown. A G-function approach to fitness minima, fitness maxima, evolutionarily stable strategies

and adaptive landscapes. *Evolutionary Ecology Research*, 1:923–942, 1999.

R. A. Cole and F. A. Ward. Optimum fisheries management policy: angler opportunity versus angler benefit. *North American Journal of Fisheries Management*, 14:22–33, 1994.

C. Darwin and R. Wallace. On the tendency of species to form varieties; and on the perpetuation of varieties and species by natural means of selection. *Journal of the Proceedings of the Linnean Society*, 1858.

R. Dawkins. *The Selfish Gene*. Oxford University Press, 1976.

R. Dawkins. *The Extended Phenotype: The Long Reach of the Gene*. Oxford University Press, 1982.

D. L. De Angelis and L. J. Gross, editors. *Individual-Based Models and Approaches in Ecology: populations, Communities and Ecosystems*. Chapman & Hall, New York, 1992.

A. M. de Roos, D. S. Boukal, and L. Person. Evolutionary regime shifts in age and size at maturation of exploited fish stoks. *Proceedings of the Royal Society of London B*, 273:1873–1880, 2006.

F. Dercole. Remarks on branching-extinction evolutionary cycles. *Journal of Mathematical Biology*, 47:569–580, 2003.

F. Dercole. The ecology of asexual pairwise interactions: A generalized law of mass action. *Journal of Mathematical Biology*, 2014. (submitted).

F. Dercole and S. Geritz. Unfolding the resident-invader dynamics of similar strategies. *Theoretical Population Biology*, 2014. (to be submitted).

F. Dercole and S. Rinaldi. Evolution of cannibalistic traits: scenarios derived from adaptive dynamics. *Theoretical Population Biology*, 62:365–374, 2002.

F. Dercole and S. Rinaldi. *Analysis of Evolutionary Processes: The Adaptive Dynamics Approach and Its Applications*. Princeton University Press, 2008.

F. Dercole and S. Rinaldi. Evolutionary dynamics can be chaotic: a first example. *International Journal of Bifurcation and Chaos*, 11: 3473–3485, 2010.

F. Dercole, R. Ferrière, and S. Rinaldi. Ecological bistability and evolutionary reversals under asymmetrical competition. *Evolution*, 56:1081–1090, 2002.

F. Dercole, J. O. Irisson, and S. Rinaldi. Bifurcation analysis of a prey-predator coevolution model. *SIAM Journal on Applied Mathematics*, 63(4):1378–1391, 2003.

F. Dercole, A. Gragnani, R. Ferriére, and S. Rinaldi. Coevolution of slow-fast populations: evolutionary sliding, evolutionary pseudo-equilibria and complex Red Queen dynamics. *Proceedings of the Royal Society of London B*, 273:983–990, 2006.

F. Dercole, U. Dieckmann, M. Obersteiner, and S. Rinaldi. Adaptive dynamics and technological change. *Technovation*, 28:335–348, 2008.

F. Dercole, R. Ferriére, and S. Rinaldi. Chaotic Red Queen coevolution in three-species food chains. *Proceedings of the Royal Society of London B*, 277:2321–2330, 2010a.

F. Dercole, C. Prieu, and S. Rinaldi. Technological change and fisheries sustanibility: the point of view of adaptive dynamics. *Ecological Modelling*, 221:379–387, 2010b.

F. Dercole, P. Landi, and F. Della Rossa. The branching bifurcation of Adaptive Dynamics. *International Journal of Bifurcation and Chaos*, 2014. (to be submitted).

A. Dhooge, W. Govaerts, and Yu. A. Kuznetsov. MATCONT: A MATLAB package for numerical bifurcation analysis of ODEs. *ACM Transactions on Mathematical Software*, 29:141–164, 2002.

U. Dieckmann and M. Doebeli. On the origin of species by sympatric speciation. *Nature*, 400:354–357, 1999.

U. Dieckmann and R. Ferriére. Adaptive dynamics and evolving biodiversity. *Evolutionary Conservation Biology*, pages 188–224, 2004. Cambridge University Press.

U. Dieckmann and M. Heino. Probabilistic maturation reaction norms: their history, strengths, and limitations. *Marine Ecology Progress Series*, 335:253–269, 2007.

U. Dieckmann and R. Law. The dynamical theory of coevolution: a derivation from stochastic ecological processes. *Journal of Mathematical Biology*, 34:579–612, 1996.

U. Dieckmann and R. Law. Relaxation projections and method of moments. *The Geometry of Ecological Interactions*, pages 412–455, 2000. Cambridge University Press.

U. Dieckmann, U. Marrow, and R. Law. Evolutionary cycling in predator-prey interactions: population dynamics and the Red Queen. *Journal of Theoretical Biology*, 176:91–102, 1995.

U. Dieckmann, M. Doebeli, J. A. J. Metz, and D. Tautz. *Adaptive Speciation*. Cambridge University Press, 2004.

U. Dieckmann, M. Heino, and K. Parvinen. The adaptive dynamics of function-valued traits. *Journal of Theoretical Biology*, 241:370–389, 2006.

U. Dieckmann, M. Heino, and A. D. Rijnsdorp. The dawn of Darwinian fishery management. *ICES Insight*, 46:34–43, 2009.

O. Diekmann, M. Gyllenberg, and J. A. J. Metz. Steady state analysis of structured population models. *Theoretical Population Biology*, 63:309–338, 2003.

U. Diekmann and J. A. J. Metz. Surprising evolutionary predictions from enhanced ecological realism. *Theoretical Population Biology*, 69:263–281, 2006.

M. Doebeli and U. Dieckmann. Evolutionary branching and sympatric speciation caused by different types of ecological interactions. *The American Naturalist*, 156:77–101, 2000.

M. Doebeli and I. Ispolatov. Continuously stable strategies as evolutionary branching points. *Journal of Theoretical Biology*, 266: 529–535, 2010.

M. Doebeli and G. D. Ruxton. Evolution of dispersal rates in metapopulation models: Branching and cyclic dynamics in phenotype space. *Evolution*, 51:1730–1741, 1997.

E. S. Dunlop, M. Heino, and U. Dieckmann. Eco-genetic modeling of contemporary life-history evolution. *Ecological Applications*, 19: 1815–1834, 2009.

M. Durinx. *Life amidst Singularities.* Doctoral thesis, Institute of Biology, Leiden University, The Netherlands, 2008.

M. Durinx, J. A. J. Metz, and G. Meszéna. Adaptive dynamics for physiologically structured population models. *Journal of Mathematical Biology*, 56:673–742, 2008.

E. Edeline, S. M. Carlson, L. C. Stige, I. J. Winfield, J. M. Fletcher, J. B. James, T. O. Haugen, L. A. Vøllestad, and N. C. Stenseth. Trait changes in a harvested population are driven by a dynamic tug-of-war between natural and harvest selection. *Proceedings of the National Academy of Science*, 104:15799–15804, 2007.

E. Edeline, A. Le Rouzic, I. J. Winfield, J. M. Fletcher, J. B. James, N. C. Stenseth, and L. A. Vøllestad. Harvest-induced disruptive selection increases variance in fitness-related traits. *Proceeding of the Royal Society of London B*, 276:4163–4171, 2009.

M. Egas, M. W. Sabelis, and U. Dieckmann. Evolution of specialization and ecological character displacement of herbivores along a gradient of plant quality. *Evolution*, 3:507–520, 2005.

G. H. Engelhard and M. Heino. Maturity changes in Norwegian spring-spawning herring *Clupea harengus*: compensatory or evolutionary responses. *Marine Ecology Progress Series*, 272:245–256, 2004.

B. Ernande, U. Dieckmann, and M. Heino. Adaptive changes in harvested populations: plasticity and evolution of age and size at maturation. *Proceedings of the Royal Society of London B*, 271:415–423, 2004.

I. Eshel. Evolutionary and continuous stability. *Journal of Theoretical Biology*, 103:99–111, 1983.

I. Eshel and U. Motro. Kin selection and strong evolutionary stability of mutual help. *Theoretical Population Biology*, 19:420–433, 1981.

D. S. Falconer. *Introduction to Quantitative Genetics.* Longman, 1989.

J. Felsenstein. Skepticism towards Santa Rosalia, or why are there so few kinds of animals? *Evolution*, 135:124–138, 1981.

R. Ferriére, J. L. Bronstein, S. Rinaldi, R. Law, and M. Gauduchon. Cheating and the evolutionary stability of mutualisms. *Proceedings of the Royal Society of London B*, 269:773–780, 2002.

G. A. Field. The status float phenomenon. *Business Horizons*, 1: 45–52, 1970.

R. A. Fisher. *The Genetical Theory of Natural Selection*. Clarendon Press, 1930.

J. M. Fromentin and J. E. Powers. Atlantic bluefin tuna: population dynamics, ecology, fisheries, and management. *Fish and Fisheries*, 6:281–306, 2005.

J. D. Futuyma and M. Slatkin. *Coevolution*. Sinauer Associates, 1983.

S. Gavrilets. *Fitness Landscapes and the Origin of Species*. Princeton University Press, Princeton, NJ, 2004.

S. A. H. Geritz. Resident-invader dynamics and the coexistence of similar strategies. *Journal of Mathematical Biology*, 50:67–82, 2005.

S. A. H. Geritz and F. Dercole. Editorial. *Journal of Biological Dynamics*, 5:103, 2011.

S. A. H. Geritz, J. A. J. Metz, E. Kisdi, and G. Meszéna. The dynamics of adaptation and evolutionary branching. *Physical Review Letters*, 78:2024–2027, 1997.

S. A. H. Geritz, E. Kisdi, G. Meszéna, and J. A. J. Metz. Evolutionarily singular strategies and the adaptive growth and branching of the evolutionary tree. *Evolutionary Ecology*, 12:35–57, 1998.

S. A. H. Geritz, E. van der Meijden, and J. A. J. Metz. Evolutionary dynamics of seed size and seedling competitive ability. *Theoretical Population Biology*, 55:324–343, 1999.

S. A. H. Geritz, M. Gyllenberg, F. J. A. Jacobs, and K. Parvinen. Invasion dynamics and attractor inheritance. *Journal of Mathematical Biology*, 44:548–560, 2002.

S. A. H. Geritz, E. Kisdi, and P. Yan. Evolutionary branching and long-term coexistence of cycling predators: critical function analysis. *Theoretical Population Biology*, 71:424–435, 2007.

W. Govaerts. *Numerical Methods for Bifurcations of Dynamical Equilibria*. SIAM, Philadelphia, PA, 2000.

A. Gårdmark and U. Dieckmann. Disparate maturation adaptations to size-dependent mortality. *Proceedings of the Royal Society of London B*, 273:2185–2192, 2006.

V. Grimm and S. F. Railsback. *Individual-based Modeling and Ecology*. Princeton University Press, 2005.

M. R. Gross. Disruptive selection for alternative life histories in salmon. *Nature*, 313:47–48, 1985.

M. R. Gross. Alternative reproductive strategies and tactics: diversity within sexes. *Trends in Ecology and Evolution*, 11:92–98, 1996.

M. Gyllenberg and G. Meszéna. On the impossibility of coexistence of infinitely many strategies. *Journal of Mathematical Biology*, 50: 133–160, 2005.

M. Gyllenberg and K. Parvinen. Necessary and sufficient conditions for evolutionary suicide. *Bulletin of Mathematical Biology*, 63:981–993, 2001.

J. B. S. Haldane. *The Causes of Evolution*. Longmans Green, 1932.

R. Hannesson. *The Economics of Fisheries*. Blackwell Science, 2002.

G. Hardin. The competitive exclusion principle. *Science*, 131:1292–1298, 1960.

P. J. B. Hart and J. Reynolds. *Handbook of Fish Biology and Fisheries*. Blackwell Science, 2002.

M. Heino. Management of evolving fish stocks. *Canadian Journal of Fisheries and Aquatic Sciences*, 55:1971–1982, 1998.

M. Heino and O. R. Godø. Fisheries-induced selection pressure in the context of sustainable fisheries. *Bulletin of Marine Science*, 70: 639–656, 2002.

E. Hernández-García, C. López, S. Pigolotti, and K. H. Andersen. Species competition: coexistece, exclusion and clustering. *Philosophical Transactions of the Royal Society of London A*, 367:3183–3195, 2009.

R. Hilborn and C. J. Walters. *Quantitative Fisheries Stock Assessment: Choice, Dynamics and Uncertainty.* Chapman & Hall, 1992.

S. B. Hsu, S. P. Hubbel, and P. Waltmann. Competing predators. *SIAM Journal on Applied Mathematics*, 35:617–625, 1978.

J. A. Hutchings and D. J. Fraser. The nature of fisheries- and farming-induced evolution. *Molecular Ecology*, 17:294–313, 2008.

J. A. Hutchings and J. D. Reynolds. Marine fish population collapses: consequences for recovery and extinction risk. *Bioscience*, 54:297–309, 2004.

G. E. Hutchinson. Homage to Santa Rosalia or why are there so many kinds of animals? *The American Naturalist*, 93:145–159, 1959.

I. C. Ito and T. Ikegami. Food-web formation with recursive evolutionary branching. *Journal of Theoretical Biology*, 238:1–10, 2006.

S. Jennings and M. J. Kaiser. The effects of fishing on marine ecosystems. *Advances in Marine Biology*, 34:201–352, 1998.

C. Jørgensen, K. Enberg, E. S. Dunlop, R. Arlinghaus, D. Boukal, K. Brander, B. Ernande, A. Gårdmark, F. Johnson, S. Matsumura, H. Pardoe, K. Raab, A. Silva, A. Vainikka, U. Dieckmann, M. Heino, and A. D. Rijnsdorp. Managing evolving fish stocks. *Science*, 318:1247–1248, 2007.

T. Kawecki. Sympatric speciation driven by beneficial mutations. *Proceedings of the Royal Society of London B*, 263:1515–1520, 1996.

I. Keller, C. E. Wagner, L. Greuter, S. Mwaiko, O. M. Selz, A. Sivasundar, S. Wittwer, and O. Seehausen. Population genomic signatures of divergent adaptation, gene flow and hybrid speciation in the rapid radiation of Lake Victoria cichlid fishes. *Molecular Ecology*, 22:2848–2863, 2013.

A. A. King and W. M. Schaffer. The geometry of a population cycle: a mechanistic model of snowshoe hare demography. *Ecology*, 3: 814–830, 2001.

E. Kisdi. Evolutionary branching under asymmetric competition. *Journal of Theoretical Biology*, 197:149–162, 1999.

E. Kisdi and S. A. H. Geritz. Adaptive dynamics in allele space: evolution of genetic polymorphism by small mutations in a heterogeneous environment. *Evolution*, 53:993–1008, 1999.

E. Kisdi, F. J. A. Jacobs, and S. A. H. Geritz. Red Queen evolution by cycles of evolutionary branching and extinction. *Selection*, 2: 161–178, 2001.

Yu. A. Kuznetsov. *Elements of Applied Bifurcation Theory*. Springer Verlag, 3rd edition, 2004.

P. Landi and F. Dercole. The evolution of fashion traits: pure social interactions promote diversity. In *Proceedings of the 8th European Nonlinear Dynamics Conference ENOC 2014*, Vienna, 2014a.

P. Landi and F. Dercole. The evolution of fashion traits: Pure social interactions promote diversity. *Journal of Mathematical Sociology*, 2014b. (to be submitted).

P. Landi, F. Dercole, and S. Rinaldi. Branching scenarios in eco-evolutionary prey-predator models. *SIAM Journal on Applied Mathematics*, 73:1634–1658, 2013.

P. Landi, C. Hui, and U. Dieckmann. Fisheries-induced disruptive selection. *Journal of Theoretical Biology*, 2014. submitted.

J. Laver. *Taste and Fashion: From the French Revolution to the Present Day*. Harrap, 1937.

R. Law. Optimal life-histories under age-specific predation. *The American Naturalist*, 114:399–417, 1979.

R. Law. Fishing, selection and phenotypic evolution. *ICES Journal of Marine Science*, 57:659–669, 2000.

R. Law and D. R. Grey. Evolution of yields from populations with age-specific cropping. *Evolutionary Ecology*, 3:343–359, 1989.

J. A. Leon. Selection in contexts of interspecific competition. *The American Naturalist*, 108:739–757, 1974.

J. Levins. *Evolution in Changing Environments*. Princeton University Press, 1968.

R. C. Lewontin. Gene, organism and environment. In D. S. Bendall, editor, *Evolution from Molecules to Men*, pages 273–285. Cambridge University Press, 1983.

C. C. Li. *Population Genetics*. The University of Chicago Press, 1955.

E. D. Lowe. Quantitative analysis of fashion change: a critical review. *Home Economics Research Journal*, 21:280–306, 1993.

E. D. Lowe and J. W. G. Lowe. Velocity of the fashion process in women's formal evening dress, 1789-1980. *Clothing & Textiles Research Journal*, 9:50–58, 1990.

J. W. G. Lowe and E. D. Lowe. Cultural pattern and process: a study of stylistic change in women's dress. *American Anthropologist*, 54: 521–544, 1982.

J. W. G. Lowe and E. D. Lowe. Model of fashion change. *Advances in Consumer Research*, 11:731–734, 1983.

A. Lurie. *The Language of Clothes*. Random House, 1981.

R. H. MacArthur. Species packing, and what interspecies competition minimizes. *Proceedings of the National Academy of Science*, 64: 1369–1371, 1969.

R. H. MacArthur and R. Levins. Competition, habitat selection and character displacement in a patchy environment. *Proceedings of the National Academy of Science*, 51:1207–1210, 1964.

R. H. MacArthur and R. Levins. The limiting similarity, convergence and divergence of coexisting species. *The American Naturalist*, 101: 377–385, 1967.

T. R. Malthus. *An Essay on the Principle of Population*. Printed for J. Johnson in St. Paul's Church-Yard, London, 1798.

P. Marrow, R. Law, and C. Cannings. The coevolution of predator-prey interactions: ESSs and Red Queen dynamics. *Proceedings of the Royal Society of London B*, 250:133–141, 1992.

P. Marrow, U. Dieckmann, and R. Law. Evolutionary dynamics of predator-prey systems: nn ecological perspective. *Journal of Mathematical Biology*, 34:556–578, 1996.

N. D. Martinez. Network evolution: exploring the change and adaptation of complex ecological systems over deep time. In *Ecological Networks: Linking Structure to Dynamics in Food Webs*, pages 287–301. Oxford University Press, 2006.

C. Matessi and C. Di Pasquale. Long term evolution of multi-locus traits. *Journal of Mathematical Biology*, 34:613–653, 1996.

H. Matsuda and P. A. Abrams. Runaway evolution to self-extinction under asymmetrical competition. *Evolution*, 48:1764–1772, 1994.

S. Matsumura, R. Arlinghaus, and U. Dieckmann. Assessing evolutionary consequences of size-selective recreational fishing on multiple life-history traits, with an application to northern pike (*Esox lucius*). *Evolutionary Ecology*, 25:711–735, 2011.

J. Maynard Smith. Sympatric speciation. *The American Naturalist*, 100:637–650, 1966.

J. Maynard Smith and J. Price. The logic of animal conflicts. *Nature*, 246:15–18, 1973.

E. Mayr. *Systematics and the Origin of Species*. Columbia University Press, 1942.

H. G. E. Meijer, F. Dercole, and B. E. Oldeman. Numerical bifurcation analysis. In R. A. Meyers, editor, *Encyclopedia of Complexity and System Science*, pages 6329–6352. 2009.

G. J. Mendel. Experiments in plant hybridization. *Abhandlungen*, 4: 3–47, 1865.

G. Meszéna, M. Gyllenberg, F. J. A. Jacobs, and J. A. J. Metz. Link between population dynamics and dynamics of Darwinian evolution. *Physical Review Letters*, 95:078195, 2005.

G. Meszéna, M. Gyllenberg, L. Pásztor, and J. A. J. Metz. Competitive exclusion and limiting similarity: a unified theory. *Theoretical Population Biology*, 69:68–87, 2006.

J. A. J. Metz, R. M. Nisbet, and S. A. H. Geritz. How should we define fitness for general ecological scenarios? *Trends in Ecology and Evolution*, 7:198–202, 1992.

J. A. J. Metz, S. A. H. Geritz, G. Meszéna, F. J. A. Jacobs, and J. S. van Heerwaarden. Adaptive dynamics: a geometrical study of the consequences of nearly faithful reproduction. In S. J. van Strien and S. M. Verduyn Lunel, editors, *Stochastic and Spatial Structures of Dynamical Systems*, pages 183–231. Elsevier Science, 1996.

C. M. Miller, S. H. McIntyre, and M. K. Mantrala. Toward formalizing fashion theory. *Journal of Marketing Research*, 30:142–157, 1993.

J. F. Nash. Equilibrium points in n-person games. *Proceedings of the National Academy of Science*, 36:48–49, 1950.

M. A. Nowak. An evolutionary stable strategy may be inasscessible. *Journal of Theoretical Biology*, 142:237–241, 1990.

A. F. Opdal. Fisheries change spawning ground distribution of north-east Arctic cod. *Biology Letters*, 6:261–264, 2010.

S. R. Palumbi. Humans as the world's greatest evolutionary force. *Science*, 293:1786–1790, 2001.

K. Parvinen. Evolutionary suicide. *Acta Biotheoretica*, 53:241–264, 2005.

W. Pesendorfer. Design innovation and fashion cycles. *The American Economic Review*, 85:771–792, 1995.

S. Pigolotti, C. López, E. Hernández-García, and K. H. Andersen. How gaussian competition leads to lumpy or uniform species distributions. *Theoretical Ecology*, 3:89–96, 2010.

J. J. Poos, Å. Brännström, and U. Dieckmann. Harvest-induced maturation evolution under different life-history trade-offs and harvesting regimes. *Journal of Theoretical Biology*, 279:102–112, 2011.

D. M. Raup and J. J. Sepkoski. Mass extinctions in the marine fossil record. *Science*, 215:1501–1503, 1982.

J. Richardson and A. L. Kroeber. Three centuries of women's dress fashions: a quantitative analysis. *Anthropological Records*, 5:111–153, 1940.

D. E. Robinson. Fashions in shaving and trimming of the beard: the men of the illustrated London News, 1842-1972. *American Journal of Sociology*, 81:1133–1141, 1976.

D. A. Roff. An allocation model of growth and reproduction in fish. *Canadian Journal of Fisheries and Aquatic Sciences*, 40:1395–1404, 1983.

D. A. Roff. *Evolutionary Quantitative Genetics*. Chapman & Hall, 1997.

M. L. Rosenzweig and R. H. MacArthur. Graphical representation and stability conditions of predator-prey interactions. *The American Naturalist*, 97:209–223, 1963.

J. Roughgarden. The theory of coevolution. *Coevolution*, pages 383–403, 1983. Sinauer Associates.

A. Salthaug. Adjustment of commercial trawling effort for Atlantic cod, *Gadus morhua*, due to increasing catching efficiency. *Fishery Bulletin*, 99:338–342, 2001.

A. Sasaki. Clumped distribution by neighborhood competition. *Journal of Theoretical Biology*, 186:415–430, 1997.

M. Scheffer. *Ecology of Shallow Lakes*. Kluwer Academic, 1st edition, 1998.

M. Scheffer and E. H. van Nes. Self-organized similarity, the evolutionary emergence of groups of similar species. *Proceedings of the National Academy of Science*, 16:6230–6235, 2006.

P. Schuster and K. Sigmund. Replicator dynamics. *Journal of Theoretical Biology*, 100:533–538, 1983.

G. Simmel. Fashion. *International Quarterly*, 10:130–155, 1904.

A. Sinclair. Fish distribution and partial recruitment: the case of eastern Scotian Shelf cod. *Journal of Northwest Atlantic Fishery Science*, 13:15–24, 1992.

G. B. Sproles. *Fashion: Consumer Behavior Toward Dress*. Burgess, 1979.

G. B. Sproles. Analyzing fashion life cycles: principles and perspectives. *The Journal of Marketing*, 45:116–124, 1981.

G. B. Sproles. Behavioral science theories of fashion. In M. R. Solomon, editor, *The Psychology of Fashion*, pages 55–70. Lexington Books, 1985.

S. C. Stearns. *The Evolution of Life Histories*. Oxford University Press, 1992.

V. Steele. *Fashion and Eroticism*. Oxford University Press, 1985.

T. K. Stokes, J. M. McGlade, and R. Law. *The exploitation of evolving resources*. Springer, Berlin, 1993.

D. P. Swain and E. J. Wade. Density-dependent geographic distribution of Atlantic cod (*Gadus morhua*) in the southern Gulf of St. Lawrence. *Canadian Journal of Fisheries and Aquatic Sciences*, 50: 725–733, 1993.

P. J. Taylor and L. Jonker. Evolutionarily stable strategies and game dynamics. *Mathematical Biosciences*, 40:145–156, 1978.

J. N. Thompson. *The Coevolutionary Process.* Chicago University Press, 1994.

P. Turchin. *Complex Population Dynamics: A Theoretical/Empirical Synthesis.* Princeton University Press, 2003.

L. Van Valen. A new evolutionary law. *Evolutionary Theory*, 1:1–30, 1973.

T. Veblen. The economic theory of woman's dress. *The Popular Science Monthly*, 46:198–205, 1894.

T. L. Vincent and J. S. Brown. *Evolutionary Game Theory, Natural Selection, and Darwinian Dynamics.* Cambridge University Press, 2005.

J. von Neumann and O. Morgenstern. *Theory of Games and Economic Behavior.* Princeton University Press, 1953.

C. J. Walters and S. J. D. Martell. *Fisheries Ecology and Management.* Princeton University Press, 2004.

P. Weeden. Study patterned on Kroeber's investigation of style. *Dress*, 3:8–19, 1977.

E. O. Wilson. *Biodiversity.* The National Academic Press, 1988.

S. Wright. Evolution in mendelian populations. *Genetics*, 16:97–159, 1931.

A. B. Young. *Recurring Cycles of Fashion.* Harper and brothers, 1937.

F. Zhang, C. Hui, and A. Pauw. Adaptive divergence in Darwin's race: how coevolution can generate trait diversity in a pollination system. *Evolution*, 67:548–560, 2013.

J. Ziman, editor. *Technological Innovation as an Evolutionary Process.* Cambridge University Press, Cambridge, UK, 2000.

List of Figures

List of Tables